EXAMINING FACE-SENSITIVE BRAIN POTENTIALS IN NATURAL ENVIRONMENTS USING MOBILE EEG

Thesis submitted in accordance with the requirements
of the University of Liverpool for the degree of
Doctor in Philosophy by

Vicente Soto

February, 2019

Frequent abbreviations

ANOVA	Analysis of variance
BESA	Brain electrical source analysis
CLARA	Classical LORETA recursively applied
EEG	Electroencephalography
EMRP	Eye-movement related potential
ERP	Event related potential
FFA	Fusiform face area
fMRI	Functional magnetic resonance imaging
fNIRS	Functional near-infrared spectroscopy
IC	Independent component
ICA	Independent component analysis
LORETA	Low resolution electromagnetic tomography
MoBI	Mobile brain and body imaging
OFA	Occipital face area
PCA	Principal component analysis
PET	Positron emission tomography
sLORETA	Standardized low resolution electromagnetic tomography
SD	Standard deviation
STS	Superior temporal sulcus
VPP	Vertex Positive Potential
ECD	Equivalent current dipole
RS	Regional source

Contents

List of Figures

This thesis is submitted in fulfilment of the conditions for a PhD by published papers. In accordance with the University of Liverpool guidelines and regulations the experimental chapters (Chapters 4 to 7) of this thesis will take the form of journal article manuscripts, which have either been published during the preparation of this thesis, or are being prepared for submission a peer-reviewed journal or are being read by co-authors before submission to a peer-reviewed journal. Specific details regarding the contribution of authors are given at the beginning of each chapter, as required.

Declaration

No part of this work was submitted in support of any other applications for degree or qualification at this or any other university or institute of learning.

Acknowledgements

Firstly, I cannot go without thanking my supervisor, Dr Andrej Stancak. His exceptional teaching, guidance, and support were invaluable and exceeded any measure of expectations I could have possibly had. Without his rigours dedication, attention to detail, and generosity none of the work presented in this thesis would have been possible. Many thanks also to Dr Nicolas Fallon and Dr Timo Giesbrecht for their insight, supervision and advice.

I would also like to thank the fellow members of my research group, in specific, to John Tyson-Carr, Hannah Roberts, Katerina Kokmotou, Adam Byrne, Danielle Hewitt and Julia Jones who were incredibly generous with their time and efforts. It was a great pleasure working with you all. I hope we can collaborate again in the future.

I would like to acknowledge the EPSRC and Unilever for funding this project. I would also like to thank the study participants for their time and excellent disposition during experimental testing.

On a personal note, I would like to thank my parents and brothers for their encouragement as well as my wonderful wife for her relentless love and support.

Gracias Cata. Tu cariño, paciencia y apoyo incondicional fueron imprescindibles a lo largo de este proyecto. No lo podría haber hecho sin ti.

I would like to dedicate this thesis to my wife, Catalina and son, Román. You are my inspiration and I love you both endlessly.

Using mobile brain and body imaging to investigate human face processing in natural environments

Vicente Soto

Abstract

Faces are a unique type of stimulus for humans. As such, they are processed differently to other types of stimuli like houses or objects. In the past, laboratory based testing has been used to examine the neural correlates of human face processing. However, viewing faces in a laboratory differs considerably from how it occurs the real world. This thesis examines the neural mechanisms underlying the processing of face images in a naturalistic setting.

A custom-design mobile brain and body imaging technique was used to explore the neural mechanisms governing naturalistic face processing. Simultaneous mobile electroencephalography (EEG) and eye-tracking data was recorded from participants while they freely viewed images presented in a mock art gallery. The synchronization of both data streams allowed us to analyse the EEG signal by time-locking markers to naturally occurring visual events captured by the eye tracker. Using this methodology the effects of emotion, familiarity and body posture on the face-sensitive N170 ERP component were investigated.

The findings demonstrated, for the first time, the possibility of detecting face-specific brain potentials in freely moving, unrestricted subjects during passive viewing of images, as well as during active interactions with another person. The results present the effects of emotional valence on the N170 amplitude and replicate previous lab-based findings. Furthermore, the effects of body posture on early visual ERPs, but not the face-sensitive N170 contribute new insights to the face processing literature. Finally, the N170 component produced during a dyadic social interaction is described in relation to previous laboratory based reports.

The experimental chapters present a novel methodology for recording mobile EEG signals as well as an adaptable experimental design that can be used in a wide variety of fields. The thesis demonstrates that EEG activity associated to the viewing static faces in laboratory conditions resemble those produced in real world environments as well as during natural social interactions. Moreover, the effects of emotional content on face processing were represented in the N170 component particularly, when disgusted faces were viewed.

Chapter 1

Brain imaging in natural settings

1.1 Introduction

The dawn of brain imaging techniques has substantially influenced our scientific understanding regarding the mind, brain functioning and behaviour. Perhaps one of the most exciting prospects for modern cognitive neuroscience research is to understand the brain mechanisms supporting human cognition as it occurs naturally during everyday life. Humans are active agents in the world, continuously adapting and integrating perpetually changing environments which more often than not, include other living things as well as objects. The idea of interdependence between sensory perception, action and the environmental setting had previously been described (Brown, Collins & Duguid, 1989; Gibson, 1979). Chiel & Beer (1997) were amongst the first to propose the need to understand cognition as interactions between brain, body and the environment. As a result, the field of cognitive neuroscience has coined the term 'embodied' as a concept used to highlight two notions; firstly that natural cognition depends on the experience that comes from having a body with various sensorimotor capacities, and secondly, that individual sensorimotor capacities are themselves embedded in a more encompassing biological, psychological and cultural context (Varela, Thompson, & Asenstorfer, 1996). Within this framework, key concepts highlight cognition as situational and time-sensitive, the role of perception and cognition in supporting directed behaviour (Churchland, Ramachandran, & Sejnowski, 1994) as well as an active integration of the environment into our cognitive system (Wilson, 2002).

One example of the dynamic relationship between sensory input and behavioural outcomes is the integration of visual-motor feedback when adjusting our behaviour due to changes in the environment (e.g. when playing ping-pong or catching a suddenly falling object). Moreover, physiological evidence shows that brain areas have evolved in

response to the need to organize motor behaviour in three-dimensional environments to support human cognition (Rizzolatti & Gentilucci, 2002). This suggests brain processes are closely tied to our sensations and actions within the environment. This idea is supported by the fact brain dynamics dramatically change when animals or humans move; as has been shown in virtual environments as well as in the real world (Bohbot, Copara, Gotman, & Ekstrom, 2017). Taken together, these findings suggest that brain activity in the real world might differ significantly from that occurring in a laboratory situation.

In the past three decades, brain imaging has revolutionized the field of cognitive neuroscience and the way we explore brain functioning as well as dramatically increased our understanding of human psychology. Technological developments to hardware and substantial increments in computational power over the past decades have quickly made brain imaging methods ubiquitous to cognitive research. Brain imaging methods like functional magnetic resonance imaging (fMRI), positron emotion tomography (PET) and electroencephalography (EEG) have contributed invaluably to our understanding of psychological processes, brain activity and the structure of the brain. However, the limitations associated with modern brain imaging methods require strictly controlled laboratory environments. The artificially isolated conditions in which cognitive testing is typically performed are not representative of the actual functioning of cognition (Brunswik, 1943). Participants are normally asked to remain still during the collection of imaging data and cognitive testing and stimuli are traditionally presented on a 2D screen. Opposing traditional understandings that the visual system must resolve a three dimensional environment from the information extracted from two dimensional images projected in the retina. Gibson, (1979) for instance, optioned that "vision does not begin with a static retinal array, but with an organism actively moving through a visually rich environment".

One remedy to this is to register behavioural information in paradigms that include some sort of natural movement. EEG and magnetoencephalography (MEG) hyperscanning techniques, for instance, have been used to investigate social cognition during human interactions (Baess et al., 2012; Hari & Kujala, 2009; Lachat, Hugueville,

Lemaréchal, Conty, & George, 2012). These techniques involve recoding simultaneous EEG's from multiple participants during normal social interactions i.e. during a game of cards (Babiloni et al., 2007), while making arm and hand movements (Ménoret et al., 2014) or during a joint musical performance (Lindenberger, Li, Gruber, & Müller, 2009). However, in these cases the issue of mobility is not fully addressed nor is the influence of free-movement in natural settings on cognitive processing.

In the past 10 years, a mobile brain and body imaging (MoBI) methodology has been developed allowing brain imaging to be performed in natural settings and during motion (Gramann, Gwin, Bigdely-Shamlo, Ferris, & Makeig, 2010; Makeig, Gramann, Jung, Sejnowski, & Poizner, 2009). This thesis capitalises on previous MoBI methodologies and developed an innovative imaging technique to examine, for the first time, face-sensitive electrocortical brain potentials in natural environments as well as during normal social interactions.

1.2 Mobile Brain and body imaging (MoBI)

The need for a real-world approach to cognitive research has received increasing attention in recent years (Smilek, Birmingham, Cameron, Bischof, & Kingstone, 2006). The motivation behind the development of a mobile brain and body imaging (MoBI) methodology is to allow unobstructed monitoring of flexible and adaptive brain dynamics that closely resemble those occurring during natural cognition. In doing so, longstanding issues relating to the ecological validity of cognitive testing can be addressed (Bronfenbrenner, 1977; Neisser, 1976).

Of modern brain imaging techniques, EEG and functional near infrared spectroscopy (fNIRS) are currently the only systems capable of fulfilling the portability requirements for mobile neuroimaging during movement. Wearable mobile fNIRS for instance, have proven to be capable of detecting task-related changes in haemoglobin in freely moving subjects during physical activity (Piper et al., 2014) as well as during fine precision walking (Koenraadt, Roelofsen, Duysens, & Keijsers, 2014). This is possible

because fNIRS does not require severely limiting subject motion; however, they have shallow depth sensitivity and rely on hemodynamic measurements. While the metabolic and hemodynamic responses in the brain occur over several seconds, the neural dynamics underlying natural cognition unfold at the millisecond to second time scale. EEG provides both high temporal resolution as well as employing sensors small enough to offer full head coverage without posing major restrictions on head and body movements (Makeig, 2009).

To this point, the methodology proposed by (Makeig et al., 2009) involves combining high-density EEG recordings with the monitoring of dynamic body movements and, optimally, eye-tracking. By doing so, it is possible to study the macroscopic brain dynamic patterns supporting behaviour in natural, 3D environments. As such, the experimental chapters in this thesis capitalize on combined wireless EEG and eye-tracking recordings to research face-sensitive brain responses in freely moving subjects.

1.2.1 Brief history of MoBI

The first successful recording of high quality EEG signals during steady motion was only performed in the past 10 years. Early studies employed force measuring treadmills to control the rate and velocity of walking and compare brain activity during stranding and walking at different speeds (Gramann et al., 2010). In most of these experiments, PC monitors raised to eye level were used to present stimuli as well as EEG amplifiers supported by overhanging mechanic arms to allow unobstructed locomotion (De Sanctis, Butler, Malcolm, & Foxe, 2014; Severens, Nienhuis, Desain, & Duysens, 2012). Assessing the effects of progressively increasing walking demands on cognitive performance these early studies effectively demonstrated that cognitive ERP experiments can be conducted while participants walk at different speeds with high levels of accuracy. Other investigations have opted to use small lightweight EEG systems with a reduced number of electrodes (i.e. the 14 channel Emotiv system as in

Aspinall, Mavros, Coyne, & Roe, 2013) to investigate cortical brain dynamics in exterior environments during steady walking (Debener, Minow, Emkes, Gandras, & de Vos, 2012). Their results demonstrate that a commercial, low-cost wireless EEG system could provide adequate quality EEG data in outdoor recording environments. However, to faithfully record the two most dominate electrocortical sources during walking and standing a minimum 35 channels has been proven necessary (Lau, Gwin, & Ferris, 2012). To demonstrate this, an auditory stimulus presentation task was used to assess single trial classification performance during simulated flight as well as during real piloting of an aircraft. The authors report a classification accuracy of single trial auditory events at statistical levels significantly higher than chance, has been shown in highly adverse scenarios with substantial vibration, winds, acoustic noise like flying a small airplane (Callan, Durantin, & Terzibas, 2015).

In recent years, the degree to which MoBI can be used in natural environments has been systematically tested by comparing differences in auditory brain responses during bicycle riding (Zink, Hunyadi, Huffel, & Vos, 2016) as well as real-world driving (Protzak & Gramann, 2018). The results from these studies have shown small effects of external noise on the signal-to-noise ratio in the EEG signals and extend the possibility of investigating cognitive functions in highly adverse environments like inside a moving an automobile. As such, the realm of testing possibilities for mobile EEG has opened substantively making it widely available as a method for measuring the brain mechanisms underlying embodied therapeutic approaches like dance (Barnstaple & Desouza, 2017) and art therapy (King, 2016).

The growing interest in the field of mobile neuroimaging could respond to the need for methodologies that allow naturally occurring brain processes to be examined. This has been reflected to some extent, in the incremental amount of scientific publications in the field. Since the publication of the seminal paper by Makeig and colleagues, roughly 200 papers have referenced it in succeeding works. In a 2018 mobile neuroimaging conference, 110 experiments using some form of MoBI were presented as posters (including the first experimental chapter in this thesis) and 60 oral presentations were given on a wide variety of related subjects (Gramann, 2018).

1.2.2 Mobile data recording and analysis problems

Due to the emerging nature of the field of mobile brain imaging there is yet to be any standardization of MoBI experimental proceedings. Nevertheless, multiple technical and theoretical issues have been identified.

Firstly, intrinsic to the measurement of brain activity using EEG is the presence of multiple sources of artifactual noise and, as such, different types of artifacts can be found in the raw EEG signal. Movement artifacts resulting from muscle contractions are unavoidably present in the mobile EEG recordings. These artifacts are known to originate in the head and neck becoming most prominent during head movement and stabilization of the head during motion (Gwin, Gramann, Makeig, & Ferris, 2010). Eye-movements artifacts including eye-blink and movement artifacts resulting from the rotation of the eye inside the ocular orbit (i.e. saccadic spike potentials) produce large artifacts in the EEG signal which tend to propagate throughout the scalp (Keren, Yuval-Greenberg, & Deouell, 2010).

In free-viewing conditions where no fixation cross is used to stabilize the position of the eyes previous to stimulation, these artifacts are enhanced due to visual scanning of the environment (Nikolaev, Meghanathan, & van Leeuwen, 2016). Additionally, electrode movement artifacts can occur when an EEG sensor shifts or lifts from the scalp resulting in a violent change in impedance. In mobile settings these artifacts are at times present do to electrode displacements resulting from locomotion as well as head movements during natural viewing. Similarly, cable-sway has been shown to be a strong contributor to motion artifacts and reductions in the signal to noise ratio in the EEG signal (Symeonidou, Nordin, Hairston, & Ferris, 2018); nevertheless these artifacts can be dealt with easily with by using Velcro straps to secure cable bundles. Following these procedures, only one study to date has demonstrated negligible effects of head motion on EEG signals during locomotion; however these measurements were taken during treadmill walking where no head rotations took place (Nathan & Contreras-Vidal, 2016).

Secondly, the co-registration of EEG and eye-tracking during free-viewing presents specific methodological challenges as well. These issues include the precise detection of gaze positions, the varying degrees of overlap between brain responses elicited by successive eye fixations as well as low-level, visual and motor influences on cortical activity (Dimigen, Sommer, Hohlfeld, Jacobs, & Kliegl, 2011). Multimodal data acquisition of data (i.e. eye-tracking, behavioural monitoring and brain imaging data) use parallel recording and multiple synchronized data streams which are often sampled at different rates and on different systems. Precisely synchronizing all data streams becomes imperative since the calculation of evoked brain responses requires precise time-locking. Within this context, the detection of a stimulus onset time during free viewing of natural scenes is an additional challenge which is yet to be fully resolved.

Besides these technical issues relating to the sensitivity of mobile EEG recordings, short-term challenges for MoBI research must also be highlighted. The extension of laboratory environments to real world settings implies a necessary trade-off; sacrificing experimental control to permit natural behaviour. Consequent issues relate to the behavioural and cognitive degrees of freedom within the MoBI paradigm, the amount of control over experimental variables, the ecological validity in the setup and interpretability of results (Parada, 2018). Along similar lines, Debener and colleagues have proposed developing a 'transparent MoBI' methodology that would measure neurophysiological dynamics along with eye movements, body topology and spatial location without interfering in the agent's evolutionarily determined degrees of freedom for interaction (Bleichner & Debener, 2017; Debener, 2018) however, there is currently no defined methodological standardization for MoBI research.

Finally, an issue relating to the management and structuring of MoBI data has been described (Parada, 2018). Multimodal data and specifically eye-tracking world video data is large (>10 Gb) and requires large amounts of computational power to process. Furthermore, containerizing MoBI data in a common format could help future replication studies as well as facilitate the development of a standardized MoBI analysis pipeline and allow sharing data between different groups.

1.2.3 Effects of walking and posture on brain responses

Due to the technical difficulties associate the assessment of cortical activity during bipedal standing and walking, only recently have EEG investigations have directly examined event related brain activity differences during locomotion.

The regulatory mechanisms of bipedal standing have previously been investigated using PET (Ouchi, Okada, Yoshikawa, Nobezawa, & Futatsubashi, 1999) as well as EEG (Bulea, Kilicarslan, Ozdemir, Paloski, & Contreras-Vidal, 2013) and a supraspinal network associated to postural control has been described. During visual stimulation, supine positions relative to standing postures activated the anterior cerebellar lobe as well as the right visual cortex (close to Brodmann area (BA) 18 and BA 19). Lifting one foot while standing increased the involvement of the cerebellar anterior vermis and the posterior lateral cortex ipsilateral to the weight-bearing foot and standing in tandem showed activations in visual association cortex as well as in the anterior and posterior vermis (Ouchi et al., 1999). These results align with other accounts of the cerebellar vermis being responsible for the modulation of gait during imagined standing and walking (Jahn et al., 2004; Sauvage, Jissendi, Seignan, Manto, & Habas, 2013) and suggest the visual system participates in regulating postural balance.

The effects of posture on brain activity and cognitive performance have been reviewed (Thibault & Raz, 2016). In broad terms, upright, relative to supine postures increases widespread oscillatory activity in high-frequency beta and gamma bands (Thibault, Lifshitz, Jones, & Raz, 2014). Beta activity has been found to be supressed during walking (Seeber, Scherer, Wagner, Solis-Escalante, & Müller-Putz, 2014) while occipital gamma power has shown the greatest and most consistent increases from prone to supine positions (Rice, Rorden, Little, & Parra, 2013). Furthermore, gamma oscillations differences have also been associated with specific stages of the gait cycle during walking. High and low gamma oscillations in central sensorimotor areas were increased in central sensorimotor areas and decreased in the left and right dorsolateral regions and during active walking and upright standing (Seeber, Scherer, Wagner, Solis-Escalante, & Müller-Putz, 2015).

Studies evaluating cortical activation patterns during walking have identified source generators of in anterior cingulate, posterior parietal and sensorimotor cortices (Gramann et al., 2010). Intra-stride changes in spectral power show that during the end of a stance (i.e. when the front stepping foot contacts the ground) alpha band power was enhanced in or near the sensorimotor and dorsal anterior cingulate cortex (Gramann et al., 2011). These power increases were more pronounced when the contralateral foot pushed off the ground, relative to when the ipsilateral foot did. In the anterior cingulate, posterior parietal and sensorimotor cortex, intra-stride high-gamma spectral power changes have also been identified (Gwin, Gramann, Makeig, & Ferris, 2011). In line with these results, decoding gait parameters from the EEG signals recorded during locomotion has been shown to be highly accurate during normal and precision treadmill walking (Presacco, Goodman, Forrester, & Contreras-Vidal, 2011).

Functional connectivity analysis on the effect of walking on sensorimotor networks in the brain has shown that standing generates enhanced connectivity between sensorimotor cortical areas relative to walking. This reduction in network connectivity during locomotion is alleged to result from differences in the attentional demands of standing relative to walking (Lau, Gwin, & Ferris, 2014).

To examine event-related brain activity during walking MoBI approaches have often used classic visual tasks during treadmill walking by presenting stimuli on a computer monitor (Gwin et al., 2011). Gramann et al., (2010) demonstrated that visual evoked responses were detectable during slow (0.8 m/s) and fast walking (1.9 m/s) as well as when standing still. Furthermore, visual evoked responses showed no modulatory effects resulting from walking speeds of maintaining a stable stance. Similarly, no task performance changes between sitting and walking were reported by De Sanctis et al., (2014) during a Go/NoGo task using emotional images. Amplitude, latency and topography differences in the N200 and P300 components of the EEG data were associated with differences in inhibitory control between the sitting and walking condition during dual-task situations. To date however, face-specific brain activity is yet to be examined during natural behaviour or while standing. Furthermore, differences in

face-related brain activity resulting from postural variations or during social interactions have not been investigated either.

1.3 Brain processing of human faces

Faces are highly important to human beings. Unlike other stimuli found in the real world, faces transmit copious amounts of information regarding identity, gender, age, ethnicity and emotion, amongst others. As a result, faces attract our attention more rapidly relative to objects (Ro, Friggel, & Lavie, 2007) and are easily detected in poor viewing conditions (Burton, Wilson, Cowan, & Bruce, 1999) or during complex visual searches (Eng, Chen, & Jiang, 2005). Due to the significance of faces for human perception, it is not surprising that face processing has been one of the most widely researched fields in visual cognitive processing. Given the perceptual stability in the processing of face stimuli as well as the consistent findings in the experimental literature; faces represent a viable candidate for scientific research in natural contexts.

1.3.1 History of face processing research

The notion of a specialized brain mechanisms involved in processing faces stems from early clinical research investigating face blindness or prosopagnosia (Damasio, Damasio, & Van Hoesen, 1982; Florence & Ellis, 1990). Early patient studies indicated that bilateral lesions in the temporal lobes as well as lesions exclusively in the right temporal lobe resulted in selective face memory impairments (Petrides & Milner, 1982). In line with these initial findings, preliminary electrophysiological studies using face stimuli processing presented a preferred right side distribution in electrocortical response to face images compared to pictures of objects (Small, 1983).

The first report of a face specific electrocortical component in the brain described a vertex positive potential (VPP) component as a medial positive deflection at electrode position Cz with a latency of approximately 150 ms post stimulus onset (Jeffreys, 1989). The component amplitude proved considerably reduced or absent when

non-face stimuli were presented (Bötzel & Grüsser, 1989) or showed shorter peak latencies in response to face stimuli (Jeffreys, 1989; Jeffreys & Tukmachi, 1992; Aled Jeffreys, 1996; Jeffreys, 1993). Shortly after, the first systematic investigation into the electrophysiological underpinnings of human face processing was presented by Bentin, Allison, Puce, Perez, & McCarthy, (1996). The authors revealed the existence of a negative face-specific EEG component appearing at 172 ms over the occipital temporal portions on the scalp was show to be apparent when faces were viewed, but not objects like cars and houses the N170. Additionally, the authors established highly relevant methodological considerations like the effect of reference electrode on N170 amplitude. During the late 1990's and early 2000s, EEG and MEG research was used to investigate cortical responses to faces.

These studies mostly confirmed previous event related potential (ERP) findings as well as describing the bilateral sources of the M170 (Linkenkaer-Hansen et al., 1998; Liu, Higuchi, Marantz, & Kanwisher, 2000). MEG presents an advantage relative to EEG in terms of spatial resolution as well as being sensitive to activations generated in cortical sulci (Hämäläinen, Hari, Ilmoniemi, Knuutila, & Lounasmaa, 1993). Functional magnetic resonance imaging (fMRI) investigations unveiled a portion of the human fusiform gyrus devoted to face-specific processing (McCarthy, Puce, Gore, & Allison, 1996). Moreover, an isolated medial section of the fusiform gyrus, the fusiform face area (FFA), was associated to the processing of face images relative to images of houses (Kanwisher & Yovel, 2006). With the advent of advanced source estimation techniques the neural generators of the N170 were investigated using combined MEG/EEG methods (Deffke et al., 2007; Hoshiyama, Kakigi, Watanabe, Miki, & Takeshima, 2003; Pizzagalli et al., 2002). In these investigations, the fusiform face area was also proposed as the neural generator of the N170 component in agreement previous fMRI results. Further, they established the possibility of accurately estimating source generators from face-specific EEG signals recorded from the scalp.

1.3.2 Electrophysiology of face perception

The study of face processing including its neural basis as well as cognitive mechanisms is a highly active research field (reviewed in Calder, Rhodes, Johnson, & Haxby, 2011). Evidence of face-specific brain activity has been primarily obtained from electrophysiological studies using intracranial recordings (e.g., Allison, Puce, Spencer, & McCarthy, 1999), as well as ERP findings suggesting the existence of face-selective cortical processing mechanisms. Multiple components have been established in association with the processing of human faces namely, the N170/VPP complex as well as the P100 and M100 component and a specialized system supporting face processing has been described.

1.3.2.1 The N170

Numerous studies have shown the N170 component presents enhanced amplitudes between 130 – 200 ms in response to faces relative to non-face images like houses, or cars (Bentin et al., 1996; Bentin & Deouell, 2000; Eimer, 2000; Itier & Taylor, 2004). Bentin et al. (1996) described the N170 component response using a target identification task where pictures of faces and other objects (i.e. cars, insects and plants) where presented successively.

The N170 has been described as a negative going waveform that shows a maximal peak at latencies surrounding 170 ms post stimulus onset and appears over bilateral occipito-temporal portions of the scalp (Eimer, 2011). The strongest waveforms are typically found over the right hemisphere, at electrode locations P8 and PO8 (Hinojosa, Mercado, & Carretié, 2015) (Figure 1.3.2.1).

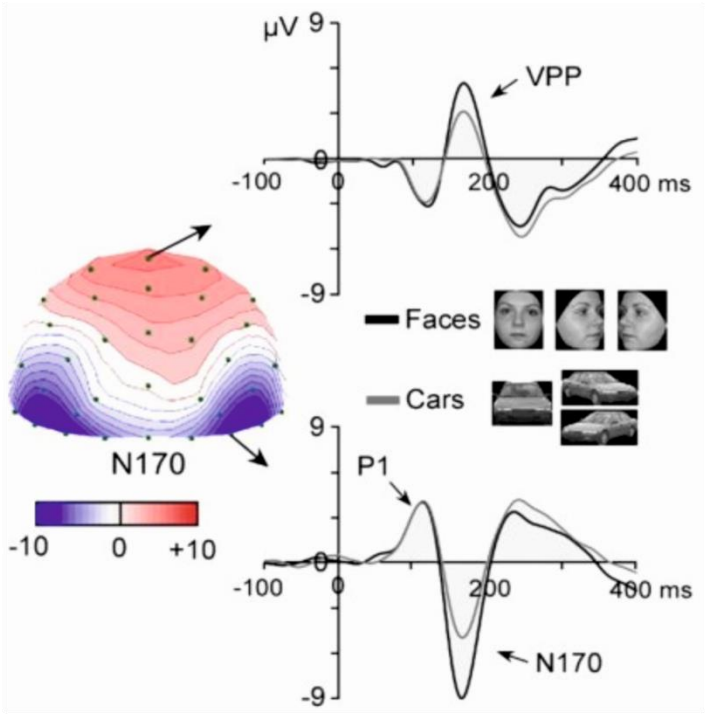

Figure 1.3.2.1: P100, N170 and VPP ERP component. The N170 is a negative component recorded from posterior lateral electrode sites following the presentation of faces and object stimuli from various categories (e.g. pictures of cars). It is most prominent at the lowest occipito-temporal electrode sites, usually maximal on right side channels P8 or PO8. The component is larger in response to faces than objects in both hemispheres, with usually a larger response in the right hemisphere. The N170 is associated with a temporally coincident positivity on the vertex (CZ), the vertex positive potential (VPP), which shows identical response properties and largely reflect the projection of the occipito-temporal dipolar sources to the vertex. Figure taken from Rossion and Jacques (2008).

Due to the N170 component's sensitivity to faces, it has been widely researched as an ERP marker for face perception in the past. As such, the specificity of the N170 to face images has since been consistently replicated in other EEG studies as well as using combined EEG and fMRI studies (Nguyen & Cunnington, 2014) as well as combined MEG research (M170) (Halgren, Raij, Marinkovic, Jousmäki, & Hari, 2000). To explore the functional significance of the N170 in the processing of faces, the effects of emotional expression have been investigated in the past (Ashley, Vuilleumier, & Swick, 2004; Mühlberger et al., 2009). The results from studies that have compared effects on the N170 in response to emotional and neutral facial expressions have shown considerable inconsistencies in their results. Early studies failing to report any effect of

facial expression on the N170 (Eimer, Holmes, & McGlone, 2003; Herrmann et al., 2002) interpreted their findings as the neural correlate of purely structural encoding of faces (Eimer & Holmes, 2002; Eimer, Kiss, & Holmes, 2008). A recent meta-analysis reported reliable emotional modulations on the N170 component amplitude (Hinojosa et al., 2015). This investigation included 57 studies examining emotional effects on the N170 component and confirmed that emotional faces result in enhanced N170 amplitudes for emotional expressions (i.e. happy, afraid and angry) relative to neutral ones. Furthermore, affective congruency between a facial expression and different sources of contextual affective information, like body posture or emotional scenes may also modulate the N170 (Hietanen & Astikainen, 2013; Righart & de Gelder, 2008 for a review see Wieser & Brosch, 2012). Interestingly, these emotional modulation effects on the N170 amplitude are reduced in some clinical patients including children with autism (McPartland, Dawson, Webb, Panagiotides, & Carver, 2004) and schizophrenic patients (Salvatore Campanella, Montedoro, Streel, Verbanck, & Rosier, 2006). In patients presenting severe prosopagnosia, for instance, the N170 component is strongly reduced or completely absent at times (Eimer & McCarthy, 1999). The reduction or absence of this component in certain clinical conditions suggests that impairments in face recognition are at least, partially caused by deficits prior to face identification, in the structural coding stage of face perception.

The encoding of identity in the N170 component amplitude has also shown mixed results. Bentin & Deouell, (2000) have shown similar responses to famous and unknown faces. The amplitude of the N170 in response to personally familiar faces as well as famous ones has however, shown to be modulated by the emotional content of faces (Kaufmann & Schweinberger, 2004; Lander & Metcalfe, 2007). Aligning with these results, overlapping neural activity during identification of emotion and identity has been demonstrated using emotional face recognition tasks (Ganel, Valyear, Goshen-Gottstein, & Goodale, 2005; LaBar, Crupain, Voyvodic, & McCarthy, 2003). Furthermore, face priming effects have shown to affect ERP amplitudes at latencies of 250 – 300 ms, but not within the N170 time-window (Schweinberger, Pickering, Jentzsch, Burton, & Kaufmann, 2002) alluding that identity is determined at earlier latencies.

Several studies have found that inversion effects severely hamper face recognition comparatively to other object images with discrimination accuracy approaching chance level in some cases (Freire, Lee, & Symons, 2000). Other studies have shown delayed recognition times and accuracy for inverted faces (Rossion et al., 1999). Face inversions show significantly delayed peaks in the N170 component as well as frequently increasing the amplitude of the component (Linkenkaer-Hansen et al., 1998; Rossion, Curran, & Gauthier, 2002).

Within the N170 latency, a VPP presenting at zenith scalp locations characteristically coincides with the N170. The VPP was the initially associated to face specific brain activity, currently however, it is well established that the VPP represents the positive side of the same dipole accounting for the N170 component (Joyce & Rossion, 2005).

Some ERP studies have recently showed the N170 component specificity effect could be abolished when controlling the interstimulus perceptual variance in the stimuli (Thierry, Martin, Downing, & Pegna, 2007) or interference is introduced (Gauthier, Curran, Curby, & Collins, 2003). Rossion & Jacques, (2008) argue however, that the methodological flaws in experimental design, like Thierry et al. studies measuring the N170 from different electrode sites (i.e. O2) and selection of the reference electrode is the underlying cause of this effect.

1.3.2.2 The P100

The P100 has received substantially less attention within the face processing literature relative to later components (i.e. the N170 and VPP). Investigations demonstrating face specific effects on the P100 component are scarce (Herrmann, Ehlis, Ellgring, & Fallgatter, 2005; Liu, Harris, & Kanwisher, 2002). Linkenkaer-Hansen et al., (1998) for example, described the P100 as an occipital positivity occurring between 80 ms - 120 ms that presents delayed latencies for degraded images of faces. The authors interpret their results alluded to ‘some degree’ of face specific processing

occurring at latencies approximating 120 ms. Most reports however, show bilateral occipital positive components within the latency interval between 80 ms – 120 ms that are indiscriminate to faces or objects (Linkenkaer-Hansen et al., 1998; Rossion, Joyce, Cottrell, & Tarr, 2003). The P100 component has more consistently been associated with all categories of stimuli, including faces and houses as well as flowers and other everyday objects like tools. Some investigations have presented results showing enhanced P100 amplitudes for faces; particularly to inverted images of faces (Itier & Taylor, 2004a), however these effects are likely to results from low-level visual differences (i.e. colour, luminescence, size and position) as proposed by (Halgren et al., 2000). These findings have led to a relative consensus favouring an interpretation of the P100 component as encoding low-level, structural physical characteristics of the stimulus (Goffaux, Gauthier, & Rossion, 2003; Liu et al., 2000; Rossion & Caharel, 2011). Nevertheless, within the P100 latency, MEG results have demonstrated M100 face-selective responses (Liu et al., 2002) involved in the categorization of the stimulus as a face relative to other non-face images.

1.3.2.3 The lambda potential

When occipital EEG signals are averaged on the basis of an eye movement (i.e. a fixation or a saccade), an ERP complex can be obtained which has been referred to as the lambda complex (Yagi, 1979a). Given that MoBI methodologies are proposed to use synchronized EEG and eye-tracking recordings, the lambda component should be considered. The lambda potential becomes increasingly relevant in MoBI research in natural settings where no stimulus presentation screens are used. The lambda component in the context of MoBI methods incorporating eye-tracking is highly relevant. It represents a powerful early ERP component and can be positive indicator that EMRP are correctly synchronized, as well as evidencing any differences in the low-level physical properties across experimental.

The main positive peak within the cortical potential complex has previously been time-locked to either the onset of an eye-movement or the offset of a saccade (Yagi,

1979b, 1981a) and peaks at latencies latency that fall within the broad latency of the P1 component (i.e. 70 ms to 120 ms). It should be noted that the lambda component can be calculated relative to the onset of offset of a saccadic eye movement. However, the lambda potential is been shown to be associated to the offset of saccades rather than the onset (Yagi, 1981a). Further, time-locking to the offset of a saccade (i.e. the onset of an eye fixation) represents an advantage for mobile EEG by minimizing the contributions of eye-movement related artifacts to the averaged waveform.

In the frequency domain, the lambda activity is pronounced in the high-theta and alpha bands (6–14 Hz) (Dimigen, Valsecchi, Sommer, & Kliegl, 2009; Ossandón, Helo, Montefusco-Siegmund, & Maldonado, 2010). There is common agreement that the positive wave at 100 ms proceeding saccade offset is a response of the visual cortex to changes in the image projected to the retina as a result of a saccade (Dimigen et al., 2009; Kazai & Yagi, 2003). The lambda potential during scanning of well illuminated contrast patterns disappears, as it does with closed eyes, in darkness, during steady fixations, or if the visual field is featureless (Evans, 1953; Lesèvre & Rémond, 1973; Rémond, & Lesèvre, 1956; Roth, 1953). The component can therefore be described as an early cortical response to retinal stimulation (Barlow & Cigánek, 1969) that can be modulated by saccade size as well as differences in low-level features like luminescence and contrast.

Relative to the P100 component in laboratory settings, the lambda component has been scarcely researched in the past, ostensibly due to the technical difficulties associated to time-locking brain responses to eye movements (Nikolaev et al., 2016). A direct comparison of the two however, showed a shared neural generator in the calcarine fissure (Kazai & Yagi, 2003). Nevertheless, Kaunitz et al., (2014) combined EEG and eye-tracking to examine brain activity during a free viewing task including faces. These authors showed classical lambda waveforms as well as face specific brain potentials resulting from naturalistic face viewing in laboratory settings.

As such, the characteristics of the lambda component can be informative for real-world MoBI results of the low-level characteristics of visual stimuli which are difficult to assess during free viewing of a three dimensional environment.

1.3.3 Neural systems supporting human face processing

The development of functional brain imaging measures has extended the scope of non-invasive EEG and MEG techniques. Early fMRI and PET research into human face processing associate multiple brain regions involved in the processing of faces (Haxby et al., 1994; Kanwisher, McDermott, & Chun, 1997; Sergent & Signoret, 1992). A core neural system for human face processing consisting of three distinct regions in occipitotemporal visual extrastriate cortex (Haxby, Hoffman, Gobbini, & Gobbini, 2000) including the inferior occipital gyri or occipital face area (OFA), the lateral fusiform gyrus or fusiform face area (FFA), the posterior portions of the superior temporal sulcus (STS) (Figure 1.3.3).

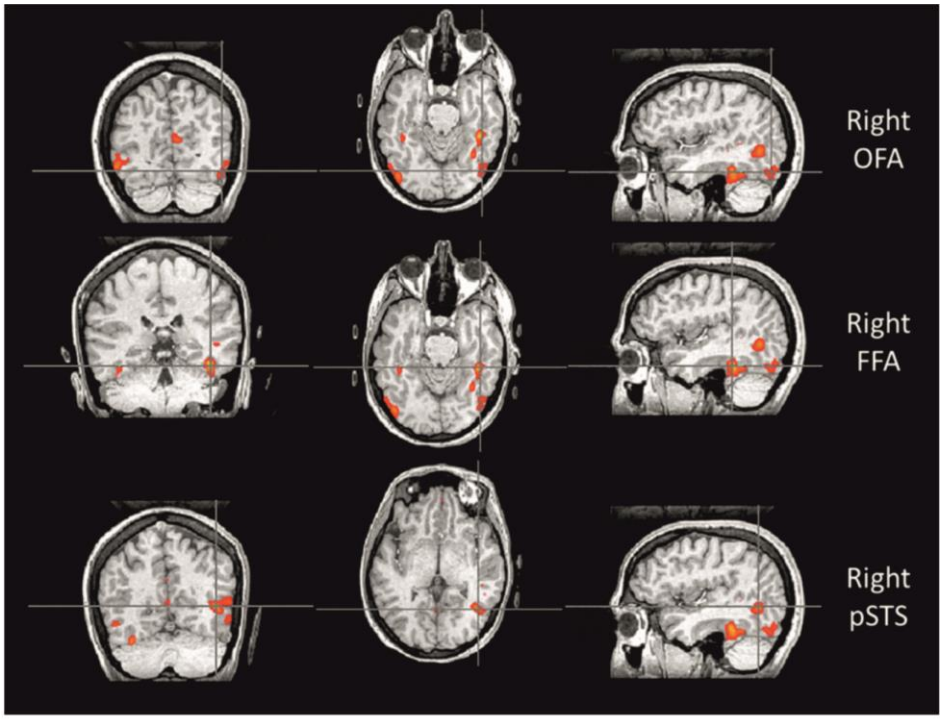

Figure 1.3.3. Neural systems supporting face processing. Three core face-selective regions in the occipitotemporal cortex. The right OFA, right FFA, and the face- selective region in the right posterior STS. The region of interest (ROI) in each row is identified using a contrast of faces greater than objects. Coronal, horizontal and sagittal slices are presented. Reproduced from Pitcher, Walsh, & Duchaine, (2011).

A highly persistent effect is that images of faces evoke larger activity in the fusiform face area than objects or places. This lateral region of the fusiform gyrus which is often reported bilaterally, but has also been consistently found isolated to the right side of the brain in some subjects (Kanwisher et al., 1997; Yovel & Kanwisher, 2004). These authors described the FFA as a sub-portion of the lateral fusiform gyrus which activates preferentially to images of faces, but not objects. Later findings presented by Calder et al. (2011) have contributed evidence of FFA activations to various aspects of face related information processing including structural encoding, recognition of identity, and processing of social cues. Aligning with this idea, lesions to this area have resulted in patients presenting face recognition impairments with prosopagnosia being more sever in bilateral lesion patients (Barton, 2008).

The OFA has similarly been functionally defined as a face-selective area located on the lateral wall of the occipital lobe broadly demarcated to Brodmann areas 18 and 19 (reviewed in Pitcher, Walsh, & Duchaine, 2011). The lateral occipital lobe, which includes the OFA, receives projections from early visual cortex prior to further analysis in higher cortical regions (Grill-Spector et al., 1998; Kourtzi, Tolias, Altmann, Augath, & Logothetis, 2003; Rotshtein, Henson, Treves, Driver, & Dolan, 2005) and has been associated with processing motion as well as bodies (Downing, Jiang, Shuman, & Kanwisher, 2001). One lesion study reported damage to the occipital cortex and the medial occipito-parietal region resulted in face and objects recognition impairments regardless of the intact functioning of the FFA (Steeves et al., 2006). As such, the OFA could be conceptualized to be between early visual cortex and the FFA in visual cortical hierarchy. fMRI research has shown enhanced OFA activation for faces relative to scrambled images and letters (Gauthier, Skudlarski, Gore, & Anderson, 2000; Puce, Allison, Asgari, Gore, & McCarthy, 1996) and has also been involved in the discrimination of familiar from novel faces (Dubois et al., 1999). These results suggest that the OFA and FFA are both necessary to correctly interpret faces. Itier & Taylor, (2004) reported the neural sources of the N170 for upright and inverted faces show no difference in their location, but show stronger source intensity on the STS for inverted faces. These authors interpreted this enhancement of the N170 amplitude as a result of stronger response in the STS rather than the involvement of additional brain regions.

Similar results have reported that the N170 amplitudes elicited by upright faces were strongly associated with BOLD responses in the FFA and STS, while activation in the OFA was correlated with the earlier P100 component, representing early visual processing at 100 ms post-stimulus (Horovitz, Rossion, Skudlarski, & Gore, 2004; Sadeh, Podlipsky, Zhdanov, & Yovel, 2010).

Several models of face perception have arisen from the evidence gathered from neuroimaging research. The most recognized models include a two-staged model (Bruce & Young, 1986), a core and extended systems model (Haxby, Hoffman, & Gobbini, 2000) as well as a modular approach (Kanwisher & Yovel, 2006) to describe the mechanisms commanding face recognition. The model proposed by Bruce and Young centres on the existence of parallel but functionally independent processing routes for different face features like identity and emotional expressions (reviewed in Atkinson & Adolphs, (2011) and in Posamentier & Abdi, (2003). This notion was extended in another influential model proposed by Haxby et al., (2000). Their model challenged the more modular view of face and object processing and proposed that faces are coded as a distributed profile of brain responses across the ventral visual pathway (Haxby et al., 2001) with distinct activation patterns in ventral temporal cortex for faces and objects (Bentin et al., 1996; Haxby et al., 2000; Haxby et al., 2001; Ishai, Ungerleider, Martin, Schouten, & Haxby, 1999; Kanwisher et al., 1997). Haxby and colleagues proposed a core system consisting of three regions in the occipitotemporal visual extrastriate cortex to detect a face as such, and an extended system of brain regions shared with neural systems for other cognitive functions resolving facial identity, biographic information and emotional expressions, amongst others. The structural encoding phase of face processing has been linked to computations occurring in the OFA and more abstract, identity-based encoding would occur in the FFA (Rotshtein et al., 2005)

Chapter 2

General Methods

2.1 Eye-tracking

Historically, attempts to describe eye-movements date back to the late 18th century (Wells, 1792) and 19th century (Javal, 1878; Lamare, 1892), however it was only in the late 1980's that small sized computers became powerful enough to enable real-time processing of gaze data. Head-mounted eye-trackers have only come into play since the mid 2000's and while early versions were slow, obtrusive and bulky; newer systems provide comfort and ease of use at higher sampling rates (Kassner, Patera, & Bulling, 2014).

2.1.1 Principles of eye tracking

Eye-tracking is the process of measuring ocular fixation points or, alternatively, assessing the motion of the ocular globe relative to the head during viewing. The aim of this procedure is to record, with high levels of accuracy and temporal resolution, where the user is looking at (i.e. gaze position). In most cases, the estimation of the gaze position implies the identification of an object or area where the gaze is directed towards at any point in time. In recent years there has been a steady increase in the use of commercially available eye trackers including head-mounted eye trackers (e.g., Pupil Labs, Tobii Glasses, SMI Glasses, Dikablis Glasses) in multiple domains including medicine, psychology, cognitive science, marketing research and autonomous driving.

In the experimental chapters of this thesis, a binocular Pupil Labs eye tracker was used to register eye-tracking data. The Pupil Labs eye tracker is a head-mounted system integrated into an open-source platform that allows for the modification of the wearable hardware as well as the source code, depending on the necessities of the user. This wearable eye tracker is an affordable, lightweight solution for mobile eye-tracking

during movement and natural viewing (Figure 2.1.1). The eye-tracking system primarily consists of infrared (IR) cameras that synchronously record eye movements with a world camera recording the subject's field of view. Pupil-Labs eye trackers use USB interfacing digital cameras that comply with the USB video class standard, making them highly adaptable to multiple research domains. The light-weight IR and world view cameras (> 50 gm) reduce visual obstruction and increase the comfort of the system. The world view camera resolution can be adjusted between 1020 × 1080 pixels sampling at 30 Hz to 640 × 480 pixels sampling at 120Hz (Kassner et al., 2014).

The eye cameras use an IR LED at 860 nm wavelength to illuminate the eye with a resolution that ranges between 200 × 200 pixels at 200 Hz to 400 × 400 pixels sampling at a rate of 120 Hz. Earlier versions of the system however, provided a 30 Hz to 120 Hz sampling rate with varying resolutions ranging between 200 × 200 pixels to 1080 × 1080 pixels.

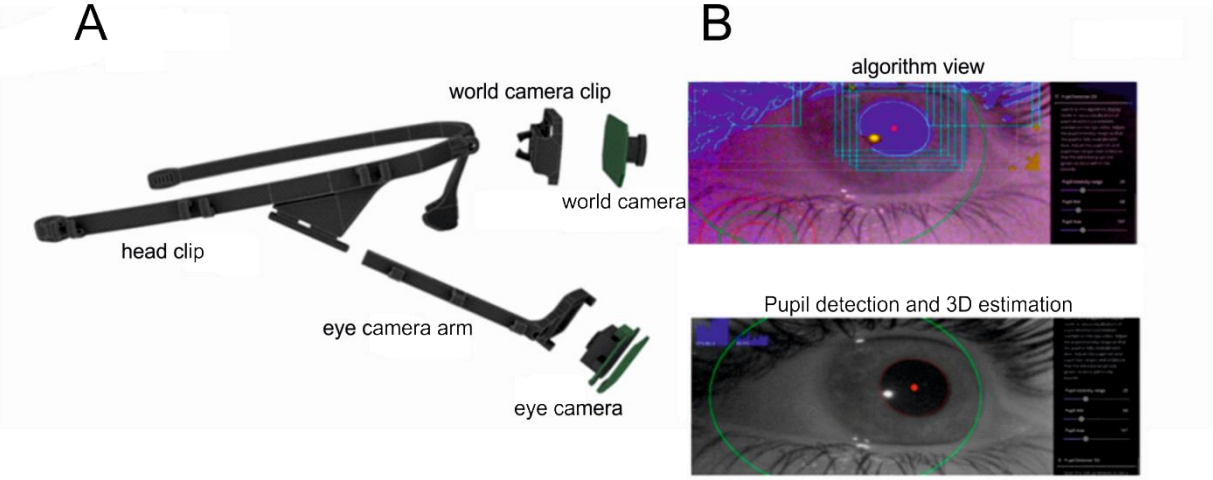

Figure 2.**1.1**. Pupil Head Set and software. A. Detailed hardware setup of the Pupil Labs eye tracker. B. Visualization of the Swirski algorithm (top) and the detection of the pupil and 3D estimation of the ocular globe (bottom). Taken form Filippucci et al., (2017).

2.1.2 Pupil detection

Multiple methods have been proposed to detect the position of the pupil in the ocular globe. These methods include cumulative distribution function algorithms (Asadifard & Shanbezadeh, 2010), projection function algorithms (Zhou & Geng, 2004)

and iris shape template matching (Boles & Boashash, 1998), amongst others. Accurately detecting the position and shape of the pupil is crucial for gaze tracking, specifically in real world environments where the distance between the subjects and the point of gaze changes continuously and eye movements are unrestricted.

The Pupil Labs eye tracker uses infrared oculography (Kumar & Krol, 1992) in combination with advanced computational algorithms (Canny, 1986) to find the contours of the pupil in the image and filters edges. In the first stage, the eye image is converted to a black and white and the initial region estimation is based on the strongest response in a centre surround feature as proposed in Świrski, Bulling, & Dodgson, (2012). A Canny algorithm is then used to detect edges based on neighbouring pixel intensity. The defined contours are then simplified using the Ramer–Douglas–Peucker algorithm (Douglas & Peucker, 1973) and filtered and split into sub-contours based on criteria of curvature continuity. All the possible pupil ellipses are found by applying an ellipse fitting procedure onto a subset of the contours that had been previously defined with a goodness-of-fit in a least squares sense. An augmented combinatorial search defines contours that can be added in support of candidate ellipses is then applied. The results are evaluated based on the fit of the ellipse and the ratio between edge length and ellipse circumference. If the ratio exceeds the threshold value, the Canny algorithm is used to refine the ellipse fit and define the pupil position (Figure 2.1.1B). The effectiveness of the Pupil Lab eye-tracking system has been compared to other benchmark systems (Fuhl, Tonsen, Bulling, & Kasneci, 2016).

2.1.3 Eye movements

Figure 2.1.3A shows the ocular globe of the human eye and the six main muscles that support it. These include two pairs of direct muscles (i.e. superior and inferior rectus muscles) as well as a pair of superior and inferior oblique muscles (Singh & Singh, 2012). The rotations of the eye result from the contraction of these muscles allowing movements in six degrees of freedom (Figure 2.1.3B). Eye movements primarily include stabilizing movements that hold the eye in place as well as saccadic

movements that move the eye around the visual field and bring the gaze to objects of interest.

Stabilizing eye movements are intended to maintain the image projected stably onto the retina and include fixations and smooth pursuits (i.e. visual tracking of a slowly moving target). Saccadic eye movements include saccades and vergence movements. The later of the two comprise inward and outward rotations of the eye involved in binocular vision. In order to focus on near targets, the eyes rotate inwards and in the opposite direction when targets are farther away in the visual field (Usakli & Gurkan, 2010).

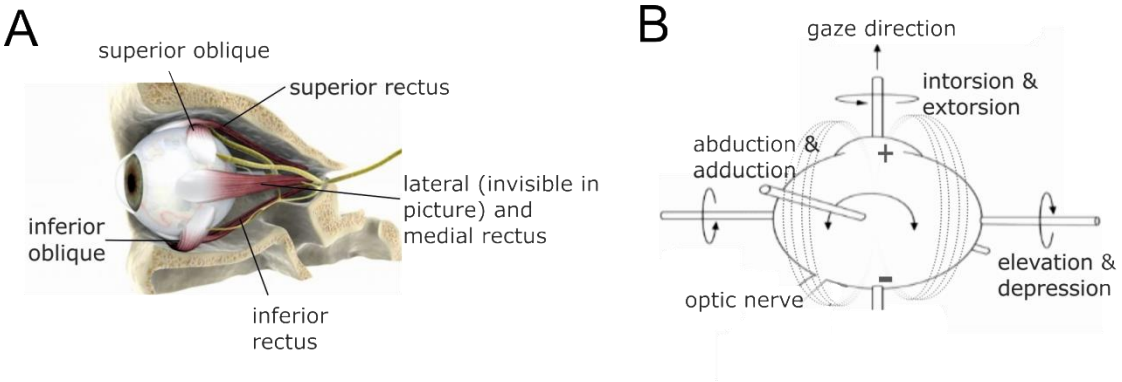

Figure 2.1.3. Eye movements. A. Main muscles involved in the movement of the eye including the superior and inferior oblique muscles, the superior and inferior rectus as well as the medial rectus. The lateral rectus cannot be seen from this angle. B. Six degrees of freedom of eye movements. Black arrows show the direction of rotations on three axes. The grey dotted lines show the flow of micro-currents from the positive to the negative pole. Adapted from Singh, H., & Singh, J. (2012)

2.1.4 Gaze tracking

Most video-based gaze tracking systems are essentially comprised of one or more digital and infrared cameras. The required eye parameters for gaze tracking include the pupil centre, the centre of curvature of the cornea as well as the optical and visual axes (described in Guestrin & Eizenman, 2006). The fovea is the portion of the retina with the highest visual sensitivity in the back of the eye. The visual axis is described as the imaginary line joining the fovea with the centre of the corneal

curvature. The visual axis defines the direction of the gaze however; it deviates slightly from the optical axis. This small deviation, which easily be accounted for, is known as the kappa angle and is normally no more than 5 degrees (Zhu & Ji, 2004). Gaze locations can be overlaid onto the scene space recorded in the world view camera and can be used determine the duration and frequency as well as the onset of the gaze a specific visual feature. The gaze point can be mapped to the worldview scene based on the calibration routine and the centre of the pupil. To map the pupil positions onto the scene space viewed by the participant, the Pupil Labs system implements a transfer function consisting of two bivariate polynomials of adjustable degree. The initial parameters for this are obtained by running a calibration routine using manual markers, an on-screen calibration protocol or using natural environmental features (Kassner et al., 2014).

In the experimental chapters of this thesis, manual markers were always used to perform calibration routines. This allowed the eye tracker to the calibrated at comparable viewing distances to the ones in the experimental sessions (i.e. approximately 1 m to 1.5 m) as well as to ensure adequate calibrations in the far corners of the visual field.

2.1.5 Eye-tracking in freely moving individuals

To undertake mobile imaging research head-mounted eye-tracking systems need be used. Unlike traditional eye-trackers, positioned in front of the participant who is viewing a screen, wearable head-mounted eye-trackers come in the form of eye-glasses. It has been shown that eye gaze can be calculated with high accuracy under normal head movement with minimal personal calibrations (Zhu & Ji, 2007).

Nevertheless, multiple studies have previously reported difficulties when eye-trackers are used in natural environments like driving (Braunagel, Kasneci, Stolzmann, & Rosenstiel, 2015; Liu, Xu, & Fujimura, 2002), while using a laptop computer (Zhang, Sugano, Fritz, Bulling, & Planck, 2015) as well as during shopping (Kasneci et al.,

2014). The main sources of error in mobile eye-tracking mainly relate to problems in the detection of the pupil in natural environments. These issues have been detailed by Schnipke & Todd, (2000) and include changes in illumination, motion blur, eyelashes covering the pupil and recording errors. Furthermore, differences in individual eye physiology as well as contact lenses and the use of make-up (i.e. mascara) have also been shown to be relevant sources of noise for mobile eye-tracking systems (Fuhl et al., 2016).

The accurate and robust detection of the pupil position is a key element for all wearable eye trackers used in natural environments. As such, it is central for MoBI research using eye-tracking to determine visual onset times must strive to achieve continuous data streams in the eye-tracking recordings performed in the mobile settings.

2.1.6 Triggering EEG data in MoBI

In the experimental chapters that follow the detection of stimulus onset times was done by visual inspection of the real-world video streams with the superimposed gaze positions. All recorded frames from the worldview camera contained an accurate timestamp based on the internal PC processor clock of the recording system. Eye-tracking videos were visually inspected, and the stimuli onset times were tabulated on a picture by picture basis. The tabulation of stimulus onset times was performed by observing gaze positions throughout all recordings and manually annotating the video frame corresponding to onset. The stimulus onset was defined as the first identifiable moment a gaze position touched or landed on a stimulus image. If the first instance of touch could not be defined in the eye-tracking data, the succeeding trial was discarded from analysis. The real times corresponding to the tabulated frames were then used to import the stimulus onset latencies onto the raw EEG data. Due to higher sampling rates in the IR eye cameras relative to the world view camera, often multiple data points were registered to one worldview frame. In these cases, the middle sample was used to determine the onset latency of the event marker.

2.2 *Electroencephalography*

Richard Caton (1842–1926) was a medical lecturer at the University of Liverpool and was the first to report that "feeble currents of varying direction pass through the multiplier when the electrodes are placed on two points of the external surface of the brain" (Caton, 1875). Although his demise came 3 years earlier to the invention of the electroencephalogram (Berger, 1929), his initial observation marked the birth of the EEG measurements from cortical surfaces of the brain; forever changing our approach to the study of brain physiology, as well as the understanding of cerebral functioning.

2.2.1 Physiological basis of the EEG signal

When sensory stimulation exceeds threshold level neurons fire. This unleashes a cavalcade of brain activity which ultimately leads to perception as well as higher cognitive functions. Neuronal ensembles are made up of hundreds of thousands of neurons which are involved in similar processes or neural computations (Sherrington, 1909). These groups of neurons rely on a biochemical mechanism, referred to as an action potential, to communicate. An action potential is a discreet change in voltage generated in the soma of a neuron that travels across the axon to the terminal buttons in the dendrites. The biochemical mechanism driving an action potential is extremely fast and causes ion channels to open and close producing a small potential field (Rowan & Tolunsky, 2003). An action potential travels along the axon fibre towards excitatory or inhibitory synapse. A post-synaptic potential is generated when neurotransmitters bind with a postsynaptic cell membrane of a neighbouring neuron. These post-synaptic action potentials, also referred to as extracellular field potentials (Speckmann, 1979), are significantly longer (50-200 ms) and have a greater field (Rowan & Tolunsky, 2003). Due to the macroscopic orientation of dendrites thousands of field potentials can occur in a similar location during a coherent response (Fisch, 1999). The summated local field potentials can be measured as a voltage difference on the scalp using non-invasive EEG sensors (Niedermeyer & da Silva, 2005; Nunez & Silberstein, 2000).

EEG electrodes are highly sensitive to current variations; the volume conduction problem relates to the spreading of EEG signals from multiple sources in the brain to all electrodes on the scalp. This problem can be defined as the propagation of currents from the primary electrocortical source through biological tissue and skull towards the measuring electrodes. As such, voltage differences detected at scalp electrodes relate to the location, size and the orientation of the dipole resulting from the cortical activation. This is influenced by brain conductivity and the resistance of the brain, as well as cerebral spinal fluid, skull thickness and skin tissue. To resolve this, specialized algorithms are continuously being developed to reduce the impact volume conduction on EEG signals (e.g. the three sphere model proposed by Geddes & Baker, 1967).

2.2.2 Mobile EEG signal acquisition and pre-processing

EEG uses small sensors to measures subtle fluctuations local electrical field potentials in the cortex of the brain over time (Kamp, Pfurtscheller, Edlinger, & da Silva, 2005). Electrodes are typically placed on the scalp of the head by means of specifically designed electrode caps. The distribution of the electrodes over the scalp of the head is in correspondence to a contemporary derivate of the Standardised International 10-20 system which is based on relative distances to measurements of recognized anatomical landmarks on the skull (Jasper, 1958; Klem, Lüders, Jasper, & Elger, 1999). The standardization of electrode locations on the scalp is crucial for consistent interpretation of results across experimental studies.

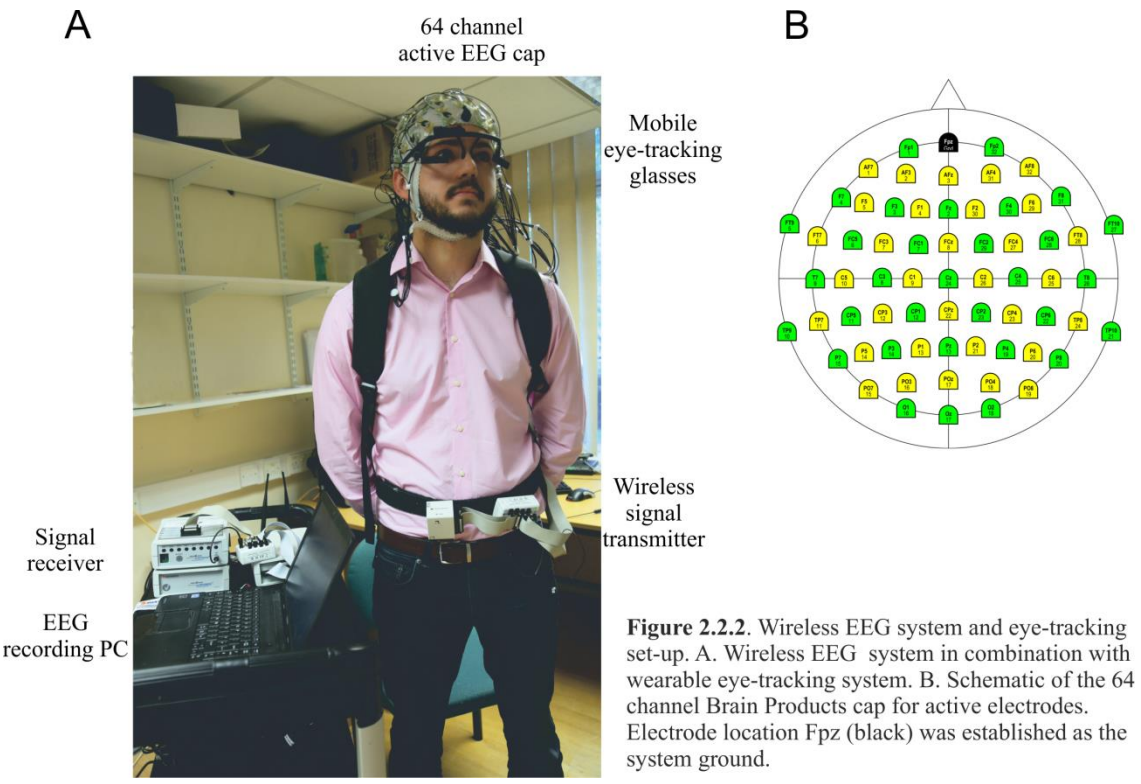

Figure 2.2.2. Wireless EEG system and eye-tracking set-up. A. Wireless EEG system in combination with wearable eye-tracking system. B. Schematic of the 64 channel Brain Products cap for active electrodes. Electrode location Fpz (black) was established as the system ground.

To maintain a stable connection conductive electrolyte gel is applied to individual electrodes to improve electrical conduction (Rowan & Tolunsky, 2003) as well as lower skin-to-electrode impedances which can distort the EEG signal (Teplan, 2002). This becomes increasingly relevant for mobile EEG recordings in adverse environments like the outdoors and/or during body movements. To reduce the impact of movement, high viscosity gel is applied to which is less likely to smear or bridge with neighbouring electrodes. Furthermore, to minimize the influence of external sources of noise active electrodes are used in mobile EEG systems. Active electrodes are shielded from external currents and have an output impedance of less than 1 Ohm, ensuring that the signal is fully insensitive to electrical interference (van Rijn, Peper, & Grimbergen, 1990).

EEG amplitudes typically range between 4 Hz – 100 Hz and, as such require to be amplified before it can be visualized as waveforms that can accurately be measured and interpreted. The signal registered in each electrode represents the difference between in voltage relative to a reference electrode signal (Luck, 2005). There are

several methods for establishing a reference signal including using the vertex electrode, linked mastoid electrode signals, using an electrode placed on the nose, the averaged signal or Laplacian data; a weighted average of the immediately neighbouring electrodes (Nunez et al., 1997). EEG signals are additionally low-pass filtered to reduce high-frequency noise like muscle potentials; and high-pass filters are used to cancel low-frequency potentials.

In the experimental chapters that follow a 64 mobile EEG system was used in combination with Pupil Labs wearable eye tracker (Figure 2.2.2A). The mobile EEG system (MOVE, Brain Products GmbH, Munich, Germany) transfers data wirelessly over the 2.4 - 2.5 GHz spectrum range by means of a small transmitter that is carried by the participant. The light-weight transmitter amplifies and digitizes the incoming raw analogue signal from the electrodes and transfers it to receiver. The receiver then converts the digital data back to an analogue signal. The transmitter-receiver conversion factor is 1:1 meaning the EEG amplifier provides unchanged raw data to the controlling computer. A mobile base unit was placed on a rolling trolley which supported the signal receiver, EEG amplifier and recording computer. This base unit was repositioned throughout recording sessions to maintain a distance no larger than 7 m to avoid transmission cuts and maintain optimum signal quality. The EEG signal was always sampled at 1000 Hz with filters between 0.1 Hz and 200 Hz.

2.2.3 Artifact rejection in mobile EEG signals

A major concern in mobile EEG research is that signals are easily contaminated by the presence of extracerebral potentials. As in standalone EEG systems, artifacts can result from multiple sources including muscle potential associated with harsh body movements, chewing, eye blinks and eye movements (i.e. electro-oculographic activity, EOG) as well as heart palpitations i.e. electrocardiographic artifacts (Rowan & Tolunsky, 2003). Additionally, artifacts relating to locomotion and postural corrections are specific to mobile EEG recording in natural environments (Gwin et al., 2010). These common artifact potentials are several magnitudes stronger than cerebral signals and can

render EEG signals uninterpretable. Other known artifacts typically relate to problems in individual electrodes as well as electrical noise from alternating current electrical appliances causing a 50 Hz wavelength artifact in recordings. Active electrodes however, are significantly less affected by the 50 Hz power line noise. To avoid artifacts from concealing the underlying EEG data, correction methods can be performed off-line. Visual inspection of the EEG data is a commonly used procedure to discard trials contaminated by the presence of artifacts. Alternatively, automatized routines can be employed to discard trials containing large artifacts. Furthermore, both principal component analysis (PCA) (Berg & Scherg, 1994) and independent component analysis (ICA) (Jung et al., 2000) techniques are classically used to separate cerebral from extra cerebral sources of noise in the data. These procedures clean the signal by isolating the average EEG signal to maximally spatially and temporally independent components allowing the removal of specific artifacts (e.g. EOG or ECG artifacts) from the EEG signal (Luck, 2005).

In actively behaving subjects, ICA is a pivotal tool as it dissociates the contribution of non-brain sources from cerebral signals (Gwin et al., 2010, 2011). These external sources of noise include mechanical artifacts, biological signals (e.g., eye movements and muscle activity) (Gramann et al., 2010) and losses in wireless signal transmission. The nature of MoBI recordings, involving moving participants and concomitant EMG and eye movement activity, requires new approaches to handling of non-brain activity. Pattern-matching procedures based on PCA, for instance, have been developed to correct stereotypical artifacts like ECG or EOG artifacts and can be implemented in the brain electrical source analysis software (BESA; MEGIS Software GmbH, Munich, Germany). The spatio-temporal pattern search cleans the EEG signals by correcting stereotyped artifacts like horizontal and vertical eye movements as well as eye blinks.

2.2.4 Eye-movement related potentials (EMRPs)

Eye-movement related potentials (EMRP), also known as saccadic eye-movement related potentials, refer to potential changes associated to a specific phase of a saccadic eye movement (i.e. the onset or offset of a saccade). More precisely, EMRP can be defined as the averaged time-locked EEG activity detected at scalp electrodes following a saccadic movement (Jagla, Jergelová, & Riečanský, 2007). In a similar manner to event related potentials (ERPs) (Luck, 2005), multiple EMRP waveforms can be averaged to generate a mean positive or negative voltage deflections, referred to as components. The averaged EMRP response to different stimulus conditions can be compared in terms of their amplitude or latency to quantify differences in the waveform at high levels of temporal resolution (< 1 msec).

Unlike fixation related potentials (fERP or FRP) (Baccino & Manunta, 2005; Dimigen, Valsecchi, Sommer, & Kliegl, 2009; Kamienkowski, Ison, Quiroga, & Sigman, 2012) which are time-locked to an eye fixation (i.e. the maintaining of the visual gaze on a single location), EMRPs are temporally fixed to a specific phase in the saccadic eye movement, before a fixation occurs. As such, EMRP include a saccadic spike potential in posterior parietal areas as well as the lambda complex (Kazai & Yagi, 2003; Yagi, 1979, 1981) and artifact potential components relating to the offset of a saccade (Thickbroom, Knezevič, Carroll, & Mastaglia, 1991; Thickbroom & Mastaglia, 1986).

The EMRPs presented in the experimental chapters of this thesis were calculated based on the first instance that the gaze position touches an image. This initial touch between the gaze and an image typically corresponds to the final part of the saccade which brought the gaze to fixation. By identifying the initial touch of a gaze with a relevant visual feature; naturally occurring eye-movements were used to inform the analysis regarding naturally occurring onset times during free-viewing of pictures.

2.2.5 Independent component analysis (ICA)

ICA is a linear decomposition approach which effectively separates multichannel EEG data into independent components (ICs). Three main ICA algorithms have been

used for EEG analysis and include the adaptive mixture of independent component analysers (AMICA) (Palmer, Kreutz-Delgado, & Makeig, 2006; Palmer, Makeig, Kreutz-Delgado, & Rao, 2008), the extended InfoMax ICA (Bell & Sejnowski, 1995; Lee, Girolami, Bell, & Sejnowski, 2000) and the FastICA (Hyvärinen & Oja, 2000). Spatial filtering based on the information content of an EEG signal can be effectively used to resolve issues arising from the mixing of source signals caused by the volume conduction problem at individual electrodes (Makeig, Bell, Jung, & Sejnowski, 1996).

ICs resulting from the ICA decomposition are maximally spatially and temporally independent from each other and differ significantly with regards to the relative strength and polarity of the volume conducted activity at each sensor. The underlying assumption is that EEG sources are spatially fixed and that the overall number of sources is equal or less than the number of scalp electrodes. The generators of the EEG signal are made up from synchronous cortical activity across highly connected areas in the cortex. ICA can effectively segregate activity from dozens of independent sources of activity that closely fit a single dipole projection expected from the EEG sources (Delorme, Palmer, Onton, Oostenveld, & Makeig, 2012; Makeig, Debener, Onton, & Delorme, 2004).

In MoBI research ICA represents a valuable computational tool as it effectively distinguishes non-cerebral sources of noise originating from eye-movements, as well as scalp muscles or movement artefacts relating to gait and postural adjustments present during movement (Gramann, Ferris, Gwin, & Makeig, 2014; Gramann et al., 2010).

2.2.6 Source modelling of mobile EEG signals

A basic problem in EEG is the estimation of neuronal sources corresponding to a distribution of electrical potentials over the scalp. In mobile EEG recordings, where non-cerebral sources relating to movement are enhanced, it has been proposed that ICA could be used to separate the problem of EEG source identification from the issue of source localization (Makeig et al., 1996). Localizing sources of neural activity can be

achieved by solving the inverse problem. By identifying the contribution of brain and non-brain sources to the data, ICA provides a pre-processing step in the identification of source locations (Jung et al., 2001). Advanced mathematical algorithms have been designed to estimate the source of the EEG signal; these estimations however are limited by the accuracy of the conductivity model and brain templates used in each case (Schneider & Strüder, 2012).

Recent investigations using MoBI have established that equivalent dipole reconstructions of ICs allow the identification of EEG sources with reasonable levels of spatial accuracy (Acar & Makeig, 2013; Jungnickel & Gramann, 2016; Scherg & Berg, 1991), specifically in high-density EEG systems recording from a high number of electrodes (Lau et al., 2012). Furthermore, source dipole modelling can be used to estimate the individual contributions of non-brain related potentials like eye-movements and blinks (Berg & Scherg, 1991).

2.2.7 Advantages and limitations of MoBI methods

The excellent temporal resolution of the EEG signal are the major advantages of the method as electrical changes in the brain occur at the millisecond time scale. In mobile settings, small sensor size of EEG electrodes and portability of the system allows the direct assessment of the processing of stimuli in real time. EEG investigation of specific aspects of sensory and cognitive processing is often more informative than explicit behavioural measures (i.e. reaction times). Furthermore, the possibility of recording brain potentials in highly ecological environments allows normal cognition and natural sensory processing to be investigated.

The major limitation of EEG however, is the low spatial resolution when compared to methods like fMRI, PET or NIRS. The distortion of the electrocortical signal measured at the scalp is due to the layers of various tissues, cerebrospinal fluid and skull the signal must permeate before reaching the sensor. The result of this is that it is impossible to definitively identify the source of electrical activity.

2.3 Synchronising eye-tracking and EEG data in MOBI studies.

To synchronize the multimodal data stream, a light emitting trigger-box was constructed. The hardware consisted of a button box connected in parallel to both a 5 V power source and an LED light protruding from the box. Digital pulses were placed within the EEG data at the beginning of each experiment and were then aligned in post processing. These digital pulses became apparent in the eye-tracking data a flash of light in the world camera view. The time series from both data streams are then synchronized by zeroing the real time clocks for each system and importing the eye-tracking events into the EEG data as markers.

At the start of each experimental session the trigger box was used flash a light que into the world video camera of the eye-tracking system and simultaneously sending a transistor-transistor logic (TTL) pulse into the EEG data. The offset of the light flash was recorded in a specific frame in the eye-tracking recording. The offset frame was time-stamped to the internal processing clock of the eye-tracking recording computer and was used to synchronize the EEG and eye-tracking data streams.

The temporal accuracy of this synchronization was previously tested in a 15 min pilot recording where synchronizing light stimuli were generated in approximately 1 min intervals. The eye-tracking frames were logged and compared to the latency at which the EEG triggers occurred. The temporal asynchrony between the triggers in the EEG and frames in the eye-tracking recording system was 0.022 ± 0.02 s (mean ± SD) over the 15 min period. The length of the pilot recording was determined by the average duration of an experimental block in the mock picture gallery that was used in the following experimental chapters.

Chapter 3

Research questions, hypotheses and overview

3.1 Research problems

Recording brain activity during natural behaviour poses problems for modern neuroimaging techniques and, as such, methodological questions relating to presence of noise in mobile EEG signal in natural settings is a specific challenge to mobile EEG research. Furthermore, within a natural environment, the lack of time-locked stimulus presentation is an additional concern.

Research problems associated with the use of combined eye-tracking and EEG in the real world relate to multi-saccadic activity during natural exploration of the visual scene. The effects of eye-movement artifacts on the EEG signal must be resolved. Similarly, pre-saccadic activity relating to planning in the visual system, such as oculomotor preparation (Kurtzberg & Vaughan, 1982; Richards, 2001) should be regarded. In natural settings, the effects of posture on event related brain potentials is of high significance, however it is yet to be investigated comprehensively. This raises an additional issue relating to the reproducibility of laboratory based results in natural settings using three dimensional, real stimuli is addressed. Along similar lines, the presence of stimuli in peripheral vision is of further concern and overlapping trans- and multi-saccadic processes are likely be present during free exploration of the visual environment.

Neuroimaging research has described the neural mechanisms underlying face perception in the past (Calder et al., 2011). It is still unknown however; if behavioural and neurobiological measures recorded under strictly controlled laboratory conditions accurately reflect the complexity of cognitive processing as it would occur in natural environments. As such, it is possible that people process faces differently in the real world relative to laboratory conditions. This question has a broader significance face

processing EEG literature, as well as general laboratory-based sensory processing neuroimaging research. Given the perceptual stability in the processing of faces, as well as the consistency in experimental findings, faces represent a viable candidate for scientific research in natural settings.

The effects of emotional expression on the N170 have been well documented in the past; here we examine the validity of these results in a natural setting during free exploration. The effects of viewing famous, relative to unknown faces are debated in the literature. Here we address this issue by comparing brain activity associated to viewing famous and anonymous faces in natural environments. Further, we examine differences in electrical potential in the brain resulting from postural variations. The N170 is a highly researched ERP; however we are still unsure it is exclusively a response to a static two dimensional image or if real faces produce a similar response during natural behaviour. This is, to the best of our knowledge, the first attempt to detect face-sensitive brain activity accompanying natural behaviour using wireless EEG in combination with mobile eye-tracking.

3.2 Hypothesis

- Mobile EEG in combination with eye-tracking recordings will distinguish electrocortical brain responses of faces relative to objects.

- Face-specific brain activations will appear over the right occipitotemporal region of the scalp at 170 ms when faces are viewed, but not objects.

- The face-sensitive EMRP will be modulated by the emotional expression of faces. Negative and positive expressions will generate larger N170 amplitudes relative to neutral ones.

- Face familiarity is indexed in the N170 face-related brain component. Famous faces will modulate the N170 component amplitude relative to unknown faces.

- Upright postures will affect the N170 amplitude in response to emotional faces relative to reclining ones. The additional processing demands associated to maintaining an upright stance will reduce the amplitude of the N170 response.

- The MoBI methodology developed throughout this thesis can be used to detect face-sensitive brain potentials during a normal social dyadic interaction.

- EEG recordings during a dyadic social interaction will reproduce face-sensitive potentials recorded in the laboratory.

3.3 Thesis chapter overview

Chapter 2 describes the experimental procedures involved in mobile neuroimaging data collection combining EEG and eye-tracking data to detect brain electrical potentials from mobile subjects in natural settings. Data analysis methods for wireless EEG data are detailed in this chapter.

Chapter 3 presents the main research problems surrounding MoBI research into face processing addressed in the experimental chapters. Briefs for each chapter and a summary of the hypothesis are presented.

Chapter 4 presents a mobile EEG study investigating face processing during viewing of a mock art gallery. Brain representations of facial expressions are investigated in freely moving subjects using mobile EEG combined with eye tracking. The effects of emotional faces on the N170 component are explored during free viewing of faces in a natural environment.

Chapter 5 investigates the effects of familiarity on face-sensitive EMRPs from natural viewing of images in an environment closely resembling an art gallery. We examine the functional significance of N170 components response to famous and unknown faces. We replicated our previous findings of the N170 component however our results deviate from those suggesting the N170 encodes higher order information of faces (i.e. identity).

Chapter 6 examined the effects of posture on emotional face processing by comparing EMRPs recorded from reclined subjects in the lab to those obtained from standing subjects within a picture gallery.

Chapter 7 presents, for the first time, evidence of face-specific potentials in the brain recorded during a natural social interaction with another person. Viewing a real human face during conversation generated a N170 component that was not present when object images were viewed.

Chapter 8 provides a general discussion where the overarching results obtained in the experimental results are summarised and discussed in light their theoretical significance and their current limitations. This chapter concludes with suggestions for future research directives as well as latent applications for this method in the future.

Chapter 4

Brain responses to emotional faces in natural settings:

A wireless mobile EEG recording study

Soto, V. [1], Tyson-Carr, J. [1], Kokmotou, K. [1,2], Roberts, H.[1], Cook, S. [1], Fallon,. [1], Giesbrecht, T. [3], Stancak, A. [1,2]

[1] Department of Psychological Sciences, University of Liverpool, Liverpool, United Kingdom,

[2] Institute for Risk and Uncertainty, University of Liverpool, Liverpool, United Kingdom,

[3] Unilever Research & Development Port Sunlight Laboratory, Merseyside, United Kingdom

This experiment investigated the effects of emotional expression on face-sensitive brain potentials using mobile EEG in a natural setting.
It is published in Frontiers in Psychology (2018), doi: 10.3389/fpsyg.2018.02003. The format of the text has been modified to match the style of this thesis.

The roles of the co-authors are summarised below:

I designed the study in collaboration with Andrej Stancak and collected the data. John Tyson-Carr, Katerina Kokmotou, Hannah Roberts and Stephanie Cook assisted with the collection of data and contributed useful comments whilst preparing the manuscript for publication. Andrej Stancak created the original computer programs for data analysis and synchronization of mobile EEG and eye-tracking data. Andrej Stancak, Nicholas Fallon and Timo Giesbrecht contributed to the experimental design as well as the large-scale planning of this project Andrej Stancak, Nicholas Fallon and Timo Giesbrecht secured funding for project.

4.1 Abstract

The detection of a human face in a visual field and correct reading of emotional expression of faces are important elements in everyday social interactions, decision making and emotional responses. Although brain correlates of face processing have been established in previous fMRI and EEG/MEG studies, little is known about how the brain represents faces and emotional expressions of faces in freely moving humans. The present study aimed to detect brain electrical potentials that occur during the viewing of human faces in natural settings.

64-channel wireless EEG and eye-tracking data were recorded in 19 participants while they moved in a mock art gallery and stopped at times to evaluate pictures hung on the walls. Positive, negative and neutral valence pictures of objects and human faces were displayed. The time instants in which pictures first occurred in the visual field were identified in eye-tracking data and used to reconstruct the triggers in continuous EEG data after synchronizing the time axes of the EEG and eye-tracking device.

EEG data showed a clear face-related event-related potential (ERP) in the latency interval ranging from 165 to 210 ms (N170); this component was not seen whilst participants were viewing non-living objects. The face ERP component was stronger during viewing disgusted compared to neutral faces. Source dipole analysis revealed an equivalent current dipole (ECD) in the right fusiform gyrus (BA37) accounting for N170 potential.

Our study demonstrates for the first time the possibility of recording brain responses to human faces and emotional expressions in natural settings. This finding opens new possibilities for clinical, developmental, social, forensic, or marketing research in which information about face processing is of importance.

4.2 Introduction

Facial expressions are evolutionarily based and culturally conditioned tools. They steer social interactions, solicit help and inform about events in social environments as well as the intentions of the expresser (Matsumoto, Keltner, Shiota, O'Sullivan, & Frank, 2008). The capacity to recognize facial expressions quickly and correctly correlates with problem solving capacity and efficient adaptation to a new environment (Matsumoto, LeRoux, Bernhard, & Gray, 2004). In contrast, the ability to recognize facial expressions is impaired in abused children (Camras et al., 1988), depressed people (Persad & Polivy, 1993), children presenting autistic traits (Ozonoff, Pennington, & Rogers, 1990), and people with a history of substance abuse (Foisy et al., 2005).

Previous brain imaging studies have shown that a set of brain regions in occipitotemporal cortex were associated with processing human faces (Haxby, Hoffman, & Gobbini, 2002; Kanwisher et al., 1997). Electroencephalographic event-related potentials (ERPs) revealed a negative potential, N170, at lateral occipitotemporal regions of the scalp which responded with greater amplitude when viewing faces compared to objects (Bentin et al., 1996). A large number of studies have confirmed that the N170 not only reflects low-level visual features of a human face, but would also signify a conscious awareness of the presence of a face in the visual field (recently reviewed in Olivares, Iglesias, Saavedra, Trujillo-Barreto, & Valdés-Sosa, 2015; Bruno Rossion, 2014). While earlier studies reported a lack of encoding of emotional facial expression by the N170 potential (Eimer et al., 2003; Herrmann et al., 2002), a recent meta-analysis confirmed the encoding of emotional facial expressions in the amplitudes of the N170 potential (Hinojosa et al., 2015).

Human perception and cognition in real life differs from that occurring in a laboratory experiment in that it offers a continuous and naturally flowing stream of perceptual and motor decisions. Unlike flashing a visual stimulus on a screen in a laboratory experiment, free viewing of scenes under natural conditions involves multi- and trans-saccadic processes which necessitate the anticipation of a visual pattern before the start of a saccadic eye movement, and integration of information across successive eye fixations (Melcher & Colby, 2008). In contrast to laboratory electroencephalography (EEG), magnetoencephalography (MEG) or functional magnetic resonance imaging

(fMRI) experiments, people often interact with real life situations while walking or standing upright. Maintaining an upright stance or walking poses further demands on the brain processing and physiological adjustments which are not encountered in laboratory settings (reviewed in Thibault et al. 2014). Visual processing is enhanced and electrical activity and the relative cerebral blood flow in occipital cortex (Goodenough, Oltman, Sigman, & Cox, 1981; Yasuomi Ouchi et al., 2001) is enhanced while standing erect compared to reclining. Therefore, brain responses to viewing human faces, which have been well established in a number of laboratory studies over past decades, cannot be taken as templates which the brain merely replays in a real life situation such as walking and meeting people.

Recent advances in EEG technology and data analysis opened new possibilities to explore human cognition, emotion and actions as they occur in natural settings. A novel non-invasive mobile brain and body imaging (MoBI) modality has been proposed (Gramann et al., 2011, 2010; Makeig et al., 2009). MoBI typically involves the use of wireless EEG recordings in freely moving individuals, and a multimodal approach to data analysis which combines EEG recordings with recordings of muscle activity, spatial head coordinates, and electro-oculography (Ojeda, Bigdely-Shamlo, & Makeig, 2014). The challenges posed by recording wireless EEG in natural settings are largely related to the presence of movement related artifacts and the separation of cerebral and extracerebral sources of EEG activity (Gwin et al., 2010). A MoBI approach has been successfully applied to recording of EEG during every-day life activities (Wascher, Heppner, & Hoffmann, 2014) like cycling (Zink et al., 2016), recording of EEG in pilots while airborne (Callan et al., 2015), and identification of brain potentials related to the control of locomotion (Seeber et al., 2015; Severens et al., 2012; Wagner et al., 2012).

Recording brain electrical potentials during viewing human faces in natural settings poses an additional specific challenge related to the absence of a time locking event in a continuous stream of EEG data, which has traditionally been provided by a stimulus control computer. In the present study, we employed continuous recordings of eye movements to identify the time instants at which the gaze first landed on a picture of a face or object. This approach capitalizes on previous laboratory studies analysing eye-

movement related potentials during free reading of words (Baccino & Manunta, 2005; Dimigen et al., 2011; Hutzler et al., 2007) or free viewing of visual scenes (Fischer, Graupner, Velichkovsky, & Pannasch, 2013; Simola, Le Fevre, Torniainen, & Baccino, 2015) and is similar to a recent study which reconstructed the face N170 potential during viewing of a continuous video stream (Johnston, Molyneux, & Young, 2014).

The primary aim of this study was to employ a MoBI approach to record face-specific brain potentials in freely moving individuals. As a secondary goal, we also analysed whether hedonic valence of faces and objects would manifest in mobile EEG data. In line with previous research studies conducted in laboratory settings (Blau, Maurer, Tottenham, & McCandliss, 2007; Kolassa & Miltner, 2006; Trautmann-Lengsfeld, Domínguez-Borràs, Escera, Herrmann, & Fehr, 2013), we hypothesized that face-specific brain activations will manifest in the right occipitotemporal region of the scalp at about 180 ms, and that the face-sensitive eye movement related potential (EMRP) component will be modulated by the emotional expressions of the faces. Pictures of objects and facial expressions consisted of pleasant, neutral, or unpleasant to explore the possibilities of mobile EEG recordings to both differentiate brain responses to faces and objects and to resolve the qualities of emotional expression of faces.

4.3 Materials and methods

4.3.1 Participants

Twenty-five healthy volunteers (27.2 ± 4.7 years old, mean ± SD) were recruited for the study. A total of six participants were excluded from the sample due to signal problems either in the eye-tracking (n = 4) or wireless EEG recording (n = 2). Thus, the final sample consisted of nineteen participants (five females) with an average age of 27 ± 5 years. All participants gave their written informed consent prior to the study. Ethical approval was obtained from the University of Liverpool Research Ethics Committee. Participants received £20 as compensation for their travel expenses and time.

4.3.2 Stimuli

Stimuli consisted of 180 colour pictures of face and non-face objects. Object stimuli included toys, flowers and gifts (positive), dirty toilets, rubbish bins and scenes of contamination (negative), and houses, stationary and household objects (neutral). Complex images such as landscapes with flowers and scenes of contamination were included in the object images to enable modulation of the emotional valence of the object category. The luminance levels of face and objects in each of three levels of hedonic valence were similar and not statistically different ($P > 0.05$). Ninety face pictures were selected from the NimStim Set of Facial Expressions (Tottenham et al., 2009) and 90 object pictures were taken from the IAPS database (Lang, Bradley, & Cuthbert, 1997) and from public domain images available under creative commons licenses. In each category (objects and faces), 30 hedonically positive, 30 negative, and 30 neutral pictures were selected. Face stimuli were comprised of happy (positive), neutral and disgusted (negative) facial expressions. The expression of disgust was chosen because this emotion best matched the emotional response to unpleasant object images. All face images showed a frontal view on a white background. Seventeen different female faces (9 White/Caucasian, 4 East-Asian and 4 Afro-Caribbean) and eighteen male (10 White/Caucasian, 6 Afro-Caribbean and 2 East-Asian) faces were used in the study.

Stimuli were presented on twenty A0 poster-size panels. Each panel contained 9 images (15 cm × 20 cm) and a fixation cross in the centre (14.3 cm × 14.3 cm) printed onto a paper sheet (Figure 4.3.2A). All images were assigned pseudo-randomly to present a minimum of 3 faces and 3 objects (one of each hedonic category) per panel. The face and object pictures were distributed quasi-randomly on each poster in such a way that no face picture would systematically fall into the visual field while shifting the gaze to a face picture in the corner of a panel.

All panels were pasted onto Styrofoam sheets and attached to the walls using adhesive tape. Two hallways within the Eleanor Rathbone Building of the University of

Liverpool were used to create a mock art gallery where the experiment took place (Figure 4.3.2 B).

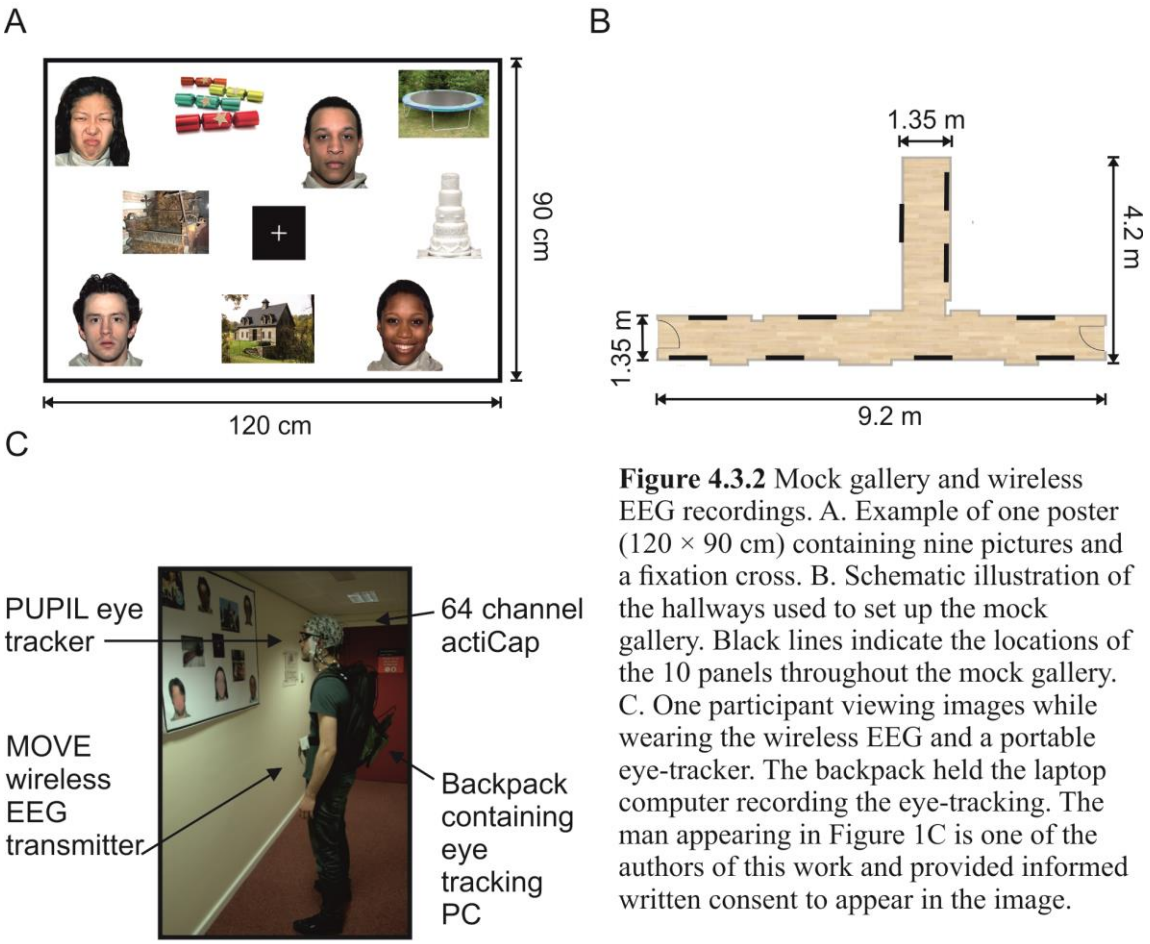

Figure 4.3.2 Mock gallery and wireless EEG recordings. A. Example of one poster (120 × 90 cm) containing nine pictures and a fixation cross. B. Schematic illustration of the hallways used to set up the mock gallery. Black lines indicate the locations of the 10 panels throughout the mock gallery. C. One participant viewing images while wearing the wireless EEG and a portable eye-tracker. The backpack held the laptop computer recording the eye-tracking. The man appearing in Figure 1C is one of the authors of this work and provided informed written consent to appear in the image.

4.3.3 Procedure

Our study is an initial attempt to record and quantify the face-sensitive ERPs that occur in natural settings such as in the street or at the supermarket. The experiment closely matches the natural settings of a picture gallery in which individuals move freely from one painting to another and visually explore a painting containing both human figures and non-living objects. The presence of the fixation cross in the middle of the board which participants fixated before shifting their gaze to a next picture on the board was the only difference relative to the settings of a picture gallery. This component was introduced to the task to reduce the possibility of overlap in viewing neighbouring pictures and to compensate for the limited capacity of our eye-tracker to quantify the

pattern of saccades and fixations during a free visual exploration which would be required to reconstruct the eye-movement related potentials using advanced processing methods such as regression analysis (Ehinger & Dimigen, 2018).

A mock art gallery was created by hanging the stimuli panels onto bare walls in designated hallways. The corridors were not closed off on either side, nor were there attempts to discourage other people from passing through while an experimental session was in progress. As in the real world, passers-by occurred spontaneously. Participants were requested to walk through the mock art gallery while viewing the images displayed on each panel. They were free to navigate the gallery in any order they chose and view individual pictures in any order and for as long as they wished. Subjects were only instructed to stand facing each panel and to view each image for at least few seconds before moving onto the next image. Participants were, additionally asked to look at the centre fixation cross before viewing each image, and to return their gaze to the fixation cross before moving to the next picture. They only continued onto a subsequent panel after viewing all images (Figure 4.3.2A). Picture preferences were indicated by marking selected pictures on a small paper printed version of each panel.

The gallery task was divided into two blocks. Each block contained ten panels with nine images presented on each one. In total, participants viewed 180 different images in the experiment. On average, each gallery block lasted approximately 15 minutes. Participants were tasked with selecting a preferred face and object as well as a disfavoured face and object from each panel.

Instructions were delivered and equipment was set up in a designated lab space. Participants were fitted with the EEG cap (actiCAP, Brain Products, Germany). The mobile EEG system was then connected and wireless signals were visually inspected on a standing participant. Next, eye-tracking glasses (PUPIL; Kassner et al. 2014) were placed on the participant over the EEG cap. The eye trackers were calibrated against a blank white panel at a distance of 1 m. Gaze-tracking was optimized by means of 3D calibration routine using manual markers.

The eye-tracking recording laptop was placed in a backpack and carried by the participant for the duration of the gallery task (Figure 4.3.2C). EEG cables running from the electrodes to the lightweight transmitter were also placed in the backpack to reduce cable sway artifacts (Gramann et al., 2010; Gwin et al., 2010). A mobile base unit was assembled using a rolling trolley where the wireless signal receiver, EEG amplifier and recording computer were placed. The base unit was positioned by the experimenter maintaining a distance of no more than 7 m from the participant in order to maintain optimal signal quality.

Electrode impedances and gaze tracking calibration were checked and corrected in the break between blocks if required. Once the gallery task concluded, subjects completed a rating task on a computer in the laboratory.

Once the gallery task had been completed, the EEG cap and the eye-tracking glasses were removed. Participants were then required to rate how much they liked and if they would approach the images previously seen in the mock gallery. Ratings were performed using two visual analogue scales (VAS) sized 10 cm and anchored on each extreme (i.e. '*0: Do not like'* up to *'100: Like very much'* and '*0: Avoid'* up to *'100: Approach'*). Pictures and rating scales were presented on a LCD screen using Cogent program v. 1.32 (Welcome Department of Imaging Neuroscience, United Kingdom) running on MATLAB v. R2014a (The MathWorks, Inc., USA).

4.3.4 EEG recordings

Whole scalp EEG data was continuously recorded using a 64-channel wireless and portable EEG system (Brain Products, GmbH, Münich, Germany). Signals were digitized at 1 kHz on a BrainAmp DC amplifier linked to Brain Vision Recorder program version 1.20.0601 running on a Windows laptop. The wireless interface (MOVE, Brain Products, GmbH) utilizes a lightweight signal transmitter which participants carry on a belt (Figure 4.3.2C). Active Ag/AgCl EEG electrodes were mounted on an electrode cap (actiCAP, Brain Products, GmbH) according to the 10-20 electrode system. Electrode FCz was used as the system ground and electrodes were

referenced to Cz. The EEG cap was aligned in respect to the midpoint between the anatomical landmarks of the nasion and inion, and the left and right preauricular points. The electrode-to-skin impedances were lowered using electrolyte gel (Signa Gel, Parker Laboratories, Inc., Fairfield, NJ) and checked to be below 50 kΩ before starting the recordings.

4.3.5 Eye movement recording and analysis

The locations of the gaze positions were recorded using a PUPIL binocular eye-tracking system and Pupil Capture software v 0.7.6. running on Ubuntu v 14.04.4. The PUPIL eye tracker is a high resolution lightweight wearable system (Figure 4.3.2C). PUPIL software is a cross-platform (Linux, Mac, and Windows) open-source software which is actively maintained and supported by the developers (Kassner et al., 2014). Here, eye-tracking data and the real-world video streams were set at a sampling rate of 60 frames per second with a resolution of 600 × 800 pixels in both the world camera and in the eye cameras. The sampling rate of 60 Hz was chosen based on pilot experiments in order to secure a continuous stream of eye-tracking data which was often discontinuous at higher sampling rates.

The ocular pupils of both eyes were located based on a centre-surround detection algorithm (Świrski, Bulling, & Dodgson, 2012). To calibrate the gaze locations, a manual marker 3D calibration protocol was used to generate a 9-point grid in the field of view of the participant. Calibration was repeated until gaze positions were accurate everywhere on the blank panel. Small calibration offsets occurred at times due to displacements in the wearable eye-tracker on the subject's face. These were adjusted using the manual gaze correction plug-in on Pupil Player during manual tabulation of stimulus onset times. If multiple time stamps were associated with one frame in the real-world recordings, the middle frame was selected as the time-locking event. The Pupil Capture software can process up to three video streams (two eye cameras and a world view camera) synchronously and allows for mid-recording calibrations. These video streams are read and exported using Pupil Capture software for real-time pupil

detection, recording, and gaze mapping. The gaze mapping function allows the eye positions to be superimposed onto the world-view scene space. Exported PUPIL raw gaze data is time-locked to the processing computer's internal clock, giving millisecond precision to the eye measurements.

Eye-tracking data were processed using Pupil Player v. 0.7.6 program. Additionally, all recorded frames contained an accurate time stamp based on the PC processor real-time clock. Eye-tracking video files were visually inspected and stimuli onsets were manually tabulated. Each stimulus was logged on a picture by picture basis with stimulus onset defined as the first instance in which the gaze position touched or landed on an image. The real times corresponding to the tabulated frames were used to import stimulus onset latencies onto the raw EEG data. Four subjects' data was excluded from the sample due to loss of gaze calibration during the recordings.

The total gaze times were calculated by additionally tabulating the earliest frame in which the gaze left an image. Of the 19 total subjects, 15 data sets were used to calculate the average gaze times per condition. Four subjects' data was not included in the calculation of mean viewing times. The four exclusions were due to difficulties or uncertainties in defining an accurate offset time when the subject's gaze left an image to return to the fixation cross. A 2 × 3 analysis of variance (ANOVA) for repeated measures was used to check any significant differences in viewing times across conditions.

At the start of each gallery block, a trigger-box fitted with a light emitting diode (LED) was used to synchronize data streams. A pulse of light was flashed into the world-view camera on the eye trackers as a simultaneous transistor-transistor logic (TTL) pulse was registered in the EEG data recording. In doing so, a visual light cue became apparent at a specific frame in the video data. This frame was then registered and used to temporally synchronize the EEG and eye-tracking data streams. The accuracy of the synchronization was tested in a 15 minute recording during which 15 synchronizing light stimuli were produced in approximately 1 minute intervals. The time-locked eye-tracking frames were logged and compared to the latency of the EEG

triggers. The temporal asynchrony between triggers simultaneously delivered to the eye-tracking and EEG recording system was of 0.022 ± 0.020 s (mean ± SD) over a 15 minute recording.

4.3.6 Eye movement related potentials

After synchronization, event markers were inserted into EEG data by synchronizing the time axes of the EEG and eye-tracking system. EEG data were pre-processed using the Brain Electrical Source Analysis program (BESA v.6.1, MEGIS Software GmbH, Munich, Germany). Data were first referenced to a common average using common averaging method (Lehmann, 1987) on the continuous EEG signal. EEG data were epoched to range from -200 ms to 1000 ms and the mean EEG activity in the baseline interval ranging from -200 ms to -100 ms was removed from each data point as it represented a more stable baseline than the 100 ms preceding viewing onset. The onset of a stimulus was defined as the first contact of the gaze with any part of a picture in each of the 180 images. This time point effectively corresponded to part of the eye movement which brought the gaze onto a particular face or object in a picture. Eye blink artifacts were removed using a pattern matching algorithm involving principal component analysis (Berg & Scherg, 1994; Ille, Berg, & Scherg, 2002). Then, EEG data was visually inspected for movement or muscle artifacts and trials contaminated with large artifacts were marked and excluded from further analysis. Post-saccadic EMRPs were computed from all trials falling into six different conditions (face vs. objects, three hedonic levels).

The data was visually inspected and corrected for the presence of artifacts. Trials were excluded if artifacts were present in either eye-tracking or EEG data. If participants skipped an image, failed to fixate, or gaze tracking was lost during fixation, the concurrent trial was discarded.

The sampling rate of the eye-tracking device was calculated offline (41.1 Hz on average). Given the relatively low sampling rate, we have not analysed in detail if the

next eye movement was a saccade or a fixation. Thus, EEG epochs were formed as cuts into a wild video scene similar to a recent study (Johnston et al., 2014).

4.3.7 Source dipole analysis

As EEG epochs were effectively locked to the first shift of the gaze onto a picture, we anticipated that EMRPs will comprise the saccade-related cortical potential (Kazai & Yagi, 2003; Thickbroom et al., 1991; Yagi, 1981a) and artifact potential components related to offsets of saccades. The eye movement artifacts primarily involve the corneoretinal potential associated with a displacement of the large electrical dipole of the eye during eye blinks or saccades, and a smaller saccade spike potential related to the contraction of oculomotor muscles at onset of a saccade (Dimigen et al., 2011; Nikolaev et al., 2016). Owing to limited sampling rate of eye-tracking data and presence of a small jitter between eye movement and EEG data, we applied source dipole modelling to separate electrical activations originating in the occipitotemporal cortex from those electrical potentials which originated in eye orbits and were volume conducted to distant regions of the scalp.

Grand average EMRP waveforms were used to determine the source dipole locations. A source dipole model was constructed using BESA v. 6.1 program. Two regional sources were used to model the electrical potentials to the residual corneoretinal artifact and saccade spike potentials (Berg & Scherg, 1991). The lambda component is an occipital potential that becomes most prominent when averaged EEG signals are time-locked with a saccadic eye movement offsets. To model the cortical sources accounting for distinct peaks of lambda potential (Thickbroom et al., 1991; Yagi, 1979b), a set of equivalent current dipoles (ECD) were fitted using a sequential strategy (Hoechstetter, Berg, & Scherg, 2010; Stancak et al., 2002). In sequential strategy, ECDs are successively fitted based on the peak latencies of the prominent ERP peaks determined in the global field power curve. Each new ECD explains the portion of data variance not explained by previously fitted ECDs. First, we placed two regional sources into the right and left eye orbit to separate any corneoretinal potentials related to eye blinks or saccades from the cerebral sources which were modelled in the next stage. A

regional source has three orthogonal dipoles with origins at the same location and can therefore model potentials emanating from one location in all possible directions. Since regional sources have three orthogonal components, they model activations from a widespread region of the scalp and activations which do not have constant orientations over the entire EMRP epoch. While placing regional sources into eye orbits is less effective than modelling saccade potentials with a set of equivalent dipoles each tuned to a specific saccade direction (Berg & Scherg, 1991), this method was an appropriate choice in the absence of information about the timing and angles of saccades.

We added another dipole with free orientation and location to the source dipole model. Fitting this additional dipole resulted in the dipole being placed beyond the boundaries of the head and not changing the residual variance which means that the extra dipole did not explain any specific topographic aspect of the potential field. Secondly, we also modelled the potentials in the time points of interest using a classical LORETA (Pascual-Marqui, Michel, & Lehmann, 1994) analysis recursively applied (CLARA) (Hoechstetter et al., 2010). CLARA did not show any new cluster beyond the locations previously tagged by equivalent current dipoles.

The CLARA analysis was also used to verify the locations of ECDs using an independent source localization method (Hoechstetter et al., 2010). A 4-shell ellipsoid head volume conductor model was employed to construct the source dipole model using the following conductivities: brain = 0.33 S/m; scalp = 0.33 S/m; bone = 0.0042 S/m; cerebrospinal fluid (CSF) = 1.0 S/m. Finally, we have compared the scalp potential maps with the potential maps predicted by the source dipole model and found a good match.

Due to the limited sampling rate of the eye tracker, presence of a small jitter between the EEG and eye-tracking data streams, and absence of calibration marks in visual scenes, we were not able to identify individual saccades and evaluate their impact on EEG potentials in the present study. Indeed, the principal orthogonal component in each of two regional sources (Figure 4.4.3A) shows the presence of an eye movement potential starting about 20 ms before the time-locking event and continuing eye-

movement potentials after the time-locking event. This variability is due to the triggering of stimulus onset which was determined as the first instance of the gaze contacting an image. Due to the position of the images on the panels relative to the fixation cross, this occurred at different instances of the saccade. Evaluation of effects of including two regional sources on residual variance is given in the Results.

4.3.8 Statistical analysis

The source waveforms representing the source activity in each of the fitted ECDs were analysed using a 2 × 3 repeated measures ANOVA (objects vs. faces, three levels of hedonic valence). To control for the risk of false positive results due to a large number of tests, P values were corrected using the false discovery rate method (Benjamini & Yekutieli, 2001). This analysis was used to identify the latency interval in which faces and objects and/or three hedonic categories would differ. Average source activity in intervals of interest was analysed further in SPSS v.22 (IBM Corp., NY, USA). Post-hoc paired t-tests were performed when necessary and considered significant at $P < 0.05$ with Bonferroni corrected for multiple comparisons. The statistical confidence level of $P < 0.05$ was always employed.

Scalp data at select electrodes were analysed similarly as source dipole waveforms. The ANOVA of the raw data was computed for the average of P8 and PO8 electrodes on the scalp. This analysis was included to enable comparisons of EMRP with previous studies (Figure 4.4.4.2).

4.4 Results

4.4.1 Behavioral ratings

Figure 4.4.1 illustrates the average liking scores for each of the experimental conditions. A 2 × 3 repeated measures ANOVA revealed a statistically significant effect of objects vs. faces likeability ($F(1,18) = 7.7$, $P = 0.012$). Subjects attributed larger

likeability to objects (52.6 ± 4.25, mean ± SD) than faces (47.5 ± 7.53). Both objects and faces showed a statistically significant effect of hedonic valence ($F(2,36) = 179.4$, $P < 0.0001$) consisting of a greater likeability of both objects and faces of positive valence compared to both neutral and negative valence, and greater likeability of neutral than negative valence ($P = 0.012$). The interaction between objects vs. faces and three hedonic categories was also statistically significant ($F(2,36) = 62.1$, $P < 0.0001$). Post-hoc tests revealed that this interaction effect was driven by a greater contrast between neutral and unpleasant objects ($t(18) = -17.4$, $P < 0.0001$) than neutral and unpleasant faces ($t(18) = 5.8$, $P < 0.0001$).

A 2 × 3 repeated measures ANOVA conducted on average approachability ratings showed a similar pattern of responses. Subjects rated objects (53.2 ± 0.98) as more approachable than faces (44.5 ± 1.6) ($F(1, 18) = 19.8$, $P < 0.0001$) as well as rating positive pictures (70.6 ± 2.3) more approachable than neutral (52.4 ± 1.4) or unpleasant ones (23.56 ± 1.8) ($F(1,16) = 140.5$, $P < 0.0001$). Post-hoc comparisons showed an interaction effect with greater contrasts shown between neutral and negative valence objects ($t(18) = -13.8$, $P < 0.0001$)
relative to the contrast between neutral and disgusted faces ($t(18) = -6.7$, $P < 0.0001$) ($F(2,36) = 44.4$, $P < 0.0001$).

The 2 × 3 ANOVA for repeated measures was performed on the average gaze time of each subject across conditions. The data from 15 subjects was used in this analysis. The four exclusions from this analysis were due to difficulties in defining an accurate offset time when the subjects gaze returned to the fixation cross. No effects of category ($F(1,14) = 2.11$, $P > 0.05$) were found in mean viewing times between face (3.346s ± 1.3s) and object (3.155s ± 1.1s) images. Nor were there any effects of hedonic valence were found on the average viewing times either ($F(1,14) = 0.451$; $P > 0.1$). Disgusted (3.15s ± 1.1s), neutral (3.28s ± 1.3s) and happy faces (3.31s ± 1.3s) were viewed equally across face and object categories ($P > 0.1$).

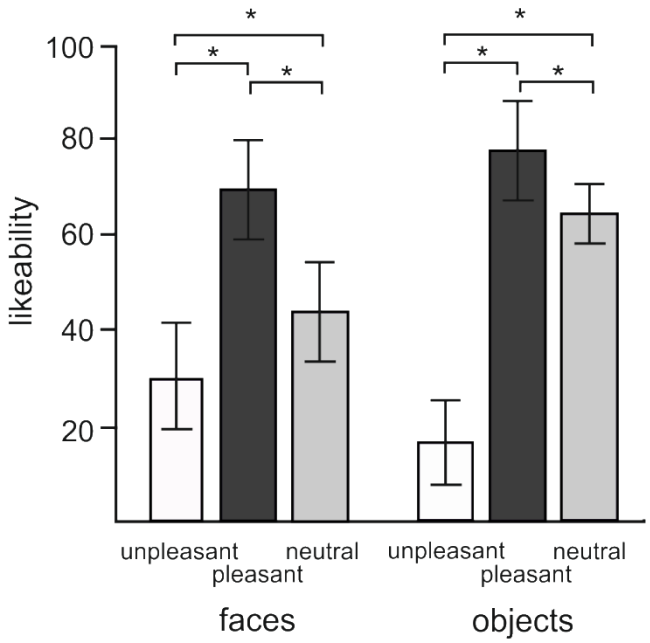

Figure 4.4.1 Mean ratings of likeability for objects and faces in three different hedonic valence conditions. Error bars stand for standard deviations. Asterisks (*) indicate the presence of statistical significance at $P < 0.05$.

4.4.2 Eye movement related potentials

Wireless EEG data maintained good quality throughout the duration of the experiment. As subjects maintained a stable stance during the viewing of pictures, EEG data showed minimal neck muscle or head movement artifacts which have been shown to heavily affect EEG data during walking or running (Gwin et al., 2011). Of the 6 excluded subjects, 2 of these were discarded at an early stage in the experiment due to loss of signal purportedly caused by drainage of the batteries in the transmitter unit resulting in incomplete EEG data. The average number of accepted trials was 72 ± 8.6 and 73 ± 6.3 (mean ± SD) for face and object pictures respectively.

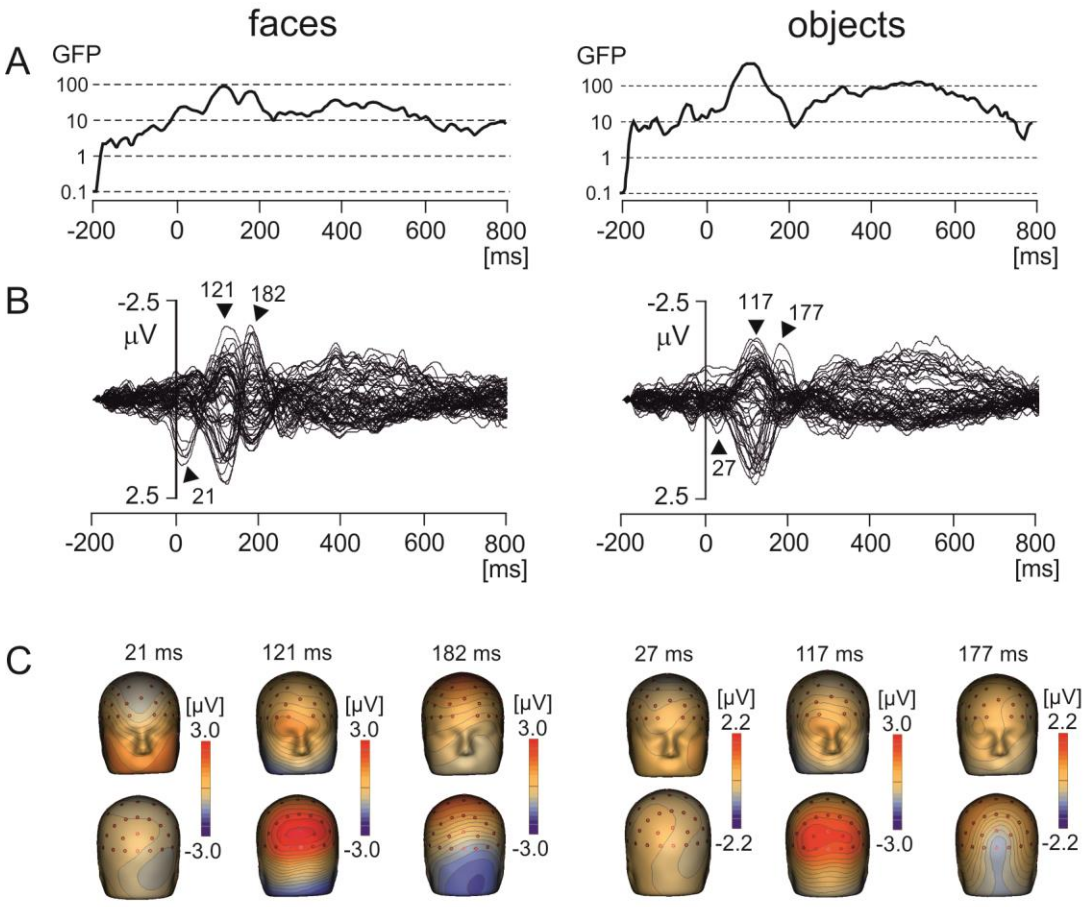

Figure 4.4.2 Grand average EMRPs during viewing of faces and objects. A. Global field power for face and object pictures. B. Butterfly plots of grand average EMRPs to face and object pictures. Peak latencies of distinct EMRPs components are highlighted with arrows. C. The topographic maps of grand average EMRPs overlaid on the volume rendering of the human head at select latency points.

Figure 4.4.2A shows the global field power and Figure 4.4.2B the butterfly plots of EMRPs for face and objects. Figure 4.4.2C illustrates the topographic maps of distinct EMRP components observed in global field power curves. An early small potential component peaking at 27 ms in objects and at 21 ms in faces was associated with a weak negative potential in the right occipital region of the scalp and another weak negative potential at the vertex (Figure 4.4.2B, C). It is unclear whether this small potential was a part of an anticipation of a face picture or whether it was related to the effects of saccades preceding the time-locking event. The lambda potential (Thickbroom

et al., 1991; Yagi, 1981a) showed a large component peaking at 117 ms in objects and at 121 ms in faces and exhibited a prominent positive component at occipital electrodes. The peak latency of the lambda potential suggests that the time-locking event coincided more often with onsets of saccades rather than with onsets of fixations because the latencies of the lambda potential occur comparatively late (~120 ms) if the time locking event is the saccade onset (Kaunitz et al., 2014). Only in face EMRPs, a distinct negative component peaking at 182 ms was seen in the right occipital-temporal region of the scalp. This negative component was associated with a positive potential component at central-parietal electrodes (Figure 4.4.2C). Both the peak latency of the negative occipitotemporal component and the presence of a positive vertex potential suggest that this particular component, responding only to face pictures, was the face-sensitive N170 component (Bentin et al., 1996). The butterfly plots for both faces and objects showed the presence of electrical activity in the latency epoch > 300 ms. However, these components had relatively small amplitudes compared to the earlier latency components and did not show distinct peaks allowing further detailed analysis.

4.4.3 Source dipole analysis

To segregate brain electrical responses generated in localized cortical regions from the extracerebral potentials, EMRP data were analysed at the source dipole level. The source dipole model was built using grand average EMRPs comprising data from six conditions (faces and objects, three hedonic valence categories) and all nineteen subjects. Figure 4.4.3A illustrates the source dipole waveforms and spatial topographic maps of EMRP waveforms for each fitted source dipole. Figure 4.4.3B illustrates the source dipole locations and orientations in a schematic transparent glass brain. Figure 4.4.3C demonstrates the locations of individual source dipoles in an anatomical brain image as well as the two regional sources in the eyes.

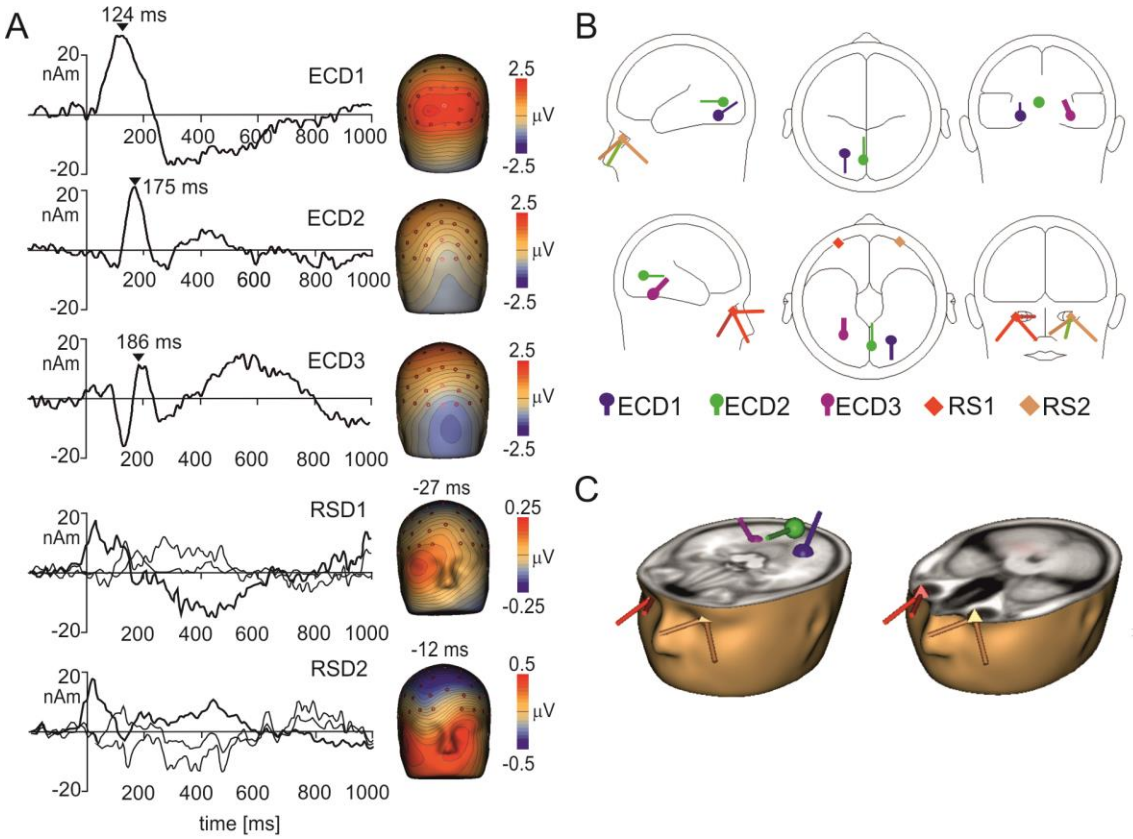

Figure 4.4.3 Source dipole model of grand average face and object EMRPs. A. The left panel shows the source dipole waveforms of three ECDs (ECD1-ECD3) and two regional sources (RS1-2). The right panel illustrates the spatial topographic maps at the latency points showing the strongest source activity (ECD1-ECD3) or at latency points showing a spatio-temporal pattern of corneoretinal potential (RS1-RS2). B. The glass brain showing locations and orientations of ECD1-ECD3 and RSD1-2. C. Locations and orientations of ECDs and RSDs in the standardized MR of a human head. The left head shows three ECDs, and the right head illustrates the two regional sources located in both eye orbits.

It should be pointed out that the use of regional sources has a drawback of having the sources just outside of the head model (Lins, Picton, Berg, & Scherg, 1993) potentially causing incomplete removal of saccadic potentials occurring during free viewing of pictures. The regional sources showed distinct peaks related to saccade offsets, and further irregular waves related to eye movements occurring later. Placing two regional sources into the eye orbits was an additional precaution, on top of the removal of eye blink artifacts from raw data using the pattern matching algorithm, in preventing the extracerebral sources from affecting the EMRPs. Nevertheless, dipole locations results must be taken with some caution due to the difficulties associated with

generating precise estimations of source locations in mobile EEG data which can, at times, be noisy (Grech et al., 2008).

ECD 1 was fitted to the visual cortex (Brodmann area 19; approximate Talairach coordinates: x = -22.5, y = -65.4, z = -18.2 mm) (Figures 4B-C) and modelled the large positive component of the lambda potential. It peaked at 124 ms and accounted for the positive potential maximum in occipital and lower parietal electrodes. ECD2 was located in the primary visual cortex (Brodmann area 17; approximate Talairach coordinates: x = -3.5, y = -74.6, z = 2.7 mm) (Figures 4.4.3B-C). This source accounted for a negative potential occurring briefly at 175 ms in occipital electrodes. This potential was mainly featured in objects EMRPs.

ECD3 accounted for the N182 potential showing a negative maximum in the right temporal-occipital electrodes and a positive potential maximum over the central and parietal regions of the scalp. This spatio-temporal pattern was prominent in face picture data and almost absent in objects data and therefore, the final fit of ECD3 was carried out in face EMRPs. The source of this potential component was located in the right fusiform gyrus (Brodmann area 37; approximate Talairach coordinates: x = 25.7, y = -56.8, z = -18.2 mm) (Figures 4.4.3B-C).

While eye-tracking data provided a useful trigger for computing the event-related potentials in the present study, the limited sampling rate and the lack of precise, calibrated markers in spontaneously occurring visual scenes did not allow quantification of oculo-motor artifacts similar to previous studies conducted in laboratory settings (Dimigen et al., 2011; Fischer et al., 2013; Kamienkowski et al., 2012; Ossandón, Helo, Montefusco-Siegmund, & Maldonado, 2010; Rämä & Baccino, 2010; Simola et al., 2015; Trautmann-Lengsfeld et al., 2013). To remove corneoretinal potentials, which may have remained in the data even after eye blink correction using the pattern matching algorithm, and those related to saccadic eye movements, we added two regional sources with origins in the left and right eye orbit to the source dipole model. To demonstrate the capacity of the regional sources to control the artifact components caused by eye movements, we have quantified each subject's residual variance in the

individual average source dipole waveforms in two time intervals, one covering the onset of the trigger event (-15 – 40 ms) and the other corresponding to the interval showing statistically significant differences between objects and faces (170 – 210 ms). The source waveforms of three ECDs and effects of the presence of these regional sources on residual variance are illustrated in Figure 4.4.3.2.

In the first interval (-15 – 40 ms), the residual variance decreased from 70.1 ± 15% to 36 ± 20.7% (mean ± SD) after including two regional source dipoles into the source model. In the latency interval 170 – 210 ms, the residual variance changed from 41% to 27.5% after including two regional sources with origins in eye orbits. According to a two-way ANOVA for repeated measures (2 latency intervals, regional sources on vs. off), the addition of the two regional sources to the model showed a significant increase in the model fit for both latency intervals ($F(1,18) = 152.7$, $P < 0.001$). The interaction between the latency intervals and presence of the regional sources in the source dipole model was also statistically significant ($F(1,18) = 32.4$, $P < 0.001$). This interaction was caused by a stronger effect of the presence of two regional sources in the latency interval -15 – 40 ms compared to 170 – 210 ms.

The five-dipole model accounted for 83% of variance in the latency interval 0 - 300 ms. Attempts to fit further ECDs in subsequent latency intervals (>300 ms) did not reduce the residual variance significantly, and new ECDs landed outside the boundaries of the head. The slightly larger residual variance of 17% compared to laboratory studies achieving a residual variance 10% or smaller could be related to an increased background noise in our data which were recorded wirelessly in freely moving individuals and in the absence of control over incidental extraneous stimuli. Alternatively, this could be due to other active brain sources not accounted by the model.

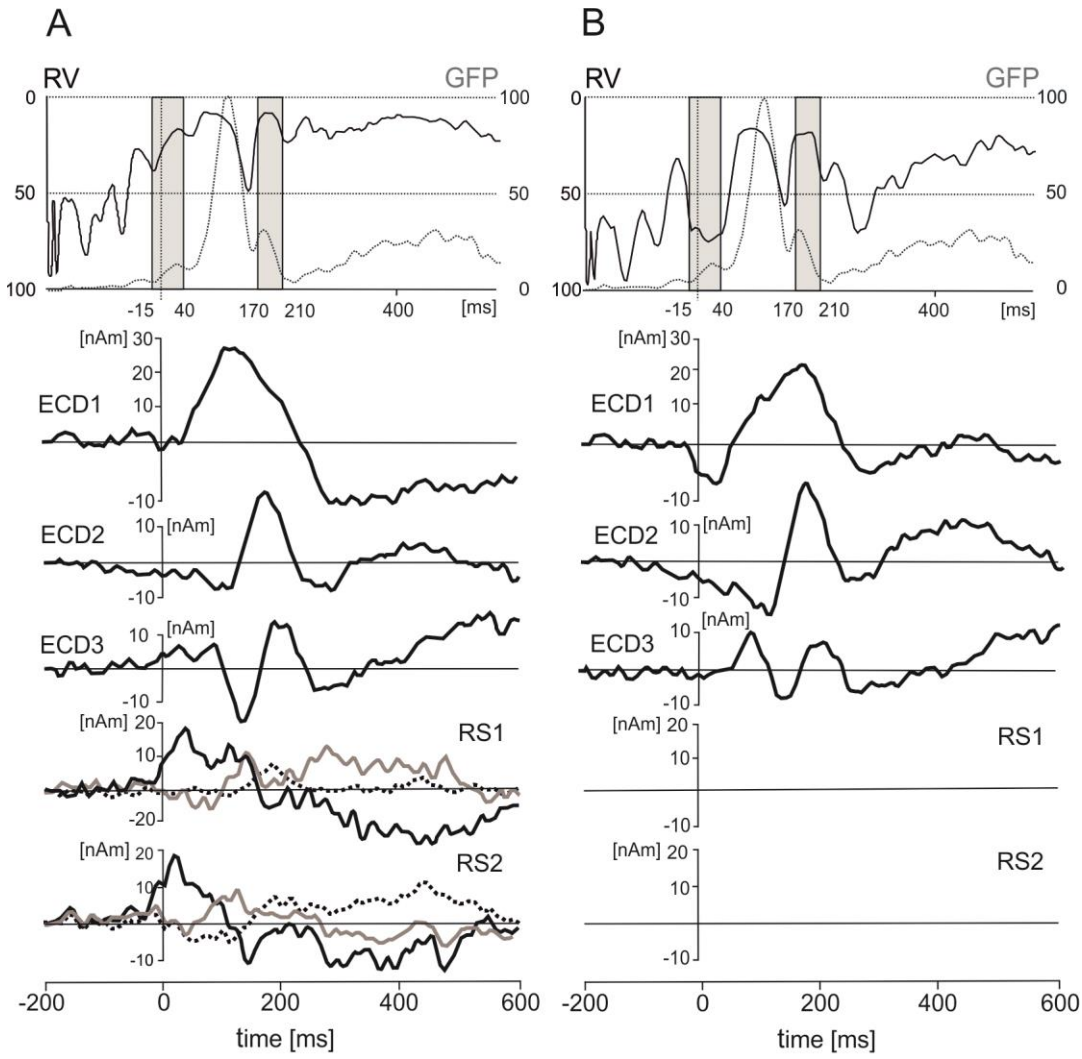

Figure 4.4.3.2 Effects of inclusion of two regional sources (RS1 and RS2) on residual variance (RV), standardized global field power (GFP), and three equivalent current dipoles (ECD1-ECD3). A. The time courses of RV (dot line), GFP (solid line), three ECDs and two RSs in a solution with the regional sources included. The two grey intervals in the top panel correspond to two intervals of interest in which residual variance was evaluated statistically (-15 - 40 ms and 170 - 210 ms). The dot lines in both rectangles stand for the latency of 0 ms. The principal of three orthogonal components in each regional source is plotted with black bold line. B. The time courses of RV, GFP and three ECDs after switching off two RSs.

4.4.4 Source dipole waveforms in face and object pictures

For each experimental condition the source dipole model was applied to the grand average data by projecting the source dipole model onto the original ERP data. The source waveforms of the three ECDs were analysed using a 2 × 3 ANOVA for repeated measures over specific interval of interest from 0 to 300 ms. P values were corrected using the false discovery rate method at P = 0.01.

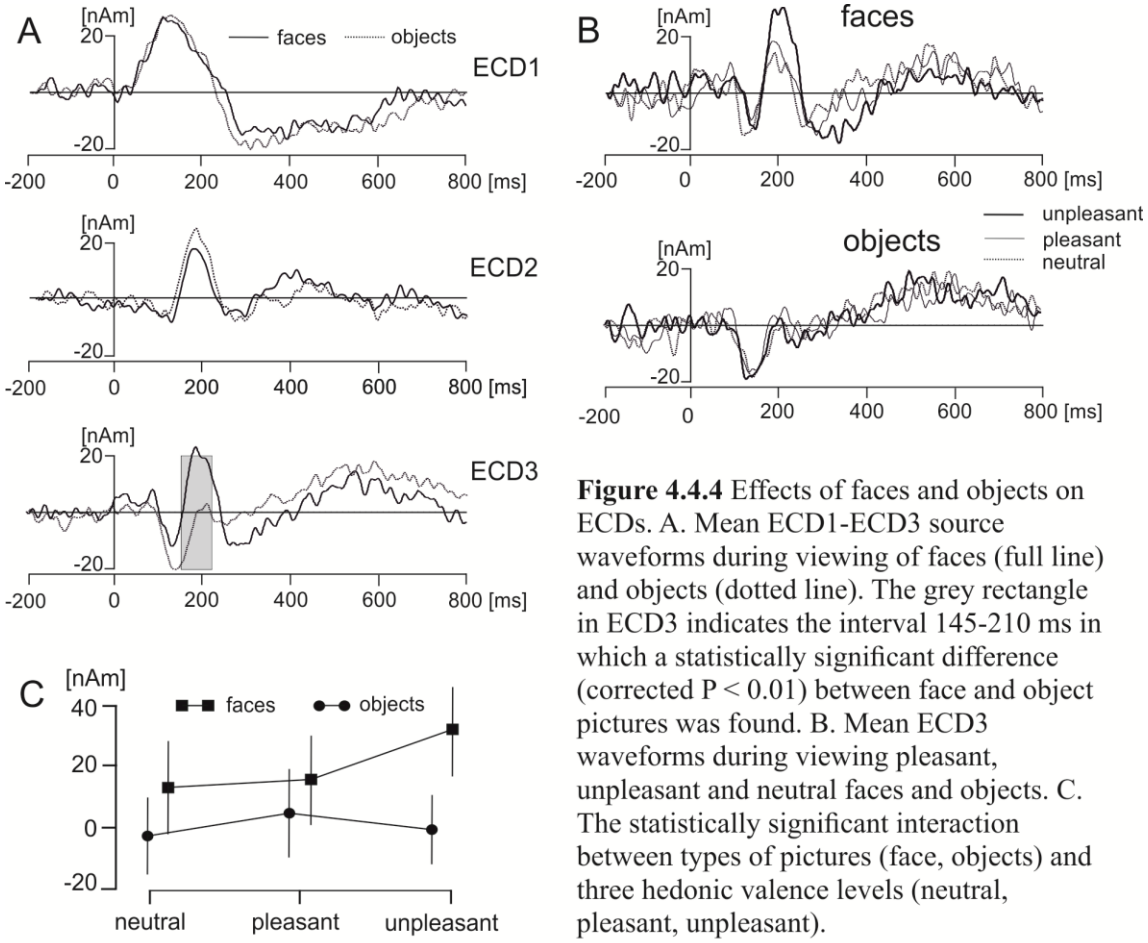

Figure 4.4.4 Effects of faces and objects on ECDs. A. Mean ECD1-ECD3 source waveforms during viewing of faces (full line) and objects (dotted line). The grey rectangle in ECD3 indicates the interval 145-210 ms in which a statistically significant difference (corrected $P < 0.01$) between face and object pictures was found. B. Mean ECD3 waveforms during viewing pleasant, unpleasant and neutral faces and objects. C. The statistically significant interaction between types of pictures (face, objects) and three hedonic valence levels (neutral, pleasant, unpleasant).

The main effect representing the difference between face and object pictures was found only in ECD3 in a broad latency interval ranging from 145 ms to 210 ms (Figure 4.4.4). The source dipole waveforms of ECD3 in faces and objects and in each of three hedonic levels are illustrated in Figure 4.4.4B. The latency interval showing a statistically significant difference between faces and objects comprised two local maxima in ECD3 source dipole waveforms. Face data showed a peak at 186 ms and

objects data showed a peak at 211 ms. To analyse further the effects of picture types and three hedonic levels in the latency intervals showing the strongest activations in each of two types of pictures, the average source dipole moments in 10-ms intervals centred at the two peak latency points (181 – 191 ms and 196 – 216 ms) were analysed using a 2 × 3 × 2 repeated measures ANOVA (2 picture types × 3 hedonic levels × 2 latency intervals). Faces showed a stronger source dipole amplitude than objects across both latency intervals (faces: 20.2 ± 4.5 nAm, objects: 0.56 ± 0.50 nAm, mean ± SD; $F(1,18) = 29.3$, $P < 0.0001$). Further, the statistically significant interaction between picture types and three hedonic levels ($F(1,18) = 9.86$, $P < 0.0001$) revealed that the amplitude of ECD3 was affected by the hedonic content in faces but not in objects (Figure 4.4.4C). Tests of simple effects demonstrated the effect of hedonic levels were only significant in faces ($F(2,36) = 15.9$, $P < 0.0001$) but not in objects ($F(2,36) = 1.58$, $P = 0.221$). The statistically significant effect of hedonic levels in face pictures was related to the greater amplitude of ECD3 in disgusted faces compared to both happy ($t(18) = 15.95$, $P < 0.0001$) and neutral faces ($t(1,18) = 18.49$, $P < 0.0001$).

EEG data recorded using a wireless system in freely moving individuals are preferably interpreted based on source dipole analysis which allows to verify that a potential waveform of interest was of cerebral origin. However, we also analysed if the differences between faces and objects and the effects of hedonic face valence shown in ECD3 would be present at select scalp electrodes. Two electrodes showing the face potential component at the latency of 189 ms, PO8 and P8 were averaged. The potential waveforms for faces and objects and the topographic maps of EMRPs at the latency of 189 ms are shown in Figure 4.4.4.2A. Figure 4.4.4.2B illustrates the PO8-P8 potential waveforms and topographic maps in neutral, pleasant and unpleasant faces and objects. The averaged PO8-P8 potential waveforms were analysed using a 2 × 3 ANOVA for repeated measures over the interval from 0 to 300 ms. A statistically significant effect of picture type was found in the latency interval 175 – 212 ms ($F(1, 18) = 32.1$, $P < 0.0001$). The amplitude of the PO8-P8 potential was more negative in faces (-1.51 ± 0.40 μV) than in objects (0.32 ± 0.36 μV). In contrast to the ECD3 data, the interaction between picture types and three hedonic levels was not statistically significant ($F(2,36) = 2.02$, $P = 0.16$).

As our recordings did not allow to evaluate parameters of individual saccades which are known to affect the strength of P1 potential (Thickbroom et al., 1991; Yagi, 1979b), we analysed whether faces and objects would differ in the amplitudes of the P1 component. The potential in electrodes PO3 and PO4 showing maximum amplitudes of the P1 component were averaged. The amplitude of the P1 component in the interval 110 – 130 ms was analysed statistically using a 2 × 3 ANOVA for repeated measures. Notably, the amplitude of the P1 component was almost identical in face and objects data (faces: 2.38 ± 0.26 mV, objects: 2.39 ± 0.36 mV (mean ± SEM); F (1, 18) = 0.08, P = 0.95).

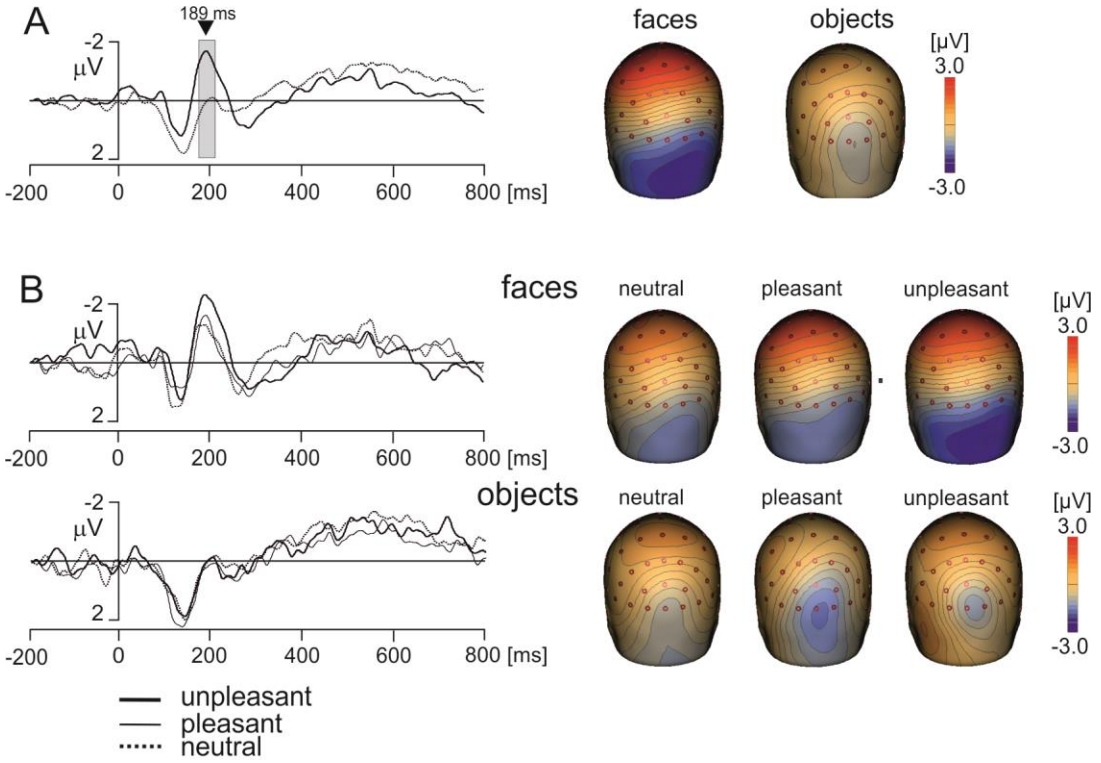

Figure 4.4.4.2 Grand average EMRP waveform for combined electrodes P8 and PO8. A. Mean EMRP for all face and object conditions. The highlighted area represents the time window (175 ms – 212 ms) in which a statistically significant effect of picture type was found (P < 0.0001). B. EMRPs for all three hedonic valence conditions for face and place images.

The P1 component was influenced neither by hedonic valence of pictures (F(2,36) = 0.41, P = 0.77) nor the interaction between the type of pictures and hedonic valence µ2, 36) = 1.86, P = 0.17). It is therefore unlikely that the findings pertaining to

the face-sensitive time interval (170 - 210 ms) would be affected either by low-level visual features of stimuli or differences in oculo-motor activity during viewing the pictures.

4.5 Discussion

Recording brain electrical activity in natural settings during free visual exploration of the environment poses both technical and data analytical challenges. To the best of our knowledge, this study is the first to demonstrate the presence of a face-sensitive scalp potential during viewing of human faces in natural settings. The detection of the face-sensitive potential in freely moving subjects using wireless EEG recordings could be accomplished owing to recent advances in EEG technology and data processing techniques. Our study uses an active electrode wireless EEG system which has been shown to cancel external electromagnetic noise (van Rijn et al., 1990). Unlike previous studies employing MoBI during walking or running (De Sanctis, Butler, Green, Snyder, & Foxe, 2012; Gramann et al., 2011; Gwin et al., 2010), head and body movement artifacts associated to the swaying of electrode cables were minimal in the present study because subjects stood calmly while viewing pictures. Furthermore, our gaze time analysis showed that all images, irrespective of their category and condition, were viewed for the same amount of time (approximately 3s).

The N182 potential in our study showed a typical spatio-temporal pattern consistent with the N170 face potential occurring during viewing faces in laboratory type of EEG recordings, however, it was virtually absent during viewing objects. The face-sensitive N182 component activity also differentiated disgusted and neutral faces evidencing that modern wireless mobile EEG recordings acquired in natural settings have the capacity to resolve emotional expressions of faces.

The face-sensitive N182 component of EMRPs was modelled by an ECD located in the right fusiform area (Brodmann area 37) in the medial occipitotemporal cortex. The presence of a source in the fusiform gyrus is consistent with its role as a dominant face processing region (Kanwisher et al., 1997; Yagi, 1981b). Localizing the source of

the N182 component in the fusiform gyrus is also consistent with previous source localization studies of face-sensitive potentials in scalp EEG data (Bötzel, Schulze, & Stodieck, 1995; Carretié et al., 2013; Deffke et al., 2007; Sadeh et al., 2010; Trautmann-Lengsfeld et al., 2013) (reviewed in Rossion & Jacques (2011)) and in intracerebral, subdural (Allison, Puce, Spencer, & McCarthy, 1999) or depth electrode recordings (Barbeau et al., 2008).

ECD3 was localized to the fusiform area. The activity originating from this region showed a peak latency of 186 ms which falls within the broad latency limit of the N170 component ranging from 120 to 200 ms (Rossion, 2014). In contrast to face pictures, the source activity in the fusiform cortex was at a baseline level at the latency of 180-190 ms when subjects were viewing objects. This sharp contrast of the activity in fusiform cortex between viewing faces and objects strongly supports our conclusion that the N182 component of EMRP is equivalent to the face-sensitive N170 component in event-related potential recordings acquired in laboratory conditions.

One of the methodological challenges consisted in the separation of the lambda complex from corneoretinal artifacts of different origins. Eye movement artifacts are generated in most cases by rotations of the corneoretinal dipole crossing each eye predominantly in antero-posterior direction during eye blinks and saccades (Berg & Scherg, 1991; Dimigen et al., 2011; Nikolaev et al., 2016). The eye movement artifacts associated with eye blinking were removed at the pre-processing stage using a well-established pattern matching algorithm (Ille et al., 2002). To separate the genuine cortical potentials from the saccadic potentials, we employed a source dipole modelling approach. As saccadic eye movements associated with shifting the gaze towards different pictures had variable orientations, it was not possible to model the saccadic potentials using a set of equivalent current dipoles tuned to different directions of saccades (Berg & Scherg, 1991). Therefore, two sets of regional sources with fixed origins were placed to model the electrical dipoles resulting from the displacement of the eyeballs during saccadic movements in any direction. As each regional source had an identical spatial origin, the regional sources captured the saccade potentials irrespectively of the exact direction of a saccade at a particular instant. Further,

employment of regional sources did not require modelling the residual corneoretinal or saccade potential at a specific latency period which allowed us to capture the components of the eye movement artifacts even in the presence of a slight latency jitter related to about 20 ms asynchrony between EEG and eye-tracking data streams.

The EMRP waveforms in the present study featured a prominent lambda potential complex (Yagi, 1979b, 1981b). The P1 component of lambda potential in the present study had a slightly longer peak latency of 120 ms compared to the 70-80 ms latency seen in earlier studies (Thickbroom et al., 1991; Yagi, 1982), but was close to the peak amplitude at a latency of 100 ms reported in more recent studies (Dimigen et al., 2011; Körner et al., 2014). These latency differences may be related to methodological and experimental variations across studies (Kamienkowski et al., 2012). For instance, the peaks of lambda potential have been shown to occur about 20 ms later if the time locking event is a saccade onset compared to setting the time-locking event to a fixation onset (Kaunitz et al., 2014).

The source activity generated in the medial occipitotemporal cortex also differentiated emotional expressions. Disgusted faces evoked stronger source activity than neutral or happy faces. Although earlier studies have questioned the capacity of the face-sensitive N170 component to differentiate emotional expressions (Martin Eimer et al., 2003; Herrmann et al., 2002), one recent study (Trautmann-Lengsfeld et al., 2013) and a recent meta-analysis involving 57 ERP studies involving a variety of emotional expressions showed that the face-sensitive N170 component also differentiated emotional faces from neutral faces (Hinojosa et al., 2015). A comparatively strong amplitude modulation of the face-sensitive component by disgusted faces in the present study suggests that emotional and neutral face expressions are perceived differently while standing and behaving spontaneously. This may be related to participants standing upright in the present study as posture has been shown to affect a number of neurophysiological and cognitive parameters (reviewed in Thibault & Raz (2016)). The specific role of posture on the face-sensitive ERP component and subjective ratings of different emotional expressions will be addressed in a future study. While this effect has

been studied for auditory evoked components in the past (De Vos, Gandras, & Debener, 2014), this has yet to be done for emotional visual stimuli.

In contrast to previous laboratory studies of which some have found a modulation of mid- and long-latency event-related potential components by emotional expressions of faces (Eimer et al., 2003; Trautmann-Lengsfeld et al., 2013), our study did not identify any distinct evoked potential components in the latency epochs >300 ms. The absence of clear EMRP in the mid- and long-latency range may be limitation of wirelessly recorded data in freely behaving individuals. In contrast to laboratory studies, exploration of environment in the real world is a trans-saccadic process involving short-term visual memory, reframing, and prediction (Melcher & Colby, 2008). These higher order perceptual and cognitive processes continue during the exploration of a scene and since they would not show a fixed phase relative to the time-locking event, the resulting event-related potentials may not show any well-defined spatio-temporal components.

It should be pointed out that the face-sensitive EMRP component analysed in individual scalp electrodes did not resolve the hedonic valence of faces pictures. In the framework of mobile brain imaging (Gramann et al., 2010; Gwin et al., 2010, 2011), source dipole localization is an important element in the data processing pipeline because it allows for separation of cerebral and extracerebral contributions to scalp potentials. In the present study, source dipole localization separated the occipital cortex activations associated with lambda potential from the face-sensitive N182 component. Therefore, source waveform data were more specific to face processing and extracted the face-sensitive activation better than scalp electrode data. The methodological feature of wirelessly recorded EEG data in freely moving individuals needs to be taken into account when comparing our data with previous lab-based studies of the N170 potential.

The difference between the current experiment and previous research may be related to the fact that, in contrast to previous studies where subjects were seated and passively viewing a computer monitor, the subjects in our study were standing and able to freely control their movements. The effects of body posture and freedom of making simple behavioral decisions on emotional expressions is still poorly understood. Humans may perceive different levels of various coping resources while standing

compared to sitting or reclining. For instance leaning forwards compared to reclining has been shown to shorten reaction times and increase the late cortical positive potential for appetitive cues (Price, Dieckman, & Harmon-Jones, 2012). Since an appraisal of coping resources contributes to the perception of a situation as taxing or stressful (Lazarus & Folkman, 1984), it is likely that emotional responses and their cortical representations may have different characteristics in people while moving and behaving freely compared to when they are seated and restrained by a laboratory setup. The finding of stronger anticipatory anxiety before a stressful mental arithmetic task during standing than supine (Lipnicki & Byrne, 2008) suggests that emotional processing of the same stimuli may vary depending on the body posture. Future studies should more carefully address the effects of body posture on emotional and cognitive processes, including face processing; as future findings acquired using mobile EEG recordings in natural settings will likely differ from those acquired in laboratory conditions.

To conclude, we showed that EMRPs acquired using combined eye-tracking and wireless EEG recordings in freely moving individuals clearly differentiated between viewing a human face and a non-living object as well as between types of emotional face expression. These findings open new questions, for instance the effect of posture on naturally occurring ERPs. The methodology presented provides a range of experimental and applied research possibilities in multiple domains including social and developmental psychology, medicine, and consumer science.

Chapter 5

Effect of face familiarity on eye-movement related potentials in natural settings

Soto, V. [1], Tyson-Carr, J. [1], Kokmotou, K. [1,2], Roberts, H.[1], Cook, S. [1], Fallon,. [1], Giesbrecht, T. [3], Stancak, A. [1,2]

[1] Department of Psychological Sciences, University of Liverpool, Liverpool, United Kingdom,

[2] Institute for Risk and Uncertainty, University of Liverpool, Liverpool, United Kingdom,

[3] Unilever Research & Development Port Sunlight Laboratory, Merseyside, United Kingdom

This experiment investigated the effects of familiar and unfamiliar faces expressed in the N170 potentials in a natural setting using mobile brain and body imaging. The manuscript for this paper is currently being prepared to submit for publication.

The roles of the co-authors are summarised below:

I designed the study in collaboration with Andrej Stancak and collected the data. John Tyson-Carr, Katerina Kokmotou, Hannah Roberts and Stephanie Cook assisted with the collection of data and contributed useful comments whilst preparing the manuscript. Andrej Stancak, Nicholas Fallon and Timo Giesbrecht contributed to the large-scale planning of this project Andrej Stancak, Nicholas Fallon and Timo Giesbrecht secured funding for project.

5.1 Abstract

In a previous study we used mobile brain and body imaging (MoBI) in freely moving subjects to identify modulations on the N170 face component resulting from differences in emotional expression. The N170 amplitude encoded negative emotional expressions of faces relative to neutral ones. The present investigation aimed to analyse the effects of familiarity on the N170 component activations recorded in unrestricted subjects.

Mobile EEG and eye movement data were recorded from 19 participants during free viewing of familiar and unfamiliar pictures of faces and places. Eye-tracking data was then used to register stimulus onset times into the continuous EEG data after synchronising both time axes. Eye movement related potentials (EMRPs) were computed from wirelessly recorded EEG data time locked to the initial contact of the subjects gaze with an image.

Independent component analysis of the grand averaged EMRPs revealed four independent components of interest. A strong positivity peaking at 90 ms over occipital electrodes was identified as the lambda component. Only when faces, but not places, were viewed, a face specific component presented as a sharp negative peak at 159 ms over occipito-temporal areas of the cortex. This component however, did not resolve overall level of familiarity faces or places images. Additionally, two distinct independent components were identified in relation to the encoding place images at different latencies. An early bilateral occipital positivity at 129 ms followed by a negative component peaking at 183 ms over the posterior midline was observed when place images were viewed. The statistical comparison of the ICs did not present any effect of familiarity on N170 component activity.

Results replicate previous findings and demonstrate further the possibility of recording face-sensitive components in unrestricted EEG subjects. The technique presented here opens new opportunities for not only cognitive neuroscience research, but also for fields including forensic psychology, developmental neuroscience and marketing research.

5.2 Introduction

Face recognition is a crucial cognitive mechanism for human behaviour. This adaptive behaviour requires, at the minimum, the fast recognition and correct interpretation of a face stimulus, normally within a crowded environment full of salient cues. As such, when scanning a natural scenes for the presence of faces, detection is aided by preferentially identifying salient features characterising faces, i.e. the mouth and eyes (Mertens, Siegmund, & Grüsser, 1993). A perceptual advantage towards faces has been shown under poor viewing conditions (Burton et al., 1999) as well as in complex crowded visual scenes (Kaunitz et al., 2014). However, humans' ability to remember or match unfamiliar relative to familiar faces is consistently less accurate (reviewed in Hancock, Bruce, & Burton, 2000) and has been shown to be worse in ecologically valid settings than in lab-based testing (Logie, Baddeley, & Woodhead, 1987). Studies employing famous faces have also shown that familiarity enhances perception and facilitates the recognition of emotional expressions in a difficult recognition tasks (i.e. very short stimulus presentation times < 100 ms) (Baudouin & Sansone, (2000). Furthermore, the recognition of personally familiar faces has also been shown to facilitate the detection of neutral facial expressions relative to emotional ones (Endo, Endo, Kirita, & Maruyama, 1992). To explain these differences, the distinction between first and second order processing has been proposed as critical mechanisms for perceiving and identifying famous faces (Maurer, Le Grand, & Mondloch, 2002).

The neural correlates of face processing have often been studied using electroencephalography (EEG). Specifically, event related potentials (ERP) are a well-established method for examining differences in brain activity arising from the viewing of faces. The face-specific (N170) component is negative brain potential appearing over lateral occipito-temporal regions of the scalp that responds selectively for faces, but not objects such as houses or cars (Bentin, Allison, Puce, Perez, & McCarthy, 1996; reviewed in Rossion & Jacques, 2008). It has been theorized the N170 would reflect an early stage of structural encoding of faces. Recent findings however, have suggested that the N170 component not only reflects low-level visual features of a human faces, but could also represent conscious awareness of the presence of a face in the visual field

(reviewed in Olivares, Iglesias, Saavedra, Trujillo-Barreto, & Valdés-Sosa, 2015; Rossion, 2014) and encodes differences in emotional facial expressions (reviewed in Hinojosa, Mercado, & Carretié, 2015). As such, the N170 component would reflect an early processing stage that would occur previous to higher order representations, like discerning identity. Previous experimental work has challenged this idea presenting conflicting results in the literature. For instance, using a face recognition task with sequentially presented matching and non-matching pairs of faces, Barrett, Rugg, & Perrett (1988) observed enhanced amplitudes in the N170 waveform in posterior scalp locations for non-matching conditions relative to matching ones. The N170 component can resolve familiar and unfamiliar faces with findings showing smaller amplitudes found for familiar relative to unfamiliar faces (Campanella et al., 2000). However, multiple studies have reported a lack of effect instead (Rossion et al., 1999; Schweinberger, Pickering, Jentzsch, Burton, & Kaufmann, 2002). Alternatively, results presented by Caharel et al., (2002) show effects of familiarity when comparing the N170 amplitudes in response to famous, relative to unknown faces during a serial visual presentation task.

While the N170 component has been successfully identified under free-viewing conditions (Johnston et al., 2014), the bulk of ERP research into familiar face processing has been performed in traditional lab-based settings. The experimental control afforded by the lab environment has allowed researchers to accurately control the presentation stimuli by flashing unfamiliar and familiar faces on a computer monitor. This has enabled time-locked EEG signals to be recorded in noise-free settings optimizing the signal to noise ratio of the EEG recordings. Nevertheless, the environmental conditions afforded by these testing conditions are significantly different from those occurring during natural cognition. To the best of our knowledge, the neural correlates of free-viewing familiar and unfamiliar faces in natural scenarios are yet to be investigated.

A recent study from our group (Soto et al., 2018) showed the possibility of recording high quality EEG signals from freely roaming human subjects. When examining face-sensitive brain potentials in freely moving subjects, significantly larger N170 waveforms to faces relative to objects and an effect of emotional condition was

found at the source waveform level. Significantly higher EMRP amplitudes presented for negative valence faces relative to neutral ones. This opens the question whether MoBI could be used to further our understanding on the role of the N170 in human face recognition. In the present investigation we apply a mobile brain and body imaging (MoBI) methodology to investigate familiar face processing in a naturalistic environment. We hypothesized that within natural settings, famous faces would generate enhanced brain responses relative to unknown ones. Following the method presented in our previous paper, mobile EEG data and parallel eye-tracking recordings were synchronized offline and used to inform the EEG analysis regarding the onset of naturally occurring events. Subjects viewed portraits of famous and unknown faces presented on panels that hung on the walls of an open corridor. The aim was to determine to the effects of familiarity on face-sensitive eye movement related potentials (EMRP) elicited in an environment resembling an art gallery. As such, we examine the functional significance and temporal dynamics of N170 components response to famous and unknown faces. A secondary aim was to replicate our previous findings suggesting the N170 components involvement in encoding higher order information of faces i.e. identity.

5.3 Materials and methods

5.3.1 Participants

Twenty-three healthy volunteers 26.9 ± 5.1 years old (mean ± SD), were recruited for the study. All participants resided in Liverpool at the moment of testing and all but two were University of Liverpool students or staff. The EEG data of three subjects were discarded due to loss of during the recording. Data from one additional subject was discarded due to a loss of registration of the synchronization light in the eye-tracking recording. Therefore the final sample was composed of nineteen normal subjects (10 females) with an average age of 26 ± 5 years. Experimental subjects gave written informed consent prior to taking part of the study in agreement with the ethical approval obtained from the University of Liverpool Research Ethics Committee.

Participants received £20 as compensation for their travel expenses and time. All experimental procedures were conducted in a single session in accordance with the Ethics committee of the University of Liverpool.

5.3.2 Stimuli

All stimuli were presented on twenty A0 poster-size panels. Each panel contained 9 different stimuli images presented in full colour approximately 20 cm × 25 cm in size and a fixation cross in the centre (14.3 cm × 14.3 cm) printed onto a blank paper sheet (Figure 5.3.2A). As such, each panel had at the minimum four faces images (two of which were familiar faces) and four place images (two of which were familiar places) were displayed on each panel. All panels were pasted onto Styrofoam sheets and attached to the walls using adhesive tape. Two hallways within the Eleanor Rathbone Building of the University of Liverpool were used to create a mock art gallery where the experiment took place.

Ninety face images and ninety place images were selected from online searches exclusive to public domain images available under creative commons licences for reuse with modification. All 180 were cropped to match in size and quality (300 dpi) using Corel Picture software. Face images were always presented as standard portrait shots including the shoulders. Place images were cropped and presented as either landscape or portrait. In each category half the images were familiar and half were unfamiliar.

Familiar faces were selected from a wide spectrum of identifiable personalities from the United Kingdom and abroad. This included well known celebrity actors (e.g. Jennifer Aniston, John Cleese), national politicians (e.g. Theresa May, James Cameron) and international politicians (e.g. Hillary Clinton, Donald Trump) as well as contemporary pop-music icons (e.g. Amy Winehouse, Justin Bieber). Familiar places included local Liverpool landmarks residents would be familiar with given that all subjects resided in Liverpool at the time of testing (e.g. The Albert's Dock, Liverpool Metropolitan Cathedral), images from the University of Liverpool campus (e.g. Victoria building, Abercrombie Square) and famous international locations (e.g. Golden Gate

Bridge, Buckingham Palace). Unfamiliar places were selected to match the familiar place images in size and general level of complexity while unfamiliar faces were selected to match the famous ones for sex, age and gender.

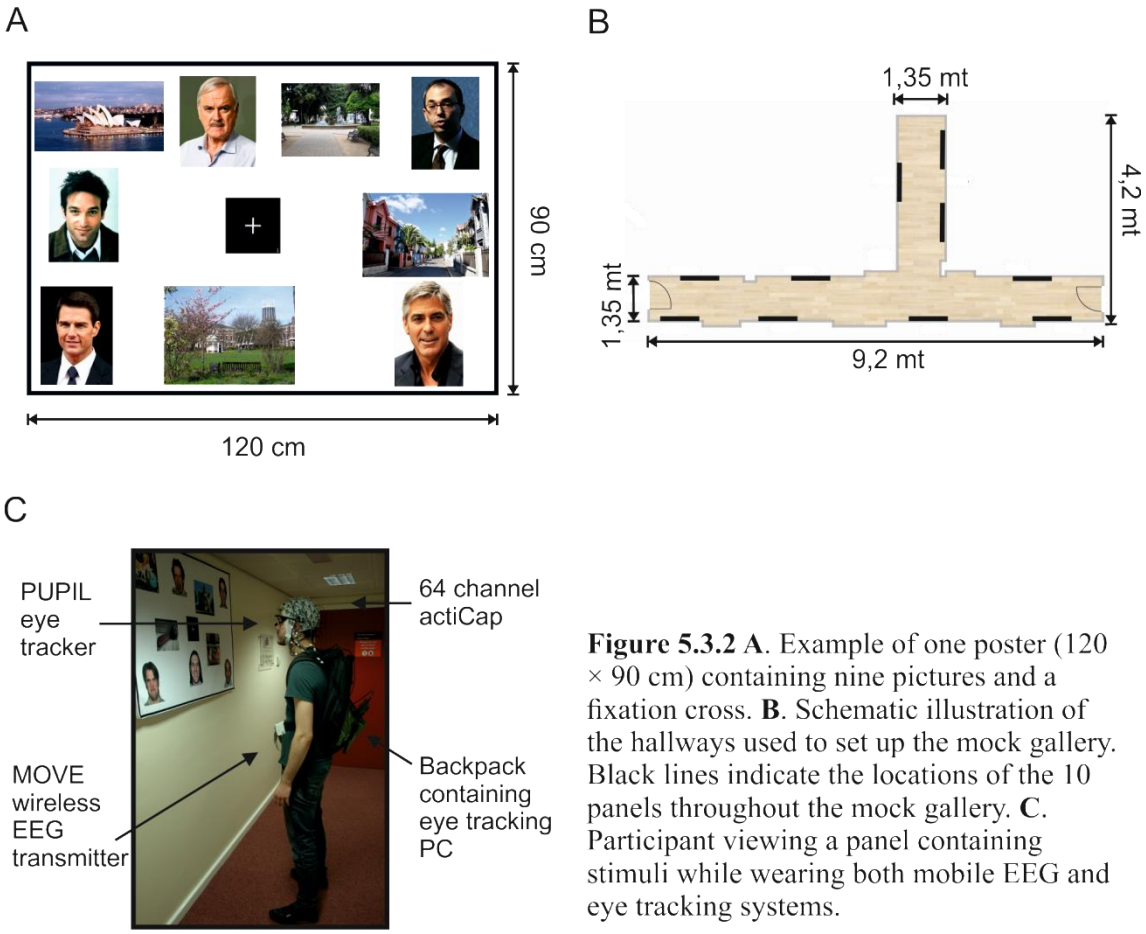

Figure 5.3.2 A. Example of one poster (120 × 90 cm) containing nine pictures and a fixation cross. **B**. Schematic illustration of the hallways used to set up the mock gallery. Black lines indicate the locations of the 10 panels throughout the mock gallery. **C**. Participant viewing a panel containing stimuli while wearing both mobile EEG and eye tracking systems.

5.3.3 *Procedure*

The mobile EEG system was connected and impedances checked on subjects before MOVE wireless system was connected. Wireless signals were inspected on a standing participant. Next, eye-tracking glasses (PUPIL) (Kassner et al., 2014) were placed on the participant over the EEG cap. The eye trackers were calibrated against a blank white panel at a distance of 1 meter. Gaze-tracking was optimized by means of a 3D calibration routine using manual markers. Following the method described in Soto et al., (2018), a MoBI framework was applied as it has proven a valid method for recording EMRP in naturally behaving individuals.

5.3.4 Gallery task

A mock art gallery was created by hanging the stimuli panels on bare walls in designated hallways (a schematic illustration can be found in Figure 5.3.2 B). Participants were requested to walk through the mock art gallery while viewing the images displayed on each panel. Subjects were free to navigate the gallery in any order they chose and view individual pictures in any order and for as long as they wished; the only instruction they received was to stand facing each panel and to view each image for a few seconds before moving onto the next image. Participants were asked to look at the centre fixation cross before commencing each image, and to return their gaze to the fixation cross before moving to a next picture. During the gallery blocks, participants selecting preferred face and object images as well as their disfavoured face and object from each panel. Picture preferences were indicated by marking selected pictures on a small paper prints. The full experiment consisted of two blocks in the mock gallery. Each gallery block contained ten panels with nine images on each. In total, participants viewed 180 different images in the experiment. On average each gallery block lasted approximately 15 to 20 minutes. The corridors were not closed off on either side nor were there attempts to discourage other people from passing through it while an experimental session was in progress. As in the real world passers-by occurred in the corridors at times.

5.3.5 Behavioural ratings

Once the gallery task was completed, the EEG cap and the eye-tracking glasses were removed. Participants were requested to rate how much they liked and how familiar each image seen in the mock gallery was. Ratings were performed using two visual analogue scales (VAS) sized 10 cm and anchored on each extreme (i.e. '*0: Do not like' up to '100: Like very much' and* '*0: Avoid' up to '100: Approach'*). Pictures and rating scales were presented on a LCD screen using Cogent program v. 1.32 (Welcome

Department of Imaging Neuroscience, United Kingdom) running on MATLAB v. R2014a (The MathWorks, Inc., USA).

5.3.6 Data synchronization

A light emitting diode (LED) was fitted to a trigger box and was used at the beginning of each experimental block to synchronise data streams. A pulse of flashing light was recorded in the world-view camera on the eye trackers as a simultaneous transistor-transistor logic (TTL) pulse was registered in the EEG data recording. In doing so, the light cue was visible at a specific frame in the eye-tracking video data. The offset frame was then registered and used to temporally synchronize the EEG and eye-tracking data streams offline. The temporal asynchrony has been tested previously by simultaneously delivering light flashes from the eye-tracking and TTL pulses to the EEG recording system. The asynchrony was of 0.022 ± 0.020 s (mean ± SD) over a 15-min recording. Electrode impedances and gaze tracking calibration were checked and corrected between blocks if required.

5.4 Eye movement recording and analysis

Gaze positions were recorded using a PUPIL 120 Hz binocular eye-tracking system and Pupil Capture software v 0.9.6. running on Ubuntu v 14.04.4. The PUPIL eye tracker is a high resolution lightweight wearable eye-tracking system. The PUPIL software suit is a cross-platform (Linux, Mac, and Windows) open-source software which is actively maintained and supported by the developers (Kassner et al., 2014). Eye-tracking data and the real world video streams were set at a sampling rate of 60 frames per seconds to avoid processing lag in the recordings.

The ocular pupils of both eyes were located based on a centre-surround detection algorithm (Świrski et al., 2012). To calibrate the gaze locations a manual marker 3D calibration protocol was used to generate a 9-point grid in the field of view of the participant. Calibration was repeated until gaze positions were accurate everywhere on

the blank panel. The Pupil Capture software processes three video streams (two eye cameras and a world view camera) synchronously and allows for mid-recording calibrations. These video streams are read and exported using Pupil Capture software for real-time pupil detection, recording, and gaze mapping. The gaze mapping function allows the eye positions to be superimposed onto the world-view scene space. Exported PUPIL gaze raw data is time-locked to the processing computer's internal clock, giving millisecond precision to the eye measurements.

Eye-tracking data were processed using Pupil Player v 0.8.1 program. Fixation offsets were corrected using manual gaze correction in Pupil Player and fixation jitters were resolved using in-house scripts on MATLAB v. 2014a and v. 2017a. Raw gaze positions were exported using the Pupil Player Raw Data Exporter plugin. Exported files contained gaze positions, eye positions and level of confidence for each individual frame and an accurate time stamp based on the PC processor real-time clock.

Eye-tracking video files were visually inspected and stimuli onsets were manually tabulated. Each stimulus was logged on a picture-by-picture basis with stimulus onset defined as the first instance where the gaze position touched or landed on an image. The onset times were always tabulated in the same manner, maintaining strict adherence to the selection criteria (i.e. first visible instance the gaze position contacted an image). The real times corresponding to the tabulated frames were used to import stimulus onset latencies onto the raw EEG data. Four subjects' data was excluded from the sample due to loss of gaze calibration during the recordings.

5.5 EEG recordings

Whole scalp EEG data was continuously recorded using a 64-channel wireless and portable EEG system (Brain Products, GmbH, Münich, Germany). The wireless interface (MOVE, Brain Products, GmbH) utilizes a lightweight signal transmitter which participants carry on a belt (Figure 5.3.2 C). Active Ag/AgCl EEG electrodes were mounted on an electrode cap (actiCAP, Brain Products, GmbH) according to the 10-20 electrode system. EEG recordings were sampled at a rate of 1000 Hz. Electrode

FPz was established as the system ground and electrodes were referenced to Fz. The EEG cap was aligned in respect to the midpoint between the anatomical landmarks of the nasion and inion, and the left and right preauricular points. Electrolyte gel (Signa Gel, Parker Laboratories, Inc., Fairfield, NJ) was applied to maintain electrode-to-skin impedances under 50 kΩ. EEG average reference was applied and signals were digitized at 1 kHz on a BrainAmp DC amplifier linked to Brain Vision Recorder program version 1.20.0601 running on a Windows laptop.

5.5.1 Eye movement related potentials

After synchronization, event markers were inserted into EEG data by synchronizing the time axes of the EEG and eye-tracking system. EEG data were pre-processed using the Brain Electrical Source Analysis program (BESA v.6.0, MEGIS Software GmbH, Munich, Germany). Data were first referenced to a common average using common averaging method (Lehmann, 1987) on the continuous EEG signal. EEG data were epoched to range from -200 ms to 600 ms and the mean EEG activity in the baseline interval ranging from -200 ms to -100 ms was removed from each data point. The onset of a stimulus was defined as the first contact of the gaze with any part of a picture in each of the 180 images. This time point effectively corresponded to part of the saccade which brought the gaze onto a particular face or object in a picture. Eye blink artifacts were removed using a pattern matching algorithm involving principal component analysis (Berg & Scherg, 1994; Ille, Berg, & Scherg, 2002). Then, EEG data was visually inspected for movement or muscle artifacts and trials contaminated with large artifacts were marked and excluded from further analysis. Post-saccadic EMRPs were computed from all trials falling into four different conditions (face vs objects and familiar and unfamiliar images). The data was visually inspected and corrected for the presence of artifacts. Trials were excluded if artifacts were present in either eye-tracking or EEG data. If participants skipped an image, failed to fixate, or gaze tracking was lost during fixation, the concurrent trial was discarded.

The sampling rate of the eye-tracking device was calculated offline from the subjects included in the analysis (44.7 Hz ± 5 Hz). Given the relatively slow sampling

rate, we have not analysed eye movement data further. Thus, EEG epochs were formed as cuts into a wild video scene similar to a recent study (Simola et al., 2015).

5.5.2 Independent component analysis

An extended Infomax independent component analysis (ICA) (Delorme & Makeig, 2003; Lee, Girolami, & Sejnowski, 1999) was applied to decompose the grand average EEG signal into temporally independent and spatially fixed components between -100 ms to 300 ms. Using the default setting in BESA v 6.1, the ICA procedure reduces the dimensionality of data via principal component analysis (PCA). All principal components explaining less than 1.0% variance are ignored, effectively reducing the rank of the data to components that are maximally uncorrelated. ICA decomposition, also referred to as blind source separation, was performed on the EMRP grand averaged waveforms across all four conditions and a super grand average condition including all trials. Twenty four independent components (ICs) were estimated from the grand averaged scalp activity. To assess the contribution of an individual IC component to the signal, temporal and spatial features of all ICs were carefully examined and those evidencing task related activity were selected between 0 ms and 300 ms.

Four ICs of interest were identified on the basis of spatio-temporal features as well as the peaks of activity in response to our different experimental conditions. Task relevant ICs were maintained whilst outlying components were removed from the data. In a method similar to that found in Vigon, Saatchi, Mayhew, Taroyan, & Frisby,(2002), the remaining ICs were then projected back onto all scalp channels, band-pass filtered at 0.5 Hz and 45 Hz and were re-referenced to the common average reference.

Further analysis was performed on the isolated IC activity. The averaged waveforms and scalp projections for each IC of interest are investigated in all experimental conditions. The amplitude of ICs were statistically compared to examine the effect of familiarity on source activity.

5.5.3 Statistical analysis

Independent component waveform activity was analysed using a 2 × 2 analysis of variance (ANOVA) (familiarity × category) for repeated measures for each relevant IC. To control for the risk of false positive results due to a large number of tests, P values were corrected using permutation analysis including 1000 permutations (Maris & Oostenveld, 2007). This analysis was used to identify the latency interval in which faces and place image categories would differ maximally. Any intervals showing statistical significance in the baseline -200 to 0 ms were not investigated. No statistical differences were apparent in the baseline period of -200 ms to -100 ms latencies for any cluster. Average IC activity in intervals of interest was analysed further using SPSS v.22 (IBM Corp., NY, USA). Post hoc paired t-tests were performed when necessary and considered significant at $P < 0.05$ with Bonferroni corrected for multiple comparisons. The statistical confidence level of $P < 0.05$ was always employed.

5.5.4 Source Analysis

An exploratory source analysis was performed on each IC weighted dataset separately using the sLORETA software v. 20150415. Source analysis was applied on the weighted back-projections of the grand average isolated IC waveforms to identify individual generators for each IC of interest. Low Resolution Electromagnetic Tomography (LORETA; (Pascual-Marqui et al., 1994) is a common method for estimating generators of cortical activity. The head model included a grid of 6239 voxels at 5×5×5 mm^3 spatial resolution, representing the full cortical surface. This method allows sources of activity to be distributed throughout the whole brain rather than only surface/cortical sources of activity. Using this method, deep and cortical sources have the same chance of being reconstructed and therefore, offer a considerable advantage over other methods which preferentially model sources close to the cortical surface (Grech et al., 2008).

5.6 Results

5.6.1 Picture ratings

Figure 5.6.1 displays the average rating-scores across three different visual analogue scales for each experimental condition. Repeated measures analyses of variance (ANOVA) were computed to test for categorical (face and place images) and familiarity (familiar and unfamiliar images) effects on rating scores for each rating scale (likability, arousal and familiarity. A 2 × 2 ANOVA (familiarity × category) for repeated measures was performed separately on each one of the three rating scales.

Likeability scores revealed a preference for place images (M= 61.9, SD =5.0) relative to faces (M = 51.4, SD = 5.0). The ANOVA showed an effect of familiarity on likability rating behaviour ($F(1,18) = 35.835$, $P < 0.001$) in which familiar images (M = 67.0, SD = 8.5) were preferred over unfamiliar images (M = 55.9, SD = 11.6) ($t(1,18) = 3.49$, $P < 0.005$). Categorical effects ($F(1,18) = 31.441$, $P < 0.001$) between faces and places were explored using paired samples t-tests. Statistical comparisons indicated that place images (M = 61.9, SD = 6.8) were rated as more liked than face images (M =51.4 , SD = 5.03) ($t(18) = -5.6$, $P < 0.001$). There was no significant interaction. As expected, average ratings for level of familiarity confirmed the existence of strong effect in rating behaviour ($F(1,18) = 31.4$, $P < 0.001$). Familiar images (M = 76,5, SD = 10,7) were indeed more recognizable to participants than their unfamiliar (M = 5.9, SD = 4.8) counterparts ($t(18)= 23.58$, $P < 0.001$). No effect of category ($F(1,18) = 0.071$, $P > 0.5$) suggests that both face and place stimuli maintained similar levels of familiarity in each category throughout the experiment.

The arousal ratings showed significant effects for familiarity ($F(1,18) = 30.5$, $P < 0.001$), but not category ($F(1,18) = 2.2$, $P > 0.05$). While familiar images (M = 55.9, SD = 15.9) were found more arousing than unfamiliar images (M = 44.4, SD = 13.4) ($F(1, 18) = 30.5$, $P < 0.001$) no differences amongst categories were encountered ($F(1,18) = 2.262$ $P = 0.15$). An interaction effect between familiarity and image categories was observed ($F(1,18) = 16.033$, $P < 0.002$). Familiar faces (M = 57.9, SD = 21.1) were considered more arousing than familiar places (M = 34.8, SD = 15.8), but this difference

was not significant (t(18) = .651 p > 0.05). Unfamiliar places (M = 44.4, SD =13.3) however, were perceived to be significantly less arousing than unfamiliar places (M = 34.8, SD = 15.7; t(18) = -3.388, P < 0.005).

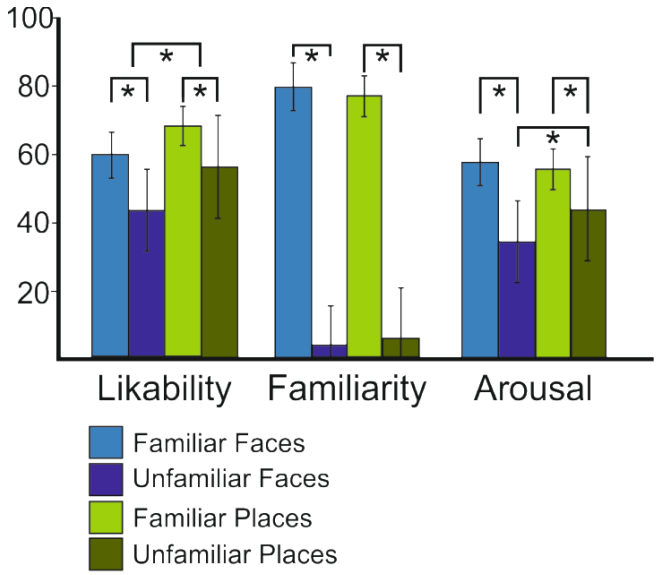

Figure 5.6.1. Grand average ratings for each visual analogue scale (VAS). Blue colours are face images and green colours are place images. Light colours represent familiar images and dark colours represent unfamiliar images * indicate significant differences (p<0.05) in rating behaviour.

5.6.2 Eye movement related potentials

Subjects maintained a stable stance during viewing the pictures minimising any neck muscle or head movement artifacts which have been shown to heavily affect EEG data during locomotion (Gwin et al., 2011). A total of 180 images (45 Familiar Faces, 45 Familiar Places, 45 Unfamiliar Faces and 45 Unfamiliar Places) were seen by each participant. All data were visually inspected and corrected for the presence of artifacts with trials being excluded if artifacts were present in either eye-tracking or EEG data. If participants skipped an image, failed to fixate, or gaze tracking was lost during viewing,

the concurrent trial was removed. The average number of accepted trials in each condition was 35.6 ± 4.65 familiar faces, 37.2 ± 3.7 unfamiliar faces, 36.8 ± 4.1 familiar places and 38.2 ± 3.7 unfamiliar places. No significant differences were found in the amount of trials included in each experimental condition ($p > 0.05$).

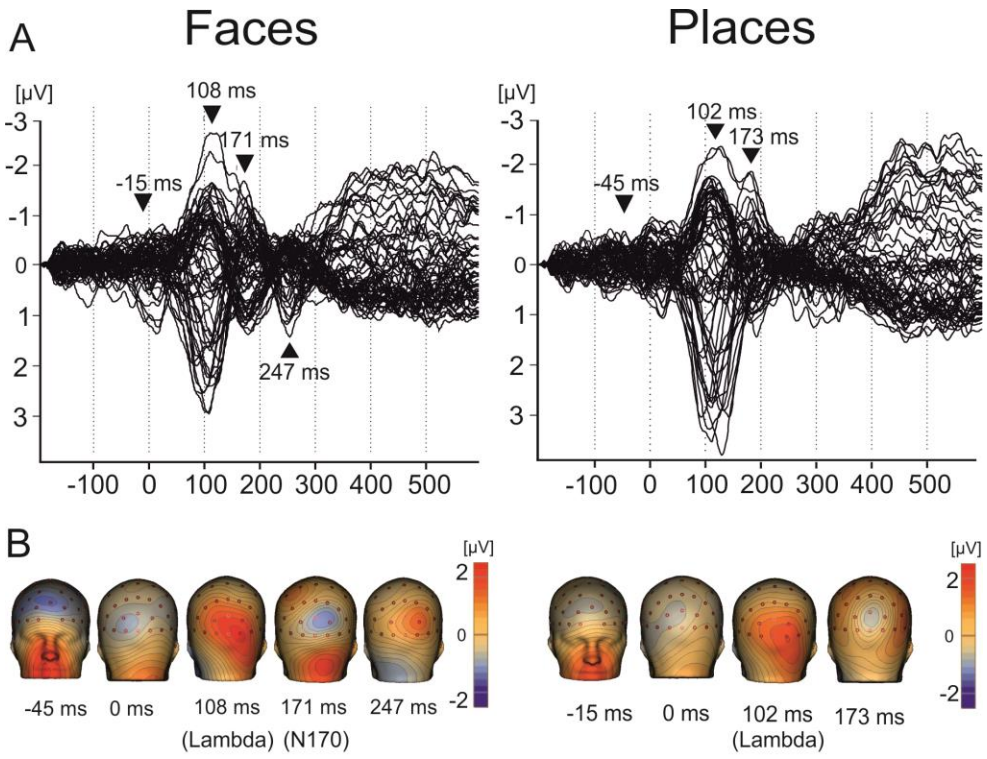

Figure 5.6.2: Grand average EMRPs in face and place pictures. A. Butterfly plots of grand average EMRPs to face and object pictures. Peak latencies of face (-45 ms, 0 ms, 108 ms, 171 ms, 247 ms) and objects (-15 ms, 0 ms,108 ms, 171 ms) EMRPs components are highlighted with arrows. B. The topographic maps of grand average EMRPs overlaid on the volume rendering of the human head at five latency points in face EMRPs (-45 ms, 0 ms, 108 ms, 171 ms, 247 ms) and object EMRPs (-15 ms, 0 ms,108 ms, 171 ms)

Figure 5.6.2A shows butterfly plots of EMRPs for face and place images and Figure 5.6.2B illustrates the spatial topographic maps of distinct EMRP components seen across the scalp. The butterfly plots show stable baselines as well as clear evoked components in the P1 and N170 latencies. A positive peak was seen at approximately 250 ms in face, but not place, conditions.

5.6.3 Independent components analysis

Grand average waveforms were decomposed into their statistically maximally independent components using the default extended Infomax ICA in EEGlab toolbox. Four ICs of interest were selected on the basis of their temporal characteristics and back projected scalp distributions (Figure 5.6.3A). Grand average IC1 presented dorsal positivity at latencies surrounding 90 ms post stimulus onset. This positive waveform was identified as the lambda potential over posterior sites on the scalp (Thickbroom et al., 1991; Yagi, 1981a). The component showed a large waveform peaking at 90 ms in place and 92 ms in face conditions. All lambda potentials showed a prominent positivity at occipital electrodes across all conditions (Figure 5.6.3B) as they show activity resulting from oculo-retinal fixations of the eye as it contacts a stimulus.

Only when faces, but not place images were viewed, a sharp negative component peaking at 159 ms and a slightly smaller peak of activity at 171 ms were apparent. The component was displayed over the right temporo-occipital region of the scalp. Both the latency of the negative peak over occipito-temporal scalp distribution of the component suggest that IC6, which responded only to face images, is the classical face-sensitive N170 component reported in lab-based studies (Bentin et al., 1996).

Two distinct ICs showed prominent activations for place images relative to faces. The first, IC2 peaking at 129 ms presented a strong bilateral positivity across posterior electrodes. The later component IC7 presents as a sharp negativity across posterior scalp locations slightly lateralized to the right hemisphere. This component peaked maximally at 183 ms. with a smaller sub peak at 205 ms. Figure 5.6.3C shows the location of the strongest differences in average source waveform activity for each IC of interest for both face and place images.

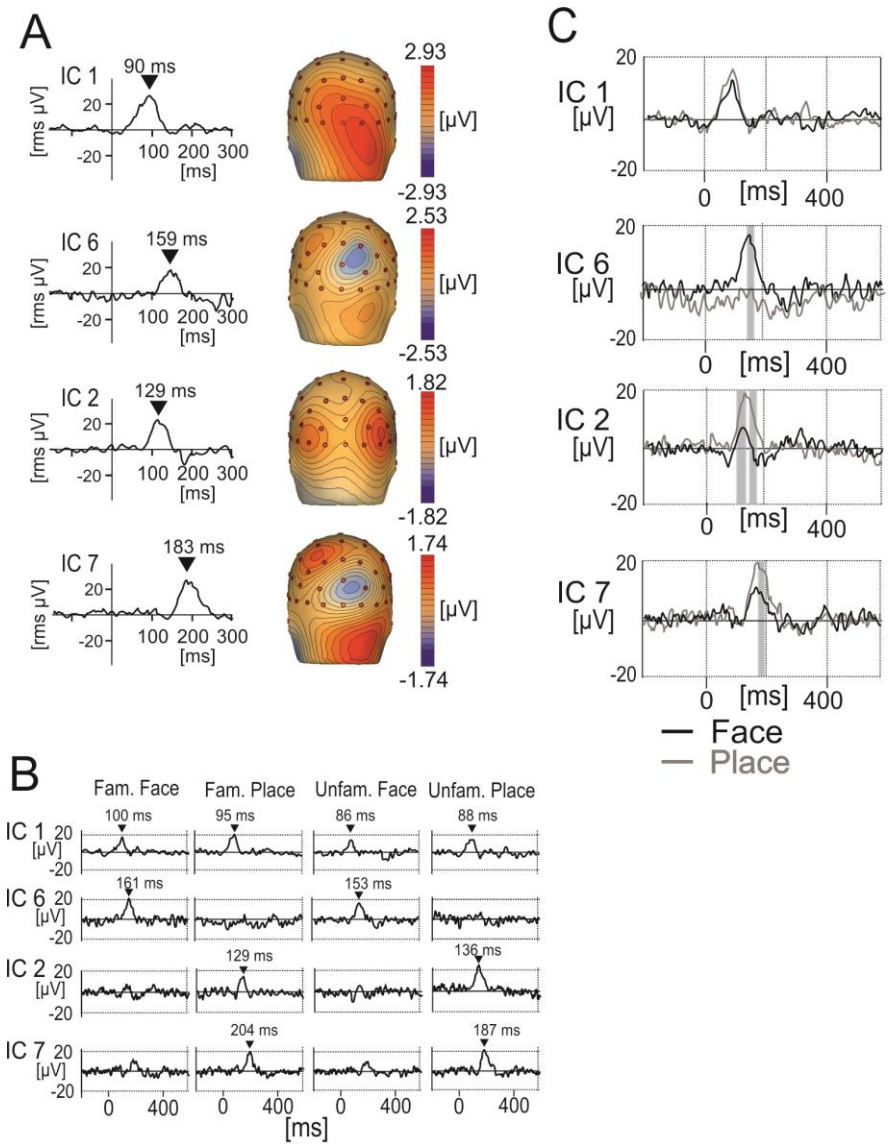

Figure 5.6.3 Independent component scalp and source activity. A. Grand average IC activity for the selected IC of interest as well as scalp topographies at the peaks in activation for each isolated IC. B. Average activation of each IC across familiar and unfamiliar pictures in both face and place experimental conditions. C. Average IC waveform for face and place categories for every IC of interest. Shaded areas signify significant differences in waveform activity ($P < 0.001$). To control for the risk of false positive results due to a large number of tests, P values were corrected using permutation analysis including 1000 permutations.

5.6.4 Independent component statistics

5.6.4.1 Independent component 1: The lambda potential: 90 – 110 ms

IC1 was prominent in all experimental conditions at the expected latency of the lambda potential. The main peak of this component reached maximum at 94 ms post image onset. ANOVA revealed no effect of familiarity present between 90 ms and 110 ms ($F(1,18) = 0{,}043$ $P > 0.1$) nor any effect of category on the evoked waveforms ($F(1,18) = 3.4$, $P > 0.05$). The lambda response did not differ across conditions presenting in all cases as a bilateral positive occipital potential on the scalp regardless of participants viewing face or place images. The lambda response has been identified as a occipital EEG potential occurring 100 ms after eye movements have been made (Thickbroom et al., 1991; Yagi, 1979b). For our results, the presence of a clear lambda component is a positive indicator that EMRP were correctly recorded and that eye-tracking data was adequately synchronized to the mobile EEG data stream. The P1 component represented as the lambda complex here shows a slightly earlier peak latency as lambda potentials shown in recent studies (Dimigen et al., 2011; Körner et al., 2014). This will be addressed in the discussion.

5.6.4.2 Independent component 6: The face-specific N170

Figure 5.6.3B shows the time course of IC6 in all experimental conditions. The waveform activity for this component was extracted across our four conditions between 150 and 170 ms. Peaks in the component waveform are seen for face, but not place conditions. A repeated measures ANOVA evidenced of a significant effect of category ($F(1,18) = 13.948$, $P < 0.003$) and no effect of familiarity ($F(1,18) = 0.044$, $P > 0.05$) on waveform amplitude. Figure 5.6.3C shows the time intervals were statistical differences ($P < 0.001$) between place and face conditions occurred. The average waveform generated by viewing faces ($M = 154.06$, $SE = 37.05$) was significantly stronger that that generated when viewing places ($M = 7.9$, $SE = 30.36$) ($t(18) = 3.735$, $P < 0.003$). No interaction effect was found for this time window ($F(1,18) = 0.342$, $P > 0.5$). IC6 presents selective activations to face images with peaks arising within the broad latency

of the N170 face-specific component presented by Bentin et al., (1996). However, unlike results presented previously face specific responses did not differ when familiar or unknown faces were freely viewed.

5.6.4.3 Independent components 2 and 7: place components

Our results show two distinct components that were active at different latencies when subject's viewed place images. The earliest component IC2 showed a peak in activity at 129 ms. A 2 (faces/places) × 2 (familiar/unfamiliar) ANOVA for repeated measures was performed between 120 ms and 140 ms. The analysis yielded a significant effect of category ($F(1,18) = 20.95$, $P < 0.001$) within this time window. The effect of familiarity on IC2 activations was not statistically significant, but a trend pointing towards an effect of familiarity on this component was encountered ($F(1,18) = 3.57$, $P = 0.075$). No interaction effect was appreciable in this time window.

In the latency interval between 180 ms and 200 ms, IC 7 also evidenced selectively towards place images, most prominently between 180 – 200 ms (Figure 5.6.5C). Statistical comparisons showed an effect of category ($F(1,18) = 29.284$, $P = 0.001$) with significantly larger activations for place images ($M = 185.53$, $SD = 155.77$) than face images ($M = 84.92$, $SD = 158.25$) across this time window. The ANOVA for repeated measures within this window of interest found a category effect ($F(1,18) = 29.284$, $P < 0.001$) in which places generate significantly greater waveforms than faces ($t(1, 18) = 3.117$, $P < 0.05$). IC7 showed no effect of familiarity on place sensitive activity ($F(1, 18) = 1.515$, $P < 0.05$). Familiar place images ($M = -0.5$, $SD = 1.81$) generated, slightly larger negativities than unfamiliar place images ($M = -0.04$, $SD = 1.53$) however this difference was not significant nor was the interaction effect observed at this latency. The place sensitive component in the brain shows enhanced sensitivity towards places, however, no strong differences resulting from familiar relative to unfamiliar images were found ($P > 0.05$).

5.6.5 Source analysis of ICA maps

For the exploratory analysis of sources, the relevant components were inspected by using the back-projected IC weights to estimate the generators of neural activity. For all electrocortical potentials occurring in the first 300 ms, intracranial sources of activity were estimated via low resolution brain electromagnetic tomography (LORETA) (Pascual-Marqui, 2002). LORETA inverse solutions were estimated in a standard 3D solution space using a lead field matrix calculated on an averaged Montreal Neurological Institute (MNI) brain template. The main clusters of activity were investigated at the peak latencies of each IC. No statistical testing was performed on source waveform activity. Figure 5.4.5A shows average waveforms for each IC (black line) and their scalp distribution, as well as averaged waveform for face and place conditions for every IC.

The local maxima underlying IC1 activations was located to the right superior parietal lobule (BA7) encompassing the right lateral wall of the parietal cortex. This components source activity presented a marked right lateralization with activation reaching its peak at 88 ms for place images and 85 ms for faces. Similar source waveforms were registered when subjects viewed faces and place images. When faces, but not places were viewed IC6 source activity reached its local activation maximal at 156 ms and was located to the right precuneus (BA7) within the superior parietal lobe. IC6 was associated to the N170 component visible on scalp electrodes. IC2 shows a reverse pattern of activity across posterior portions of the scalp with its maxima located to the right extrastriate visual area within the occipital cortex (BA19) and responded selectively to place images. Another IC encoding place images (IC7) was also located to the precuneus (BA7), but unlike IC6, this component presented a central distribution and responded preferentially for place, but not faces irrespective of familiarity.

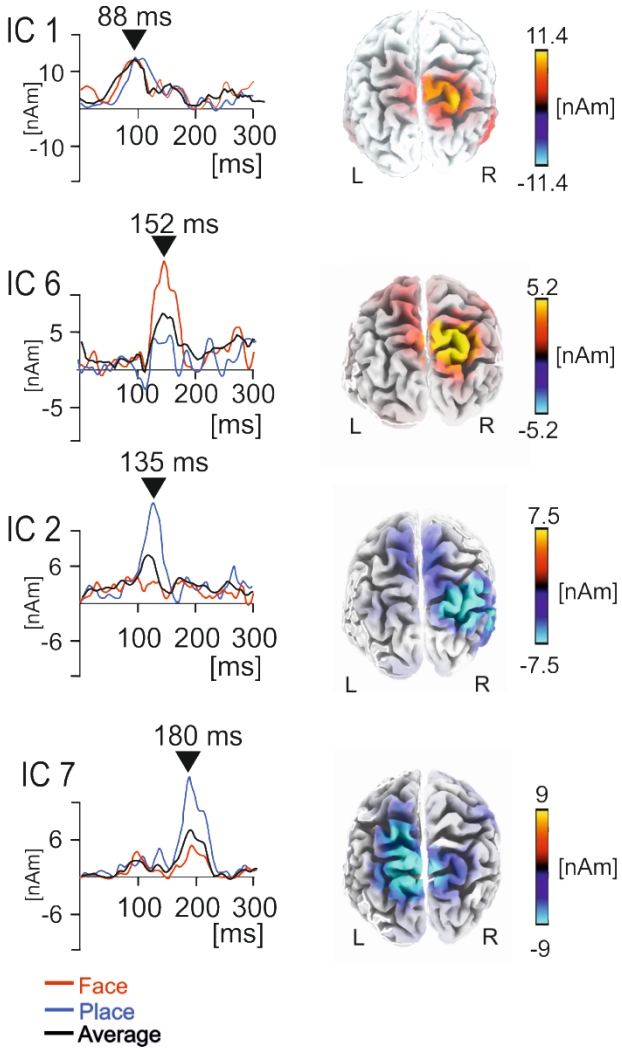

Figure 5.6.5. Source localization of independent components of interest. IC waveforms between 0 ms and 300 ms as well as the location of the average activation on the cortical surface. The time courses of the average IC activity is shown for face (red lines) and place (blue lines) conditions as well as the average between both (black lines). sLORETA source images show the main differences between faces and places of each relevant IC. No statistical testing was performed on this data.

5.7 Discussion

The present study employed combined eye-tracking and EEG recordings to examine the neural correlates of familiar and unfamiliar image processing within an unconstrained setting that mimicked natural behaviour. Independent components responding selectively to face and place images were identified using ICA and isolated for analysis. The N170 face-sensitive component showed no distinct effects of familiarity on waveform amplitude nor did either of the place sensitive components.

The detection of the N170 was accomplished by employing modern active EEG electrodes that cancel external sources of noise (van Rijn et al., 1990) and wireless transmission of the EEG signal. EEG recordings were made in tandem with mobile eye-tracking which was then used to inform the EEG analysis regarding natural viewing onset of each image. Unlike previous MoBI investigations performed during locomotion (De Sanctis et al., 2012; Gwin et al., 2010). In the present study, head movement and body motion artefacts were naturally minimized as subjects stood still to view each of the images. Furthermore, cable-sway artefacts which have been shown to strongly influence mobile EEG recordings (Symeonidou et al., 2018) were mitigated by attaching EEG cable strands to the backpack carried by the participants. An additional concern related to the synchronizing of multiple data streams as well as accurately detecting the onset time of visual stimuli. Unlike traditional paradigms where the onset of a visual stimulus on a screen is co-registered to the EEG data, in this study eye-tracking gaze data was used to determine real-world viewing onset times in the EEG data stream. Onset latencies were detected via visually inspecting the gaze-tracking data superimposed onto the world-view recording and manually registering the instances of first contact on an image. A methodological challenge brought on by this process consisted in the separation of the lambda potential from artifacts originating from eye movements. Eye movement artefacts were generated by rotations of the corneoretinal dipole across each eye in primarily anterior-posterior during blinking and saccades (Dimigen et al., 2011; Nikolaev et al., 2016; Scherg & Berg, 1991). Eye movement artifacts associated with eye blinks and eye movements were corrected at the pre-processing stage using a well-established pattern matching algorithm (Ille et al., 2002).

Then, to further clean the EEG signal from any residual artefactual activity non-relevant ICs were extracted from the data and discarded from further analysis.

The P1 component of the lambda complex present in the EMRP waveforms evidenced a strong peak between 86 ms and 100 ms across experimental conditions. This is minimally later than the peak latency of 70 ms reported in earlier eye movement EEG studies (Yagi, 1982) and coincides with more current reports of 100 ms lambda peak latencies (Dimigen et al., 2011). The differences reported between these studies are likely due to experimental variations and methodological differences such as time locking events to saccade onsets rather than the saccade offset (Kaunitz et al., 2014). In our data set, the temporal asynchrony jitter must be also considered as an explanation for these small inconsistencies in peak latencies of the lambda component.

The face-sensitive component displayed a spatio-temporal pattern on the scalp characteristic of the N170 component occurring in lab-based EEG studies. ICA was applied to separate the scalp ERP into the maximally independent components and remove non brain related activity. In doing so, IC6 was identified as accounting for the scalp-level N170 potential. With respect to the amplitude of the N170 our results are contrary to previous findings using famous faces in priming and serial visual presentation studies (Caharel et al., 2002) as well as studies using personally familiar faces (one's own face or that of a parent). Personal familiarity has shown to affect the N170 amplitude in adults (Caharel, Courtay, Bernard, Lalonde, & Rebaï, 2005) as well as in young children (Parker & Nelson, 2005). The N170 component recorded from our standing participants showed no sensitivity to the effects of familiarity on waveform amplitude. Our results more closely resemble previous findings showing similar N170 waveform amplitudes to familiar and unknown faces in serial presentation studies (Tanaka, Curran, Porterfield, & Collins, 2006) and visual priming tasks (Henson et al., 2003; Jemel, Pisani, Calabria, Crommelinck, & Bruyer, 2003). The results of this experiment support the hypothesis that the N170 is not susceptible to influences of familiarity and, as such, would not be encode higher order information like identity.

One explanation for the conflicting evidence in the literature has been offered by research exploring different recognition stages expressed in the N170 component

(Barrett et al., 1988; Eimer, 2000a). These authors report no strong effects of familiarity in the N170 component, but significant effects at latencies later than 400ms. Others have shown that complex processes involved in the recognition of identity are resolved at mid latency ERP components as early as 250 ms. (Gosling & Eimer, 2011; Tanaka et al., 2006). Our results partially align with lab-based findings presented in the past and favour the idea that the N170 potential is representative of a pre-categorical encoding of the structural characteristics of faces (Bentin, Allison, Puce, Perez, & Mccarthy, 1996). The ICs presented in our results showed no strong peaks in activity at 250 ms to 300 ms and later components were not investigated. Further research is warranted to explore the effects of familiarity on succeeding brain activity, however a current limitation of the mobile EEG method presented here is that signal quality deteriorates at longer latencies (< 300ms).

The exploratory LORETA analysis was performed to explore the source generators of relevant ICs and to contrast these findings with previous neuroimaging results. Similarly to the generators located in the precuneus found in our results, Gobbini & Haxby, (2006) have shown the involvement of the precuneus when subjects evaluated personally familiar faces. Comparable results have also been presented in experiments using mothers and their children's faces (Leibenluft, Gobbini, Harrison, & Haxby, 2004) alluding to the involvement of the precuneus in resolving the identity of a face. Additionally, the precuneus was active when places were viewed in our study and has been linked with episodic memory retrieval (Wagner, Shannon, Kahn, & Buckner, 2005) as well as the regeneration of rich episodic contextual associations in the past. The involvement of the precuneus when subjects viewed images of places might be due to multiple images of personally familiar places (i.e. places in Liverpool and London) included in the stimuli set. Functional magnetic resonance imaging (fMRI) studies have previously identified multiple brain regions; including the fusiform face area (FFA) (Kanwisher & Yovel, 2006), fusiform gyrus (FG) (Kanwisher, McDermott, & Chun, 1997), and the amygdala (Alumit Ishai, Haxby, & Ungerleider, 2002) as main contributors to the detection and recognition of identity as well as emotional content of faces. The FFA located in human extrastriate cortex, for instance, evidences augmented blood oxygen level dependant (BOLD) signals towards faces relative to other images

(Allison et al., 1994; Kanwisher et al., 1997) and has been reported previously as a visual association area, with facial feature-extracting (reviewed in Haxby, Hoffman, & Gobbini, 2000), word expertise (McCandliss, Cohen, & Dehaene, 2003), attention and multimodal integrative functions (Kreifelts, Ethofer, Grodd, Erb, & Wildgruber, 2007).

The differences found between our results and previous accounts of the N170 could be partially explained to the methodological differences with lab-based research. Unlike previous EEG research of familiar face processing where subjects sat passively viewing a monitor, participants in our experiment were allowed to freely view printed images from a standing position with no constraints to their eye-blinks or head movements. Furthermore, postural modifications have shown to affect a number of cognitive and neurophysiological processes (Thibault, Lifshitz, & Raz, 2015). Nevertheless, the effect of maintaining an upright stance on the N170 component has still not been fully explored. It is likely that the additional coping resources associated maintaining an upright stance and will affect the perceptual processing of different stimuli. We address this in a future study aimed at quantifying the influence of standing postures on face specific brain activity.

Here we provided evidence showing that mobile EEG recordings combined with wearable eye trackers represent a viable method for the detection of EMRPs in unobstructed, naturally behaving participants. Furthermore, we replicated a classical N170 component to face images. Interestingly however, we report no significant modulations resulting from varying levels of familiarity on the N170 component activity. These findings support the notion of a staged mechanism for face identification, aligning with the dual mechanisms account for face processing (Bentin & Deouell, 2000; Eimer, 2000b). The methodology applied here represents a pioneering innovation and is easily adaptable for testing multiple domains including social cognition, developmental psychology and consumer science in settings approaching ecological validity.

Chapter 6

Effect of body posture on eye-movement related potentials.

Soto, V. [1], Tyson-Carr, J. [1], Roberts, H.[1], Kokmotou, K. [1,2], Hewitt D. [1], Byrne, A. [1,2], Fallon, N.[1], Giesbrecht, T. [3], Stancak, A. [1,2]

[1] Department of Psychological Sciences, University of Liverpool, Liverpool, United Kingdom,

[2] Institute for Risk and Uncertainty, University of Liverpool, Liverpool, United Kingdom,

[3] Unilever Research & Development Port Sunlight Laboratory, Merseyside, United Kingdom

This experiment examined the effects of body posture expressed in the N170 potentials in a natural setting. EMRPs recorded while standing in a mock art gallery were compared to those produced while viewing emotional faces from a recumbent position. The manuscript for this paper is currently being prepared to submit for publication.

The roles of the co-authors are summarised below:

I designed the study in collaboration with Andrej Stancak carried out the data acquisition. John Tyson-Carr, Katerina Kokmotou, Hannah Roberts, Adam Byrne and Danielle Hewitt assisted with the collection of data and contributed useful comments whilst preparing the manuscript. John Tyson-Carr created the original computer programs for the EEG clustering analysis that were adapted for our dataset. Andrej Stancak, Nicholas Fallon and Timo Giesbrecht contributed to the large-scale planning of this project Andrej Stancak, Nicholas Fallon and Timo Giesbrecht secured funding for project.

6.1 Abstract

Brain imaging performed in natural settings is known as mobile brain and body imaging (MoBI), an upcoming neuroimaging technique that allows amongst other things, the recording of brain responses outside of a laboratory in ecologically valid surroundings. We have recently identified a MoBI N170 component in response to images of emotional human faces. To date however, it is not known whether maintaining an upright stance affects face specific brain processing. The present study aimed at investigating the effects of maintaining an upright stance on brain activations in a naturalistic setting. Emotional human faces were used to test the effects of posture on the N170 face-sensitive ERP component.

64-channel wireless EEG data was recorded from 14 participants while standing and sitting in a reclined position. Subjects freely viewed pictures of emotional faces in both positions. The natural viewing onset times were detected for each stimulus from the eye tracker and inserted as event markers into the EEG time series. Subjective rating scores for each image were registered post-hoc at both postures. Grand average eye-movement related potentials (EMRP's) displayed post-saccadic lambda components and the face-sensitive N170/vertex positive potential (VPP) complex. Spatial filtering of the EEG data was performed using independent component analysis (ICA) and two main EMRP features were explored. The group level analysis was performed on clustered IC activity.

One component of interest associated with the lambda potential and showed amplitude peaks at latencies between 110 ms and 130 ms. The lambda component was significantly reduced in standing, relative to reclining conditions. Additionally, components were associated to the N170/VPP, but no effects of body posture on component amplitude were found in either component.

Results demonstrated that posture affected the amplitude of the primary EMRP component when related to initial processing of image information, but not the later N170 face-sensitive component or its VPP counterpart. The effects of posture on the lambda component indicated that visual spatial attention may be affecting early visual processing. We additionally consider physiological effects like cerebral spinal fluid

shifting thickness within the brain should be considered when interpreting MoBI results and planning future research.

6.2 Introduction

Maintaining an upright stance has often been construed as a simple behaviour, at times assumed equal to sitting recumbent or laying supine. However, maintaining a standing balanced posture requires the rapid processing and integration of continuous vestibular, somatosensory and visual information (Mergner & Rosemeier, 1998; Nashner, 1976). The purpose of the current investigation was to test this assumption by applying an innovative mobile brain and body imaging (MoBI) technique to investigate the effects of body posture on brain activity associated to viewing faces within a naturalistic environment.

The effect of posture on concurrent brain activity has been notoriously difficult to study and as such, brain researchers have typically used neuroimaging results tacitly assuming that evoked brain activity in a laboratory setting translates to real world cognition. The lack of insight could be partially attributable to the inherent postural requirements of modern brain imaging techniques. The ecological nuances associated with functional magnetic resonance imaging (fMRI) have previously been described (Raz et al., 2005), these revolve around the necessity of supine participants to be restrained and remain still as flashing stimuli appear onscreen. Electroencephalographic (EEG) recordings classically position sitting subjects alone in dimly lit rooms viewing monitors, whereas magnetoencephalography (MEG) uses both sitting and supine participants. Furthermore, body and head movements are sometimes minimized via chin rests and head braces. The most glaring difference between these imaging modalities is the position of the participants' body during testing and the type of restriction to subject's body movements. More interestingly, the experimental tasks being performed are at times, incongruent with the body position that subjects must assume; for instance performing arithmetic calculations while laying supine (Lipnicki & Byrne, 2008).

Moreover, modifications to body posture have been shown not only to affect normal human physiology, but also behaviour and cognition. For instance, compared to laying supine, sitting has been shown to improve intelligence and augment perception (Lundström, Boyle, & Jones-Gotman, 2006). Relative to maintaining a reclined sitting position, increased cortical activity and shortened reaction times have been described in subjects leaning forward to view appetitive cues (Harmon-Jones, Gable, & Price, 2011). Furthermore, different body postures have been shown to also affect behaviour; for example slumped body positions have been shown to lead to more 'helpless' behaviours (Riskind & Gotay, 1982). Upright stances have shown to aid psychomotor performance (Caldwell, Prazinko, & Caldwell, 2003; Caldwell, Prazinko, & Hall, 2000) and to heighten levels of anticipatory anxiety during challenging mental arithmetic tasks (Lazarus & Folkman, 1984; Lipnicki & Byrne, 2005). Conversely, supine body positions have been shown to reduce anger evocation (Harmon-Jones & Peterson, 2009) and induce more relaxed and calm emotional states. Even small body movements like the adoption of different facial expressions affect emotional judgments and the generation of memories (Laird & Lacasse, 2014). These findings suggest that neural processing of emotional stimuli could vary resulting from changes in body positions, alluding to a close-knit relationship between posture and emotional processing.

Nitschke and colleagues (1996), showed the central lobule in the anterior cerebellum was activated by foot movements performed in the supine position. However, producing foot movements in a supine position is different from sustaining a standing posture. To tackle this problem, mobile gantries to support PET systems have been used to test visual processing of objects at different body postures (Ouchi et al., 1999). In doing so, these authors describe the contributions of cortical structures like the right primary and secondary visual cortices (Brodmann area (BA) 17/18), the left cerebellar anterior lobe (culmen) and the anterior vermis have been described as mechanisms for the regulation of bipedal standing relative to supine positions. The visual cortex proved more active when standing with feet together than feet apart and the cerebellar anterior vermis as well as the lateral posterior lobe cortex were preferentially active on ipsilateral hemispheres to the weight-bearing side when adjusting posture (Ouchi, Okada, Yoshikawa, Futatsubashi, & Nobezawa, 2001). Patient

reports showing deficits in cerebellum have shown to hinder normal motor functioning (Gottwald, Wilde, Mihajlovic, & Mehdorn, 2004). Furthermore, thalamic lesions have been shown to strongly hinder spatial attention (Rafal & Posner, 1987). For neuroimaging researchers however, the aforementioned methodological difficulties and environmental testing differences are rarely addressed and have assumed to be invariant, limiting our understanding of the involvement of cortical and subcortical structures in postural maintenance.

Recently, a mobile brain and body imaging (MoBI) methodology has been developed allowing untampered brain activity to be investigated in natural environments (Gramann et al., 2010; Gwin et al., 2010). Studying these processes in real-world situations could provide a deeper understanding and offer a point of comparison for laboratory based research. In the present investigation, we implemented MoBI to study the effects of posture on the neural correlates of emotional human face processing. The approach is based upon previous MoBI results into emotional processing of objects and faces where a N180 face-specific ERP components were identified in mobile participants (Soto et al., 2018). In the current investigation, we built upon these previous findings and investigated the effects of posture on the N170 component produced by emotional faces at two different postures. We hypothesised that an upright, standing posture will reduce the N170 face specific component amplitude due to the additional processing demands brought on by maintaining a stable posture. Wireless EEG and eye-tracking data was recorded while our participants performed the same free-viewing task while sitting in a reclined position and standing upright. As such, the main aim of this investigation was to explore the effects of natural body posture on the neural processing emotional facial expressions expressed in the N170 component amplitude.

6.3 Materials and methods

6.3.1 Participants

Fourteen healthy volunteers 24.6 ± 3.2 years old (mean ± SD), were recruited for the study by online advertisements and word of mouth. One participant was excluded from the sample due to an excessively noisy EEG signal during the reclining session.

Therefore the final sample was composed of fourteen subjects (8 females) with an average age of 24.6 ± 3.3 years. Experimental subjects gave written informed consent prior to taking part of the study in agreement with the ethical approval obtained from the University of Liverpool Research Ethics Committee. Participants received £30 (£15 per session attended) as compensation for their travel expenses and time. All experimental procedures were conducted in a single session in accordance with the Declaration of Helsinki.

6.3.2 Stimuli

Face images expressing four emotional categories (afraid, disgusted, happy and neutral) were selected from the Karolinska Directed Emotional Faces (KDEF; Lundqvist, Flykt, & Öhman, 1998) set and from the NimStim face inventory (Tottenham et al., 2009). The full stimulus set consisted of 180 emotional humans faces, 45 images in each emotional category presented on twenty A0 poster-size sheets. 120 images were taken from the KDEF and 60 from the NimStim set. All 180 images used in the experiment were cropped to match in size and quality (300 DPI) using Corel Picture software. Additionally, all images were matched for temperature and brightness and were always presented as standard portrait shots including the shoulders. A0 size panels were constructed containing 9 different stimuli images presented in full colour approximately 20 cm × 25 cm in size. Additionally, a white on black square fixation cross was presented in the centre (14.3 cm × 14.3 cm) printed onto an A0-size paper sheet (Figure 6.3.2). Twenty panels contained all emotional face categories pseudo-randomly distributed and maintained similar distances from the fixation cross in the centre. All panels were pasted onto Styrofoam sheets and attached to the walls using adhesive tape.

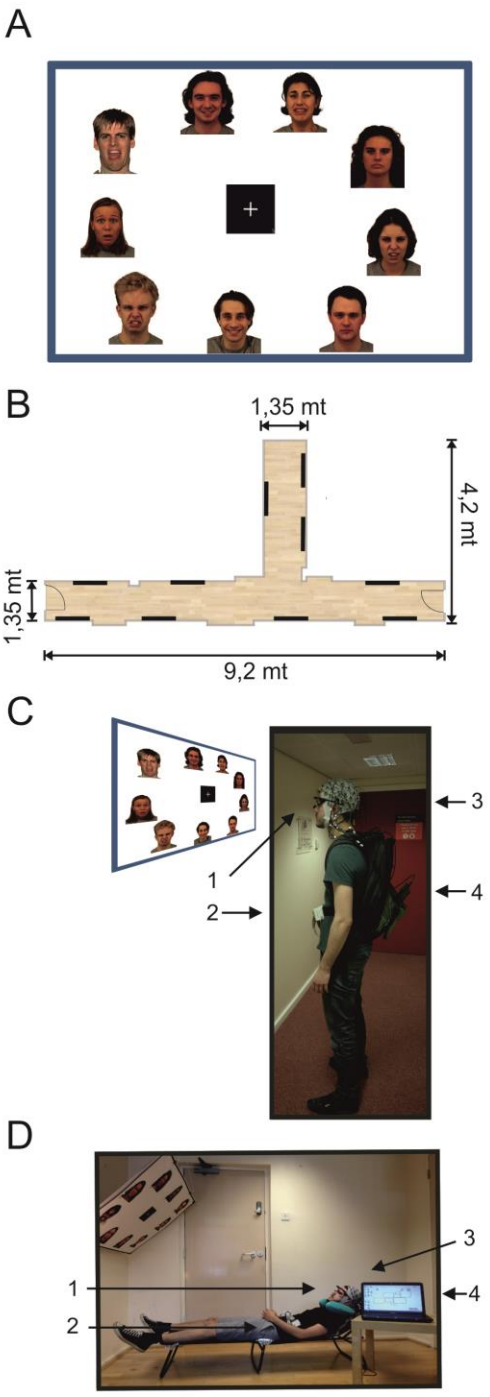

Figure 6.3.2. Experimental setup of mock gallery and reclining session A. Example of one poster panel (120 cms × 90 cms) presenting face images. B. Schematic illustration of the hallway used to setup the mock picture gallery. Black lines indicate the position of each panel within the hallway. C and D. One subject wearing the full equipment and experimental setup for the standing and reclining sessions. 1) Pupil eye tracker; 2) MOVE wireless EEG transmitter; 3) 64 channel actiCap; 4) Eye tracking PC in the backpack.

6.3.3 EEG Recordings

EEG data was continuously recorded using a 64-channel wireless and a portable EEG system (Brain Products, GmbH, Münich, Germany). Brain Products MOVE system (Brain Products, GmbH) employs a lightweight signal transmitter which participants carry on a belt (Figure 6.3.2 C and D). Active Ag/AgCl EEG electrodes were mounted on an electrode cap (actiCAP, Brain Products, GmbH) according to the 10-20 electrode system and aligned to the midpoint between the anatomical landmarks of the nasion and inion, and the left and right preauricular points. Electrode FCz was used as the system ground and electrodes were referenced to AFz. Electrolyte gel was applied to maintain electrode-to-skin impedances under 50 kΩ. EEG recordings were sampled at a rate of 1000 Hz. EEG average reference was applied to the signals and were digitized at 1 kHz with a BrainAmp DC amplifier linked to Brain Vision Recorder program version 1.20.0601 running on Windows operating system. Data were filtered online using a 0.1-200 Hz bandpass filter.

6.3.4 Eye movement recording

A PUPIL (Kassner et al., 2014) binocular eye-tracking system was used to record the locations of the gaze position. Pupil Capture software v 0.9.6 running on Ubuntu v 14.04.4 was used to generate the recordings. PUPIL eye tracker is an open source, high resolution wearable system (Figure 6.2.3C) that provides a lightweight solution for mobile gaze-tracking. Pupil locations were recorded using infra-red cameras sampling at 90 Hz with a resolution of 320 × 240 pixels. The real-world video streams were set at a sampling rate of 60 frames per second with a resolution of 600 × 800 pixels.

To calibrate the gaze locations, a manual marker 3D calibration protocol was used to generate a 9-point grid in the field of view of the participant. Calibration was repeated until gaze positions were accurate everywhere on the blank panel. Small calibration offsets occurred at times due to displacements in the wearable eye-tracker on

the subject's face. These offsets were adjusted offline using the manual gaze correction plug-in on Pupil Player during manual tabulation of stimulus onset times. Eye-tracking data were processed using Pupil Player v. 0.9.6 program. The ocular pupils of both eyes were located based on a centre-surround detection algorithm (Świrski et al., 2012). Exported raw gaze data is time-locked to the processing computer's internal clock, giving millisecond precision to the eye measurements. Additionally, all recorded frames contained an accurate time stamp based on the PC processor real-time clock. Eye-tracking video files were visually inspected and stimuli onsets were manually tabulated. Each stimulus was logged on a picture by picture basis with stimulus onset defined as the first instance in which the gaze position landed on an image. The real times corresponding to the tabulated frames were used to import stimulus onset latencies onto the raw EEG data.

6.3.5 Data synchronization

A trigger-box fitted with a light emitting diode (LED) was constructed to synchronise data streams at the start of every recording. The light-flash on the trigger-box was recorded by the world-view camera on the eye trackers as a simultaneous transistor-transistor logic pulse was registered in the EEG data recording. The visual light cue that became apparent at a specific frame in the eye-tracking video data was used to synchronise the data streams. The accuracy of the synchronisation was tested in a 15 minute EEG and eye-tracking recording. In this test 15 synchronising light stimuli were produced in approximately 1 minute intervals. The time-locked eye-tracking frames were logged and compared to the latency of the EEG triggers. The temporal asynchrony between triggers simultaneously delivered to the eye-tracking and EEG recording system was of 0.022 ± 0.020 s (mean ± SD) over a 15 minute recording.

6.3.6 Procedure

Subjects assisted to two testing days, a standing session where stimuli was viewed while upright, and a reclining session where they laid supine on a lounge chair. In both sessions instructions were delivered and equipment was set up in a designated

lab space following identical procedures. Half of the subjects did the reclining task first and the other half did the standing task first. Experimental sessions were separated by a minimum of one week.

6.3.7 Standing session

Participants were fitted with the EEG cap and electrode-to-skin impedances were kept below 50 kΩ before commencing the task. Mobile EEG system was then connected and wireless signals were visually inspected on a standing participant. Next, eye-tracking glasses were placed on the participant over the EEG cap.

A mobile base unit was assembled using a rolling trolley where the wireless signal receiver, EEG amplifier and recording computer were placed. The base unit was positioned by the experimenter keeping a distance of no more than 7m from the participant in order to maintain optimal signal quality. The eye trackers were calibrated on a standing participant against a blank white panel at a distance of approximately 1 m. Gaze-tracking was optimised by means of 3D calibration routine using manual markers. The laptop registering the eye-tracking was placed in a backpack and carried by the participant for the duration of the task (Figure 6.2.3C & D). EEG cables running from the electrodes to the lightweight transmitter were also placed in the backpack to reduce cable sway artifacts (Gramann et al., 2010; Gwin et al., 2010).

Two hallways within the Eleanor Rathbone Building of the University of Liverpool were used to create a naturalistic picture gallery where the standing session took place (Figure 6.3.2B). Participants were requested to walk through the hall, stopping to view the images displayed on each panel. They were free to navigate the gallery in any order they chose and were only instructed to stand facing each panel and to view each image for a minimum of a few seconds before moving onto the next image. To do so, subjects were instructed to look at the centre fixation cross before viewing each image, and to return their gaze to the fixation cross before moving to the next picture. They only continued onto a subsequent panel after viewing all images. To maintain task engagement, participants were asked to select a preferred face as well as a

disfavoured face from each panel and to mark the selected pictures on a small paper printed version of each panel. The full experiment consisted of two blocks in the mock gallery. In each block, subjects viewed ten panels with nine images on each one. In total, participants viewed 180 different images in the experiment. On average, each of the two gallery block lasted approximately 15 minutes.

5.3.8 Reclining session

The wireless EEG was placed on the participant in the same manner as in the standing session. For the reclining task, the eye trackers were calibrated on a blank white panel with the participant lying on the lounge chair. The blank panel was hung at a distance of approximately 1 m with 140° angle to match viewing conditions across both sessions. The inclination angle of the lounge chair was lifted approximately 40° (Figure 6.3.2D). In this session subjects laid on a lounge chair that provided full body support as high as the neck. A foam neck support was used to prevent electrodes on the back of the scalp smearing against the chair. An identical 3D calibration routine using manual markers was used to optimise the gaze-tracking for the reclined condition. The eye-tracking computer was placed on the same mobile base unit where the EEG recording computer rested in this session.

Participants were requested to view the images displayed on each panel. The experimenters hung each panel as they were completed. Subjects were only instructed to relax and view each face for a couple of seconds before moving onto the next image. No restrictions were placed on eye-movements or blinks. The same selection task was used here to maintain engagement. As in the standing session, participants viewed the same 180 different images in the experiment divided in two blocks. Each block in the reclined session also lasted approximately 15 minutes.

In both sessions, electrode impedances and gaze tracking calibration were checked and corrected in the break between blocks if required. Once the viewing task was completed, the EEG cap and the eye-tracking glasses were removed. Participants were then required to rate how much they liked and if they would approach the images

that had been previously seen. Ratings were performed using three visual analogue scales (VAS) sized 10 cm and anchored on each extreme. The scales evaluated the general likability of each face image as well as the level of arousal and emotional valence. Subjects were instructed to use the middle of the scale for expressions deemed neutral. (i.e. '*0: Do not like'* up to *'100: Like very much'; '0: Unrousing'* up to *'100: Very Arousing and* '*0: Very negative'* up to *'100: Very positive'*). Pictures and rating scales were presented on a LCD screen using Cogent program v. 1.32 (Welcome Department of Imaging Neuroscience, United Kingdom) running on MATLAB v. R2014a (MathWorks, Inc., USA). Participants rated the same faces after each session.

6.4 EEG analysis

6.4.1 Eye movement related potentials

EEG data were pre-processed using the Brain Electrical Source Analysis program (BESA v.6.0, MEGIS Software GmbH, Munich, Germany). Data were initially referenced using common averaging method (Lehmann, 1987) and digital filters were applied to remove frequencies lower than 0.5 Hz and higher than 35 Hz from the EEG data. Oclulographic artefacts including blinks as well as vertical and horizontal eye-movement artifacts were removed using pattern matching averaged artefact topographies (Berg & Scherg, 1994; Ille et al., 2002). This method is based on a principal component analysis. Additionally, EEG data was visually inspected for movement or muscle artifacts and trials contaminated with large artifacts were marked and excluded from further analysis.

Event markers were inserted into EEG data by synchronising the time axes of the EEG and eye-tracking system. EEG data were epoched to range from -200 ms to 600 ms relative to the first contact of the gaze with any part of a picture in each of 180 pictures. This time point effectively corresponded to part of the saccade which brought the gaze onto a particular face or object in a picture. Artifact-corrected EEG signals were then exported into EEGLAB v.14.1.1 (http://www.sccn.ucsd.edu/eeglab/) an open source environment for processing EEG data (Delorme & Makeig, 2003). During averaging,

the mean EEG activity in the baseline interval ranging from -200 ms to -100 ms was removed from each data point. Post-saccadic EMRPs were computed from all trials falling into eight different conditions including postural conditions (reclining and standing) and emotional facial expressions (afraid, disgusted, neutral and happy). The sampling rate of the eye-tracking system was previously calculated offline (average sampling rate: 41.1 Hz). The sampling rate was chosen based on 15 minute pilot experiments to secure a continuous stream of eye-tracking data which was often discontinuous at higher sampling rates. However, due to the relatively low sampling rate, further analysis of the eye movements was not performed and eye-tracking data was used exclusively to detect stimuli onsets times. EEG epochs were generated as cuts into the world video scene in a similar manner as the method described in our previous experiment. Artifact-corrected EEG data was then exported to EEGLAB for group-level analysis.

6.4.2 Data analysis and independent component clustering

Individual subject data was entered into the EEGLAB STUDY structure (Delorme et al., 2011). Data were analysed using in-house scripts built on the open source EEGLAB toolbox for Matlab (Delorme & Makeig, 2003). Independent component analysis (ICA) was performed within EEGLAB for all subjects using an extended Infomax ICA algorithm to parse EEG by defining maximally statistically independent components (IC) (Makeig et al., 1996) using the default training parameters on EEGLAB. This method allows an accurate detection and removal of extra-cerebral sources of noise. ICA was performed on concatenated epochs for each subject individually. Event related potentials (ERPs) and IC scalp maps were then computed across experimental conditions and used to construct a pre-clustering array to group ICs into 9 clusters. The DIPFIT2 routine from EEGLAB was used to model each IC as equivalent current dipole by using a standardized boundary element (Oostenveld & Oostendorp, 2002). If the residual variance of the single-dipole exceeded 30% or if the location landed outside the head the IC was removed previous to clustering. The clustering of ICs was performed across all 14 subjects based on similarities in scalp

topographies, equivalent dipole locations and event related potential waveforms by means of the *k*-means clustering routine available in EEGLAB (Lee, Miyakoshi, Delorme, Cauwenberghs, & Makeig, 2015). Three clusters of interest were identified and selected based on IC activity and average dipole locations and only if ICs were present in at least half of our subjects (≥ 7). Furthermore, two peak features in the global field power were used to identify component clusters for analysis. Cluster 2 presented 33 ICs across 13 subjects and accounted for the N170 component. Cluster 8 (16 ICs) were clustered from 9 subjects and presented a small peak in activity at around 90 ms and accounted for the VPP peaking in medial scalp locations as well as a larger secondary peak at around 170 ms. Custer 6 was composed of 18 ICs present in 10 subjects and represented the major contributor to the lambda component. Statistical testing was performed on the grand averaged IC cluster activity across all experimental condition for these three components.

6.4.3 Statistical analysis

The source waveforms representing the averaged clustered IC activity in each of the fitted dipoles were analysed using a 2 × 4 analysis of variance (ANOVA) for repeated measures ANOVA (Reclining vs. standing, four emotional face conditions). Statistical testing was performed on the averaged source activity across the intervals of interest in SPSS v.22 (IBM Corp., NY, USA). We focused the analysis on 20 ms time intervals (- 10 ms to 10 ms) relative to the peak in IC activity for each selected cluster. Post-hoc paired t-tests were performed when necessary and considered significant at $P < 0.05$ with Bonferroni corrected for multiple comparisons. The statistical confidence level of $P < 0.05$ was always employed.

6.5 Results.

6.5.1 Face ratings

Figure 6.5.1 shows the average rating scores for each visual analogue scale across all four experimental conditions. To test the effects of body posture on the overt rating behaviour, each of the three individual visual analogue scale ratings were submitted to separate 2 × 4 ANOVAs for repeated measures. Across all rating scales we found no effects of posture observed on overt rating behaviour between standing and reclining conditions (arousal scale: $F(1, 14) = 0.009$; $P = 0.927$; emotion detection scale: $F(1, 14) = 1.112$; $P = 0.31$; and pleasantness scale: $F(1, 14) = 0.251$; $P = 0.624$). A significant effect of emotional condition on arousal level was also found in this analysis ($F(3,42) = 100.62$, $p < 0.001$) as well as for the emotion ($F(3,42) = 69.008$, $p < 0.001$) and pleasantness scale ($F(3,42) = 84.883$, $p < 0.001$)

Pairwise t-tests were used to test differences amongst all pair of emotional categories. Paired comparisons confirmed that arousal rating were significantly different across emotional expressions specifically; disgusted expressions rated as less arousing than afraid facial expressions ($t(14) = -6.1$; $P = 0.003$) and more arousing than neutral faces ($t(14) = -2.9$; $P = 0.012$). Unexpectedly, afraid and neutral facial expressions were rated as equally arousing by our participants ($t(14) = 0.104$; $P = 0.92$). Similarly, the emotional scale ratings showed happy faces (80.7± 7.8) were consistently rated as highly positive while disgusted (35.2 ± 6.6), and afraid (39.1 ± 5.7) were rated on the negative end of the scale. Neutral facial expressions however, were perceived to be slightly negative (41.1 ± 6.8; mean ±SD). As expected, this effect was additionally encountered in the pleasantness ratings where faces reflecting happy emotional expressions were perceived as more pleasant than disgusted ($t(14) = -12.6$, $P < 0.001$), afraid ($t(14) = 14.1$; $P < 0.001$) or neutral faces ($t(14) = 10.4$, $P < 0.001$). Again, neutral faces were rated equally pleasant as disgusted faces ($t(14) = -2.1$; $P > 0.05$) and afraid expressions ($t(14) = 0.012$, $P > 0.05$) irrespective of the postural position.

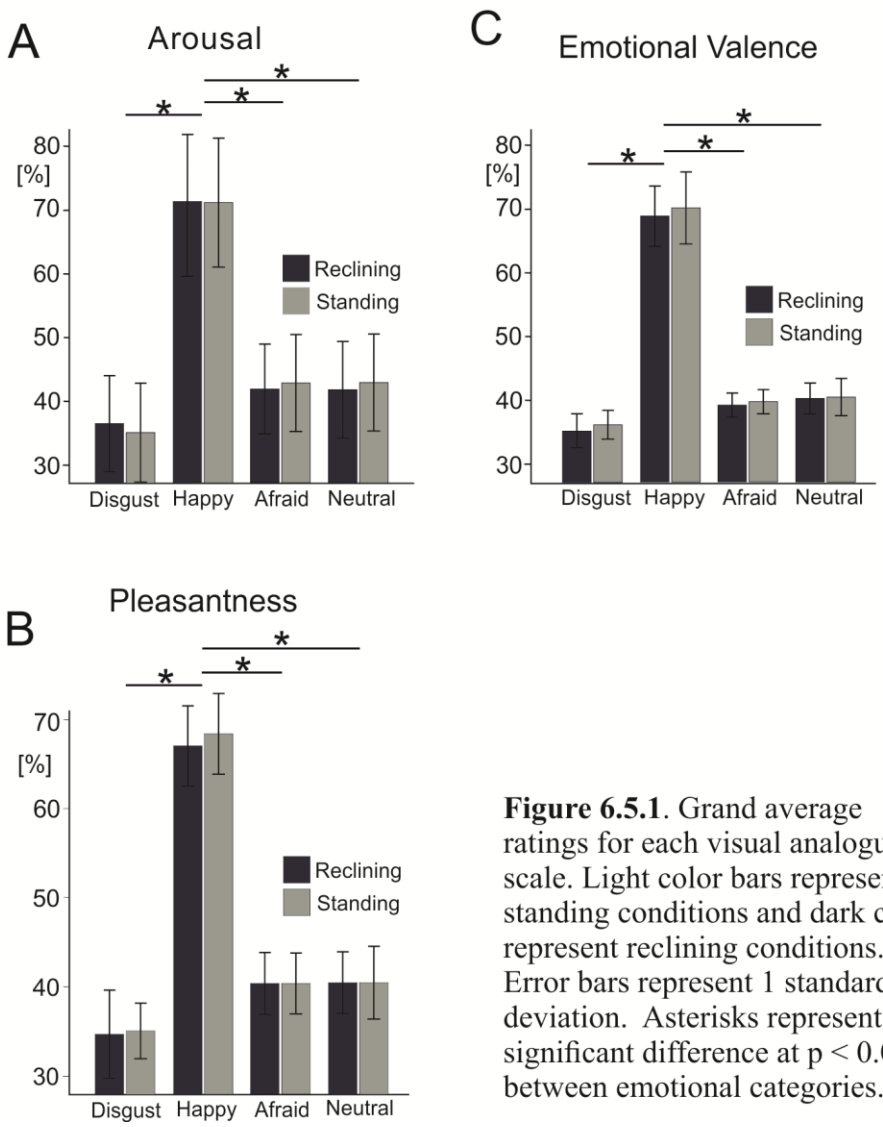

Figure 6.5.1. Grand average ratings for each visual analogue scale. Light color bars represent standing conditions and dark colors represent reclining conditions. Error bars represent 1 standard deviation. Asterisks represent a significant difference at $p < 0.05$ between emotional categories.

6.5.2 Eye movement related potentials

EMRP were constructed from -200 ms to 600 ms relative to the first instance of contact of the subjects gaze with an image. Throughout both experimental sessions subjects maintained a stationary reclined sitting position or a still upright stance during the viewing of pictures. As such, the EEG data showed minimal neck muscle or head movement artifacts which have been shown to affect EEG data during walking or running (Gwin et al., 2010). The data was visually inspected and corrected for the presence of artifacts. Trials were excluded if artifacts were present in either eye-tracking or EEG data. If participants skipped an image, failed to fixate, or gaze tracking was lost during fixation, the trial was discarded from any further analysis.

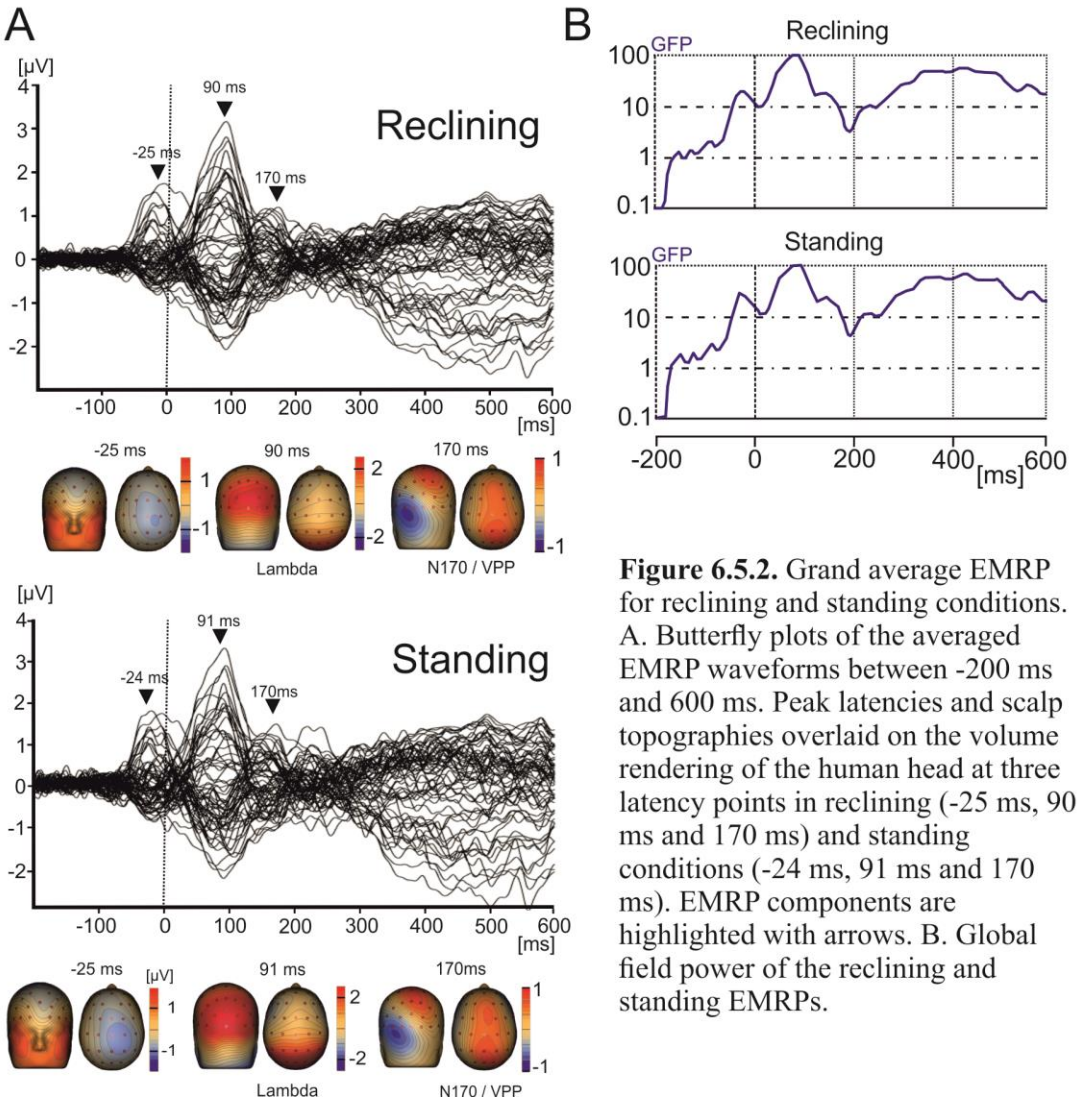

Figure 6.5.2. Grand average EMRP for reclining and standing conditions. A. Butterfly plots of the averaged EMRP waveforms between -200 ms and 600 ms. Peak latencies and scalp topographies overlaid on the volume rendering of the human head at three latency points in reclining (-25 ms, 90 ms and 170 ms) and standing conditions (-24 ms, 91 ms and 170 ms). EMRP components are highlighted with arrows. B. Global field power of the reclining and standing EMRPs.

Figure 6.5.2 presents the butterfly plots of EMRPs for reclining and standing conditions and the topographic maps of distinct EMRP components detected in the global field power (GFP) curves. The butterfly plots for both faces and objects show a stable baseline period at – 200 ms to –100 ms and the presence of clear peaks in the EEG signal between 0 ms and 300 ms. At latencies after 300 ms however signal became noisy and, as such later components were not investigated. The first peaks in GFP are visible in the time interval occurring previous to viewing onset (-25 ms and -24 ms for reclining and standing conditions respectively) and is related to residual eye-movement activity not fully removed in the pattern matching procedure. The peak latency of the negative occipitotemporal component and the presence of a positive vertex potential

suggest that this particular component was the face-sensitive N170/VPP complex (Bentin et al., 1996).

6.5.3 Independent component clusters

IC clusters were selected on the basis of their maximum explained variance being greater than 70% and that clusters were composed of IC from a minimum nine of the subjects. Additionally, the spatial-temporal characteristics of the scalp maps and dipole locations were used to select ICs.

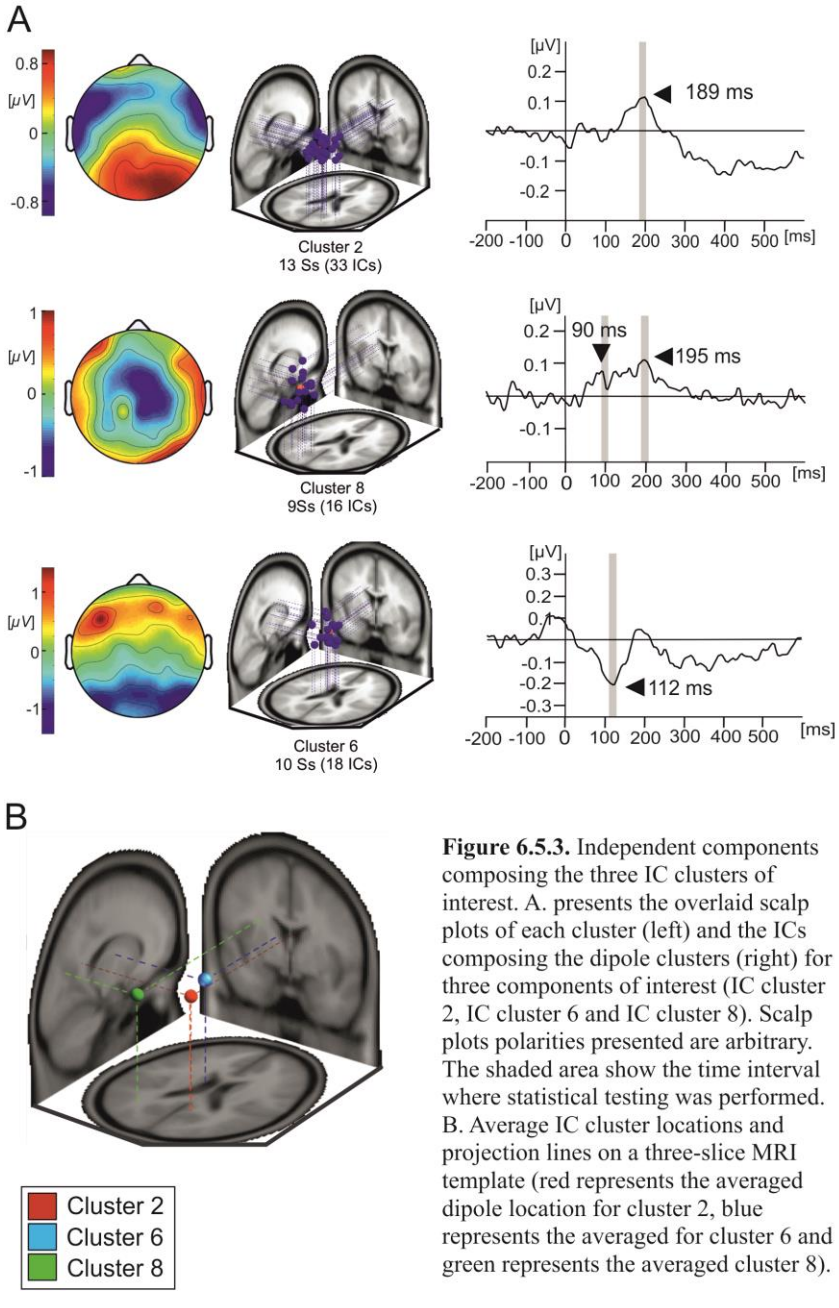

Figure 6.5.3. Independent components composing the three IC clusters of interest. A. presents the overlaid scalp plots of each cluster (left) and the ICs composing the dipole clusters (right) for three components of interest (IC cluster 2, IC cluster 6 and IC cluster 8). Scalp plots polarities presented are arbitrary. The shaded area show the time interval where statistical testing was performed. B. Average IC cluster locations and projection lines on a three-slice MRI template (red represents the averaged dipole location for cluster 2, blue represents the averaged for cluster 6 and green represents the averaged cluster 8).

Three IC clusters were selected based on the peak in their averaged waveforms and scalp distributions (Figure 6.5.3). The mean IC dipole for each IC cluster of interest was located in, or near to the posterior cingulate cortex (cluster 2), the left thalamus (cluster 6) and the left angular gyrus (cluster 8). The average waveform activations of each of these IC cluster was statistically tested using a 2 × 4 (body posture × emotional condition) ANOVA for repeated measured.

Cluster 2 presents as a tight grouped cluster of 33 ICs in occipito-temporal portions of the brain present in 13 subjects. Figure 6.5.3.2A illustrates the averaged IC activity across experimental conditions as well as the location of individual ICs composing cluster. Due to the peak latency and location of the cluster we have associated it to the N170 face-sensitive component. The average IC dipole location of this cluster was placed medially in the posterior cingulate cortex behind the splenium of the corpus callosum (Talairach coordinates x, y, and z: 9, -48, 23; Brodmann Area 23). The mean IC dipole accounted for 86.72% of the total explained variance (13.28% RV ± 8.8; $\bar{x}$ ± SD). Across the different experimental conditions cluster 2 shows peaks in mean activity occurring between 150 ms and 230 ms with an average peak at 189 ms. The ANOVA performed over the 180 ms to 200 ms time interval reflected no effects of body position on cluster 2 ($F(1,13) = 0.033$; $p > 0.05$). No effects of emotional condition were present in the data ($F(3,39) = 0.776$; $p > 0.05$) nor was there an observable interaction effect ($F(3,39) = 0.235$; $p > 0.05$).

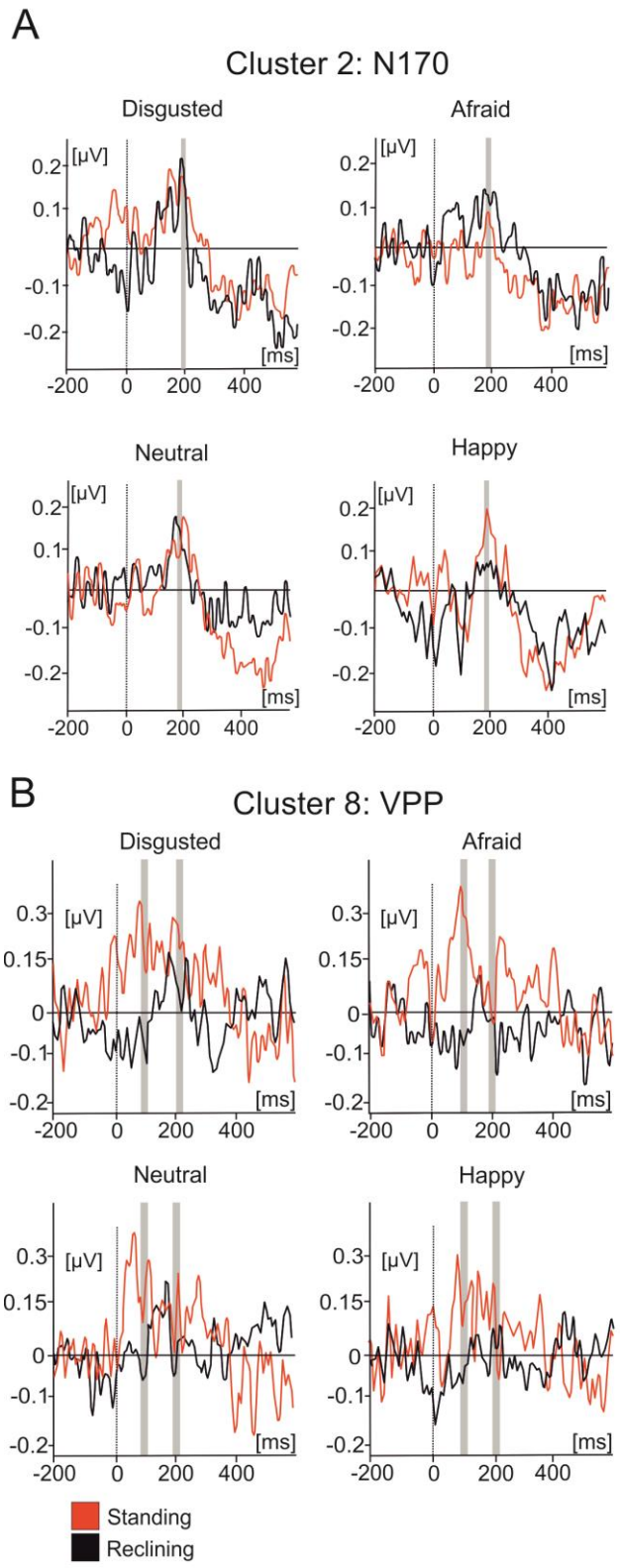

Figure 6.5.3.1 Average IC cluster activations for the N170 and VPP. A. IC activity accounting for the N170 between -200 ms and 600 ms for each emotional condition. B. Average IC activity accounting for the VPP between -200 ms and 600. Red lines represent the standing condition and black lines represent the reclining condition. Shaded areas represent the time interval where statistical testing was performed.

Cluster 8 was composed by 16 components present in nine subjects. The scalp distributions presented over the occipito-parietal regions of the scalp with a first small deflection occurring at roughly 100 ms and a main, larger peak at a latency of about 200 ms (Figure 6.5.3.1B). This cluster modelled the VPP which represent the same brain mechanism as the N170 component, given their co-occurrence and shared neural generators. The averaged dipole explained 81.17% of the residual variance (19.83% ± 5.94; $\bar{x}$ ± SD) and was located to the left angular gyrus (Brodmann Area 39, Talairach coordinates: -26, -62, 17). Statistical comparisons were performed in the time interval between 90 ms and 110 ms as well as between 190 ms and 210 ms. Within the first time interval no significant effect of posture on evoked source activity of cluster 8 ($F(1,13) = 2.603$, $p > 0.1$) was found in the latency period surrounding the peak. Additionally, no emotional effect ($F(3,39) = 0.198$, $p > 0.5$) nor was there any effect of interactions between posture and emotional categories ($F(3,39) = 0.99$, $p > 0.1$). A similar pattern of results are

presented at the peak latency. In interval ranging from 190 ms to 210 ms, no effects of posture ($F(1,14) = 0.007$, $p > 0.5$) or emotional category were found ($F(3,39) = 1.426$, $p > 0.1$) nor was there any interaction effects present ($F(3,39) = 1.677$, $p > 0.05$) in the data.

Cluster 6 was comprised of 18 IC from ten of the subjects, which became active within similar latencies as the lambda potential (Figure 6.5.3.2). The scalp distribution of the component shows a clear occipital distribution. The averaged IC dipole was fit to the left thalamus (Talairach coordinates -10, -6, 9; close to Brodmann area 17) and the mean dipole accounted for 84.6% of the explained variance (16.4% ± 9.63). Cluster 6 activations showed significant effects of body posture on IC activity ($F(1,13) = 6.424$; $p < 0.05$). When subjects reclined, the averaged IC activity was larger (-0.15 ± 0.621μV) relative to when they stood (-0.085 ± 0.415μV). There was no effect of emotion on the mean IC cluster activity ($F(3,39) = 0.475$; $p > 0.05$) nor interaction effect was found in this interval ($F(3,39) = 0.694$; $p < 0.05$).

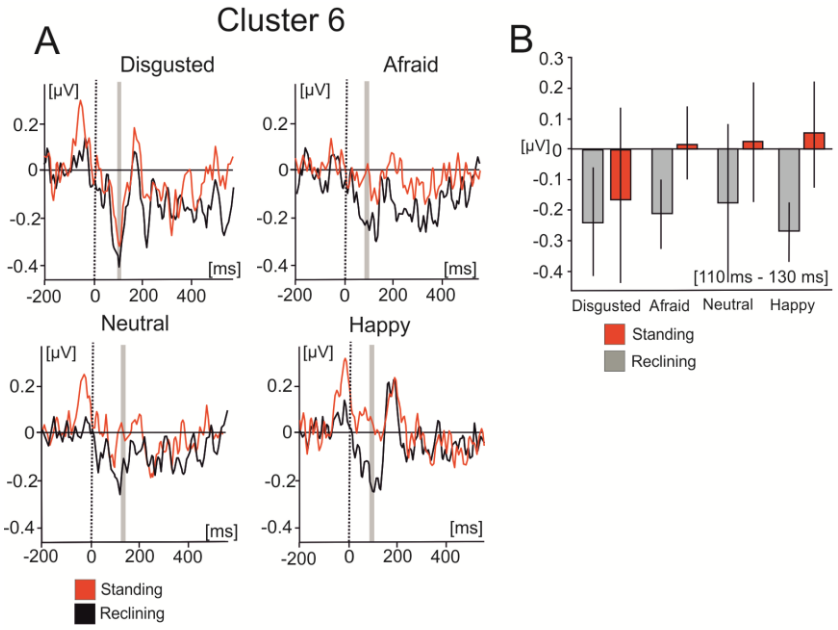

Figure 6.5.3.2. Mean IC cluster activations for cluster 6. A. IC activity between -200 ms to 600 ms for each emotional condition. Red lines represent the standing condition and black lines represent the reclining condition. B. Bar graph represents the averaged IC activity over the shaded area between 120 ms – 140 ms.

6.6 Discussion

The present study contrasted multi-postural wireless EEG signals recorded in naturalistic settings in order to investigate the effect of posture on face specific EEG activity. Our results indicated that upright body postures strongly reduced the lambda component amplitude, but not the later N170/VPP complex. When subjects viewed the faces in a standing posture reduced lambda amplitudes were produced relative to when a reclined sitting posture was assumed during viewing. Our results demonstrated reduced lambda waveforms were present during the standing condition. This difference was greatest in the afraid and happy emotional categories subjects were reclined relative to when standing. In both postures, the EMRPs displayed similar GFP profiles and scalp topographies. ICA and subsequent dipole fitting was then used to group IC across subjects based on the spatio-temporal distributions of IC activity. The IC clustering routine was used to spatially filter the mobile EEG data recorded in a naturalistic environment. The IC-based artifact rejection and subsequent dipole fitting procedure as implemented in EEGLAB provides a single dipole solution for the averaged component, limiting the spatial resolution and accuracy of the source model. As such, we are hesitant to interpret the source localization of the average IC for each cluster.

The lambda response has been identified primarily as a visual response during natural viewing (Thickbroom et al., 1991) and is regarded as the analogue of the P100 component elicited in laboratory based testing. The lambda potential is similarly elicited by the afferent inflow beginning at onset of the visual stimulus (Yagi, 1981b); it is thought to represent rapid indexing of visual stimuli and like the P100 component is also modulated by low-level visual features (Pourtois, Dan, Grandjean, Sander, & Vuilleumier, 2005) as well as saccade size (Dimigen et al., 2011). Contrary to our results, previous research has shown that leaning forward in a sitting position enhances the P100 component in response to sexually erotic images (Price et al., 2012) shortens reaction times and increases left frontal cortical activity in response to appetitive food cues when compared to recumbent sitting positions (Harmon-Jones et al., 2011). This has yet to been demonstrated for standing postures. It has been suggested that the P100 component additionally reflects discrete attentional mechanisms in which the

enhancement of the P100 component would be invoked by the suppression of unattended stimuli (Clark & Hillyard, 1996). The focusing of visual attention has consistently yielded enhanced P1 amplitudes in laboratory based testing in the past (Di Russo & Spinelli, 1999; Hillyard & Anllo-Vento, 1998). The P100 enhancement effect has been explained by the recruitment of additional extrastriate neurons when attention is focused on the image (Luck, Woodman, & Vogel, 2000). In general, it is well established that visual evoked potentials are larger during focused attention (Van Voorhis & Hillyard, 1977) and previous ERP research has shown colour, shapes and motion can modulate visual ERPs staring at about 100ms (Anllo-Vento, Luck, & Hillyard, 1998; Torriente, Valdes-Sosa, Ramirez, & Bobes, 1999). Following this, the reduction of the lambda component found in our standing condition likely results from the additional attentional demands on the visual system during natural viewing. Further, the focusing of visual attention could explain this reduction given that the in sitting condition there was no need for subjects to attend to environmental factors, nor incur in planning of motor actions.

As such, the lambda component would be indexing sustained visual attention in natural environments. Visual processing in a natural setting includes both multi- and trans-saccadic processes involving short term visual memory, planning, and prediction (Melcher & Colby, 2008). The continuous stream of visual information becomes increasingly relevant when exploring a naturalistic environment, moving from one location to another to view images. Furthermore, evidence that visual search involves the rapid shift in distribution of attention among scanned objects has been presented in the past (Woodman & Luck, 1999). Conversely, the enhanced lambda amplitudes elicited from the recumbent positions likely results from the narrowing focus of visual attention in the more consistent with the constraint, stationary setting.

Alternative explanations including at least one physiological and one methodological consideration must be considered when interpreting these results. Firstly, upright postures have been associated with increased high frequency oscillatory activity (i.e. gamma), but reduced power in the lower frequency EEG bands (i.e. delta; theta; alpha) (Chang et al., 2011; Thibault et al., 2014). Unfortunately, high-frequency

neural activity overlaps with the spectral bandwidth of muscle artifacts (~30 – 300 Hz) (Muthukumaraswamy, 2013) which are inevitably present in wireless EEG data recorded from freely moving participants. During the pre-processing procedure of the mobile EEG signals, high frequency oscillatory activity was low-pass filtered at 35 Hz to reduce the influence of muscle artifacts and prevent aliasing (Oken, 1986). As such, it is possible that the strong reduction in lambda amplitude is determined by the reduction in power over lower frequency bands resulting from upright postures relative to supine (Chang et al., 2011). Previous research into the energy distribution in the frequency domain has shown that the P100 component corresponds to increases in power in a wide range of frequency bands, but primarily within the theta and alpha bands (Quian Quiroga, Rosso, Basar, & Schurmann, 2001). Secondly, we must consider the displacement of the brain inside the skull and changes in thickness of the cerebral spinal fluid surrounding the brain. Changing from a prone to supine position has shown to generate decreases in cerebral spinal fluid thickness of approximately 30% which can in strongly influence occipital EEG signals (Rice, Rorden, Little, & Parra, 2013).

To the best of our knowledge, this is the first study to investigate postural effects on face-sensitive visual evoked activations. The N170/VPP face-sensitive components were the main features of the EMRP and have previously been hypothesized to represent the same brain process given their shared neural generator (Joyce & Rossion, 2005). However, contrary to our predictions, neither face-sensitive potentials showed any effects of posture on waveform amplitude nor were they affected by the emotional expressions on the faces at either posture. Similar results presenting a lack of emotional modulation on the N170 have been reported in laboratory experiments in the past (Ashley et al., 2004; Dennis & Chen, 2007; Eimer & Holmes, 2002). However, a recent meta-analysis has confirmed the N170 component does indeed encode the emotional content of faces (Hinojosa, Mercado, & Carretié, 2015). Furthermore, our previous MoBI experiment also showed emotional encoding of face expression in the N170 amplitude in natural environments (Soto et al., 2018). However in most of these studies face images were typically contrasted to non-face object images. Here, object images were not included into the stimuli and only faces were used. This was done to maximize the number of face presentations in each emotional condition. It is possible however,

that habituation effects known to dampen the peak of the N170 amplitude reduced the magnitude of the expected emotional effects (Maurer, Rossion, & McCandliss, 2008).

We demonstrated that the N170/VPP face-sensitive EMRPs were clearly identified during natural standing as well as during reclined sitting, but showed no influence of posture on face-sensitive information processing. An effect of posture was however, detected on the averaged IC activity within the latency of the lambda potential. While standing, reduced lambda waveforms were obtained relative to the sitting position. We partially attribute this effect to modulations in attentional shifts during natural vision relative to laboratory based free-viewing. Future MoBI research into visual information processing during natural behaviour should consider these results when investigating early evoked visual potentials in upright postures. Additionally, we pose that further research is needed to investigate the effect of cerebral spinal fluid thickness shifts on ERPs in mobile settings. Furthermore, methodological issues like high frequency band filtering of EEG activity must be overcome and should be addressed by future MoBI investigations.

Chapter 7

Face-related electrocortical potentials during a natural dyadic interaction.

Soto, V.[1], Roberts, H.[1], Hewitt, D.[1], Tyson-Carr, J.[1], Kokmotou, K.[1,2], Byrne, A.[1,2], Fallon, N.[1], Giesbrecht, T.[3], Stancak, A.[1,2]

[1] Department of Psychological Sciences, University of Liverpool, Liverpool, United Kingdom,

[2] Institute for Risk and Uncertainty, University of Liverpool, Liverpool, United Kingdom,

[3] Unilever Research & Development Port Sunlight Laboratory, Merseyside, United Kingdom

This investigation examined face-sensitive brain potentials generated from viewing a real face while sustaining a spontaneous conversation. We described the neural correlates of face processing during a natural social dyadic interaction. The manuscript for this paper is currently being prepared to submit for publication.

The roles of the co-authors are summarised below:

I designed the study in collaboration with Andrej Stancak and carried out the data acquisition. Hannah Roberts, Danielle Hewitt, John Tyson-Carr, Katerina Kokmotou, and Adam Byrne assisted with the collection of data and contributed useful comments whilst preparing the manuscript. I modified original computer programs created by Andrej Stancak for data analysis and synchronization of mobile EEG and eye-tracking data. Andrej Stancak, Nicholas Fallon and Timo Giesbrecht contributed to the large-scale planning of this project Andrej Stancak, Nicholas Fallon and Timo Giesbrecht secured funding for the project.

7.1 Abstract

The possibility of detecting brain electrical potentials in natural environments has recently been established using combined electroencephalography and eye-tracking systems. The way in which the brain represents real human faces during natural dyadic interactions is yet to be investigated. The aim of the current investigation was to detect, for the first time, face-sensitive brain potentials that arise from viewing a real face during a conversation with another person.

64-channel wireless electroencephalography (EEG) combined with mobile eye-tracking was recorded from 10 healthy participants during a poster presentation session conducted by a confederate. The poster session consisted of an informal conversation where subjects viewed both the presenter's face and images displayed on a poster. Data streams were synchronized at the start of each experiment and gaze data from the eye tracker was then used to inform the EEG analysis. The initial instance in which the gaze marker made contact with a stimulus (face or image) within a continuous stream of fixations was identified and inserted as triggers into the continuous EEG data. Eye movement related potentials (EMRPs) were calculated from the initial instances of a participant's gaze contacted the real face or an object image.

The EEG analysis revealed a negative EMRP within the broad latency interval of the N170 component occurred during face viewing and was not present when the poster was viewed. The N170 peaked at 154 ms and was observed at an occipito-parietal electrode location on the scalp when participants viewed a real face during a conversation. A clear lambda component was also observed in the averaged EEG data and was present for both image and real face categories. An independent component analysis (ICA) was used to extract genuine brain potentials from extracerebral sources of noise. Source dipole modelling was used to examine the generators of the main contributors to the grand averaged visual evoked potential. The analysis revealed one equivalent current dipole (ECD) in the secondary visual cortex (BA 19) that modelled the lambda response.

One ECD was located in the lower portions of the parietal lobe (BA 7) and another in the orbitofrontal cortex (BA 10).

Our results demonstrate the feasibility of recording brain responses to a real human faces during a natural social interaction. The results presented here resemble findings obtained from previous laboratory-based N170 reports; alluding to similar neural mechanisms active during a normal conversation. These findings open new possibilities for future EEG research in the real world.

7.2 Introduction

Natural vision presents humans with a steady stream of visual stimuli which, in most cases includes physical objects as well as human faces. The correct detection and discrimination of a face from an object within our visual field is important for normal perception (Towler, Gosling, Duchaine, & Eimer, 2012) and for human social interactions (Frith, 2009). Previous brain imaging research has indicated a set of specialized brain regions associated with the processing of human faces (Haxby, Hoffman, & Gobbini, 2000; Haxby, Hoffman, & Gobbini, 2002; Kanwisher, McDermott, & Chun, 1997). EEG investigations into the mechanisms commanding face processing have discovered a face-specific negative event related potential (ERP) that peaks at 170 ms when faces, but not objects are viewed (N170) (Bentin et al., 1996). These investigations, however, are rarely performed using stimuli like tangible objects or real human faces. Instead, the bulk of the research into human visual processing is performed on isolated subjects using two dimensional pictures as stimuli; highly removed from real world viewing behaviour. This investigation attempted, for the first time, to examine face-sensitive brain potentials that arise from viewing a real face in a setting closely matching a natural dyadic social interaction.

Dyadic interactions are characterized by intricate reciprocal relationships of relayed information which prompts behaviours that are simultaneously processed and responded to within the social context (Schilbach et al., 2013). Verbal exchanges have previously been associated with enhanced inter-brain synchrony between the speaker

and the listener (Pérez, Carreiras, & Duñabeitia, 2017) as well as increases in synchronous neural activity in the alpha, beta and gamma bands over parietal locations after cooperative interactions (Dumas, Nadel, Soussignan, Martinerie, & Garnero, 2010). Strong alpha and beta modulations have been shown to occur bilaterally in the sensory-motor cortices and stronger beta modulation has been reported in followers relative to leaders during motor entrainment (Zhou, Bourguignon, Parkkonen, & Hari, 2016). These oscillations originated in early visual cortices alluding to the involvement of visual information processing during social entrainment and hand motion mimicking. These investigations however, have classically used video feeds to monitor and time-lock behavioral events to the EEG time series.

As such, a specific methodological challenge is the synchronization of a cognitive process with an electrocortical potential in a natural environment. To resolve this issue, an innovative mobile brain and body imaging (MoBI) technique was used to record simultaneous EEG data and eye-tracking data during a natural conversation. MoBI systems have been of interest in the field of cognitive neuroscience and psychophysiology for almost a decade (Makeig et al., 2009). Seminal investigations examined visual processing during standing and walking (Gramann et al., 2010), as well as the effects of locomotion on visual cortical activity (Gwin et al., 2011). More recently, studies have started using MoBI to explore brain activity in real world environments during natural cognition (Cruz-Garza et al., 2017; Zink et al., 2016). Currently however, the neural correlates of real human face processing during a normal dyadic interaction are yet to be examined using this technique.

Our group has recently conducted a combined mobile EEG and eye-tracking experiment that evaluated neural activity in response to emotional faces images presented in a mock picture gallery (Soto et al., 2018). A face-sensitive N170 component was detected in the mobile EEG signals establishing the possibility of using eye-tracking data to compute EMPR in freely moving individuals. The N170 component is an early negative potential that occurs over occipito-temporal electrodes and has been well established as an index of early visual information processing (Bentin et al., 1996). It can be modulated by a number of experimental influences including the emotional

expression of a face (Hinojosa et al., 2015), the viewer's level of expertise (Tanaka & Curran, 2001) or simple inversion effects (Eimer, 2000; Rossion et al., 2000). As a result, it has been proposed that well controlled inter-stimulus perceptual variability differences between stimulus categories would abolish the face-sensitive N170 effect (Thierry et al., 2007). Other researchers have debated this showing face specificity in the N170 amplitude using stimuli that have been matched in terms of low-level features (Bentin et al., 2007). These factors may also modulate the perception of faces and, hence, the face-related potentials during a natural dyadic interaction.

The primary aim of the current investigation was to employ the MoBI methodology presented in our previous experiment (Soto et al., 2018) to examine neural responses to a real human face during a natural dyadic interaction. We expected to find a N170 component would be present when subjects viewed a real face, but would not exist when viewing images of objects. Additional components encoding low-level features of the object images as well as the real face were additionally anticipated. As such, a secondary aim of this investigation was to evaluate the extent to which previous laboratory based ERP results would carry over into the real world during natural cognition.

7.3 Materials and methods

7.3.1 Participants

14 healthy volunteers were initially recruited to participate in the study. Data from 2 subjects was discarded due to a loss of synchronization in the beginning of the experiment. Two additional subjects' data were discarded, one due to a loss of gaze information in the eye-tracking recording and another due excessive noise in the EEG signal. Therefore, the final sample was composed of 10 subjects (5 females) with an average of 27.4 ± 5.6 years of age (mean ± SD). All subjects gave written informed consent prior to taking part of the study in agreement with the ethical approval obtained from the University of Liverpool Research Ethics Committee. Participants received £15

as compensation for their travel expenses and time. All experimental procedures were conducted in a single session in accordance with the Declaration of Helsinki.

7.3.2 Stimuli and materials

Two co-authors of this paper (HR and DH, both females) participated in the experiment as confederates for the poster session. The role of the confederates was to maintain a conversation with the participant regarding the topic displayed on the poster. The confederates were briefed and given documentation on the four topics to prepare each presentation in advance (i.e. future technologies, travel destinations, hobbies and fun and electric v/s gasoline vehicles). The real world stimuli consisted of both the confederate's face and the images of objects displayed on the posters. Each topic had its own poster which included images of objects and landscapes as well as a title and image labels (example in Figure 7.3.2A). All posters were printed onto A0-sized paper sheets and attached to a stand using Velcro. These topics were designed to engage the participant's interests and allow a natural conversation to occur. Participants selected and viewed one poster at a time, however if the conversation suddenly became stagnant or came to a natural conclusion subjects were asked to select a new poster to discuss.

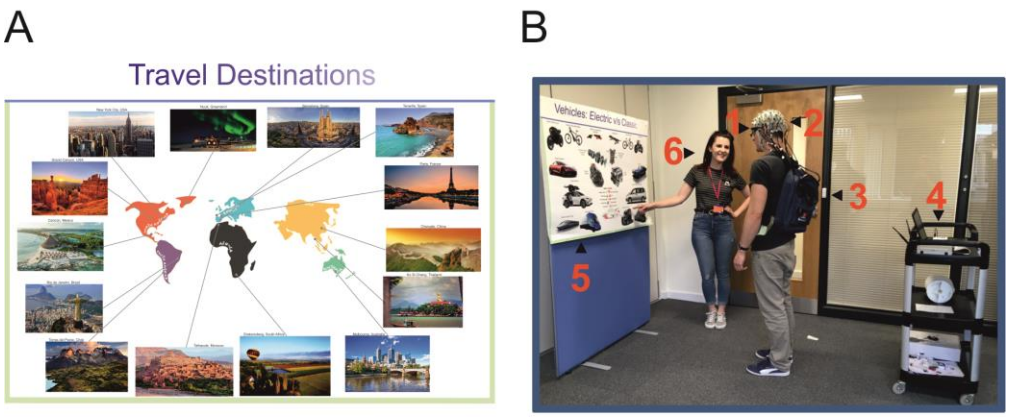

Figure 7.3.2 Experimental setup and wireless EEG recordings. A. Example of one poster (120 cm × 90 cm). B. One participant viewing images while wearing the wireless EEG and a portable eye-tracker. (1) Pupil wearable eye tracker. (2) MOVE wireless EEG 64 channel actiCap. (3) Eye tracking PC contained in the backpack. (4) EEG receiver and recording PC. (5) Poster panel. (6) Confederate. The man and woman appearing in (B) are authors of this work and provided informed written consent to appear in this figure.

7.3.3 Procedure

Once the EEG and eye-tracking equipment was setup, participants were walked into a testing space where the confederate was waiting. A designated room within the Brain and Behaviour Laboratory of the University of Liverpool was used because of the open plan space and plentiful natural light. The laptop registering the eye-tracking was placed in a backpack and was worn by the participant for the duration of the task. The laptop was checked once, in the middle of the session, to ensure no loss of calibration or gaze position had occurred throughout the task. EEG cables running from the electrodes to the lightweight transmitter were also placed under the backpack to reduce cable sway artifacts which can influence the EEG data (Gramann et al., 2010; Gwin et al., 2010). A mobile base unit was assembled using a rolling trolley where the wireless signal receiver, EEG amplifier and recording computer were placed. The base unit was positioned by the experimenter keeping a distance of about 1.5 m behind the participant in order to maintain optimal signal quality (Figure 7.3.2B).

Participants were requested to stand while they took part in the conversation and to look at both the images and the presenter. Subjects were not instructed to avoid movements or eye-blinks, rather, they were asked to behave normally and be inquisitive. Subjects took part in a single experimental session which lasted no more than 60 minutes including setup, testing and debriefing. During the presentation, subjects viewed at least one poster on their selected topic and the confederate. The task commenced with a short presentation given by the confederate (5 minutes) and then an informal discussion took place where participants were encouraged to ask questions and give their opinions (10 minutes). The presentation and discussion lasted approximately 15 minutes. After the conversation concluded, equipment was removed and participants were thanked and debriefed.

7.4 EEG recordings

EEG data was recorded using a 64-channel wireless EEG system (Brain Products, GmbH, Münich, Germany). A lightweight EEG signal transmitter which participants carry on a belt was used to transmit the EEG signal to the recording

computer (Figure 7.3.2B). Active Ag/AgCl electrodes were mounted on an electrode cap (actiCAP, Brain Products, GmbH) according to the 10-20 electrode system and aligned to the midpoint between the anatomical landmarks of the nasion and inion, and selected left and right preauricular points. Electrode FCz was used as the system ground and electrodes were referenced to AFz. EEG recordings were sampled at a rate of 1000 Hz. Electrolyte gel was applied to lower electrode-to-skin impedances under 50 kΩ at the start of the experiment. An average reference was applied to the EEG signals that were digitized at 1 kHz with a BrainAmp DC amplifier controlled by the Brain Vision Recorder program version 1.20.0601 running on Windows machine. Data were filtered online using a 0.1-200 Hz bandpass filter. The mobile EEG MOVE system (Brainproducts) was then connected and wireless signals were visually inspected on a standing participant before commencing the experiment.

7.5 Eye movement recording

A PUPIL (Kassner et al., 2014) eye-tracking system was used to record the locations of the gaze position of the right eye in all subjects. Pupil Capture software v. 1.6.11 running on Windows 10 was used to generate the recordings. The wearable PUPIL eye tracker is a lightweight solution for mobile gaze-tracking (Figure 7.3.2B). Pupil locations were recorded using infra-red cameras sampling at 200 Hz with a resolution of 240 × 240 pixels. The real-world video streams were set at a sampling rate of 60 frames per second with a resolution of 600 × 800 pixels.

To calibrate the gaze positions, a manual marker 3D calibration protocol was used to generate a 9-point grid in the field of view of the participant. Calibration was repeated until gaze positions were accurate at all location on the blank panel. Eye-tracking data were processed using Pupil Player v. 1.9.1 program. The ocular pupil the right eye was located based on a centre-surround detection algorithm (Świrski et al., 2012). Exported raw data is time-locked to the processing computer's internal clock, giving millisecond precision to the eye measurements. Additionally, all recorded frames contained an accurate time stamp based on the PC processor real-time clock. The first detectable frame in which the gaze contacted a stimulus after leaving a stimulus of the

opposing category was detected from the world video recordings. The real times corresponding to the tabulated frames were then used to import stimulus onset latencies onto the raw EEG data.

7.6 Data synchronization

A trigger-box fitted with a light emitting diode (LED) was constructed to synchronise data streams at the start of every recording. The flash of the LED light on the trigger-box was recorded by the world-view camera on the eye trackers as a simultaneous transistor-transistor logic pulse was registered in the EEG data recording. The visual light cue became apparent at a specific frame in the eye-tracking video data and this was used to synchronize the time axis of the data streams. The asynchrony was tested in a previous pilot study and resulted in 0.022 ± 0.020 s (mean ± SD) asynchrony over a 15-min recording.

7.7 EEG analysis

7.7.1 Eye movement related potentials

EEG data were analysed using the Brain Electrical Source Analysis program (BESA v.7.0, MEGIS Software GmbH, Munich, Germany). Data were initially referenced using common average method (Lehmann, 1987) and digital filters were applied to remove frequencies lower than 0.5 Hz and higher than 35 Hz from the EEG data. Electro-oculographic artefacts topographies (i.e. blinks, vertical and horizontal eye-movement artifacts) were removed using a pattern matching based on a principal component analysis (Berg & Scherg, 1994; Ille et al., 2002). Additionally, EEG data was visually inspected for movement, cable sway and muscle artifacts and trials contaminated with large artifacts were marked and excluded from further analysis. The average amount of stimuli in the object condition was 39.5 ± 13.4 (mean ± SD) and 44.2 ± 12.4 (mean ± SD) for the real face condition.

Event markers were inserted into EEG data by synchronizing the time axes of the EEG and eye-tracking system. The onset of a stimulus was defined as the first 'new' contact of the gaze with the confederates' face or any image on the poster. This time point effectively corresponded to end of the saccade which brought the gaze onto a particular fixation after leaving a stimulus of the opposing condition. Succeeding fixations on the same stimulus type were disregarded from the analysis and EEG data were epoched to range from -200 ms to 400 ms. The mean EEG activity in the baseline interval ranging from -200 ms to -100 ms was removed from each data point as it represented a more stable baseline than the 100 ms preceding viewing onset which contained large part of the eye-movement artifact that brought the eye to fixation on a stimulus' The average EMRPs were computed from the gaze onset of trials falling into the two conditions. EEG epochs were generated as cuts into the real-world video scene in the same manner as described in Soto et al. (2018).

7.7.2 Idependent component analysis

To extract the task-related components in the EEG signal, ICA was performed in BESA using the extended Infomax ICA algorithm (Lee, Girolami, & Sejnowski, 1999). ICA was applied on the grand average EMRP waveforms for both conditions. Before ICA was calculated, the dimensionality of the data was reduced by principal component analysis (PCA). PCA solutions are constrained by orthogonality of components, and by those that account for greatest common variance. As a default in BESA, PCA components explaining less than 1% of the variance are ignored. ICA was applied as it is an established method for solving the blind source separation problem (Jung et al., 2000). Without presuming any prior knowledge of the nature and location of the neural generators, ICA is constrained to find temporally independent components and it distinguishes sources that are maximally statistically independent from each other. As such, BESA solutions are constrained by the geometry of the head, the volume conduction of the dipoles, and the anatomical constraints dictated by the user.

7.7.3 Source dipole analysis

Source dipole modeling was used to separate electrical activations originating in the occipitotemporal cortex from those electrical potentials which originated in eye orbits and were volume conducted to distant regions of the scalp. EEG epochs were time-locked to the initial shift of the gaze onto a face or a picture on the poster. Due to this, we anticipated that EMRPs will include the presence of a small, saccade-related cortical potential and artefacts associated with offsets of saccades (Kazai & Yagi, 2003; Thickbroom et al., 1991; Yagi, 1981a). The eye-movement artifacts are the manifestations of the corneoretinal potential resulting from the displacement of the large electrical dipole of the eye during blinks, saccades and eye movements; as well as smaller saccade spike potential related to the contraction of oculomotor muscles during the saccade (Dimigen et al., 2011; Nikolaev et al., 2016).

A source dipole model was constructed using BESA v. 7.0 to investigate the cortical sources of the peaks in the average EMRP of the face related potential. Three equivalent current dipoles were fitted using a sequential strategy (Hoechstetter et al., 2010; Stancak et al., 2002). ECDs were sequentially fitted based on the peak latencies of the prominent EMRP peaks determined in the global field power curve. In the sequential fitting procedure, each additional ECD explains the portion of data variance not accounted for by previously fitted ECDs. To confirm the location of the ECDs, a classical LORETA (Pascual-Marqui et al., 1994) analysis recursively applied (CLARA) was utilized (Hoechstetter et al., 2010). CLARA did not show any new cluster beyond two locations previously tagged by ECDs. Additional ECDs added to the model did not improve the amount of explained residual variance or resulted in the dipole being placed outside of the head. This meant the extra dipoles did not explain any specific topographic aspect of the potential field. A 4-shell ellipsoid head volume conductor model was employed to construct the source dipole model using the following conductivities for each layer: brain = 0.33 S/m; scalp = 0.33 S/m; bone = 0.0042 S/m; cerebrospinal fluid = 1.0 S/m.

Due to the presence of a small jitter between the EEG and eye-tracking data streams and changes in the distance between the participant and the viewed stimulus, we were not able to quantify the parameters of individual saccades or evaluate their impact on EEG potentials in the present study.

7.8 Result

7.8.1 EMRPs

EMRPs were time-locked to the initial shift of gaze onto a new image or the confederate's face. Figure 7.8.1A illustrates the EMRP butterfly plots for object and face conditions between -200 ms to 400 ms post stimulus onset. Two prominent features are highlighted in the global field power plots in the face condition while only one can be observed for object images (Figure 7.8.1B). The topographic maps at peak latencies in the grand average EMRPs are depicted in Figure 7.8.1C. In both conditions, small negative component was found over frontal electrode sites at approximately 20 ms prior to an image or face being viewed. These small potentials could represent the anticipation of a face or an image picture, but could also be related to small influences of saccades preceding the time-locking event of the evoked waveforms. The lambda potential (Thickbroom et al., 1991; Yagi, 1981a) represented the main component with a large component peaking at 60 ms in the face condition and 85 ms for object condition. Only when faces were viewed an additional negative component with posterior distributions was present at 135 ms. Due to the peak latency, topographical scalp distribution and enhanced waveform amplitude for faces relative to objects, this potential was associated with the classical N170 component.

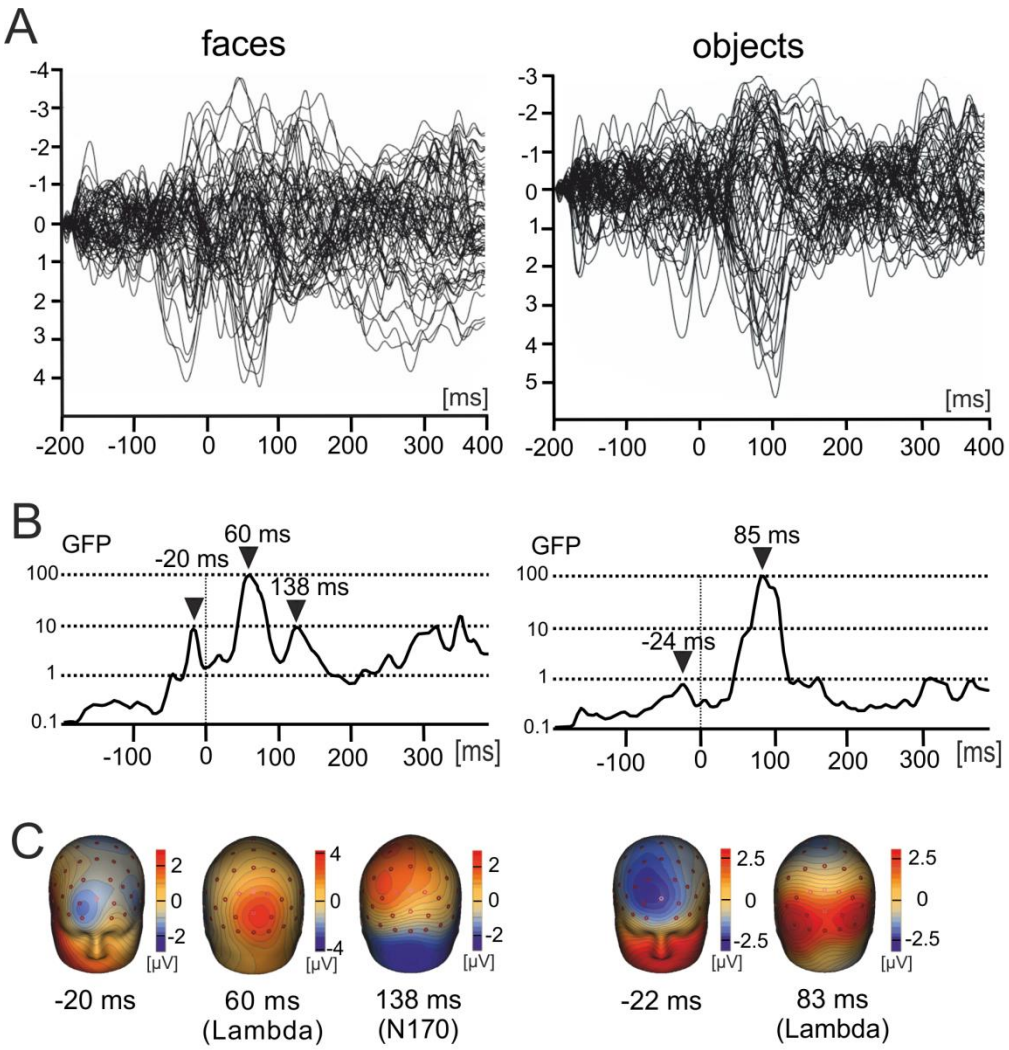

Figure 7.8.1 Grand average EMRPs during viewing of the face and object images. A. Butterfly plots of grand average EMRPs to face and object pictures. Peak latencies of distinct EMRPs components are highlighted with arrows. B. Global field power for face and object pictures. The highlighted latencies correspond to the peaks in GFP. C. The topographic maps of grand average EMRPs overlaid on the volume rendering of the human head at the highlighted latencies.

Figures 7.8.1.1A presents the negative scalp level N170 component at 155 ms over posterior locations for the face condition. The positive lambda component at 60 ms was present for both conditions. At electrode site PO8 the N170 waveform shows a maximum negative peak at 155 ms that was elicited exclusively for real faces, but not for object images. The lambda component was maximal at electrode site POz. The positive peak ranging between 60 and 90 ms was present for both conditions, aligning with previous reports of 80 ms - 100 ms peak latency of the lambda wave when

calculated from the offset of a saccade (Yagi, 1979a). The peak latency of this component represents a positive indicator that the EMRP were synchronized closely to the offset of the saccade that brought the gaze onto a stimulus of either condition. Figure 7.8.1.1B shows the topographical maps at peak latencies for the lambda and N170 component.

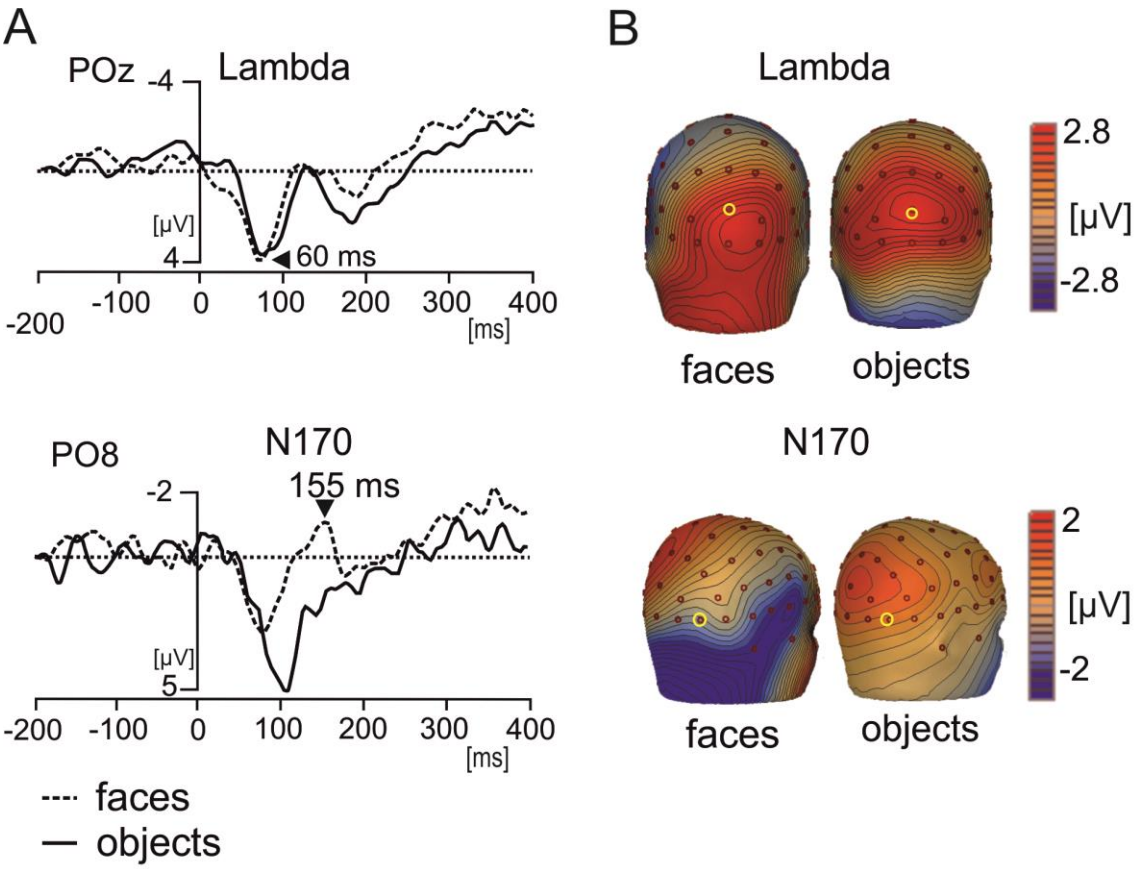

Figure 7.8.1.1. Grand average EMRP waveform at electrodes POz and PO8. A. Mean EMRP for the face and object conditions. The lambda EMRP was calculated at electrode POz and the N170 component at electrode PO8. B. The spatial topographic maps at the latency points showing the largest peaks for the lambda and N170 component.

7.8.2 ICA

Independent component analysis was used to explore the individual generators underlying the EMRP waveforms. The results of the ICA are presented in full in Figure 7.8.2A. The ICA showed clean decompositions extracting cerebral components as well as components accounting for extracerebral sources of noise like small saccadic activity not fully resolved using the pattern matching procedure during the pre-processing stage. Figure 7.8.2B presents the topographies and scalp distributions of the ICA components of interest in each condition. For the face and object image conditions two ICA components (ICA#1 & ICA#4 in face and ICA#1 and ICA#2 in object condition) accounted for the posterior positive potential within the latency of the lambda potential. In the real face category, one additional ICA component accounted for the N170

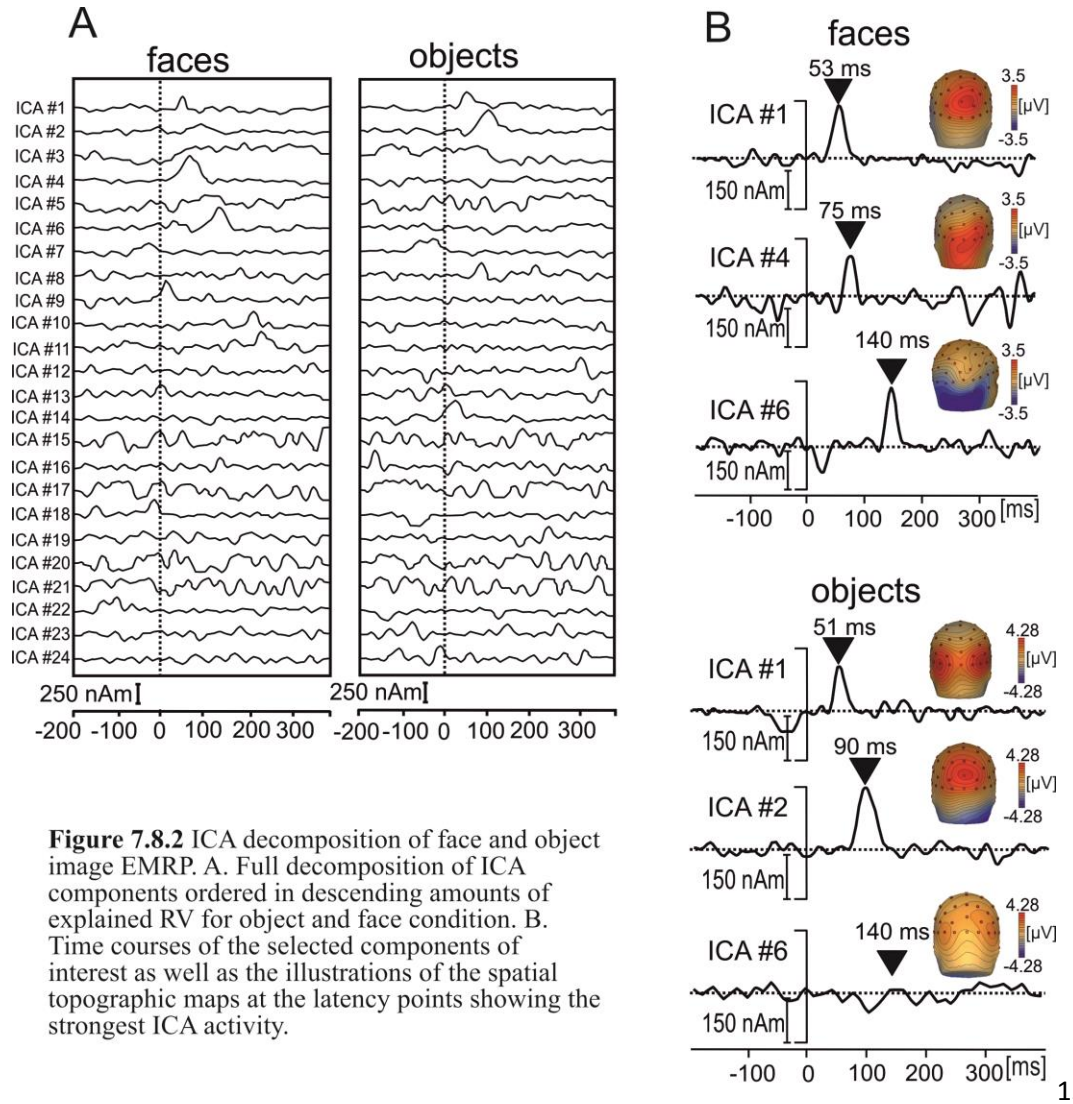

Figure 7.8.2 ICA decomposition of face and object image EMRP. A. Full decomposition of ICA components ordered in descending amounts of explained RV for object and face condition. B. Time courses of the selected components of interest as well as the illustrations of the spatial topographic maps at the latency points showing the strongest ICA activity.

potential. ICA#5 peaked at 140 ms and showed a right hemispheric distribution over posterior and temporal portions scalp. This component was not present in the object image condition.

7.8.3 Source dipole analysis

Figure 7.8.3A shows the GFP and of RV of the three ECD source solution for the object and face conditions. The source dipole waveforms and spatial topographic maps and ECD waveforms for each dipole fitted in the source model to each condition are presented in Figure 7.8.3B. The dipole orientations and estimated ECD locations are illustrate glass brains in Figure 7.8.3C. To compared the effectiveness of the ECD solution in modelling the sources of for face and object EMRPs individually the model was applied separately to the grand average waveforms for both conditions. In the latency interval between 60 ms and 70 ms the source model accounted for 81.3 % of the data in the objects condition and 79.9% in the real face condition. Within the 125 ms to 145 ms latency interval of the face related secondary peak, the source model explained 71.4% of the residual variance in the data.

ECD 1 was fitted to inferior portions of the occipital cortex aloo referred to as the visual association area in the brain (Brodmann area (BA) 18; approximate Talairach coordinates: x = 3.7, y = -60, z = -5.1 mm). This dipole modelled the large positive component of the lambda potential (Figures 5B-C). EDC1 explained the main positive potential peak at 60 ms in face and 63 ms objects conditions at posterior portions brain areas. ECD2 was located in the orbitofrontal cortex close to the medial frontal gyrus (BA 10; approximate Talairach coordinates: x = 3.5, y = 53.9, z = 2.7 mm). ECD3 modeled the N170 component and was located to the anterior portion of the extrastriate cortex in the occipital lobe (BA 19; approximate Talairach coordinates: x = -17, y = -47.5, z = -4 mm). This source accounted for a smaller negative potential occurring at 141 ms in occipital electrodes present only in the face condition. For the object images this ECD did not show a peak in activity at 141 ms.

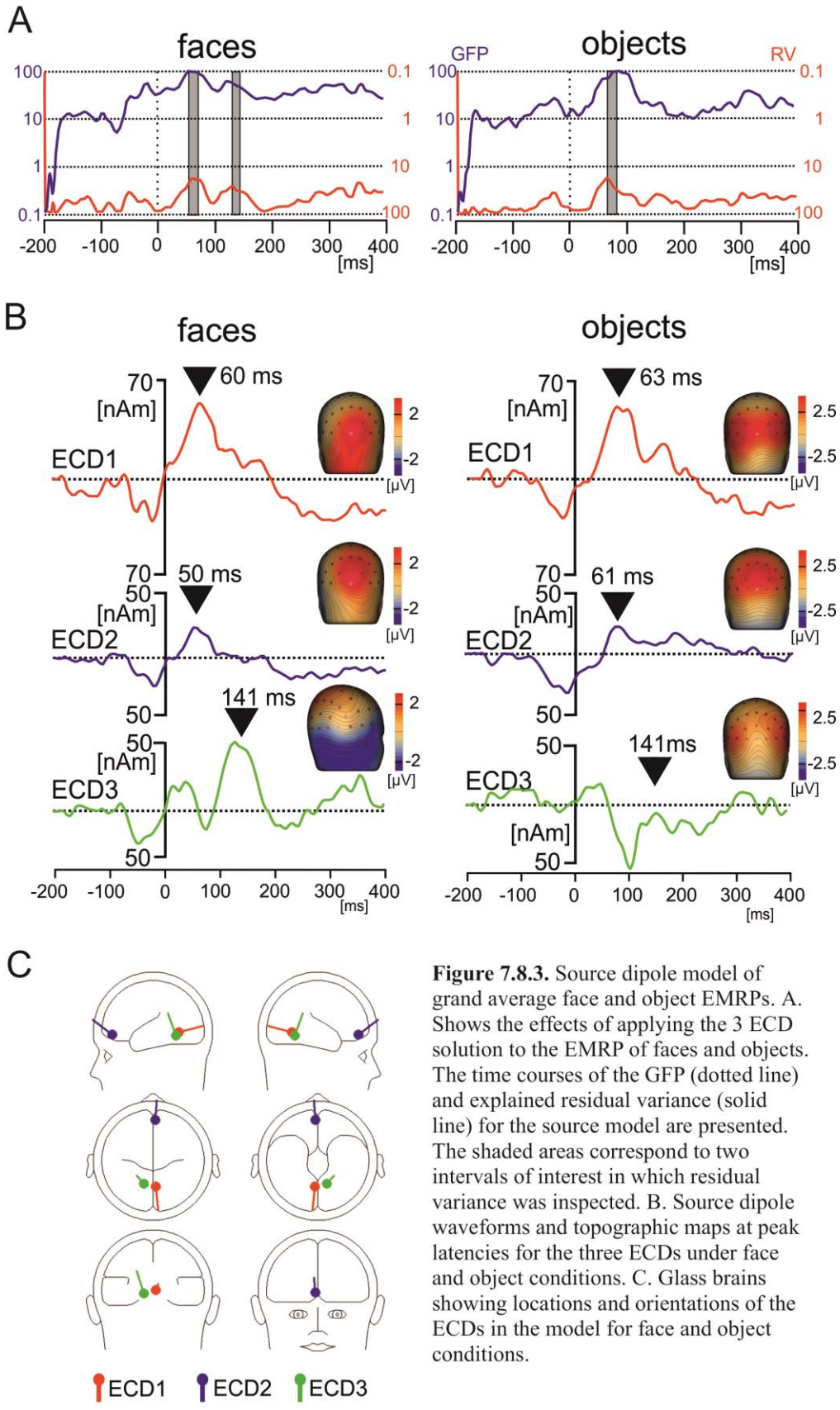

Figure 7.8.3. Source dipole model of grand average face and object EMRPs. A. Shows the effects of applying the 3 ECD solution to the EMRP of faces and objects. The time courses of the GFP (dotted line) and explained residual variance (solid line) for the source model are presented. The shaded areas correspond to two intervals of interest in which residual variance was inspected. B. Source dipole waveforms and topographic maps at peak latencies for the three ECDs under face and object conditions. C. Glass brains showing locations and orientations of the ECDs in the model for face and object conditions.

7.9 Discussion

Understanding the brain processes involved during a dyadic social interaction is a challenging problem in contemporary neuroscience. This exploratory investigation represents, to the best of our knowledge, the first piece of evidence of a face-sensitive electrocortical potential identified in the stream of EEG data during a normal conversation.

The main aim of this investigation was to determine whether it was possible to detect the face specific N170 potential during a naturalistic dyadic social interaction. This is similar to recent attempts to record similar to recent attempts to record EEG from interacting individuals using hyperscanning techniques (Hari, Himberg, Nummenmaa, Hämäläinen, & Parkkonen, 2013; Zhou et al., 2016) during social and cooperative interactions (Babiloni et al., 2006). Neuroimaging research using EEG, magnetif functional resonance imaging (MEG) and functional magnetic resonance imaging (fMRI) systems have provided important insights into brain-to-brain communication in social dyads and groups (Babiloni et al., 2007; Hirata et al., 2014; Konvalinka & Roepstorff, 2012). EEG hyperscanning studies have illustrated the role of the phi complex during synchronized movements (Tognoli, Lagarde, DeGuzman, & Kelso, 2007), as well as involve the suppression of beta oscillations in social cooperation (Ménoret et al., 2014) . Furthermore, dual EEG studies have provided evidence of increased phase synchronization, both within subjects and between brains during a joint musical performance (Lindenberger et al., 2009). Inter-brain connections in the inferior frontal gyrus, anterior cingulate, parahippocampal gyrus, and postcentral gyrus have additionally been exposed using this technique (Yun, Watanabe, & Shimojo, 2012). However, the interpretation of hyperscanning results must be taken with some caution, particularily in regards to interpreting hyperconnectivity (Burgess, 2013).

Low-level mechanisms commanding visual perception, including face specific information processing during social interactions have not yet been adressed. Furthermore, the influences of the environment on real-face information processing in a context of social communication are not fully understood. Our results show that only when the real face was viewed a negative component appeared in occipital electrode

sites within the broad latency of the N170 (Bentin et al., 1996; Bötzel et al., 1995; Joyce & Rossion, 2005). The right hemispheric distribution and the presence of a co-occurring vertex positive peak at a latency of 155 ms latency provide definitive evidence of faces sensitive brain responses produced during a normal dyadic interaction. The ICA decomposition of the EMPR separated the genuine brain components from non-cerebral potentials, as well as from other overlapping generators of brain activity. ICA#6 accounted for the N170 component that was only present in the real face condition with a peak latency of 140 ms. This ICA component showed a right hemispheric distribution across temporo-posterior electrode locations, characteristic of the N170 component (Eimer, 2011). This finding represents the first report of a N170 component resulting from the viewing of a real human face, establishing the possibility of using MoBI methodologies to study social dyadic interactions during normal behaviour.

The EMRPs for face and object image conditions presented a prominent positive component within the latency of the lambda component. At electrode site POz, both evoked waveforms showed a similar spatio-temporal profile. The lambda component has classically been understood to represent an index of low-level feature extraction and is the free-viewing equivalent to the P100 component in classical lab-based results (Kazai & Yagi, 2003). As such, we expected to find this component regardless of which stimulus condition is being viewed. Previous reports of the peak latency of the lambda component at 80 – 100 ms suggests that the stimulus onset time for the lambda component in the current study effectively coincided with the final portion of the saccade that brought the gaze to fixation (Yagi, 1981b). Averaging to the offset of a saccade has been proven to be advantageous as it reduces the number of eye-movement artefacts associated with the onset of the saccade (Yagi, 1981a).

A source modelling approach was used to further explore the neural generators of the grand averaged evoked response. The lambda component in the EMRPs was modelled by ECD1 located in visual cortex (BA 18). The N170 component in the data was modelled by EDC3 located in the left BA 19 which is bounded rostrally by occipitotemporal area BA 37 classically associated with human face processing (Itier & Taylor, 2004; Kanwisher et al., 1997). The presence of a source in the visual cortex that

modelled for the lambda component is consistent with previous results and its role as a visual processing region (Kazai & Yagi, 2003). The slight location inaccuracies between these results and previous studies could be explained by differences in the source estimations; ostensibly due to the lack of electrodes in lower posterior locations on the scalp. The source model had a slightly lower level of 'goodness-of-fit' to the data relative to traditional EEG studies. The model accounted for roughly 80% of the residual variance during the peak latency of the lambda potential and 60% of the residual variance in the latency period between 125 – 145 ms where the N170 was maximal. One possible explanation for this is the increased noise in mobile EEG recordings made it difficult to locate the source of the N170 component to the fusiform gyrus in the occipitotemporal cortex (Deffke et al., 2007; Kanwisher et al., 1997). The CLARA analysis that was used to seed the ECDs did not show occipitotemporal activation either. This could be due to the confederate's face being constantly present in visual field during the experiment. Comparable N170 amplitudes for peripherally and centrally presented emotional faces have been shown in the past (Rigoulot et al., 2011; Rigoulot, D'Hondt, Honoré, & Sequeira, 2012). The presence of a real face present in peripheral vision while gazes fell on object images could have activated the fusiform gyrus throughout the experimental session. As such, anticipatory effects could additionally be present in the averaged EMRPs as a result of prolonged visual stimulation (Ran, Chen, Pan, Hu, & Ma, 2014). Furthermore, given that only one face was viewed, adaptation effects could also be influencing the amplitude of the face-sensitive component as well (Amihai, Deouell, & Bentin, 2011).

To the best of our knowledge, only one other study has attempted to replicate the laboratory based N170 using real faces in an ecologically valid setting. Koenig, (2018) has recently presented results showing N170 component produced from the natural viewing of real human faces in a MoBI methodology similarly combining eye-tracking with mobile EEG recordings. This group showed that N170 responses to real faces where less robust than previously reported N170 effects in the literature. Authors demonstrated that when viewing static images of faces in natural environments the results more closely resembled previous accounts of the N170 in mobile and laboratory settings. The findings presented in this thesis align with this report and confirm that it is

indeed possible to capture the N170 face-sensitive EMRP by employing a MoBI methodology and using a real face. The relatively small negative deflection relative to laboratory based results additionally align with the idea that event related brain activations are reduced in the real world as a result of the increased cognitive load resulting from the additional influences of noise associated with the real world environment (Protzak & Gramann, 2018; Zink et al., 2016).

While our results can be viewed as a novel achievement in the field of mobile neuroimaging, some limitations must be considered. The manual tabulation of viwing onsets, for instance, is a time-consuming process which could be improoved using automatic face detection algorithms (i.e. CamSHIFT or the KLT algorithm for Matlab). This could additionally standardise the criteria for detecting and establishing viewing onset in real world environments as it would not require visual inspection of the video feeds. Furthermore, three main technical issues must be considered when interpreting these results. The synchronization jitter between the eye-tracking and EEG data streams (of 20 ms ± 22 ms) could explain inconsistencies in peak latency of the lambda and N170 component relative to previous reports. Secondly, small calibration displacements that occurred in the eye tracker made it difficult to detect all the stimuli onset times, lowering the number of usable trails in the EEG analysis. Finally, the low number of participants that composed the final sample is an inherent limitation to this study; currently more subjects are being tested to moderate this limitation.

We must additionally consider that the free viewing parameters of the real world experiment allow for overlapping neural processes in the EEG data (Dimigen et al., 2011; Makeig, Ca, Bell, & Sejnowski, 1996). Even in controlled laboratory ERP experiments, results often contain a mixture of overlapping brain responses (Eimer & Forster, 2003). Research in real world or quasi-naturalistic environments involve fast and continuous multisensory stimulation as well as complex behavioral responses. To resolve the mixture of neural signals, sophisticated regression-based approaches have been proposed in the past (Frömer, Maier, & Rahman, 2018; Hauk, Davis, Ford, Pulvermüller, & Marslen-Wilson, 2006; Van Humbeeck, Meghanathan, Wagemans, van Leeuwen, & Nikolaev, 2018). Recently, a novel software solution (*unfold* toolbox) has

been presented for implementing advanced deconvolution models and spline regressions in ERP research (Ehinger & Dimigen, 2018). Unlike traditional averaging techniques, regression based modelling can isolate overlapping potentials as well as control the effects of linear and non-linear covariates contributing to the neural responses. Future MoBI investigations using combined mobile EEG and eye-tracking recordings should consider implementing computational tools like the *unfold* toolbox in their analysis pipeline. Additional considerations regard the synchronization of multiple sources of data. The Lab Streaming Layer software allows the exchange of time series between programs and computers in real time, optimizing the synchronization between multimodal data streams (Kothe, 2014).

To conclude, our results demonstrate the possibility of recording face-specific electrocortical responses in naturally interacting individuals during social interactions. These findings support the notion that laboratory-based N170 results could closely translate to natural cognition in the real world. Furthermore, the methodology presented in ths investigation provides a range of experimental possibilities for multiple research domains including social cognition, as well as medical and consumer science.

Chapter 8

General discussion and concluding remarks

8.1. General Discussion

Quotidian perception rarely presents faces in isolation; as such it becomes increasingly relevant to study face processing in complex perceptual environments. The overall aim of this thesis was to explore the neural mechanisms commanding face processing in natural environments. A MoBI methodology was implemented to explore the effects of emotional valence, familiarity and posture on face-specific brain potentials in mobile subjects. Anticipated findings included that the information contained in faces (i.e. emotional expressions and identity) would produce modulations on face-specific brain responses. Further, these modulations were expected to be affected by different body positions. Finally, the possibility of detecting the N170 component during a dyadic social interaction was explored.

8.2 Summary of findings

- The findings established the possibility of combining mobile EEG and eye-tracking recordings to detect face-sensitive cortical potentials in response to face images presented in a mock art gallery setting.
- The results demonstrated that EMRPs acquired using combined eye-tracking and wireless EEG recordings in freely moving individuals clearly differentiated between viewing images of a human face and a non-living object during free viewing.
- The source of the activity generated in the right FFA encoded not only the presence of a face in the visual field, but also the emotional content of faces.

- The effects of emotional expression were observed on the N170 face-sensitive component. Disgusted faces produced an enhanced neural response relative to faces conveying neutral expressions.
- Familiar faces and place images were rated to be more familiar, likable and arousing than unknown faces and places. Images of familiar places were also deemed more pleasant than face images presented in the mock gallery.
- The N170 component did not present modulations resulting from familiarity on source activations in the precuneus.
- Place specific components were detected at distinct latencies, but did not encode the perceived level of familiarity of an image.
- Posture did not strongly influence the N170 component or the VPP counterpart.
- Analysis of independent component clusters revealed an effect of posture on the lambda component activity (100 ms). The lambda amplitude was enhanced at a standing posture relative to reclining.
- The findings provide the first piece of evidence that real human faces elicit N170 electrocortical potentials in the brain during a natural dyadic social interaction.
- These findings support the notion that real-world responses to real faces resemble those produced in a laboratory setting.

8.3 Themes

Several themes emerged from the experimental findings in this thesis. The overarching finding was the detection of the face-sensitive N170 component in the mobile EEG data of subjects in environments approaching natural settings using a mobile brain imaging technic based which incorporates mobile eye tracking. Furthermore, the effects of emotional expression, face familiarity and body posture on the N170 component were examined. Preferential brain responses to faces were represented in the EMRP data acquired in natural settings. The neural correlates associated to processing of real faces were investigated by describing brain components during a real social interaction.

8.3.1 Detecting face related cortical potentials in naturalistic settings

Brain imaging techniques in the past have required participants to maintain a fixed head position during data acquisition. The restriction of head movements is intended to avoid major sources of contamination to EEG signal as well as minimizing eye movement artifacts by presenting stimuli in a fixed position. However, our cognition is closely linked to a dynamic environments that requires adaptive behavioural changes as well as the evaluation of salient features in our environment (Wilson, 2002). The detection of the face-sensitive potential in freely moving subjects using wireless EEG recordings was largely accomplished by capitalizing on recent advances in active electrodes, wearable eye-tracking systems and modern data processing techniques.

A lightweight eye-tracking system was used to incorporate synchronized mobile gaze detection to the EEG data stream. The viewing onset latency for each stimulus was identified and incorporated into the EEG data as event markers. As such, natural viewing behaviour was used to inform the EMRP analysis; dispending of the need to use stimulus presentation systems and computer screens. This affordance however, is unavoidably accompanied by eye movement related noise affecting the EEG signal. In unrestricted subjects, movement artifacts and external sources of are also known to contaminate the ongoing EEG signal. Electromyogenic or muscle artifacts are a major problem for EEG research in general because the relative low signal activity from the brain is overlaid with a high signal activity of muscles. These artifacts are enhanced in mobile scenarios lacking any kind of restriction. To perform the viewing task within the mock gallery, for instance, head displacements allowing the viewing of the images on the panels had to be accounted for. Neck muscles have shown to contribute non-cerebral sources of noise to the ongoing EEG signal while performing looking and pointing tasks (Gramann et al., 2010; Makeig et al., 2009) as well as during locomotion (Gwin et al., 2010; Leutheuser et al., 2013). A specially designed mock art gallery task was created to allow free exploration of the visual scene while naturally minimizing head and body movements. The gallery task was used in all but one of the experimental chapters in this thesis. Within the gallery, the presence of body movement related artifacts was effectively diminished as subjects maintained a stable stance while viewing the images

presented on panels. As such, the major contributions of non-cerebral activity to the EEG signal came from eye-movements.

As described in the experimental chapters, the impact of eye-movement artifacts on the EEG signal was resolved using data analysis method involving ICA which demonstrated to be effective in separating eye-movement artifacts from genuine brain activity. The standard BESA PCA-based pattern matching algorithm for data correction provided a instrumental tool and was included as part of the pre-processing pipeline (Scherg, 2005). The pattern search function scanned the EEG time series is and corrected by calculating the correlation between the subject-specific pattern and all time pointes in the EEG time series (the correlation threshold was always set to 0.75). Due to the presence of movement artifacts, the corrected EEG signals where then visually inspected to detect and exclude any muscle movement artifact or noise present in the data. Automatic artifact rejection routines did not satisfactorily mark noisy segments during EEG processing. Data-driven ICA source decomposition approaches were used to parse the mobile EEG signals into spatially static and maximally temporally independent component processes (Makeig et al., 1996). This spatial filtering technique distinguished ICs contributing maximally to each cortical brain component recorded at the scalp. Furthermore, the generators of distinct ICs were estimated using source localisation techniques which included dipole fitting and IC clustering. The ICA approach provided an accurate and substantial tool for decomposing EEG signals.

Our results demonstrated that dipole modelling and ICA techniques enabled the detection and analysis of face-specific brain potentials while subjects performed a free-viewing task as well as during a natural conversation. Furthermore, the consistency in the identification of the lambda potential, demonstrates the possibility of analysing early eye-movement related brain activity in natural environments. The findings presented in the experimental chapters of this thesis show a bias in neural responses favouring faces over images of objects and places. Furthermore, source dipole analysis revealed a current dipole in the right fusiform gyrus that produced enhanced activations in response to negative emotional facial expressions. Our initial source modelling approach incorporated two regional sources to model the electrical potentials of residual

corneoretinal artifact and saccade spike potentials still remaining after pre-processing (Berg and Scherg, 1991). This method proved effective in removing a major part of the contributions of eye-movement artifacts from the EMRP waveforms.

Combined mobile EEG recordings with a wearable eye-tracking system is a novel approach to examining face-sensitive brain cortical potentials recorded from mobile subjects during natural behaviour. The results presented in Chapter 4 represent a first report of a N170 potential recorded in a natural environment using this methodology. Further, the characteristics of the N170 component presented in the findings in Chapter 7 resemble classic N170 component results and demonstrate the viability of using this method in to examine face processing during social interactions. This represents a valuable innovation on existing EEG and MoBI methods and addresses, to some extent at least, issues of ecological validity as well as the reproducibility of previous laboratory EEG results. The experimental procedure and analysis methods used here extend the examination of the neural mechanisms underlying face processing and can be used in a wide variety of research fields.

8.3.2 Effects of emotional expression and familiarity on the N170 component

Across the experimental chapters in this thesis, the mobile neuroimaging data suggests that face-sensitive electrocortical potentials were detectable using a combined wireless EEG and eye-tracking system. Furthermore, an effect of emotional expression was found on the amplitude of the N170 component. The results presented in the experimental chapters suggests a specialized neural response to faces, but not objects, commands perception of face stimuli in natural settings. The source of the activity generated in the medial occipitotemporal cortex encoded both the presence of a face in the visual field, but also its emotional content.

The strength of the N170 component has shown to linearly increase in magnitude with emotional intensity. Findings from Utama, Takemoto, Koike, & Nakamura, (2009) showed a significant correlation between N170 amplitude and emotional intensity. N170 waveform amplitude would reflect the perception of intensity as has been previously

reported (Sprengelmeyer & Jentzsch, 2006). These results align with the general consensus regarding the sensitivity of the N170 to the emotional content of faces (Hinojosa et al., 2015). Our findings further support previous results showing negative emotional faces generated stronger EMRP responses relative to neutral faces (Blau et al., 2007; Hendriks, Van Boxtel, & Vingerhoets, 2007). Disgusted faces produced significantly stronger N170 amplitudes than neutral faces and similar N170 amplitudes as happy facial expressions when subject stood to view emotional faces. These results support a larger evolutionary argument for the role of emotion as an indicator of potential danger in the environment and pre-empting an adaptive behavioural response. Further, they align with a wide body of literature supporting the negative valence hypothesis which poses negative stimuli often evoke stronger responses than positive stimuli of similar intensity (Ito, Larsen, Smith, & Cacioppo, 1998; Smith et al., 2006; Smith, Cacioppo, Larsen, & Chartrand, 2003). Furthermore, similar effects towards negative valence stimuli have been demonstrated as physiological responses as well as ERPs findings of stronger responses to monetary losses in comparison to equivalent gains in gambling tasks (Kokmotou et al., 2017; Stancak et al., 2015) and financial monetary losses (Takahashi et al., 2013).

The effects of face familiarity on face-sensitive brain potentials did not show any significant effects, similar to those produced by emotional expressions. Within scientific inquiry, it becomes necessary to determine if the effects presented in our findings are produced by the amount of direct contact with a face or level of familiarity. Familiarity could be characterized as the amount of explicit memory content available regarding a face (Voss & Paller, 2006, 2007). As such, experimental studies investigating the effects of familiarity on face processing employ categories of images including recently learnt faces (Rossion et al., 1999), famous faces (Caharel et al., 2005; Martens, Schweinberger, Kiefer, & Burton, 2006), personally familiar faces (i.e. parents, siblings and partners). Personally relevant faces would produce higher levels of familiarity compared to recently learnt or famous faces, due to the greater amount of exposure. Given the difficulty of photographing close relatives of all the participants in an experiment, famous faces were used in our experiment.

Previous results from studies investigating face familiarity effects on the N170 component amplitude present discrepant results (Caharel et al., 2002; Caharel, Fiori, Bernard, Lalonde, & Rebaï, 2006; Marzi & Viggiano, 2007). Marzi and Viggiano reported reduced N170 amplitudes produced by familiar faces, whereas the opposite pattern of results using personally familiar faces are presented by Caharel and colleagues. Our results show a face-specific N170 component, localized to right-posterior portions of the cortex that was not affected by the level of familiarity of the faces. Similar results have shown a lack of effects on the N170 resulting from either personally familiar or learnt faces (Tanaka et al., 2006) as well as famous faces (Eimer, 2000). The question regarding the involvement of the N170 in categorising the identity of faces is still not fully resolved. The methodology presented in this thesis shows the possibility of further investigating the neural correlates of emotional and facial identity processing in natural environments and during interactions involving other people.

8.3.3 Postural effects on early but not face-specific visual processing

The extent to which postural position affects brain responses has seldom been researched in the past, ostensibly due to the methodological issues associated to the movement restrictions posed by modern imaging techniques (e.g. Raz et al., 2005). A result of these restrictions is that the sitting and laying positions typically assumed during cognitive testing are, at times, incongruent with the task being performed. Furthermore, the effects of postural on neuroimaging results in natural settings have not been fully addressed in the past.

Body posture has shown to clearly influence cognition producing modulatory effects on sensory processing like olfactory processing (Lundström et al., 2006), pain perception (Spironelli & Angrilli, 2011) and visual awareness (Goodenough et al., 1981). The effects of body posture on cortical brain activity are considerably less research, nevertheless. To the best of our knowledge, Chapter 6 of this thesis is the first experimental attempt to examine the effect of posture on face-sensitive brain potentials using EEG. Our results showed that face-sensitive brain activity did not change as a

response to the position of the subjects bodies; suggesting the detection of faces was unaffected by reclining relative to maintaining a standing position.

Unexpectedly, the amplitude of the lambda peak did show an effect resulting from positioning subjects in a recumbent position relative to a standing one. When upright, a reduced lambda response was found compared to the average lambda component produced during recumbent sitting. Previous results have shown leaning forward enhanced the amplitude of the P100 component relative to reclined sitting when arousing images were viewed (Price et al., 2012). This effect has been similarly demonstrated in response to appetitive food ques, as well (Harmon-Jones et al., 2011). The effects of posture on cognitive processing however have not been fully addressed in the past. Natural exploration of the visual environment involves multi- and trans-saccadic processes continuously integrating new information (Melcher & Colby, 2008). This posits that additional attentional demands placed on the visual system likely attenuated the lambda component produced in a standing, natural scenario. Additionally, erect body positions have shown to increase high frequency oscillatory activity (30 Hz – 100 Hz) which largely overlaps with the spectral bandwidth of muscle artifacts (Muthukumaraswamy, 2013). In mobile EEG research stringent filtering parameters are typically applied to reduce the effect of non-cerebral sources from contaminating the EEG signal in noisy environments, eliminating the contributions of high-frequency oscillatory activity to the averaged EMRPs. Methodological issues, as well as the effects of cortical-spinal fluid shifts on wireless EEG signals (Rice et al., 2013) during movement should be addressed in future MoBI research, but escape the current scope of this thesis.

8.3.4 Cortical responses to real faces during a social dyadic interaction

Human beings are social by nature. Social exchanges with other people represent a large part of the normal human experience. Dyadic social interactions like a conversation, involve an exchange of information as well as the parallel processing of auditory and visual information. The comprehension of speech has been associated to

enhancements in the intra-brain synchrony of dyads, specifically in brain areas associated with the processing of verbal information (Stephens, Silbert, & Hasson, 2010). Further, cognitive resources must additionally be devoted to processing visual information which is highly informative during social interactions. Gaze for instance, is an important social signal (Argyle, Ingham, Alkema, & McCallin, 1973; Patterson, 1982) and aids in regulating dyadic interactions. Seeing someone's reaction during a conversation for instance, represents a salient cue and produces, in turn, a reaction in the observer. These are fast acting mechanism and as such, the high temporal resolution of EEG is ideally suited to examine brain activity during social behaviour.

Brain dynamics during social interactions have previously been associated to increased arousal during face-to-face contact which produced reduced alpha oscillations recorded during gaze contact with an interlocutor (Gale, Lucas, Nissim, & Harpham, 1972). Recently, EEG and fMRI hyperscanning techniques have been used to investigate social neural processing and brain connectivity in interacting subjects (Antfolk et al., 2018; Hari et al., 2013; Konvalinka & Roepstorff, 2012; Montague et al., 2002). Coordinated brain rhythms have been observed as local and distant regional synchronizations at the individual level (Kawasaki, Kitajo, & Yamaguchi, 2010; Varela, Lachaux, Rodriguez, & Martinerie, 2001), as well as inter-brain synchronizations between subjects (Hasson, Ghazanfar, Galantucci, Garrod, & Keysers, 2012). Other authors have shown similar phase synchronizations between individuals during the imitation of hand movement (Ménoret et al., 2014) and during cooperative games and actions (Babiloni et al., 2006)**.** During alternating speech, theta/alpha (6–12 Hz) band amplitudes synchronized in the same temporal and lateral-parietal regions across subjects (Kawasaki, Yamada, Ushiku, Miyauchi, & Yamaguchi, 2013). Face-sensitive brain potentials are yet to be investigated using EEG hyperscanning or MoBI methods during social dyadic interactions. In fact, the event-related EEG literature is scarce in this field.

The findings presented in Chapter 7 establish, for the first time, the possibility of recording EMRPs during a dyadic interaction at high levels of ecological validity. Further, they provide evidence that ERPs, investigated under controlled laboratory

conditions resemble those produced in unrestricted settings during normal behaviour. Additionally, our results provide a strong piece of evidence supporting the ecological validity of the N170 component during spontaneous conversation.

8.4 Limitations

The mobile EEG experiments in the present thesis were limited to the investigation of face-sensitive EMRP responses in natural settings. The methodology used may also prove useful to investigate a broad array of visual and auditory ERPs as well as the effects of natural behaviour on brain activity.

One evident limitation in the combined eye-tracking and EEG system the low sampling rate in the mobile eye-tracking system does not allow the measurement of saccadic movements. The use of the mobile eye-tracker was limited to the identification of gaze position and latency. Accurate measurement of the characteristics of eye-movements will have allowed better modelling of the contributions of eye-movements to the EMRR. The temporal asynchrony between the two systems (0.022 ± 0.02 s) can be further reduced implementing a unified collection of measurement time series in experiments involving combined measurements (Kothe, 2014). As with traditional EEG research, the experimental results presented in this thesis are limited by the relatively low spatial resolution of EEG. The spatial mixing of source signals by volume conduction to neighbouring electrodes severely limits the spatial accuracy in the EEG measurement. However, dipole modelling and IC clustering approaches offer a cm-scale spatial estimation of the cortical sources (reviewed in Onton, Westerfield, Townsend, & Makeig, 2006). Nevertheless, the regions of neural activations, as well as the location of neural generators reported in the experimental chapters are approximate rather than exact and should be considered when interpreting our results. Further, given that free viewing was used in all the experimental chapters the overlap of consecutive eye movements, limited our analysis to early ERP components (i.e. < 300 ms).

The general limitations relating to the speed and range of movement during mobile EEG recordings have been described in the past (Gramann et al., 2011, 2010;

Gwin et al., 2011), however more current investigations using MoBI have shown reliable ERPs can be obtained in what was previously thought to be highly noisy environments (Protzak & Gramann, 2018). In the experimental chapters in this thesis movements were limited to walking within a mock art gallery; however subjects maintained a calm standing position to view the stimuli, as did they when talking to the confederate in Chapter 7.

The mock art gallery environment allowed a comparatively small number of stimuli relative to classical event-related EEG experiments. Along this same line, the limited amount of stimuli did not allow the inclusion of large number of experimental conditions. For instance, in Chapters 4 only three emotional conditions (including the neutral control) were used in the experiment. A common limitation across these studies is that participants were mostly graduate and post-graduate students from the University of Liverpool. This is a common issue in investigations of this type. Further, small samples may not be the most representative for generalising results to the wider population (Henrich, Heine, & Norenzayan, 2010). Caution is advised until these results have been replicated using different population and different environments.

8.5 Suggestions for future research

The identification of face-sensitive brain potentials in natural environments during viewing of static face images, as well as in response to real faces during conversation, opens new questions and provides a wide range of possibilities for experimental neuroimaging research as well as in applied neuroscience.

The methodology presented in the experimental chapters provides new opportunities in multiple domains including social and developmental psychology, medicine, and consumer science. Furthermore, the progressive transfer of the knowledge gathered from traditional laboratory ERP reports into ecological tasks will produce invaluable insights regarding the brain dynamics of actively behaving humans. As such, future research should examine well established EEG components in natural settings as well as validate EEG markers for clinical research. Along these lines, potential clinical

applications include research on neuromuscular control in motor disorders as well as assessing brain connectivity during locomotion in geriatric populations. Further, in the growing field of brain computer interfaces (BCI), EEG signals are used to the control of advanced prosthetics for upper and lower limb amputees (Li et al., 2017; Murphy et al., 2017; Scherberger, 2009). The integration of the combined mobile EEG and eye-tracking could integrate visual environmental information into the EEG-based control system of future prosthetics.

Newly developing fields, like music cognition, sports psychology and social cognition could also strongly benefit from the implementation of similar MoBI techniques. The eye-tracking based approach to a mobile EEG technique could additionally lead to the development of new methods and applications, e.g. real-world hyperscanning or automatized error detection monitoring during driving or cycling. Similarly, future research should consider implementing a multimodal data analysis tool like MoBILAB (Ojeda et al., 2014) or the lab streaming layer toolbox (Kothe, 2014; Ojeda et al., 2014). Future research should examining later ERP components involved in face processing like the LLP (Diéguez-risco, Aguado, Albert, & Hinojosa, 2013) in natural setting. This could be achieved by addressing the issue of overlapping neural processing using new computational tools like the *unfold* toolbox (Ehinger & Dimigen, 2018) to apply advanced deconvolution models and spline regression in EMRP research.

Along similar themes to the ones addressed in this thesis, future MoBI research employing similar experimental set-ups could addition a simple clip-on microphone to examine auditory processing in the real or the effects of language production and perception on face-specific brain activity during dyadic social interactions, for instance.

8.6 Concluding remarks

The relevance of faces for human behaviour has evolved specialized brain systems to decode information contained in faces, as is evidenced by previous neuroimaging research. There is a growing consensus within the field of the need for cognitive ethology in our methods, i.e. the observation of brain activity as it occurs in

real life or in settings closely approximating ecological validity (Kingstone, Smilek, & Eastwood, 2008; Ladouce, Donaldson, Dudchenko, & Ietswaart, 2017; Makeig et al., 2009; Wilson, 2002). The inherent compromise between strict methodological constraints and the ecological need for tasks to closely match natural behaviour is slowly being overcome. The current thesis presents a novel methodology that effectively diminishes the aforementioned trade-off by incorporating eye-tracking measurements to mobile EEG recordings. These findings further contribute to our general understanding of the neural correlated of visual exploration in a natural setting and expand previous N170 results and offer new insights into the processing of faces in natural environments. Furthermore, the results presented in this thesis advance our understanding of the involvement of the N170 component generated in the FFA in the processing of emotional faces. Further, the findings of the final study demonstrate that the face specific N170 component produced during a dyadic social interaction under natural environmental conditions resemble previous laboratory based research.

In closing, the present thesis expands previous laboratory-based findings and offers new insights to the scientific literature regarding electrophysiological brain correlates of emotional and familiar face processing in natural settings and during dyadic social interactions. It is hoped that the methodology and results presented in the experimental chapters provide a strong foundation for future mobile neuroimaging research as well as research examining face-specific cortical potentials the real world and during social interactions.

References

Akalin Acar, Z., & Makeig, S. (2013). Effects of forward model errors on EEG source localization. *Brain Topography*, *26*(3), 378–396. http://doi.org/10.1007/s10548-012-0274-6

Allison, T., Ginter, H., McCarthy, G., Nobre, A. C., Puce, A., Luby, M., & Spencer, D. D. (1994). Face recognition in human extrastriate cortex. *Journal of Neurophysiology*, *71*(2), 821–825. http://doi.org/8176446

Allison, T., Puce, A., Spencer, D., & McCarthy, G. (1999). Electrophysiological studies of human face perception. I: Potentials generated in occipitotemporal cortex by face and non-face stimuli. *Cerebral Cortex*, *9*(5), 415–430.

Amihai, I., Deouell, L. Y., & Bentin, S. (2011). Neural adaptation is related to face repetition irrespective of identity: A reappraisal of the N170 effect. *Experimental Brain Research*, *209*(2), 193–204. http://doi.org/10.1007/s00221-011-2546-x

Anllo-Vento, L., Luck, S. J., & Hillyard, S. A. (1998). Spatio-temporal dynamics of attention to color: Evidence from human electrophysiology - Anllo-Vento - 1998 - Human Brain Mapping - Wiley Online Library, *238*, 216–238. Retrieved from http://onlinelibrary.wiley.com/doi/10.1002/(SICI)1097-0193(1998)6:4%3C216::AID-HBM3%3E3.0.CO;2-6/pdf

Antfolk, J., Dumas, G., Liu, S., Zhang, X., Liu, D., Liu, X., … Wang, H. (2018). Interactive Brain Activity: Review and Progress on EEG-Based Hyperscanning in Social Interactions. *Front. Psychol*, *9*(October), 1862. http://doi.org/10.3389/fpsyg.2018.01862

Argyle, M., Ingham, R., Alkema, F., & McCallin, M. (1973). The Different Functions of Gaze. *Semiotica*, *7*(1), 19–32.

Asadifard, M., & Shanbezadeh, J. (2010). Automatic Adaptive Center of Pupil Detection Using Face Detection and CDF Analysis. *Proceedings of the International MultiConference of Engineers and Computer Scientists 2010*, *I*, 17–20.

Ashley, V., Vuilleumier, P., & Swick, D. (2004). Time course and specificity of event-related potentials to emotional expressions. *NeuroReport*, *15*(1), 211–216. http://doi.org/10.1097/00001756-200401190-00041

Aspinall, P., Mavros, P., Coyne, R., & Roe, J. (2013). The urban brain: analysing outdoor physical activity with mobile EEG. *British Journal of Sports Medicine*, *online*(November 2015), 1–6. http://doi.org/10.1136/bjsports-2012-091877

Atkinson, A. P., & Adolphs, R. (2011). The neuropsychology of face perception: Beyond simple dissociations and functional selectivity. *Philosophical Transactions of the Royal Society B: Biological Sciences*, *366*(1571), 1726–1738. http://doi.org/10.1098/rstb.2010.0349

Babiloni, F., Cincotti, F., Mattia, D., De Vico Fallani, F., Tocci, A., Bianchi, L., … Astolfi, L. (2007). High Resolution EEG Hyperscanning During a Card Game. In *2007 29th Annual International Conference of the IEEE Engineering in Medicine and Biology Society* (pp. 4957–4960). IEEE. http://doi.org/10.1109/IEMBS.2007.4353453

Babiloni, F., Cincotti, F., Mattia, D., Mattiocco, M., De Fallani, F. V, Tocci, A., … Astolfi, L. (2006). Hypermethods for EEG hyperscanning. *Annual International Conference of the IEEE Engineering in Medicine and Biology - Proceedings*, 3666–3669. http://doi.org/10.1109/IEMBS.2006.260754

Baccino, T., & Manunta, Y. (2005). Eye-fixation-related potentials: Insight into parafoveal processing. *Journal of Psychophysiology*, *19*(3), 204–215. http://doi.org/10.1027/0269-8803.19.3.204

Baess, P., Zhdanov, A., Mandel, A., Parkkonen, L., Hirvenkari, L., Mäkelä, J. P., … Hari, R. (2012). MEG dual scanning: a procedure to study real-time auditory interaction between two persons. *Frontiers in Human Neuroscience*, *6*(April), 1–7. http://doi.org/10.3389/fnhum.2012.00083

Barbeau, E. J., Taylor, M. J., Regis, J., Marquis, P., Chauvel, P., & Liégeois-Chauvel, C. (2008). Spatio temporal dynamics of face recognition. *Cerebral Cortex*, *18*(5), 997–1009.

Barlow, J. S., & Cigánek, L. (1969). Lambda responses in relation to visual evoked responses in man. *Electroencephalography and Clinical Neurophysiology*, *26*(2), 183–192.

Barnstaple, R., & Desouza, J. F. X. (2017). Dance and Neurorehabilitation - Mixed-Methods Research Models. *Journal of Functional Neurology, Rehabilitation, and Ergonomics*, *7*(1), 12–17.

Barrett, S. E., Rugg, M. D., & Perrett, D. I. (1988). Event-related potentials and the matching of familiar and unfamiliar faces. *Neuropsychologia*, *26*(1), 105–117. http://doi.org/10.1016/0028-3932(88)90034-6

Barton, J. J. S. (2008). Structure and function in acquired prosopagnosia: lessons from a series of 10 patients with brain damage. *Journal of Neuropsychology*, *2*(Pt 1), 197–225. http://doi.org/10.1348/174866407X214172

Baudouin, J. Y., & Sansone, S. (2000). Recognizing expression from familiar and unfamiliar faces. *Pragmatics & Cognition*, *8*(1), 123–146. http://doi.org/10.1075/pc.8.1.07bau

Bell, A. J., & Sejnowski, T. J. (1995). An Information-Maximization Approach to Blind Separation and Blind Deconvolution. *Neural Computation*, *7*(6), 1129–1159. http://doi.org/10.1162/neco.1995.7.6.1129

Benjamini, Y., & Yekutieli, D. (2001). The control of the false discovery rate in multiple testing under dependency. *The Annals of Statistics*, *29*(4), 1165–1188. http://doi.org/10.1214/aos/1013699998

Bentin, S., Allison, T., Puce, A., Perez, E., & McCarthy, G. (1996). Electrophysiological Studies of Face Perception in Humans. *Journal of Cognitive Neuroscience*, *8*(6), 551–565. http://doi.org/10.1162/jocn.1996.8.6.551

Bentin, S., & Deouell, L. Y. (2000). Structural Encoding and Identification in Face Processing: Erp Evidence for Separate Mechanisms. *Cognitive Neuropsychology*, *17*(1–3), 35–55. http://doi.org/10.1080/026432900380472

Bentin, S., Taylor, M. J., Rousselet, G. A., Itier, R. J., Caldara, R., Schyns, P. G., … Rossion, B. (2007). Controlling interstimulus perceptual variance does not abolish N170 face sensitivity [1]. *Nature Neuroscience*, *10*(7), 801–802. http://doi.org/10.1038/nn0707-801

Berg, P., & Scherg, M. (1991). Dipole models of eye movements and blinks. *Electroencephalography and Clinical Neurophysiology*, *79*(1), 36–44. http://doi.org/10.1016/0013-4694(91)90154-V

Berg, P., & Scherg, M. (1994). A multiple source approach to the correction of eye artifacts. *Electroencephalography and Clinical Neurophysiology*, *90*(3), 229–241. http://doi.org/10.1016/0013-4694(94)90094-9

Berger, H. (1929). Über das elektrenkephalogramm des menschen. *Archiv Für Psychiatrie Und Nervenkrankheiten*, *87*(1), 527–570.

Blau, V. C., Maurer, U., Tottenham, N., & McCandliss, B. D. (2007). The face-specific N170 component is modulated by emotional facial expression. *Behavioral and Brain Functions : BBF*, *3*, 7. http://doi.org/10.1186/1744-9081-3-7

Bleichner, M. G., & Debener, S. (2017). Concealed, Unobtrusive Ear-Centered EEG Acquisition: cEEGrids for Transparent EEG. *Frontiers in Human Neuroscience*, *11*(April), 1–14. http://doi.org/10.3389/fnhum.2017.00163

Bohbot, V. D., Copara, M. S., Gotman, J., & Ekstrom, A. D. (2017). Low-frequency theta oscillations in the human hippocampus during real-world and virtual navigation. *Nature Communications*, *8*, 1–7. http://doi.org/10.1038/ncomms14415

Boles, W. W., & Boashash, B. (1998). A Human Identification Technique Using Images of the Iris and Wavelet Transform. *IEEE Transactions on Signal Processing*, *46*(4), 1185–1188. http://doi.org/10.1109/78.668573

Bötzel, K., & Grüsser, O. J. (1989). Electric brain potentials evoked by pictures of faces and non-faces: a search for "face-specific" EEG-potentials. *Experimental Brain Research. Experimentelle Hirnforschung. Experimentation Cerebrale*, *77*(2), 349–360. http://doi.org/10.1007/BF00274992

Bötzel, K., Schulze, S., & Stodieck, S. R. (1995). Scalp topography and analysis of intracranial sources of face-evoked potentials. *Experimental Brain Research*, *104*(1), 135–43. http://doi.org/10.1007/BF00229863

Braunagel, C., Kasneci, E., Stolzmann, W., & Rosenstiel, W. (2015). Driver-Activity Recognition in the Context of Conditionally Autonomous Driving. In *2015 IEEE 18th International Conference on Intelligent Transportation Systems* (pp. 1652–1657). http://doi.org/10.1109/ITSC.2015.268

Bronfenbrenner, U. (1977). Toward an Experimental Ecology of Human Development. *American Psychologist*, *32*(7), 513.

Brown, J. S., Collins, A., & Duguid, P. (1989). Situated cognition and the culture of learning. Educational researcher, 18(1), 32-42.

Bruce, V. V., & Young, A. A. (1986). Understanding face recognition. *British Journal of Psychology*, *77*(3), 305–327. http://doi.org/10.1111/j.2044-8295.1986.tb02199.x

Brunswik, E. (1943). Organismic achievement and environmental probability, *50*(3), 255–272. Retrieved from http://psycnet.apa.org.ezproxy.northampton.ac.uk/journals/rev/50/3/255.pdf

Bulea, T. C., Kilicarslan, A., Ozdemir, R., Paloski, W. H., & Contreras-Vidal, J. L. (2013). Simultaneous Scalp Electroencephalography (EEG), Electromyography (EMG), and Whole-body Segmental Inertial Recording for Multi-modal Neural Decoding. *Journal of Visualized Experiments*, (77), 1–13. http://doi.org/10.3791/50602

Burgess, A. P. (2013). On the interpretation of synchronization in EEG hyperscanning studies: a cautionary note. *Frontiers in Human Neuroscience*, *7*(December), 1–17. http://doi.org/10.3389/fnhum.2013.00881

Burton, A. M., Wilson, S., Cowan, M., & Bruce, V. (1999). Face recognition in poor-quality video: Evidence From Security Surveillance. *Psychological Science*, *10*(3), 243–248. http://doi.org/10.1111/1467-9280.00144

Caharel, S., Courtay, N., Bernard, C., Lalonde, R., & Rebaï, M. (2005). Familiarity and emotional expression influence an early stage of face processing: An electrophysiological study. *Brain and Cognition*, *59*(1), 96–100. http://doi.org/10.1016/j.bandc.2005.05.005

Caharel, S., Fiori, N., Bernard, C., Lalonde, R., & Rebaï, M. (2006). The effects of inversion and eye displacements of familiar and unknown faces on early and late-stage ERPs. *International Journal of Psychophysiology*, *62*(1), 141–151. http://doi.org/10.1016/j.ijpsycho.2006.03.002

Caharel, S., Poiroux, S., Bernard, C., Thibaut, F., Lalonde, R., & Rebai, M. (2002). ERPs associated with familiarity and degree of familiarity during face recognition. *International Journal of Neuroscience*, *112*(12), 1499–1512. http://doi.org/10.1080/00207450290158368

Caharel, S. S. S., Poiroux, S. S. S., Bernard, C., Thibaut, F., Lalonde, R., & Rebai, M. (2002). ERPs associated with familiarity and degree of familiarity during face recognition. *International Journal of Neuroscience*, *112*(12), 1499–1512. http://doi.org/10.1080/00207450290158368

Calder, A., Rhodes, G., Johnson, M., & Haxby, J. (2011). *Oxford handbook of face perception*. (A. Calder, G. Rhodes, M. Johnson, & J. Haxby, Eds.). Oxford University Press.

Caldwell, J. A., Prazinko, B., & Caldwell, J. L. (2003). Body posture affects electroencephalographic activity and psychomotor vigilance task performance in sleep-deprived subjects. *Clinical Neurophysiology*, *114*(1), 23–31. http://doi.org/10.1016/S1388-2457(02)00283-3

Caldwell, J. A., Prazinko, B. F., & Hall, K. K. (2000). The effects of body posture on resting electroencephalographic activity in sleep-deprived subjects. *Clinical Neurophysiology*, *111*(3), 464–470. http://doi.org/10.1016/S1388-2457(99)00289-8

Callan, D. E., Durantin, G., & Terzibas, C. (2015). Classification of single-trial auditory events using dry-wireless EEG during real and motion simulated flight. *Frontiers in Systems Neuroscience*, *9*(Ferbruary), 1–12. http://doi.org/10.3389/fnsys.2015.00011

Campanella, S., Hanoteau, C., Dépy, D., Rossion, B., Bruyer, R., Crommelinck, M., & Guérit, J. M. (2000). Right N170 modulation in a face discrimination task: an account for categorical perception of familiar faces. *Psychophysiology*, *37*, 796–806. http://doi.org/10.1017/s0048577200991728

Campanella, S., Montedoro, C., Streel, E., Verbanck, P., & Rosier, V. (2006). Early visual

components (P100, N170) are disrupted in chronic schizophrenic patients: an event-related potentials study. *Neurophysiologie Clinique/Clinical Neurophysiology*, *36*(2), 71–78.

Camras, L. A., Ribordy, S., Hill, J., Martino, S., Spaccarelli, S., & Stefani, R. (1988). Recognition and posing of emotional expressions by abused children and their mothers. *Developmental Psychology*, *24*(6), 776–781. http://doi.org/10.1037/0012-1649.24.6.776

Canny, J. F. (1986). A Computational Approach To Edge Detection. *IEEE Transactions on Pattern Analysis and Machine Intelligence*, *8*(6), 679–714.

Carretié, L., Kessel, D., Carboni, A., López-Martín, S., Albert, J., Tapia, M., … Hinojosa, J. A. J. A. (2013). Exogenous attention to facial vs non-facial emotional visual stimuli. *Social Cognitive and Affective Neuroscience*, *8*(7), 764–773. http://doi.org/10.1093/scan/nss068

Caton, R. (1875). Electrical currents of the brain. *The Chicago Journal of Nervous & Mental Disease:*, *2*(4), 610.

Chang, L. J., Lin, J. F., Lin, C. F., Wu, K. T., Wang, Y. M., & Kuo, C. D. (2011). Effect of body position on bilateral EEG alterations and their relationship with autonomic nervous modulation in normal subjects. *Neuroscience Letters*, *490*(2), 96–100. http://doi.org/10.1016/j.neulet.2010.12.034

Chiel, H. J., & Beer, R. D. (1997). Processing of inputs to and outputs from the nervous system. *Tins*, *20*(12), 553–557. http://doi.org/10.1016/S0166-2236(97)01149-1

Churchland, P., Ramachandran, V. S., & Sejnowski, T. J. (1994). A Critique of Pure Vision. In *Large-Scale Neuronal Theories of the Brain* (pp. 23–60).

Clark, V. P., & Hillyard, S. A. (1996). Spatial selective attention affects early extrastriate but not striate components of the visual evoked potential. *Journal of Cognitive Neuroscience*, *8*, 387–402.

Cruz-Garza, J. G., Brantley, J. A., Nakagome, S., Kontson, K., Megjhani, M., Robleto, D., & Contreras-Vidal, J. L. (2017). Deployment of Mobile EEG Technology in an Art Museum Setting: Evaluation of Signal Quality and Usability. *Frontiers in Human Neuroscience*, *11*(November). http://doi.org/10.3389/fnhum.2017.00527

Damasio, A., Damasio, H., & Van Hoesen, G. (1982). Prosopagnosia: Anatomic basis and behavioral mechanisms. *Neurology*, *32*(4), 331–331. http://doi.org/10.1212/WNL.32.4.331

De Sanctis, P., Butler, J. S., Green, J. M., Snyder, A. C., & Foxe, J. J. (2012). Mobile brain/body imaging (MoBI): High-density electrical mapping of inhibitory processes during walking. *Proceedings of the Annual International Conference of the IEEE Engineering in Medicine and Biology Society, EMBS*, 1542–1545. http://doi.org/10.1109/EMBC.2012.6346236

De Sanctis, P., Butler, J. S., Malcolm, B. R., & Foxe, J. J. (2014). Recalibration of inhibitory control systems during walking-related dual-task interference: A Mobile Brain-Body Imaging (MOBI) Study. *NeuroImage*, *94*, 55–64. http://doi.org/10.1016/j.neuroimage.2014.03.016

De Vos, M., Gandras, K., & Debener, S. (2014). Towards a truly mobile auditory brain-computer interface: Exploring the P300 to take away. *International Journal of Psychophysiology*, *91*(1), 46–53. http://doi.org/10.1016/j.ijpsycho.2013.08.010

Debener, S. (2018). Developing portable, mobile, and transparent EEG. In K. Gramann (Ed.), *Proceedings of the 3rd International Mobile Brain/Body Imaging Conference*. Berlin.

Debener, S., Minow, F., Emkes, R., Gandras, K., & de Vos, M. (2012). How about taking a low-cost, small, and wireless EEG for a walk? *Psychophysiology*, *49*(11), 1617–1621. http://doi.org/10.1111/j.1469-8986.2012.01471.x

Deffke, I., Sander, T., Heidenreich, J., Sommer, W., Curio, G., Trahms, L., & Lueschow, A. (2007). MEG/EEG sources of the 170-ms response to faces are co-localized in the fusiform gyrus. *NeuroImage*, *35*(4), 1495–1501. http://doi.org/10.1016/j.neuroimage.2007.01.034

Delorme, A., & Makeig, S. (2003). EEGLAB: An open source toolbox for analysis of single-trial EEG dynamics including independent component analysis. *Journal of Neuroscience Methods*, *134*(1), 9–21. http://doi.org/10.1016/j.jneumeth.2003.10.009

Delorme, A., Mullen, T., Kothe, C., Akalin Acar, Z., Bigdely-Shamlo, N., Vankov, A., & Makeig, S. (2011). EEGLAB, SIFT, NFT, BCILAB, and ERICA: New tools for advanced EEG processing. *Computational Intelligence and Neuroscience*, *2011*. http://doi.org/10.1155/2011/130714

Delorme, A., Palmer, J., Onton, J., Oostenveld, R., & Makeig, S. (2012). Independent EEG sources are dipolar. *PLoS ONE*, *7*(2). http://doi.org/10.1371/journal.pone.0030135

Dennis, T. A., & Chen, C. C. (2007). Emotional face processing and attention performance in three domains: Neurophysiological mechanisms and moderating effects of trait anxiety. *International Journal of Psychophysiology*, *65*(1), 10–19. http://doi.org/10.1016/j.ijpsycho.2007.02.006

Di Russo, F., & Spinelli, D. (1999). Electrophysiological evidence for an early attentional mechanism in visual processing in humans. *Vision Research*, *39*(18), 2975–2985. http://doi.org/10.1016/S0042-6989(99)00031-0

Diéguez-risco, T., Aguado, L., Albert, J., & Hinojosa, J. A. (2013). Faces in context : Modulation of expression processing by situational information. *Social Neuroscience*, *8*(6), 601–620. http://doi.org/10.1080/17470919.2013.834842

Dimigen, O., Sommer, W., Hohlfeld, A., Jacobs, A., & Kliegl, R. (2011). Co-Registration of Eye Movements and EEG in Natural Reading: Analyses & Review. *Review. Journal of Experimental Psychology: General*, *140*(4), 552–572. http://doi.org/10.1037/a0023885

Dimigen, O., Valsecchi, M., Sommer, W., & Kliegl, R. (2009). Human Microsaccade-Related Visual Brain Responses. *Journal of Neuroscience*, *29*(39), 12321–12331. http://doi.org/10.1523/JNEUROSCI.0911-09.2009

Douglas, D. H., & Peucker, T. K. (1973). Algorithms for the reduction of the number of points required to represent a digitized line or its caricature. *Cartographica: The International Journal for Geographic Information and Geovisualization*, *10*(2), 112–122.

Downing, P. E., Jiang, Y., Shuman, M., & Kanwisher, N. (2001). A Cortical Area Selective for Visual Processing of the Human Body. *Science*, *293*(September), 2470–2473.

Dubois, S., Rossion, B., Schiltz, C., Bodart, J. M., Michel, C., Bruyer, R., … Crommelinck, M. (1999). Effect of familiarity on the processing of human faces. *NeuroImage*, *9*(3), 278–289. http://doi.org/10.1006/nimg.1998.0409

Dumas, G., Nadel, J., Soussignan, R., Martinerie, J., & Garnero, L. (2010). Inter-Brain Synchronization during Social Interaction. *PLoS ONE*, *5*(8), e12166. http://doi.org/10.1371/journal.pone.0012166

Ehinger, B., & Dimigen, O. (2018). Unfold: An integrated toolbox for overlap correction, non-linear modeling, and regression-based EEG analysis. *BioRxiv*, 360156. http://doi.org/10.1101/360156

Eimer, M. (2000a). Effects of face inversion on the structural encoding and recognition of faces - Evidence from event-related brain potentials. *Cognitive Brain Research*, *10*(1–2), 145–158. http://doi.org/10.1016/S0926-6410(00)00038-0

Eimer, M. (2000b). The face-specific N170 component reflects late stages in the structural encoding of faces. *Neuroreport*, *11*(10), 2319–2324. http://doi.org/10.1097/00001756-200007140-00050

Eimer, M. (2011). The face-sensitive N170 component of the event-related brain potential. In *Oxford Handbook of Face Perception* (pp. 329–44).

Eimer, M. C., & Holmes, A. (2002). An ERP study on the time course of emotional face processing. *Neuroreport*, *13*(4), 427–31. http://doi.org/10.1097/00001756-200203250-00013

Eimer, M., & Forster, B. (2003). Modulations of early somatosensory ERP components by transient and sustained spatial attention. *Experimental Brain Research*, *151*(1), 24–31. http://doi.org/10.1007/s00221-003-1437-1

Eimer, M., Holmes, A., & McGlone, F. P. (2003). The role of spatial attention in the processing of facial expression: an ERP study of rapid brain responses to six basic emotions. *Cognitive, Affective & Behavioral Neuroscience*, *3*(2), 97–110. http://doi.org/10.3758/CABN.3.2.97

Eimer, M., Kiss, M., & Holmes, A. (2008). Links between rapid ERP responses to fearful faces and conscious awareness. *J Neuropsychol*, *2*(Pt 1), 165–181. http://doi.org/10.1348/174866407X245411

Eimer, M., & McCarthy, R. A. (1999). Prosopagnosia and structural encoding of faces: Evidence from event-related potentials. *NeuroReport*, *10*(2), 255–259. http://doi.org/10.1097/00001756-199902050-00010

Endo, N., Endo, M., Kirita, T., & Maruyama, K. (1992). The effects of expression on face recognition. *Tohoku Psychologica Folia*, *51*(May), 37–44.

Eng, H. Y., Chen, D., & Jiang, Y. (2005). Visual working memory for simple and complex visual stimuli, *12*(6), 1127–1133.

Evans, C. C. (1953). Spontaneous excitation of the visual cortex and association areas—lambda waves. *Electroencephalography and Clinical Neurophysiology*, *5*(1), 69–74.

Fisch, B. J. (1999). *Fisch and Spehlmann's EEG Primer: Basic Principles of Digital and Analog EEG, 3e*. Amsterdam: Elsevier.

Fischer, T., Graupner, S. T., Velichkovsky, B. M., & Pannasch, S. (2013). Attentional dynamics during free picture viewing: Evidence from oculomotor behavior and electrocortical

activity. *Frontiers in Systems Neuroscience*, *7*(17), 1–9. http://doi.org/10.3389/fnsys.2013.00017

Florence, M., & Ellis, H. D. (1990). Bodamer's (1947) Paper on Prosopagnosia. *Neuropsychologia*, *7*(2), 81–105. http://doi.org/10.1080/02643299008253437

Foisy, M. L., Philippot, P., Verbanck, P., Pelc, I., van der Straten, G., & Kornreich, C. (2005). Emotional facial expression decoding impairment in persons dependent on multiple substances: impact of a history of alcohol dependence. *Journal of Studies on Alcohol*, *66*(5), 673–681. http://doi.org/10.15288/jsa.2005.66.673

Freire, A., Lee, K., & Symons, L. A. (2000). The face-inversion effect as a deficit in the encoding of configurai information: Direct evidence. *Perception*, *29*(2), 159–170. http://doi.org/10.1068/p3012

Frith, C. (2009). Role of facial expressions in social interactions. *Philosophical Transactions of the Royal Society B: Biological Sciences*, *364*(1535), 3453–3458. http://doi.org/10.1098/rstb.2009.0142

Frömer, R., Maier, M., & Rahman, R. A. (2018). Group-level EEG-processing pipeline for flexible single trial-based analyses including linear mixed models. *Frontiers in Neuroscience*, *12*(FEB), 1–15. http://doi.org/10.3389/fnins.2018.00048

Fuhl, W., Tonsen, M., Bulling, A., & Kasneci, E. (2016). Pupil detection for head-mounted eye tracking in the wild: an evaluation of the state of the art. *Machine Vision and Applications*, *27*(8), 1275–1288. http://doi.org/10.1007/s00138-016-0776-4

Gale, A., Lucas, B., Nissim, R., & Harpham, B. (1972). Some EEG correlates of face-to-face contact. *British Journal of Social and Clinical Psychology*, *11*(4), 326–332.

Ganel, T., Valyear, K. F., Goshen-Gottstein, Y., & Goodale, M. A. (2005). The involvement of the "fusiform face area" in processing facial expression. *Neuropsychologia*, *43*(11), 1645–1654. http://doi.org/10.1016/j.neuropsychologia.2005.01.012

Gauthier, I., Curran, T., Curby, K., & Collins, D. (2003). Perceptual interference supports a non-modular account of face processing. *Nature Neuroscience*, *6*(4), 428–432. http://doi.org/10.1038/nn1029

Gauthier, I., Skudlarski, P., Gore, J. C., & Anderson, A. W. (2000). Expertise for cars and birds recruits brain areas involved in face recognition. *Nature Neuroscience*, *3*(2), 191–197. http://doi.org/10.1038/72140

Geddes, L. A., & Baker, L. E. (1967). The specific resistance of biological material—A compendium of data for the biomedical engineer and physiologist. *Medical & Biological Engineering*, *5*(3), 271–293. http://doi.org/10.1007/BF02474537

Gibson, J. (1979). The ecological approach to visual perception. *Dallas: Houghtom Mifflin*.

Gobbini, M. I., & Haxby, J. V. (2006). Neural response to the visual familiarity of faces. *Brain Research Bulletin*, *71*(1–3), 76–82. http://doi.org/10.1016/j.brainresbull.2006.08.003

Goffaux, V., Gauthier, I., & Rossion, B. (2003). Spatial scale contribution to early visual differences between face and object processing. *Cognitive Brain Research*, *16*(3), 416–424. http://doi.org/10.1016/S0926-6410(03)00056-9

Goodenough, D. R., Oltman, P. K., Sigman, E., & Cox, P. W. (1981). The rod-and-frame illusion in erect and supine observers. *Attention, Perception, & Psychophysics*, *29*(4), 365–370.

Gosling, A., & Eimer, M. (2011). An event-related brain potential study of explicit face recognition. *Neuropsychologia*, *49*(9), 2736–2745. http://doi.org/10.1016/j.neuropsychologia.2011.05.025

Gottwald, B., Wilde, B., Mihajlovic, Z., & Mehdorn, H. M. (2004). Evidence for distinct cognitive deficits after focal cerebellar lesions. *Journal of Neurology, Neurosurgery and Psychiatry*, *75*(11), 1524–1531. http://doi.org/10.1136/jnnp.2003.018093

Gramann, K. (2018). Proceedings of the 3rd International Mobile Brain/Body Imaging Conference. In K. Gramann (Ed.), *3rd International Mobile Brain/Body Imaging Conference Berlin* (pp. 1–149). Berlin: TU Berlin Repository DepositOnce. http://doi.org/10.14279/depositonce-7236

Gramann, K., Ferris, D. P., Gwin, J., & Makeig, S. (2014). Imaging natural cognition in action. *International Journal of Psychophysiology*, *91*(1), 22–29. http://doi.org/10.1016/j.ijpsycho.2013.09.003

Gramann, K., Gwin, J. T., Bigdely-Shamlo, N., Ferris, D. P., & Makeig, S. (2010). Visual Evoked Responses During Standing and Walking. *Frontiers in Human Neuroscience*, *4*(October), 202. http://doi.org/10.3389/fnhum.2010.00202

Gramann, K., Gwin, J. T., Ferris, D. P., Oie, K., Tzyy-Ping, J., Chin-Teng, L., … Makeig, S. (2011). Cognition in action: imaging brain/body dynamics in mobile humans. *Reviews in the Neurosciences*, *22*(6), 593–608. http://doi.org/10.1515/RNS.2011.047

Grech, R., Cassar, T., Muscat, J., Camilleri, K. P., Fabri, S. G., Zervakis, M., … Vanrumste, B. (2008). Review on solving the inverse problem in EEG source analysis. *Journal of NeuroEngineering and Rehabilitation*, *5*, 1–33. http://doi.org/10.1186/1743-0003-5-25

Grill-Spector, K., Kushnir, T., Hendler, T., Edelman, S., Itzchak, Y., & Malach, R. (1998). A sequence of object-processing stages revealed by fMRI in the human occipital lobe. *Human Brain Mapping*, *6*(4), 316–328. http://doi.org/10.1002/(SICI)1097-0193(1998)6:4<316::AID-HBM9>3.0.CO;2-6

Guestrin, E. D., & Eizenman, M. (2006). General theory of remote gaze estimation using the pupil center and corneal reflections. *IEEE Transactions on Biomedical Engineering*, *53*(6), 1124–1133. http://doi.org/10.1109/TBME.2005.863952

Gwin, J. T., Gramann, K., Makeig, S., & Ferris, D. P. (2010). Removal of movement artifact from high-density EEG recorded during walking and running. *Journal of Neurophysiology*, *103*(6), 3526–34. http://doi.org/10.1152/jn.00105.2010

Gwin, J. T., Gramann, K., Makeig, S., & Ferris, D. P. (2011). Electrocortical activity is coupled to gait cycle phase during treadmill walking. *NeuroImage*, *54*(2), 1289–1296. http://doi.org/10.1016/j.neuroimage.2010.08.066

Halgren, E., Raij, T., Marinkovic, K., Jousmäki, V., & Hari, R. (2000). Cognitive Response Profile of the Human Fusiform Face Area as Determined by MEG. *Cerebral Cortex*, *10*(1), 69–81. http://doi.org/10.1093/cercor/10.1.69

Hämäläinen, M., Hari, R., Ilmoniemi, R. J., Knuutila, J., & Lounasmaa, O. V. (1993). Magnetoencephalography—theory, instrumentation, and applications to noninvasive studies of the working human brain. *Modern Healthcare*, *65*(2), 413.

Hancock, P. J. B., Bruce, V., & Burton, A. M. (2000). Recognition of unfamiliar faces. *Trends in Cognitive Sciences*, *4*(9), 330–337.

Hari, R., Himberg, T., Nummenmaa, L., Hämäläinen, M., & Parkkonen, L. (2013). Synchrony of brains and bodies during implicit interpersonal interaction. *Trends in Cognitive Sciences*, *17*(3), 105–106. http://doi.org/10.1016/j.tics.2013.01.003

Hari, R., & Kujala, M. V. (2009). Brain Basis of Human Social Interaction: From Concepts to Brain Imaging. *Physiological Reviews*, *89*(2), 453–479. http://doi.org/10.1152/physrev.00041.2007

Harmon-Jones, E., Gable, P. A., & Price, T. F. (2011). Leaning embodies desire: Evidence that leaning forward increases relative left frontal cortical activation to appetitive stimuli. *Biological Psychology*, *87*(2), 311–313. http://doi.org/10.1016/j.biopsycho.2011.03.009

Harmon-Jones, E., & Peterson, C. K. (2009). Supine body position reduces neural response to anger evocation: Short report. *Psychological Science*, *20*(10), 1209–1210. http://doi.org/10.1111/j.1467-9280.2009.02416.x

Hasson, U., Ghazanfar, A. A., Galantucci, B., Garrod, S., & Keysers, C. (2012). Brain-to-brain coupling: a mechanism for creating and sharing a social world. *Trends in Cognitive Sciences*, *16*(2), 114–121.

Hauk, O., Davis, M. H., Ford, M., Pulvermüller, F., & Marslen-Wilson, W. D. (2006). The time course of visual word recognition as revealed by linear regression analysis of ERP data. *NeuroImage*, *30*(4), 1383–1400. http://doi.org/10.1016/j.neuroimage.2005.11.048

Haxby, J. J., Hoffman, E., & Gobbini, I. (2002). Human neural systems for face recognition and social communication. *Biological Psychiatry*, *51*(1), 59–67. http://doi.org/10.1016/S0006-3223(01)01330-0

Haxby, J. V., Horwitz, B., Ungerleider, L. G., Maisog, J. M., Pietrini, P., & Grady, C. L. (1994). The functional organization of human extrastriate cortex: a PET-rCBF study of selective attention to faces and locations. *J Neurosci*, *14*(11 Pt 1), 6336–53. http://doi.org/7965040

Haxby, J. V, Gobbini, M. I., Furey, M. L., Ishai, A., Schouten, J. L., & Pietrini, P. (2001). Distributed and Overlapping Representations of Faces and Objects in Ventral Temporal Cortex. *Science*, *293*(5539), 2425–2430. Retrieved from www.sciencemag.org

Haxby, J. V, Hoffman, E. A., Gobbini, I., & Gobbini, M. I. (2000). The distributed human neural system for face perception. *Trends in Cognitive Sciences*, *4*(6), 223–233.

Hendriks, M. C. P., Van Boxtel, G. J. M., & Vingerhoets, A. J. F. M. (2007). An event-related potential study on the early processing of crying faces. *NeuroReport*, *18*(7), 631–634. http://doi.org/10.1097/WNR.0b013e3280bad8c7

Henrich, J., Heine, S. J., & Norenzayan, A. (2010). The weirdest people in the world? *Behavioral and Brain Sciences*, *33*(2–3), 61–83. http://doi.org/10.1017/S0140525X0999152X

Henson, R. N., Goshen-Gottstein, Y., Ganel, T., Otten, L. J., Quayle, A., & Rugg, M. D. (2003). Electrophysiological and haemodynamic correlates of face perception, recognition and priming. *Cerebral Cortex*, *13*(7), 793–805. http://doi.org/10.1093/cercor/13.7.793

Herrmann, M. J., Aranda, D., Ellgring, H., Mueller, T. J., Strik, W. K., Heidrich, A., & Fallgatter, A. J. (2002). Face-specific event-related potential in humans is independent from facial expression. *International Journal of Psychophysiology*, *45*(3), 241–244. http://doi.org/10.1016/S0167-8760(02)00033-8

Herrmann, M. J., Ehlis, A. C., Ellgring, H., & Fallgatter, A. J. (2005). Early stages (P100) of face perception in humans as measured with event-related potentials (ERPs). *Journal of Neural Transmission*, *112*(8), 1073–1081. http://doi.org/10.1007/s00702-004-0250-8

Hietanen, J. K., & Astikainen, P. (2013). N170 response to facial expressions is modulated by the affective congruency between the emotional expression and preceding affective picture. *Biological Psychology*, *92*(2), 114–124. http://doi.org/10.1016/j.biopsycho.2012.10.005

Hillyard, S. A., & Anllo-Vento, L. (1998). Event-related brain potentials in the study of visual selective attention. *Proceedings of the National Academy of Sciences*, *95*(3), 781–787. http://doi.org/10.1073/pnas.95.3.781

Hinojosa, J. A., Mercado, F., & Carretié, L. (2015). N170 sensitivity to facial expression: A meta-analysis. *Neuroscience and Biobehavioral Reviews*, *55*, 498–509. http://doi.org/10.1016/j.neubiorev.2015.06.002

Hirata, M., Ikeda, T., Kikuchi, M., Kimura, T., Hiraishi, H., Yoshimura, Y., & Asada, M. (2014). Hyperscanning MEG for understanding mother-child cerebral interactions. *Frontiers in Human Neuroscience*, *8*(March), 118. http://doi.org/10.3389/fnhum.2014.00118

Hoechstetter, K., Berg, P., & Scherg, M. (2010). BESA Research Tutorial 4 : Distributed Source Imaging BESA Research Tutorial 4 :, 1–29. Retrieved from http://www.besa.de/be/besa.de/demonstrations_and_tutorials/BESA Reserach Tutorial 4 - Distributed Source Imaging.pdf

Horovitz, S. G., Rossion, B., Skudlarski, P., & Gore, J. C. (2004). Parametric design and correlational analyses help integrating fMRI and electrophysiological data during face processing. *NeuroImage*, *22*(4), 1587–1595. http://doi.org/10.1016/j.neuroimage.2004.04.018

Hoshiyama, M., Kakigi, R., Watanabe, S., Miki, K., & Takeshima, Y. (2003). Brain responses for the subconscious recognition of faces. *Neuroscience Research*, *46*(4), 435–442. http://doi.org/10.1016/S0168-0102(03)00121-4

Hutzler, F., Braun, M., Võ, M. L.-H., Engl, V., Hofmann, M., Dambacher, M., … Jacobs, A. M. (2007). Welcome to the real world: Validating fixation-related brain potentials for ecologically valid settings. *Brain Research*, *1172*(1), 124–129. http://doi.org/10.1016/j.brainres.2007.07.025

Hyvärinen, A., & Oja, E. (2000). Independent component analysis: algorithms and applications. *Neural Networks*, *13*(4–5), 411–430. http://doi.org/10.13031/trans.56.9922

Ille, N., Berg, P., & Scherg, M. (2002). Artifact correction of the ongoing EEG using spatial filters based on artifact and brain signal topographies. *Journal of Clinical Neurophysiology : Official Publication of the American Electroencephalographic Society*, *19*(2), 113–24. http://doi.org/10.1097/00004691-200203000-00002

Ishai, A., Haxby, J. V., & Ungerleider, L. G. (2002). Visual imagery of famous faces: Effects of memory and attention revealed by fMRI. *NeuroImage*, *17*(4), 1729–1741. http://doi.org/10.1006/nimg.2002.1330

Ishai, A., Ungerleider, L. G., Martin, A., Schouten, J. L., & Haxby, J. V. (1999). Distributed representation of objects in the human ventral visual pathway. *Proceedings of the National Academy of Sciences*, *96*(16), 9379–9384. http://doi.org/10.1073/pnas.96.16.9379

Itier, R. J., & Taylor, M. J. (2004a). N170 or N1? Spatiotemporal Differences between Object and Face Processing Using ERPs. *Cerebral Cortex*, *14*(2), 132–142. http://doi.org/10.1093/cercor/bhg111

Itier, R. J., & Taylor, M. J. (2004b). Source analysis of the N170 to faces and objects. *Neuroreport*, *15*(8), 1261–1265. http://doi.org/10.1097/01.wnr.0000127827.73576.d8

Ito, T., Larsen, J., Smith, K., & Cacioppo, J. (1998). Negative information weighs more heavily on the brain: The negativity bias in evaluative categorizations. *Journal of Personality and Social Psychology*, *75*(4), 887–900. http://doi.org/10.1055/s-0044-100614

Jagla, F., Jergelová, M., & Riečanský, I. (2007). Saccadic eye movement related potentials. *Physiological Research*, *56*(6), 707–713. http://doi.org/1368 [pii]

Jahn, K., Deutschländer, A., Stephan, T., Strupp, M., Wiesmann, M., & Brandt, T. (2004). Brain activation patterns during imagined stance and locomotion in functional magnetic resonance imaging. *NeuroImage*, *22*(4), 1722–1731. http://doi.org/10.1016/j.neuroimage.2004.05.017

Jasper, H. H. (1958). The ten-twenty electrode system of the International Federation. *Electroencephalogr. Clin. Neurophysiol.*, *10*, 370–375.

Javal, E. (1878). Essai sur la physiologie de la lecture. *Annales d'Ocilistique*, *80*, 61–73.

Jeffreys, D. A. (1989). A face-responsive potential recorded from the human scalp. *Experimental Brain Research*, *78*(1), 569–576. http://doi.org/10.1007/BF00230699

Jeffreys, D. A. (1993). on the vertex positive scalp potential evoked by faces, 163–172.

Jeffreys, D. A. (1996). Evoked Potential Studies of Face and Object Processing. *Visual Cognition*, *3*(1), 1–38. http://doi.org/10.1080/713756729

Jeffreys, D. A., & Tukmachi, E. S. A. (1992). The vertex-positive scalp potential evoked by faces and by objects. *Experimental Brain Research*, *91*(2), 340–350. http://doi.org/10.1007/BF00231668

Jemel, B., Pisani, M., Calabria, M., Crommelinck, M., & Bruyer, R. (2003). Is the N170 for faces cognitively penetrable? Evidence from repetition priming of Mooney faces of familiar and unfamiliar persons. *Cognitive Brain Research*, *17*(2), 431–446. http://doi.org/10.1016/S0926-6410(03)00145-9

Johnston, P., Molyneux, R., & Young, A. W. (2014). The N170 observed "in the wild": Robust event-related potentials to faces in cluttered dynamic visual scenes. *Social Cognitive and Affective Neuroscience*, *10*(7), 938–944. http://doi.org/10.1093/scan/nsu136

Joyce, C., & Rossion, B. (2005). The face-sensitive N170 and VPP components manifest the same brain processes: The effect of reference electrode site. *Clinical Neurophysiology*, *116*(11), 2613–2631. http://doi.org/10.1016/j.clinph.2005.07.005

Jung, T., Makeig, S., Humphries, C., Lee, T., McKeown, M. J., Iragui, I., & Sejnowski, T. J. (2000). Removing Electroencephalographic aretfacts by blind source seperation. *Psychophysiology*, *37*(02), 163–178. http://doi.org/10.1111/1469-8986.3720163

Jung, T. P., Makeig, S., McKeown, M. J., Bell, A. J., Lee, T.-W., & Sejnowski, T. J. (2001). Imaging Brain Dynamics Using Independent Component Analysis. *Proceedings of the IEEE. Institute of Electrical and Electronics Engineers*, *89*(7), 1107–1122. http://doi.org/10.1109/5.939827

Jungnickel, E., & Gramann, K. (2016). Mobile Brain/Body Imaging (MoBI) of Physical Interaction with Dynamically Moving Objects. *Frontiers in Human Neuroscience*, *10*(June), 306. http://doi.org/10.3389/fnhum.2016.00306

Kamienkowski, J. E., Ison, M. J., Quiroga, R. Q., & Sigman, M. (2012). Fixation-related potentials in visual search: A combined EEG and eye tracking study. *Journal of Vision*, *12*(7), 4. http://doi.org/10.1167/12.7.4

Kamp, A., Pfurtscheller, G., Edlinger, G., & da Silva, F. L. (2005). Technological basis of EEG recording. In *Electroencephalography, Basic principles, Clinical applications and related fields*. Lippincott Williams & Wilkins.

Kanwisher, N., McDermott, J., & Chun, M. M. (1997). The fusiform face area: a module in human extrastriate cortex specialized for face perception. *The Journal of Neuroscience : The Official Journal of the Society for Neuroscience*, *17*(11), 4302–11. http://doi.org/10.1098/Rstb.2006.1934

Kanwisher, N., & Yovel, G. (2006). The fusiform face area: a cortical region specialized for the perception of faces. *Philosophical Transactions of the Royal Society B: Biological Sciences*, *361*(1476), 2109–2128. http://doi.org/10.1098/rstb.2006.1934

Kasneci, E., Sippel, K., Heister, M., Aehling, K., Rosenstiel, W., Schiefer, U., & Papageorgiou, E. (2014). Homonymous Visual Field Loss and Its Impact on Visual Exploration: A Supermarket Study. *Translational Vision Science & Technology*, *3*(6), 2. http://doi.org/10.1167/tvst.3.6.2

Kassner, M., Patera, W., & Bulling, A. (2014). Pupil. In *Proceedings of the 2014 ACM International Joint Conference on Pervasive and Ubiquitous Computing Adjunct Publication - UbiComp '14 Adjunct* (pp. 1151–1160). New York, New York, USA: ACM Press. http://doi.org/10.1145/2638728.2641695

Kaufmann, J. M., & Schweinberger, S. R. (2004). Expression influences the recognition of familiar faces. *Perception*, *33*(4), 399–408. http://doi.org/10.1068/p5083

Kaunitz, L. N., Kamienkowski, J. E., Varatharajah, A., Sigman, M., Quiroga, R. Q., & Ison, M. J. (2014). Looking for a face in the crowd: Fixation-related potentials in an eye-movement

visual search task. *NeuroImage*, *89*, 297–305. http://doi.org/10.1016/j.neuroimage.2013.12.006

Kawasaki, M., Kitajo, K., & Yamaguchi, Y. (2010). Dynamic links between theta executive functions and alpha storage buffers in auditory and visual working memory. *European Journal of Neuroscience*, *31*(9), 1683–1689.

Kawasaki, M., Yamada, Y., Ushiku, Y., Miyauchi, E., & Yamaguchi, Y. (2013). Inter-brain synchronization during coordination of speech rhythm in human-to-human social interaction. *Scientific Reports*, *3*, 1–8. http://doi.org/10.1038/srep01692

Kazai, K., & Yagi, A. (2003). Comparison between the lambda response of eye-fixation-related potentials and the P100 component of pattern-reversal visual evoked potentials. *Cognitive, Affective & Behavioral Neuroscience*, *3*(1), 46–56. http://doi.org/10.3758/CABN.3.1.46

Keren, A. S., Yuval-Greenberg, S., & Deouell, L. Y. (2010). Saccadic spike potentials in gamma-band EEG: Characterization, detection and suppression. *NeuroImage*, *49*(3), 2248–2263. http://doi.org/10.1016/j.neuroimage.2009.10.057

King, J. L. (2016). *Art therapy, trauma, and neuroscience: Theoretical and practical perspectives*. Routledge.

Kingstone, A., Smilek, D., & Eastwood, J. D. (2008). Cognitive Ethology: A new approach for studying human cognition. *British Journal of Psychology*, *99*(3), 317–340. http://doi.org/10.1348/000712607X251243

Klem, G. H., Lüders, H. O., Jasper, H. H., & Elger, C. (1999). The ten-twenty electrode system of the International Federation. *Electroencephalogr Clin Neurophysiol*, *52*(3), 3–6.

Koenig, P. (2018). Ecological Validity of the N170 – a mobile EEG study. In *3rd International Mobile Brain/Body Imaging Conference Berlin, Ju*. http://doi.org/10.14279/depositonce-7236

Koenraadt, K. L. M., Roelofsen, E. G. J., Duysens, J., & Keijsers, N. L. W. (2014). Cortical control of normal gait and precision stepping: An fNIRS study. *NeuroImage*, *85*(January 2015), 415–422. http://doi.org/10.1016/j.neuroimage.2013.04.070

Kokmotou, K., Cook, S., Xie, Y., Wright, H., Soto, V., Fallon, N., … Stancak, A. (2017). Effects of loss aversion on neural responses to loss outcomes: An event-related potential study. *Biological Psychology*, *126*(April), 30–40. http://doi.org/10.1016/j.biopsycho.2017.04.005

Kolassa, I.-T., & Miltner, W. H. R. (2006). Psychophysiological correlates of face processing in social phobia. *Brain Research*, *1118*(1), 130–141. http://doi.org/10.1016/j.brainres.2006.08.019

Konvalinka, I., & Roepstorff, A. (2012). The two-brain approach: how can mutually interacting brains teach us something about social interaction? *Frontiers in Human Neuroscience*, *6*(July), 1–10. http://doi.org/10.3389/fnhum.2012.00215

Körner, C., Braunstein, V., Stangl, M., Schlögl, A., Neuper, C., & Ischebeck, A. (2014). Sequential effects in continued visual search: Using fixation-related potentials to compare distractor processing before and after target detection. *Psychophysiology*, *51*(4), 385–395.

Kothe, C. (2014). Lab Streaming Layer (LSL). Retrieved from https://github.com/sccn/labstreaminglayer

Kourtzi, Z., Tolias, A. S., Altmann, C. F., Augath, M., & Logothetis, N. K. (2003). Integration of Local Features into Global Shapes. *Neuron*, *37*(2), 333–346. http://doi.org/10.1016/S0896-6273(02)01174-1

Kreifelts, B., Ethofer, T., Grodd, W., Erb, M., & Wildgruber, D. (2007). Audiovisual integration of emotional signals in voice and face: An event-related fMRI study. *NeuroImage*, *37*(4), 1445–1456. http://doi.org/10.1016/j.neuroimage.2007.06.020

Kumar, A., & Krol, G. (1992). Binocular Infrared Oculography. *Laryngoscope*, *102*(April), 367–378.

Kurtzberg, D., & Vaughan, H. G. (1982). Topographic analysis of human cortical potentials preceding self-initiated and visually triggered saccades. *Brain Research*, *243*, 1–9. http://doi.org/10.1016/0006-8993(82)91115-5

LaBar, K. S., Crupain, M. J., Voyvodic, J. T., & McCarthy, G. (2003). Dynamic perception of facial affect and identity in the human brain. *Cerebral Cortex*, *13*(10), 1023–1033. http://doi.org/10.1093/cercor/13.10.1023

Lachat, F., Hugueville, L., Lemaréchal, J.-D., Conty, L., & George, N. (2012). Oscillatory Brain Correlates of Live Joint Attention: A Dual-EEG Study. *Frontiers in Human Neuroscience*, *6*(June), 1–12. http://doi.org/10.3389/fnhum.2012.00156

Ladouce, S., Donaldson, D. I., Dudchenko, P. A., & Ietswaart, M. (2017). Understanding Minds in Real-World Environments: Toward a Mobile Cognition Approach. *Frontiers in Human Neuroscience*, *10*(January), 1–14. http://doi.org/10.3389/fnhum.2016.00694

Laird, J. D., & Lacasse, K. (2014). Bodily influences on emotional feelings: Accumulating evidence and extensions of William James's theory of emotion. *Emotion Review*, *6*(1), 27–34. http://doi.org/10.1177/1754073913494899

Lamare, M. (1892). Des mouvements des yeux dans la lecture. *Bulletins et Mémoires de La Société Française d'Ophthalmologie*, *10*, 354–364.

Lander, K., & Metcalfe, S. (2007). The influence of positive and negative facial expressions on face familiarity. *Memory*, *15*(1), 63–69. http://doi.org/10.1080/09658210601108732

Lang, P. J., Bradley, M. M., & Cuthbert, B. N. (1997). International Affective Picture System (IAPS): Technical Manual and Affective Ratings. *NIMH Center for the Study of Emotion and Attention*, 39–58. http://doi.org/10.1027/0269-8803/a000147

Lau, T. M., Gwin, J. T., & Ferris, D. P. (2012). How Many Electrodes Are Really Needed for EEG-Based Mobile Brain Imaging? *Journal of Behavioral and Brain Science*, *2*(7), 387–393.

Lau, T. M., Gwin, J. T., & Ferris, D. P. (2014). Walking reduces sensorimotor network connectivity compared to standing. *Journal of NeuroEngineering and Rehabilitation*, *11*(1), 1–10. Retrieved from http://www.embase.com/search/results?subaction=viewrecord&from=export&id=L53010152%5Cnhttp://dx.doi.org/10.1186/1743-0003-11-14%5Cnhttp://elvis.ubvu.vu.nl:9003/vulink?sid=EMBASE&issn=17430003&id=doi:10.11

86%2F1743-0003-11-14&atitle=Walking+reduces+sensori

Lazarus, R., & Folkman, S. (1984). *Stress, Appraisal, and Coping.* New York: Springer Publishing.

Lee, C., Miyakoshi, M., Delorme, A., Cauwenberghs, G., & Makeig, S. (2015). Non-parametric group-level statistics for source-resolved ERP analysis. In *Proceedings of the Annual International Conference of the IEEE Engineering in Medicine and Biology Society, EMBS*. http://doi.org/10.1109/EMBC.2015.7320114

Lee, T.-W., Girolami, M., Bell, A. J., & Sejnowski, T. J. (2000). A unifying information-theoretic framework for independent component analysis. *Computers & Mathematics with Applications*, *39*(11), 1–21.

Lee, T.-W., Girolami, M., & Sejnowski, T. J. (1999). Independent Component Analysis Using an Extended Infomax Algorithm for Mixed Subgaussian and Supergaussian Sources. *Neural Computation*, *11*(2), 417–441. http://doi.org/10.1162/089976699300016719

Lee, T., Girolami, M., & Sejnowski, T. J. (1999). Independent Component Analysis for Mixed Sub-Gaussian and Super-Gaussian Sources. *Joint Symposium on Neural Computation*, *441*, 417–441. Retrieved from http://ukpmc.ac.uk/abstract/CIT/106463

Lehmann, D. (1987). Principles of spatial analysis. *Handbook of Electroencephalography and Clinical Neurophysiology*, *1*, 309–354.

Leibenluft, E., Gobbini, M. I., Harrison, T., & Haxby, J. V. (2004). Mothers' neural activation in response to pictures of their children and other children. *Biological Psychiatry*, *56*(4), 225–232. http://doi.org/10.1016/j.biopsych.2004.05.017

Lesèvre, N., & Rémond, A. (1973). Effects of contrast on the visual evoked potentials related to eye movements. *The Oculomotor System and Brain Functions*, 119–134.

Leutheuser, H., Gabsteiger, F., Hebenstreit, F., Reis, P., Lochmann, M., & Eskofier, B. (2013). Comparison of the AMICA and the InfoMax algorithm for the reduction of electromyogenic artifacts in EEG data. In *Proceedings of the Annual International Conference of the IEEE Engineering in Medicine and Biology Society, EMBS* (pp. 6804–6807). http://doi.org/10.1109/EMBC.2013.6611119

Li, X., Samuel, O. W., Zhang, X., Wang, H., Fang, P., & Li, G. (2017). A motion-classification strategy based on sEMG-EEG signal combination for upper-limb amputees. *Journal of NeuroEngineering and Rehabilitation*, *14*(1), 1–13. http://doi.org/10.1186/s12984-016-0212-z

Lindenberger, U., Li, S. C., Gruber, W., & Müller, V. (2009). Brains swinging in concert: Cortical phase synchronization while playing guitar. *BMC Neuroscience*, *10*, 1–12. http://doi.org/10.1186/1471-2202-10-22

Linkenkaer-Hansen, K., Palva, J. M., Sams, M., Hietanen, J. K., Aronen, H. J., & Ilmoniemi, R. J. (1998). Face-selective processing in human extrastriate cortex around 120 ms after stimulus onset revealed by magneto- and electroencephalography. *Neuroscience Letters*, *253*(3), 147–150. http://doi.org/10.1016/S0304-3940(98)00586-2

Lins, O., Picton, T., Berg, P., & Scherg, M. (1993). Ocular artifacts in recording EEGs and event related potentials II.

Lipnicki, D. M., & Byrne, D. G. (2005). Thinking on your back: Solving anagrams faster when supine than when standing. *Cognitive Brain Research*, *24*(3), 719–722. http://doi.org/10.1016/j.cogbrainres.2005.03.003

Lipnicki, D. M., & Byrne, D. G. (2008). An effect of posture on anticipatory anxiety. *International Journal of Neuroscience*, *118*(2), 227–237. http://doi.org/10.1080/00207450701750463

Liu, J., Harris, A., & Kanwisher, N. (2002). Stages of processing in face perception: an MEG study. *Nature Neuroscience*, *5*(9), 910–6. http://doi.org/10.1038/nn909

Liu, J., Higuchi, M., Marantz, A., & Kanwisher, N. (2000). The selectivity of the occipitotemporal M170 for faces. *NeuroReport*, *11*(2), 337–341. http://doi.org/10.1097/00001756-200002070-00023

Liu, X., Xu, F., & Fujimura, K. (2002). Real-time eye detection and tracking for driver observation under various light conditions. In *Intelligent Vehicle Symposium, 2002. IEEE* (Vol. 2, pp. 344–351 vol.2). http://doi.org/10.1109/IVS.2002.1187975

Logie, R. H., Baddeley, A. D., & Woodhead, M. M. (1987). Face recognition, pose and ecological validity. *Applied Cognitive Psychology*, *1*(1), 53–69. http://doi.org/10.1002/acp.2350010108

Luck, S. J. (2005). An Introduction to Event-Related Potentials and Their Neural Origins. *An Introduction to the Event-Related Potential Technique*, 2–50. http://doi.org/10.1007/s10409-008-0217-3

Luck, Woodman, & Vogel. (2000). Event-related potential studies of attention. *Trends in Cognitive Sciences*, *4*(11), 432–440. http://doi.org/10.1016/S1364-6613(00)01545-X

Lundqvist, D., Flykt, A., & Öhman, A. (1998). The Karolinska Directed Emotional Faces (KDEF). *CD ROM from Department of Clinical Neuroscience, Psychology Section, Karolinska Institutet*, *91*, 630.

Lundström, J. N., Boyle, J. A., & Jones-Gotman, M. (2006). Sit up and smell the roses better: Olfactory sensitivity to phenyl ethyl alcohol is dependent on body position. *Chemical Senses*, *31*(3), 249–252. http://doi.org/10.1093/chemse/bjj025

Makeig, S. (2009). Mind monitoring via mobile brain-body imaging. *Lecture Notes in Computer Science (Including Subseries Lecture Notes in Artificial Intelligence and Lecture Notes in Bioinformatics)*, *5638 LNAI*, 749–758. http://doi.org/10.1007/978-3-642-02812-0_85

Makeig, S., Bell, A. J., Jung, T.-P., & Sejnowski, T. J. (1996). Independent Component Analysis of Electroencephalographic Data. *Advances in Neural Information Processing Systems*, (3), 145–151.

Makeig, S., Debener, S., Onton, J., & Delorme, A. (2004). Mining event-related brain dynamics. *Trends in Cognitive Sciences*, *8*(5), 204–210. http://doi.org/10.1016/j.tics.2004.03.008

Makeig, S., Gramann, K., Jung, T. P., Sejnowski, T. J., & Poizner, H. (2009). Linking brain, mind and behavior. *International Journal of Psychophysiology*, *73*(858), 95–100. http://doi.org/10.1016/j.ijpsycho.2008.11.008

Maris, E., & Oostenveld, R. (2007). Nonparametric statistical testing of EEG- and MEG-data.

Journal of Neuroscience Methods, *164*(1), 177–190. http://doi.org/10.1016/j.jneumeth.2007.03.024

Martens, U., Schweinberger, S. R., Kiefer, M., & Burton, A. M. (2006). Masked and unmasked electrophysiological repetition effects of famous faces. *Brain Research*, *1109*(1), 146–157. http://doi.org/10.1016/j.brainres.2006.06.066

Marzi, T., & Viggiano, M. P. (2007). Interplay between familiarity and orientation in face processing: An ERP study. *International Journal of Psychophysiology*, *65*(3), 182–192. http://doi.org/10.1016/j.ijpsycho.2007.04.003

Matsumoto, D., Keltner, D., Shiota, M., O'Sullivan, M., & Frank, M. (2008). Facial expressions of emotion. In *Handbook of emotions* (pp. 211–234). Gilford Press.

Matsumoto, D., LeRoux, J. A., Bernhard, R., & Gray, H. (2004). Unraveling the psychological correlates of intercultural adjustment potential. *International Journal of Intercultural Relations*, *28*(3–4), 281–309. http://doi.org/10.1016/j.ijintrel.2004.06.002

Maurer, D., Le Grand, R., & Mondloch, C. J. (2002). The many faces of configural processing. *Trends in Cognitive Sciences*, *6*(6), 255–260. http://doi.org/10.1016/S1364-6613(02)01903-4

Maurer, U., Rossion, B., & McCandliss, B. D. (2008). Category specificity in early perception: face and word N170 responses differ in both lateralization and habituation properties. *Frontiers in Human Neuroscience*, *2*(December), 1–7. http://doi.org/10.3389/neuro.09.018.2008

McCandliss, B. D., Cohen, L., & Dehaene, S. (2003). The visual word form area: Expertise for reading in the fusiform gyrus. *Trends in Cognitive Sciences*, *7*(7), 293–299. http://doi.org/10.1016/S1364-6613(03)00134-7

Mccarthy, G., Puce, A., Gore, J. C., & Allison, T. (1996). Face - Specific Processing in the Human Fusiforrn Gyms, 605–610. http://doi.org/10.1162/jocn.1997.9.5.605

McPartland, J., Dawson, G., Webb, S. J., Panagiotides, H., & Carver, L. J. (2004). Event-related brain potentials reveal anomalies in temporal processing of faces in autism spectrum disorder. *Journal of Child Psychology and Psychiatry and Allied Disciplines*, *45*(7), 1235–1245. http://doi.org/10.1111/j.1469-7610.2004.00318.x

Melcher, D., & Colby, C. L. (2008). Trans-saccadic perception. *Trends in Cognitive Sciences*, *12*(12), 466–473. http://doi.org/10.1016/j.tics.2008.09.003

Ménoret, M., Varnet, L., Fargier, R., Cheylus, A., Curie, A., des Portes, V., … Paulignan, Y. (2014). Neural correlates of non-verbal social interactions: A dual-EEG study. *Neuropsychologia*, *55*(1), 85–97. http://doi.org/10.1016/j.neuropsychologia.2013.10.001

Mergner, T., & Rosemeier, T. (1998). Interaction of vestibular, somatosensory and visual signals for postural control and motion perception under terrestrial and microgravity conditions - A conceptual model. *Brain Research Reviews*, *28*(1–2), 118–135. http://doi.org/10.1016/S0165-0173(98)00032-0

Mertens, I., Siegmund, H., & Grüsser, O. J. (1993). Gaze motor asymmetries in the perception of faces during a memory task. *Neuropsychologia*, *31*(9), 989–998. http://doi.org/10.1016/0028-3932(93)90154-R

Montague, P. R., Berns, G. S., Cohen, J. D., McClure, S. M., Pagnoni, G., Dhamala, M., … Fisher, R. E. (2002). Hyperscanning: Simultaneous fMRI during linked social interactions. *NeuroImage*, *16*(4), 1159–1164. http://doi.org/10.1006/nimg.2002.1150

Mühlberger, A., Wieser, M. J., Herrmann, M. J., Weyers, P., Tröger, C., & Pauli, P. (2009). Early cortical processing of natural and artificial emotional faces differs between lower and higher socially anxious persons. *Journal of Neural Transmission*, *116*(6), 735–746. http://doi.org/10.1007/s00702-008-0108-6

Murphy, D. P., Bai, O., Gorgey, A. S., Fox, J., Lovegreen, W. T., Burkhardt, B. W., … Fei, D. Y. (2017). Electroencephalogram-based brain-computer interface and lower-limb prosthesis control: A case study. *Frontiers in Neurology*, *8*(DEC), 1–8. http://doi.org/10.3389/fneur.2017.00696

Muthukumaraswamy, S. D. (2013). High-frequency brain activity and muscle artifacts in MEG/EEG: a review and recommendations. *Frontiers in Human Neuroscience*, *7*(April), 1–11. http://doi.org/10.3389/fnhum.2013.00138

Nashner, L. M. (1976). Adapting reflexes controlling the human posture. *Experimental Brain Research*, *26*(1), 59–72. http://doi.org/10.1007/BF00235249

Nathan, K., & Contreras-Vidal, J. L. (2016). Negligible Motion Artifacts in Scalp Electroencephalography (EEG) During Treadmill Walking. *Frontiers in Human Neuroscience*, *9*(January), 1–12. http://doi.org/10.3389/fnhum.2015.00708

Neisser, U. (1976). Cognition and reality. Principles and implication of cognitive psychology. *San Francisko: WH Freeman and Company*.

Nguyen, V. T., & Cunnington, R. (2014). NeuroImage The superior temporal sulcus and the N170 during face processing : Single trial analysis of concurrent EEG – fMRI. *NeuroImage*, *86*, 492–502. http://doi.org/10.1016/j.neuroimage.2013.10.047

Niedermeyer, E., & da Silva, F. H. L. (2005). *Electroencephalography: basic principles, clinical applications, and related fields*. Lippincott Williams & Wilkins.

Nikolaev, A. R., Meghanathan, R. N., & van Leeuwen, C. (2016). Combining EEG and eye movement recording in free viewing: Pitfalls and possibilities. *Brain and Cognition*, *107*, 55–83. http://doi.org/10.1016/j.bandc.2016.06.004

Nitschke, M., Kleinschmidt, A., Wessel, K., & Frahm, J. (1996). Somatotopic motor representation in the human anterior cerebellum. *Brain*, 1023–1029. http://doi.org/10.1093/brain/119.3.1023

Nunez, P. L., & Silberstein, R. B. (2000). On the Relationship of Synaptic Activity to Macroscopic Measurements: Does Co-Registration On the Relationship of Synaptic Activity to Macroscopic Measurements: Does Co-Registration of EEG with fMRI Make Sense? Macroscopic Measurements: Does Co-Registrati. *Brain Topography*, *13*(2), 79–95. Retrieved from papers3://publication/uuid/201BCB34-9C24-49C7-BC9C-7D5A49BD8B8D

Nunez, P. L., Srinivasan, R., Westdorp, A. F., Wijesinghe, R. S., Tucker, D. M., Silberstein, R. B., & Cadusch, P. J. (1997). EEG coherency I: statistics, reference electrode, volume conduction, Laplacians, cortical imaging, and interpretation at multiple scales.

Electroencephalography and Clinical Neurophysiology, *103*(5), 499–515. http://doi.org/10.1016/S0013-4694(97)00066-7

Ojeda, A., Bigdely-Shamlo, N., & Makeig, S. (2014). MoBILAB: an open source toolbox for analysis and visualization of mobile brain/body imaging data. *Frontiers in Human Neuroscience*, *8*(March), 121. http://doi.org/10.3389/fnhum.2014.00121

Oken, B. S. (1986). Filtering and aliasing of muscle activity in EEG frequency analysis. *Electroencephalography and Clinical Neurophysiology*, *64*(1), 77–80. http://doi.org/10.1016/0013-4694(86)90045-3

Olivares, E. I., Iglesias, J., Saavedra, C., Trujillo-Barreto, N. J., & Valdés-Sosa, M. (2015). Brain Signals of Face Processing as Revealed by Event-Related Potentials. *Behavioural Neurology*, *2015*(May), 514361. http://doi.org/10.1155/2015/514361

Onton, J., Westerfield, M., Townsend, J., & Makeig, S. (2006). Imaging human EEG dynamics using independent component analysis. *Neuroscience and Biobehavioral Reviews*, *30*(6), 808–822. http://doi.org/10.1016/j.neubiorev.2006.06.007

Oostenveld, R., & Oostendorp, T. F. (2002). Validating the boundary element method for forward and inverse EEG computations in the presence of a hole in the skull. *Human Brain Mapping*, *17*(3), 179–192. http://doi.org/10.1002/hbm.10061

Ossandón, J. P., Helo, A. V., Montefusco-Siegmund, R., & Maldonado, P. E. (2010). Superposition model predicts EEG occipital activity during free viewing of natural scenes. *The Journal of Neuroscience : The Official Journal of the Society for Neuroscience*, *30*(13), 4787–95. http://doi.org/10.1523/JNEUROSCI.5769-09.2010

Ossandón, J. P., Helo, A. V., Montefusco-Siegmund, R., & Maldonado, P. E. (2010). Superposition Model Predicts EEG Occipital Activity during Free Viewing of Natural Scenes. *Journal of Neuroscience*, *30*(13), 4787–4795. http://doi.org/10.1523/JNEUROSCI.5769-09.2010

Ouchi, Y., Kanno, T., Okada, H., Yoshikawa, E., Futatsubashi, M., Nobezawa, S., … Tanaka, K. (2001). Changes in dopamine availability in the nigrostriatal and mesocortical dopaminergic systems by gait in Parkinson's disease. *Brain*, *124*(4), 784–792.

Ouchi, Y., Okada, H., Yoshikawa, E., Futatsubashi, M., & Nobezawa, S. (2001). Absolute changes in regional cerebral blood flow in association with upright posture in humans: an orthostatic PET study. *Journal of Nuclear Medicine : Official Publication, Society of Nuclear Medicine*, *42*(5), 707–712. Retrieved from http://www.ncbi.nlm.nih.gov/entrez/query.fcgi?cmd=Retrieve&db=PubMed&dopt=Citation&list_uids=11337564

Ouchi, Y., Okada, H., Yoshikawa, E., Nobezawa, S., & Futatsubashi, M. (1999). Brain activation during maintenance of standing posture in humans. *Brain*, *122*(May), 329–338. Retrieved from file:///Users/Domingo/Documents/Literature/E_Lit/

Ozonoff, S., Pennington, B. F., & Rogers, S. J. (1990). Are there Emotion Perception Deficits in Young Autistic Children? *Journal of Child Psychology and Psychiatry*, *31*(3), 343–361. http://doi.org/10.1111/j.1469-7610.1990.tb01574.x

Palmer, J. A., Kreutz-Delgado, K., & Makeig, S. (2006). Super-Gaussian mixture source model

for ICA. *Lecture Notes in Computer Science (Including Subseries Lecture Notes in Artificial Intelligence and Lecture Notes in Bioinformatics)*, *3889 LNCS*, 854–861. http://doi.org/10.1007/11679363_106

Palmer, J. A., Makeig, S., Kreutz-Delgado, K., & Rao, B. D. (2008). Newton method for the ICA mixture model. In *Icassp* (pp. 1805–1808).

Parada, F. J. (2018). Understanding Natural Cognition in Everyday Settings: 3 Pressing Challenges. *Frontiers in Human Neuroscience*, *12*(September), 1–5. http://doi.org/10.3389/fnhum.2018.00386

Parker, S. W., & Nelson, C. A. (2005). An event-related potential study of the impact of institutional rearing on face recognition. *Development and Psychopathology*, *17*(03), 621–639. http://doi.org/10.1017/S0954579405050303

Pascual-Marqui, R. D. (2002). Standardized low-resolution brain electromagnetic tomography (sLORETA): technical details. *Methods and Findings in Experimental and Clinical Pharmacology*, *24 Suppl D*, 5–12. http://doi.org/841 [pii]

Pascual-Marqui, R. D., Michel, C. M., & Lehmann, D. (1994). Low resolution electromagnetic tomography: a new method for localizing electrical activity in the brain. *International Journal of Psychophysiology*, *18*(1), 49–65. http://doi.org/10.1016/0167-8760(84)90014-X

Patterson, M. L. (1982). A sequential functional model of nonverbal exchange. *Psychological Review*, *89*(3), 231–249. http://doi.org/10.1037/0033-295X.89.3.231

Pérez, A., Carreiras, M., & Duñabeitia, J. A. (2017). Brain-To-brain entrainment: EEG interbrain synchronization while speaking and listening. *Scientific Reports*, *7*(1), 1–12. http://doi.org/10.1038/s41598-017-04464-4

Persad, S. M., & Polivy, J. (1993). Differences between depressed and nondepressed individuals in the recognition of and response to facial emotional cues. *Journal of Abnormal Psychology*. US: American Psychological Association. http://doi.org/10.1037/0021-843X.102.3.358

Petrides, M., & Milner, B. (1982). Deficits on subject-ordered and temporal-lobe tasks after frontal-lobe lesions in man. *International Journal of Pediatric Otorhinolaryngology*, *20*(3), 249–262. http://doi.org/10.1016/j.ijporl.2012.05.023

Piper, S. K., Krueger, A., Koch, S. P., Mehnert, J., Habermehl, C., Steinbrink, J., … Schmitz, C. H. (2014). A wearable multi-channel fNIRS system for brain imaging in freely moving subjects. *NeuroImage*, *85*, 64–71. http://doi.org/10.1016/j.neuroimage.2013.06.062

Pitcher, D., Walsh, V., & Duchaine, B. (2011). The role of the occipital face area in the cortical face perception network. *Experimental Brain Research*, *209*(4), 481–493. http://doi.org/10.1007/s00221-011-2579-1

Pizzagalli, D. a, Lehmann, D., Hendrick, A. M., Regard, M., Pascual-Marqui, R. D., & Davidson, R. J. (2002). Affective judgments of faces modulate early activity (approximately 160 ms) within the fusiform gyri. *NeuroImage*, *16*(3 Pt 1), 663–677. http://doi.org/10.1006/nimg.2002.1126

Posamentier, M. T., & Abdi, H. (2003). Processing faces and facial expressions. *Neuropsychology Review*, *13*(3), 113–43. http://doi.org/1040-7308/03/0900-0113

Pourtois, G., Dan, E. S., Grandjean, D., Sander, D., & Vuilleumier, P. (2005). Enhanced extrastriate visual response to bandpass spatial frequency filtered fearful faces: Time course and topographic evoked-potentials mapping. *Human Brain Mapping*, *26*(1), 65–79. http://doi.org/10.1002/hbm.20130

Presacco, A., Goodman, R., Forrester, L., & Contreras-Vidal, J. L. (2011). Neural decoding of treadmill walking from noninvasive electroencephalographic signals. *Journal of Neurophysiology*, *106*(4), 1875–1887. http://doi.org/10.1152/jn.00104.2011

Price, T. F., Dieckman, L. W., & Harmon-Jones, E. (2012). Embodying approach motivation: Body posture influences startle eyeblink and event-related potential responses to appetitive stimuli. *Biological Psychology*, *90*(3), 211–217.

Protzak, J., & Gramann, K. (2018). Investigating Established EEG Parameter During Real-World Driving. *Frontiers in Psychology*, *9*, 275396. http://doi.org/10.3389/fpsyg.2018.02289

Puce, A., Allison, T., Asgari, M., Gore, J. C., & McCarthy, G. (1996). Differential Sensitivity of Human Visual Cortex to Faces, Letterstrings, and Textures: A Functional Magnetic Resonance Imaging Study Aina. *The Journal of Neuroscience*, *16*(16). http://doi.org/16(16):5205–5215

Quian Quiroga, R., Rosso, O. A., Basar, E., & Schurmann, M. (2001). Wavelet entropy in event-related potentials: a new method shows ordering of EEG oscillations. *Biological Cybernetics*, *84*(4), 291–299. http://doi.org/10.1007/s004220000212

Rafal, R. D., & Posner, M. I. (1987). Deficits in human visual spatial attention following thalamic lesions. *October*, *84*(June 1986), 7349–7353.

Rämä, P., & Baccino, T. (2010). Eye fixation-related potentials (EFRPs) during object identification. *Visual Neuroscience*, *27*(5–6), 187–192. http://doi.org/10.1017/S0952523810000283

Ran, G. M., Chen, X., Pan, Y. G., Hu, T. Q., & Ma, J. (2014). Effects of Anticipation on Perception of Facial Expressions. *Perceptual and Motor Skills*, *118*(1), 195–209. http://doi.org/10.2466/24.PMS.118k13w4

Raz, A., Lieber, B., Soliman, F., Buhle, J., Posner, J., Peterson, B. S., & Posner, M. I. (2005). Ecological nuances in functional magnetic resonance imaging (fMRI): Psychological stressors, posture, and hydrostatics. *NeuroImage*, *25*(1), 1–7. http://doi.org/10.1016/j.neuroimage.2004.11.015

Rémond, A., & Lesèvre, N. (1956). The conditions of appearance and the statistical importance of the lambda waves in normal subjects. *ELECTROENCEPHALOGRAPHY AND CLINICAL NEUROPHYSIOLOGY*, *8*(1).

Rice, J. K., Rorden, C., Little, J. S., & Parra, L. C. (2013). Subject position affects EEG magnitudes. *NeuroImage*, *64*(1), 476–484. http://doi.org/10.1016/j.neuroimage.2012.09.041

Richards, J. E. (2001). Cortical Indexes of Saccade Planning Following Covert Orienting in 20-Week-Old Infants. *Infancy*, *2*(2), 135–157. http://doi.org/10.1207/S15327078IN0202_2

Righart, R., & de Gelder, B. (2008). Rapid influence of emotional scenes on encoding of facial

expressions: An ERP study. *Social Cognitive and Affective Neuroscience*, *3*(3), 270–278. http://doi.org/10.1093/scan/nsn021

Rigoulot, S., D'Hondt, F., Defoort-Dhellemmes, S., Despretz, P., Honoré, J., & Sequeira, H. (2011). Fearful faces impact in peripheral vision: Behavioral and neural evidence. *Neuropsychologia*, *49*(7), 2013–2021. http://doi.org/10.1016/j.neuropsychologia.2011.03.031

Rigoulot, S., D'Hondt, F., Honoré, J., & Sequeira, H. (2012). Implicit emotional processing in peripheral vision: Behavioral and neural evidence. *Neuropsychologia*, *50*(12), 2887–2896. http://doi.org/10.1016/j.neuropsychologia.2012.08.015

Riskind, J. H., & Gotay, C. C. (1982). Physical Posture : Could It Have Regulatory pr Feedback Effects on Motivation and Emoton? *Motivation and Emotion*, *6*(3), 273–297.

Rizzolatti, G., & Gentilucci, M. (2002). Motor and visuo-motor functions of the premotor cortex. *Current Opinion in Neurobiology*, *12*(2), 149–154.

Ro, T., Friggel, A., & Lavie, N. (2007). Attentional biases for faces and body parts. *Visual Cognition*, *15*(3), 322–348. http://doi.org/10.1080/13506280600590434

Rossion, B. (2014). Understanding face perception by means of human electrophysiology. *Trends in Cognitive Sciences*, *18*(6), 310–318. http://doi.org/10.1016/j.tics.2014.02.013

Rossion, B., & Caharel, S. (2011). ERP evidence for the speed of face categorization in the human brain: Disentangling the contribution of low-level visual cues from face perception. *Vision Research*, *51*(12), 1297–1311. http://doi.org/10.1016/j.visres.2011.04.003

Rossion, B., Campanella, S., Gomez, C. ., Delinte, A., Debatisse, D., Liard, L., … Guerit, J. . (1999). Task modulation of brain activity related to familiar and unfamiliar face processing: an ERP study. *Clinical Neurophysiology*, *110*(3), 449–462. http://doi.org/10.1016/S1388-2457(98)00037-6

Rossion, B., Curran, T., & Gauthier, I. (2002). A defense of the subordinate-level expertise account for the N170 component. *Cognition*, *85*(2), 189–196. http://doi.org/10.1016/S0010-0277(02)00101-4

Rossion, B., Delvenne, J.-F., Debatisse, D., Goffaux, V., Bruyer, R., Crommelinck, M., & Guerit, J. M. (1999). Spatio-temporal localization of the face inversion effect: an event-related potentials study. *Biological Psychology*, *50*, 173–189. Retrieved from https://insights.ovid.com/crossref?an=00005053-200106000-00009

Rossion, B., Gauthier, I., Tarr, M. J., Despland, P., Bruyer, R., Linotte, S., & Crommelinck, M. (2000). The N170 occipito-temporal component is delayed and enhanced to inverted faces but not to inverted objects: an electrophysiological account of face-specific processes in the human brain. *Neuroreport*, *11*(1), 69–74. http://doi.org/10.1097/00001756-200001170-00014

Rossion, B., & Jacques, C. (2008). Does physical interstimulus variance account for early electrophysiological face sensitive responses in the human brain? Ten lessons on the N170. *NeuroImage*, *39*(4), 1959–1979. http://doi.org/10.1016/j.neuroimage.2007.10.011

Rossion, B., & Jacques, C. (2011). The N170: understanding the time-course of face perception in the human brain. *The Oxford Handbook of ERP Components*, 115–142.

Rossion, B., Joyce, C. A., Cottrell, G. W., & Tarr, M. J. (2003). Early lateralization and orientation tuning for face, word, and object processing in the visual cortex. *NeuroImage*, *20*(3), 1609–1624. http://doi.org/10.1016/j.neuroimage.2003.07.010

Roth, M. (1953). The lambda wave as a normal physiological phenomenon in the normal electroencephalogram. *Nature*, *172*(4384), 864–6. Retrieved from http://www.ncbi.nlm.nih.gov/pubmed/13111214

Rotshtein, P., Henson, R. N. A., Treves, A., Driver, J., & Dolan, R. J. (2005). Morphing Marilyn into Maggie dissociates physical and identity face representations in the brain. *Nature Neuroscience*, *8*(1), 107–113. http://doi.org/10.1038/nn1370

Rowan, A. J., & Tolunsky, E. (2003). *A primer of EEG: with a mini-atlas*. Butterworth-Heinemann Medical.

Sadeh, B., Podlipsky, I., Zhdanov, A., & Yovel, G. (2010). Event-related potential and functional MRI measures of face-selectivity are highly correlated: a simultaneous ERP-fMRI investigation. *Human Brain Mapping*, *31*(10), 1490–1501. http://doi.org/10.1002/hbm.20952

Sauvage, C., Jissendi, P., Seignan, S., Manto, M., & Habas, C. (2013). Brain areas involved in the control of speed during a motor sequence of the foot: Real movement versus mental imagery. *Journal of Neuroradiology*, *40*(4), 267–280. http://doi.org/10.1016/j.neurad.2012.10.001

Scherberger, H. (2009). Neural control of motor prostheses. *Current Opinion in Neurobiology*, *32*(1), 480–94. http://doi.org/10.1016/j.neuron.2008.10.037

Scherg, M. (2005). BESA®.

Scherg, M., & Berg, P. (1991). Use of prior knowledge in brain electromagnetic source analysis. *Brain Topography*, *4*(2), 143–150. http://doi.org/10.1007/BF01132771

Schilbach, L., Timmermans, B., Reddy, V., Costall, A., Bente, G., Schlicht, T., & Vogeley, K. (2013). A second-person neuroscience in interaction. *Behavioral and Brain Sciences*, *36*(4), 441–462. http://doi.org/10.1017/S0140525X12002452

Schneider, S., & Strüder, H. K. (2012). EEG: Theoretical background and practical aspects. In *Functional neuroimaging in exercise and sport sciences* (pp. 197–212). Springer.

Schnipke, S. K., & Todd, M. W. (2000). Trials and tribulations of using an eye-tracking system. In *CHI '00 extended abstracts on Human factors in computing systems - CHI '00* (p. 273). New York, New York, USA: ACM Press. http://doi.org/10.1145/633292.633452

Schweinberger, S. R., Pickering, E. C., Jentzsch, I., Burton, A. M., & Kaufmann, J. M. (2002). Event-related brain potential evidence for a response of inferior temporal cortex to familiar face repetitions. *Cognitive Brain Research*, *14*(3), 398–409. http://doi.org/10.1016/S0926-6410(02)00142-8

Seeber, M., Scherer, R., Wagner, J., Solis-Escalante, T., & Müller-Putz, G. R. (2014). EEG beta suppression and low gamma modulation are different elements of human upright walking. *Frontiers in Human Neuroscience*, *8*(July), 1–9. http://doi.org/10.3389/fnhum.2014.00485

Seeber, M., Scherer, R., Wagner, J., Solis-Escalante, T., & Müller-Putz, G. R. (2015). High and

low gamma EEG oscillations in central sensorimotor areas are conversely modulated during the human gait cycle. *NeuroImage*, *112*(July), 318–326. http://doi.org/10.1016/j.neuroimage.2015.03.045

Sergent, J., & Signoret, J. (1992). Functional and anatomical decomposition of face processing: evidence from prosopagnosia and PET study of normal subjects. *Phil. Trans. R. Soc. Lond*, *335*(1273), 55–62.

Severens, M., Nienhuis, B., Desain, P., & Duysens, J. (2012). Feasibility of measuring event Related Desynchronization with electroencephalography during walking. *Proceedings of the Annual International Conference of the IEEE Engineering in Medicine and Biology Society, EMBS*, *8*, 2764–2767. http://doi.org/10.1109/EMBC.2012.6346537

Sherrington, C. S. (1909). The integrative action of the nervous system. *CUP Archive*.

Simola, J., Le Fevre, K., Torniainen, J., & Baccino, T. (2015). Affective processing in natural scene viewing: Valence and arousal interactions in eye-fixation-related potentials. *NeuroImage*, *106*, 21–33. http://doi.org/10.1016/j.neuroimage.2014.11.030

Singh, H., & Singh, J. (2012). Human Eye Tracking and Related Issues: A Review. *International Journal of Scientific and Research Publications*, *2*(1), 2250–3153. Retrieved from www.ijsrp.org

Small, M. (1983). Asymmetrical Evoked Potentials in Response to Face Stimuli. *Cortex*, *19*(4), 441–450. http://doi.org/10.1016/S0010-9452(83)80026-4

Smilek, D., Birmingham, E., Cameron, D., Bischof, W., & Kingstone, A. (2006). Cognitive Ethology and exploring attention in real-world scenes. *Brain Research*, *1080*(1), 101–119. http://doi.org/10.1016/j.brainres.2005.12.090

Smith, K., Larsen, J., Chartrand, T., Cacioppo, J., Katafiasz, H., & Moran, K. (2006). Being bad isn't always good: Affective context moderates the attention bias toward negative information. *Journal of Personality and Social Psychology*, *90*(2), 210–220. http://doi.org/10.1037/0022-3514.90.2.210

Smith, N. K., Cacioppo, J. T., Larsen, J. T., & Chartrand, T. L. (2003). May I have your attention, please: Electrocortical responses to positive and negative stimuli. *Neuropsychologia*, *41*(2), 171–183. http://doi.org/10.1016/S0028-3932(02)00147-1

Soto, V., Tyson-Carr, J., Kokmotou, K., Roberts, H., Cook, S., Fallon, N., … Stancak, A. (2018a). Brain responses to emotional faces in natural settings: a wireless mobile EEG Brain responses to emotional faces in natural settings: a wireless mobile EEG recording study. natural settings: a wireless mobile EEG recording study.

Soto, V., Tyson-Carr, J., Kokmotou, K., Roberts, H., Cook, S., Fallon, N., … Stancak, A. (2018b). Brain Responses to Emotional Faces in Natural Settings: A Wireless Mobile EEG Recording Study. *Frontiers in Psychology*, *9*(October), 1–15. http://doi.org/10.3389/fpsyg.2018.02003

Speckmann, E.-J. (1979). *Origins of cerebral field potentials: International Symposium Muenster, Germany*. Thieme.

Spironelli, C., & Angrilli, A. (2011). Influence of body position on cortical pain-related somatosensory processing: An ERP study. *PLoS ONE*, *6*(9).

http://doi.org/10.1371/journal.pone.0024932

Sprengelmeyer, R., & Jentzsch, I. (2006). Event related potentials and the perception of intensity in facial expressions. *Neuropsychologia*, *44*(14), 2899–2906. http://doi.org/10.1016/j.neuropsychologia.2006.06.020

Stancak, A., Hoechstetter, K., Tintera, J., Vrana, J., Rachmanova, R., Kralik, J., & Scherg, M. (2002). Source activity in the human secondary somatosensory cortex depends on the size of corpus callosum. *Brain Research*, *936*(1–2), 47–57. http://doi.org/10.1016/S0006-8993(02)02502-7

Stancak, A., Xie, Y., Fallon, N., Bulsing, P., Giesbrecht, T., Thomas, A., & Pantelous, A. A. (2015). Unpleasant odors increase aversion to monetary losses. *Biological Psychology*, *107*, 1–9. http://doi.org/10.1016/j.biopsycho.2015.02.006

Steeves, J. K. E., Culhama, J., Duchaineb, B., Valyear, C. C. P. K. F., Schindler, I., Humphrey, G. K., … Goodale, M. A. (2006). The fusiform face area is not sufficient for face recognition: Evidence from a patient with dense prosopagnosia and no occipital face area. *Neuropsychologia*, *44*, 549–609. http://doi.org/:10.1016/j.neuropsychologia.2005.06.013

Stephens, G. J., Silbert, L. J., & Hasson, U. (2010). Speaker-listener neural coupling underlies successful communication. *Proceedings of the National Academy of Sciences*, *107*(32), 14425–14430. http://doi.org/10.1073/pnas.1008662107

Świrski, L., Bulling, A., & Dodgson, N. (2012a). Robust real-time pupil tracking in highly off-axis images. In *Proceedings of the Symposium on Eye Tracking Research and Applications - ETRA '12* (pp. 173–176). http://doi.org/10.1145/2168556.2168585

Świrski, L., Bulling, A., & Dodgson, N. (2012b). Robust real-time pupil tracking in highly off-axis images. *Proceedings of the Symposium on Eye Tracking Research and Applications - ETRA '12*, 173. http://doi.org/10.1145/2168556.2168585

Symeonidou, E. R., Nordin, A. D., Hairston, W. D., & Ferris, D. P. (2018). Effects of cable sway, electrode surface area, and electrode mass on electroencephalography signal quality during motion. *Sensors (Switzerland)*, *18*(4), 1–13. http://doi.org/10.3390/s18041073

Takahashi, H., Fujie, S., Camerer, C., Arakawa, R., Takano, H., Kodaka, F., … Suhara, T. (2013). Norepinephrine in the brain is associated with aversion to financial loss. *Molecular Psychiatry*, *18*(1), 3–4. http://doi.org/10.1038/mp.2012.7

Tanaka, J. W., & Curran, T. (2001). A neural basis for expert object recognition. *Psychological Science*, *12*(1), 43–7. http://doi.org/10.1111/1467-9280.00308

Tanaka, J. W., Curran, T., Porterfield, A. L., & Collins, D. (2006). Activation of preexisting and acquired face representations: the N250 event-related potential as an index of face familiarity. *Journal of Cognitive Neuroscience*, *18*(9), 1488–1497. http://doi.org/10.1162/jocn.2006.18.9.1488

Teplan, M. (2002). Fundamentals of EEG measurement. *Measurement Science Review*, *2*, 1–11. http://doi.org/10.1021/pr070350l

Thibault, R. T., Lifshitz, M., Jones, J. M., & Raz, A. (2014). Posture alters human resting-state. *Cortex*, *58*, 199–205. http://doi.org/10.1016/j.cortex.2014.06.014

Thibault, R. T., Lifshitz, M., & Raz, A. (2015). Body position alters human resting-state: Insights from multi-postural magnetoencephalography. *Brain Imaging and Behavior*, *10*(3), 772–780. http://doi.org/10.1007/s11682-015-9447-8

Thibault, R. T., & Raz, A. (2016). Imaging Posture Veils Neural Signals. *Frontiers in Human Neuroscience*, *10*(October), 1–8. http://doi.org/10.3389/fnhum.2016.00520

Thickbroom, G. W., Knezevič, W., Carroll, W. M., & Mastaglia, F. L. (1991). Saccade onset and offset lambda waves: relation to pattern movement visually evoked potentials. *Brain Research*, *551*(1–2), 150–156. http://doi.org/10.1016/0006-8993(91)90927-N

Thickbroom, G. W., & Mastaglia, F. L. (1986). Presaccadic spike potential. Relation to eye movement direction. *Electroencephalography and Clinical Neurophysiology*, *64*(3), 211–214.

Thierry, G., Martin, C. D., Downing, P., & Pegna, A. J. (2007). Controlling for interstimulus perceptual variance abolishes N170 face selectivity. *Nature Neuroscience*, *10*(4), 505–511. http://doi.org/10.1038/nn1864

Tognoli, E., Lagarde, J., DeGuzman, G. C., & Kelso, J. A. S. (2007). The phi complex as a neuromarker of human social coordination. *Proceedings of the National Academy of Sciences*, *104*(19), 8190–8195. http://doi.org/10.1073/pnas.0611453104

Torriente, I., Valdes-Sosa, M., Ramirez, D., & Bobes, M. A. (1999). Visual evoked potentials related to motion-onset are modulated by attention. *Vision Research*, *39*(24), 4122–4139. http://doi.org/10.1016/S0042-6989(99)00113-3

Tottenham, N., Tanaka, J. W., Leon, A. C., McCarry, T., Nurse, M., Hare, T. A., … Nelson, C. (2009). The NimStim set of facial expressions: Judgements from untrained research participants. *Psychiatry Research*, *168*(3), 242–249. http://doi.org/10.1016/j.psychres.2008.05.006.The

Towler, J., Gosling, A., Duchaine, B., & Eimer, M. (2012). The face-sensitive N170 component in developmental prosopagnosia. *Neuropsychologia*, *50*(14), 3588–3599. http://doi.org/10.1016/j.neuropsychologia.2012.10.017

Trautmann-Lengsfeld, S. A., Domínguez-Borràs, J., Escera, C., Herrmann, M., & Fehr, T. (2013). The Perception of Dynamic and Static Facial Expressions of Happiness and Disgust Investigated by ERPs and fMRI Constrained Source Analysis. *PLoS ONE*, *8*(6). http://doi.org/10.1371/journal.pone.0066997

Usakli, A. B., & Gurkan, S. (2010). Design of a novel efficient human-computer interface: An electrooculagram based virtual keyboard. *IEEE Transactions on Instrumentation and Measurement*, *59*(8), 2099–2108. http://doi.org/10.1109/TIM.2009.2030923

Utama, N. P., Takemoto, A., Koike, Y., & Nakamura, K. (2009). Phased processing of facial emotion: An ERP study. *Neuroscience Research*, *64*(1), 30–40. http://doi.org/10.1016/j.neures.2009.01.009

Van Humbeeck, N., Meghanathan, R. N., Wagemans, J., van Leeuwen, C., & Nikolaev, A. R. (2018). Presaccadic EEG activity predicts visual saliency in free-viewing contour integration. *Psychophysiology*, (October 2016), 1–21. http://doi.org/10.1111/psyp.13267

van Rijn, A., Peper, A., & Grimbergen, C. (1990). High-quality recording of biometric events.

Medical and Biological Engineering and Computing, *5*(28), 389–397.

Van Voorhis, S., & Hillyard, S. A. (1977). Visual evoked potentials and selective attention to points in space. *Perception & Psychophysics*, *22*(1), 54–62. http://doi.org/10.3758/BF03206080

Varela, F. J., Thompson, E., & Asenstorfer, C. (1996). Cognitive Science and Human Expierience.

Varela, F., Lachaux, J.-P., Rodriguez, E., & Martinerie, J. (2001). The brainweb: phase synchronization and large-scale integration. *Nature Reviews Neuroscience*, *2*(4), 229.

Vigon, L., Saatchi, R., Mayhew, J. E. W., Taroyan, N. A., & Frisby, J. P. (2002). Effect of signal length on the performance of independent component analysis when extracting the lambda wave. *Medical & Biological Engineering & Computing*, *40*(2), 260–268. http://doi.org/10.1007/BF02348134

Voss, J. L., & Paller, K. A. (2006). Fluent Conceptual Processing and Explicit Memory for Faces Are Electrophysiologically Distinct. *Journal of Neuroscience*, *26*(3), 926–933. http://doi.org/10.1055/s-0029-1218721

Voss, J. L., & Paller, K. A. (2007). Neural correlates of conceptual implicit memory and their contamination of putative neural correlates of explicit memory. *Learning and Memory*, *14*(4), 259–267. http://doi.org/10.1101/lm.529807

Wagner, A. D., Shannon, B. J., Kahn, I., & Buckner, R. L. (2005). Parietal lobe contributions to episodic memory retrieval. *Trends in Cognitive Sciences*, *9*(9), 445–453. http://doi.org/10.1016/j.tics.2005.07.001

Wagner, J., Solis-Escalante, T., Grieshofer, P., Neuper, C., Müller-Putz, G., & Scherer, R. (2012). Level of participation in robotic-assisted treadmill walking modulates midline sensorimotor EEG rhythms in able-bodied subjects. *NeuroImage*, *63*(3), 1203–1211. http://doi.org/10.1016/j.neuroimage.2012.08.019

Wascher, E., Heppner, H., & Hoffmann, S. (2014). Towards the measurement of event-related EEG activity in real-life working environments. *International Journal of Psychophysiology*, *91*(1), 3–9. http://doi.org/10.1016/j.ijpsycho.2013.10.006

Wells, W. C. (1792). *An Essay Upon Single Vision with Two Eyes: Together with Experiments and Observations on Several Other Subjects in Optics. By William Charles Wells, MD*. T. Cadell, in the Strand.

Wieser, M. J., & Brosch, T. (2012). Faces in context: A review and systematization of contextual influences on affective face processing. *Frontiers in Psychology*, *3*(NOV), 1–13. http://doi.org/10.3389/fpsyg.2012.00471

Wilson, M. (2002). Six views of embodied cognition. *Psychonomic Bulletin and Review*, *9*(4), 625–636. http://doi.org/10.3758/BF03196322

Woodman, G. F., & Luck, S. J. (1999). Electrophysiological measurement of rapid shifts of attention during visual search. *Nature*, *400*(6747), 867–869. http://doi.org/10.1038/23698

Yagi, A. (1979a). Lambda waves associated with the offset of saccades: a subject with large lambda waves, *8*, 235–238.

Yagi, A. (1979b). Saccade size and lambda complex in man. *Physiological Psychology*, *7*(4), 370–376. http://doi.org/10.3758/BF03326658

Yagi, A. (1981a). Averaged cortical potentials (lambda responses) time-locked to onset and offset of saccades. *Physiological Psychology*, *9*(3), 318–320.

Yagi, A. (1981b). Visual signal detection and lambda responses. *Electroencephalography and Clinical Neurophysiology*, *6*(52), 604–610.

Yagi, A. (1982). Short Report response as an index of visual perception. *Japanese Psychological Research*, *24*(2), 106–110.

Yovel, G., & Kanwisher, N. (2004). Face perception: Domain specific, not process specific. *Neuron*, *44*(5), 889–898. http://doi.org/10.1016/j.neuron.2004.11.018

Yun, K., Watanabe, K., & Shimojo, S. (2012). Interpersonal body and neural synchronization as a marker of implicit social interaction. *Scientific Reports*, *2*, 1–8. http://doi.org/10.1038/srep00959

Zhou, G., Bourguignon, M., Parkkonen, L., & Hari, R. (2016). Neural signatures of hand kinematics in leaders vs. followers: A dual-MEG study. *NeuroImage*, *125*, 731–738. http://doi.org/10.1016/j.neuroimage.2015.11.002

Zhou, Z. H., & Geng, X. (2004). Projection functions for eye detection. *Pattern Recognition*, *37*(5), 1049–1056. http://doi.org/10.1016/j.patcog.2003.09.006

Zhu, Z., & Ji, Q. (2004). Eye and gaze tracking for interactive graphic display. *Machine Vision and Applications*, *15*(3), 139–148. http://doi.org/10.1007/s00138-004-0139-4

Zhu, Z., & Ji, Q. (2007). Novel Eye Gaze Tracking Techniques Under Natural Head Movement. *IEEE Transactions on Biomedical Engineering*, *54*(12), 2246–2260. http://doi.org/10.1109/TBME.2007.895750

Zink, R., Hunyadi, B., Huffel, S. Van, & Vos, M. De. (2016). Mobile EEG on the bike: Disentangling attentional and physical contributions to auditory attention tasks. *Journal of Neural Engineering*, *13*(4). http://doi.org/10.1088/1741-2560/13/4/046017